frontiers | Research Topics

Inflammation in the pathogenesis of COVID-19

Edited by
Pietro Ghezzi, Gilles Kaplanski, Fabrice Cognasse and Veronique Godot

Published in
Frontiers in Immunology

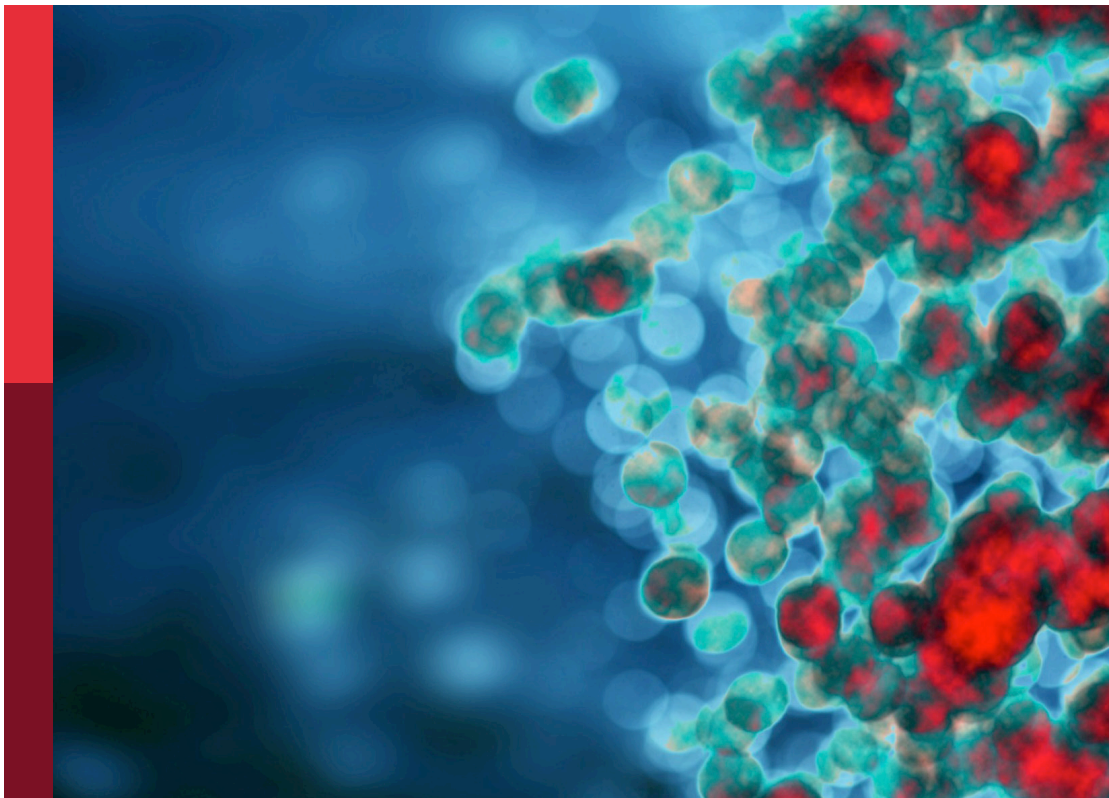

ISSN 1664-8714
ISBN 978-2-8325-3748-0
DOI 10.3389/978-2-8325-3748-0

About Frontiers

Frontiers is more than just an open access publisher of scholarly articles: it is a pioneering approach to the world of academia, radically improving the way scholarly research is managed. The grand vision of Frontiers is a world where all people have an equal opportunity to seek, share and generate knowledge. Frontiers provides immediate and permanent online open access to all its publications, but this alone is not enough to realize our grand goals.

Frontiers journal series

The Frontiers journal series is a multi-tier and interdisciplinary set of open-access, online journals, promising a paradigm shift from the current review, selection and dissemination processes in academic publishing. All Frontiers journals are driven by researchers for researchers; therefore, they constitute a service to the scholarly community. At the same time, the *Frontiers journal series* operates on a revolutionary invention, the tiered publishing system, initially addressing specific communities of scholars, and gradually climbing up to broader public understanding, thus serving the interests of the lay society, too.

Dedication to quality

Each Frontiers article is a landmark of the highest quality, thanks to genuinely collaborative interactions between authors and review editors, who include some of the world's best academicians. Research must be certified by peers before entering a stream of knowledge that may eventually reach the public - and shape society; therefore, Frontiers only applies the most rigorous and unbiased reviews. Frontiers revolutionizes research publishing by freely delivering the most outstanding research, evaluated with no bias from both the academic and social point of view. By applying the most advanced information technologies, Frontiers is catapulting scholarly publishing into a new generation.

What are Frontiers Research Topics?

Frontiers Research Topics are very popular trademarks of the *Frontiers journals series*: they are collections of at least ten articles, all centered on a particular subject. With their unique mix of varied contributions from Original Research to Review Articles, Frontiers Research Topics unify the most influential researchers, the latest key findings and historical advances in a hot research area.

Find out more on how to host your own Frontiers Research Topic or contribute to one as an author by contacting the Frontiers editorial office: frontiersin.org/about/contact

Inflammation in the pathogenesis of COVID-19

Topic editors

Pietro Ghezzi — University of Urbino Carlo Bo, Italy
Gilles Kaplanski — Assistance Publique Hôpitaux de Marseille, France
Fabrice Cognasse — INSERM U1059 SAnté INgéniérie BIOlogie, France
Veronique Godot — INSERM U955 Institut Mondor de Recherche Biomédicale (IMRB), France

Citation

Ghezzi, P., Kaplanski, G., Cognasse, F., Godot, V., eds. (2023). *Inflammation in the pathogenesis of COVID-19*. Lausanne: Frontiers Media SA.
doi: 10.3389/978-2-8325-3748-0

Table of contents

frontiers | Frontiers in Immunology

TYPE Original Research
PUBLISHED 30 September 2022
DOI 10.3389/fimmu.2022.1012027

OPEN ACCESS

EDITED BY
Veronique Godot,
INSERM U955 Institut Mondor de Recherche Biomédicale (IMRB), France

REVIEWED BY
Kenneth A. Jacobson,
National Institutes of Health (NIH), United States
Gabor Tajiti,
Medical University of Vienna, Austria
Francisco G. Vázquez-Cuevas,
Universidad Nacional Autónoma de México, Mexico
Gilson Dorneles,
Federal University of Health Sciences of Porto Alegre, Brazil

*CORRESPONDENCE
Maria Notomi Sato
marisato@usp.br

SPECIALTY SECTION
This article was submitted to Inflammation, a section of the journal Frontiers in Immunology

RECEIVED 05 August 2022
ACCEPTED 14 September 2022
PUBLISHED 30 September 2022

CITATION
Pietrobon AJ, Andrejew R, Custódio RWA, Oliveira LM, Scholl JN, Teixeira FME, de Brito CA, Glaser T, Kazmierski J, Goffinet C, Turdo AC, Yendo T, Aoki V, Figueiró F, Battastini AM, Ulrich H, Benard G, Duarte AJS and Sato MN (2022) Dysfunctional purinergic signaling correlates with disease severity in COVID-19 patients.
Front. Immunol. 13:1012027.
doi: 10.3389/fimmu.2022.1012027

Dysfunctional purinergic signaling correlates with disease severity in COVID-19 patients

Anna Julia Pietrobon[1,2], Roberta Andrejew[3], Ricardo Wesley Alberca Custódio[1], Luana de Mendonça Oliveira[1,2], Juliete Nathali Scholl[4], Franciane Mouradian Emidio Teixeira[1,2], Cyro Alves de Brito[5], Talita Glaser[3], Julia Kazmierski[6,7], Christine Goffinet[6,7], Anna Claudia Turdo[8], Tatiana Yendo[1], Valeria Aoki[1], Fabricio Figueiró[4], Ana Maria Battastini[4], Henning Ulrich[3], Gill Benard[1], Alberto Jose da Silva Duarte[1] and Maria Notomi Sato[1]*

[1]Laboratory of Dermatology and Immunodeficiencies, LIM-56, Department of Dermatology, Tropical Medicine Institute of São Paulo, University of São Paulo Medical School, São Paulo, Brazil, [2]Department of Immunology, Institute of Biomedical Sciences, University of São Paulo, São Paulo, Brazil, [3]Department of Biochemistry, Institute of Chemistry, University of São Paulo, São Paulo, Brazil, [4]Department of Biochemistry, Federal University of Rio Grande do Sul, Porto Alegre, Brazil, [5]Technical Division of Medical Biology, Immunology Center, Adolfo Lutz Institute, São Paulo, Brazil, [6]Institute of Virology, Charité - Universitätsmedizin Berlin, Berlin, Germany, [7]Department and Division of Infectious and Parasitic Diseases, Berlin Institute of Health, Berlin, Germany, [8]Department and Division of Infectious and Parasitic Diseases, Hospital das Clinicas, University of São Paulo Medical School, São Paulo, Brazil

Ectonucleotidases modulate inflammatory responses by balancing extracellular ATP and adenosine (ADO) and might be involved in COVID-19 immunopathogenesis. Here, we explored the contribution of extracellular nucleotide metabolism to COVID-19 severity in mild and severe cases of the disease. We verified that the gene expression of ectonucleotidases is reduced in the whole blood of patients with COVID-19 and is negatively correlated to levels of CRP, an inflammatory marker of disease severity. In line with these findings, COVID-19 patients present higher ATP levels in plasma and reduced levels of ADO when compared to healthy controls. Cell type-specific analysis revealed higher frequencies of CD39+ T cells in severely ill patients, while CD4+ and CD8+ expressing CD73 are reduced in this same group. The frequency of B cells CD39+CD73+ is also decreased during acute COVID-19. Interestingly, B cells from COVID-19 patients showed a reduced capacity to hydrolyze ATP into ADP and ADO. Furthermore, impaired expression of ADO receptors and a

compromised activation of its signaling pathway is observed in COVID-19 patients. The presence of ADO in vitro, however, suppressed inflammatory responses triggered in patients' cells. In summary, our findings support the idea that alterations in the metabolism of extracellular purines contribute to immune dysregulation during COVID-19, possibly favoring disease severity, and suggest that ADO may be a therapeutic approach for the disease.

KEYWORDS

adenosine, ATP, CD39, CD73, COVID-19, SARS-CoV-2, purinergic signaling

Introduction

Coronavirus Disease 2019 (COVID-19) is an inflammatory disease caused by the infection with the SARS coronavirus 2 (SARS-CoV-2). Clinical manifestations of the disease can range from no symptoms or mild upper airway symptoms to severe lower airway symptoms that can evolve to acute respiratory distress syndrome and death (1, 2). Despite the preferential tropism to the lungs, SARS-CoV-2 can be detected in several organs, triggering exacerbated inflammatory responses not only in the target tissues but also systemically, which seems to be responsible for multi-organ failure (3, 4).

Adenosine triphosphate (ATP) is a nucleotide that is present in high concentrations in the cytosol and can be released into the extracellular space upon cellular activation or death (5–7). Extracellular ATP (eATP) can act as a "danger" signal, promoting immune cell activation and eliciting proinflammatory responses (6, 8). Alternatively, eATP can be converted into adenosine (ADO) by ectonucleoside triphosphate diphosphohydrolases (ENTPDases), ecto-nucleotide pyrophosphatases/phosphodiesterases (ENPPs), ecto-5'-nucleotidases, and alkaline phosphatases expressed in the membrane of several immune cells (9–11). Among them, the ectonucleotidase CD39 (ENTPD1) dephosphorylates ATP and ADP to AMP, which is subsequently converted to ADO by CD73 (NT5E) (11). While eATP has proinflammatory properties, ADO can promote immunosuppression *via* inhibition of T cell proliferation and function and induction of anti-inflammatory cytokines (12, 13).

Alterations in the expression and frequency of CD39 and CD73 in leukocytes have already been reported during viral infections and seem to contribute to the inflammatory immunopathology of those diseases (14–16). In addition, it has been reported that viral infection and the viral load itself might influence the purinergic signaling in different viral infections (17, 18). In COVID-19 patients, specifically, there is evidence that the expression of ectoenzymes is modified in T cell lymphocytes and monocytes (19–22). However, whether alterations in this pathway might contribute to the exacerbated inflammatory response associated with COVID-19 is still unclear.

Here we suggest that purinergic signaling might contribute to disease severity during SARS-CoV-2 acute infection. We present evidence to support that the decreased expression of ectonucleotidases in COVID-19 patients' blood compromises the hydrolysis of ATP in ADO and, together with the reduction in ADO receptors, might favor systemic inflammation. Consistently, ADO partially attenuates inflammatory responses in patients' cells activated *in vitro*, suggesting that ADO can be considered as a potential therapeutic intervention for COVID-19.

Materials and methods

Human subjects

A total of 88 patients with COVID-19 hospitalized at Hospital das Clínicas da Faculdade de Medicina da Universidade de São Paulo (HC-FMUSP) from May 2020 to August 2021 were enrolled in this study. The participants were not vaccinated against COVID-19 and diagnosis was confirmed by reverse-transcriptase polymerase chain reaction (RT-PCR). Patients were divided according to WHO criteria into (1) mild cases, in which no oxygen therapy or oxygen by mask/nasal prong was required, and (2) severe cases, which were submitted to non-invasive ventilation or invasive mechanical ventilation support by the time of sample collection (23). Mild and severe COVID-19 patients had underlying medical conditions including hypertension, diabetes, and obesity, consistent with previously published studies (24, 25). Supplementary Table 1 summarizes clinical, laboratory, and treatment records from patients. We observed a ~45.5% mortality rate among patients with severe COVID-19 and ~9% among those with mild forms of the disease (Supplementary Figure 1). We also collected samples from 29 age- and gender-matched healthy unvaccinated controls and with no COVID-19 associated symptoms.

Sample processing

Blood samples were collected into EDTA tubes and centrifuged at 300 x g for 5 min. Plasma was stored at -80°C for subsequent analysis. The remaining cellular fraction was either stored in RNA Later Solution (Sigma-Aldrich) or processed for leukocyte isolation.

Gene expression by real-time PCR

Relative gene expression levels of the ectonucleotidases ENPP1, ENPP2, ENPP3, ENTPD1 (CD39), ENTPD5, and NT5E (CD73), as well as the adenosine receptors ADORA1R, ADORA2aR, ADORA2bR, and ADORA3R, were obtained by real-time PCR. Whole blood mRNA was obtained using the RiboPure RNA Purification kit (Thermo Fisher Scientific) and reverse transcribed with the iScript kit (Biorad). For real-time PCR reaction, cDNA was incubated with SYBR Green (Applied Biosystem) and the primers for all target genes, using GAPDH as an internal control. Primers sequences are listed in Supplementary Table 2. DNA amplification was carried out in a 7500 Real-time PCR system (Applied Biosystems), and data analysis was performed with the 7500 Software v2.0.6 (Applied Biosystems) according to the delta-CT method (26).

Plasmatic quantification of nucleotides

ATP and ADO levels in plasma were determined by high-performance liquid chromatography (HPLC), as previously described (27). Briefly, plasma samples were denatured with 0.6 M perchloric acid by centrifugation at 4°C, 16,000 x g for 20 min. After, 4 M KOH was used to neutralize the supernatants, and samples were submitted to second centrifugation. The supernatants were collected and stored at -80°C. Purine levels in the plasma were determined using a reverse-phase HPLC (Shimadzu) using a C18 column (Ultra C18, 25 cm, 4.6 mm, 5 µm, Restek). The elution was carried out using a linear gradient from 100% solvent A (60 mM KH2PO4 and 5 mM of tetrabutylammonium chloride, pH 6.0) to 100% solvent B (solvent A + 30% methanol). The amounts of purines were measured by absorption at 254 nm and the retention times of standards were used as parameters for identification and quantification.

Immunophenotyping

The expression of CD39 and CD73 in leukocytes was determined by flow cytometry. Samples were incubated with Fc block solution and stained with the following antibodies: anti-CD39 APC (BD-Biosciences), anti-CD73 BB515 (BD-Biosciences), anti-CD3 BV605 (BD-Biosciences), anti-CD14 PerCP (BD-Biosciences) anti-CD19 PE (Beckman Coulter), anti-CD4 V450 (BD-Biosciences) and anti-CD8 V500 (BD-Biosciences). LIVE/DEAD dye (Invitrogen) was used to distinguish dead cells. Samples were fixed with 4% paraformaldehyde and erythrocytes were removed using the FACS Lysing solution (BD Biosciences). Fluorescent cell data acquisition was done using the LSR Fortessa equipment (BD Biosciences) and analyzed with FlowJo software (BD Life Sciences). Fluorescence controls (FMO - Fluorescence Minus One) were realized for all the fluorochromes in the panel.

In cases in which the expression of ADO receptors was evaluated, blood samples depleted of erythrocytes were fixed with 4% paraformaldehyde and permeabilized with Triton-X 100. Cells were stained with primary rabbit polyclonal antibodies against A_1R, $A_{2A}R$, $A_{2B}R$, and A_3R (1:500) (Abcam) for 2h at room temperature, followed by incubation with secondary antibody Alexa Fluor 488 goat anti-rabbit (1:1000) (Thermo Fisher). Cells were acquired in an Attune cytometer (Life Technologies) and analyzed with the FlowJo software. Granulocytes and Lymphocytes were differentiated based on the forward/side scatter profile.

Single-cell data collection and nucleotidases expression analysis

Kazmierski et al. (28) recently performed single cells RNA-Seq experiments investigating the global transcriptional profile of PBMCs from HDs exposed *in vitro* to SARS-CoV-2 for 24h (data accessible at NCBI Gene Expression Omnibus [GEO] accession GSE197665 (28)). We retrieved the data sets to characterize the ectonucleotidase mRNA signature. Analysis of the single-cell RNA data was performed using R Studio v3.6 (R Core Team, 2017) and the Seurat v3.1.4 package (29) and differentially expressed genes were analyzed using the 10x Genomics Loupe Browser (v. 5.0.1).

Measurement of soluble CD73

The concentration of soluble CD73 in plasma was determined by the human CD73 ELISA kit (NT5E) (Abcam) according to the manufacturer's instructions. The minimum detection limit was 156 pg/ml.

Isolation of B cell and the extracellular metabolism of ATP

CD19+ B cells were isolated from blood samples by magnetic separation. Briefly, peripheral blood mononuclear cells were obtained from freshly heparinized blood by density gradient

centrifugation. The CD19+ B cells were separated by negative selection using the EasySep Direct HLA B Cell Isolation kit (Stemcell Technologies). The purity of the separated cells determined by flow cytometry exceeded 92%.

B cells were resuspended in phenol red-free RPMI 1640 medium (Gibco) plus 10% fetal bovine serum (FBS) (Sigma-Aldrich) at a concentration of $2.5x10^5$ cells/mL, and 100 µl were plated into a 96-well plate (Jet Bio-Fil). After 18h incubation, the cells were transferred to 1.5ml tubes and resuspended in the incubation buffer containing KCl 5 mM, CaCl2 1.5 mM, EDTA 0.1 mM, glucose 10 mM, sucrose 225 mM, Tris HCl 45 mM, and MgCl2 10 mM, pH 8. ATP (500 µM) (Sigma-Aldrich) was added and cells were incubated for 15, 30, and 60 min. at 37°C and 5% CO2. The reaction was stopped on ice, and cells were centrifuged at 600 x g for 5 min at 4°C. Supernatants were collected and incubated with 10% methanol on ice for 30 min, followed by final refrigerated centrifugation at 25000 x g for 30 min. Samples were stored at -80°C until being analyzed by HPLC as already described.

Isolation of mononuclear cells

For cell culture experiments, mononuclear cells (MNCs) were obtained by diluting 1mL of buffy coat from EDTA tubes into 11mL of PBS. Samples were layered over a buffered 60% solution of Percoll PLUS reagent (GE Healthcare) and centrifuged at 800 × g for 30 min. Cells at the interphase were collected and counted for the next assays.

PKA activity assay

MNCs were resuspended in supplemented medium at a concentration of $1x10^6$ cells/mL and were plated into a 48-well plate. After 18h incubation, either ATP or ADO (100µM) (Sigma-Aldrich) were added to the cultures for 30min. Total cellular proteins were extracted and 30ng were used to access the protein kinase A (PKA) activity using the PKA Kinase Activity Assay kit (Abcam) according to the manufacturer's instructions. The absorbance was measured at 450 nm with a microplate reader ELx800 (BioTek).

ADO immunomodulation assay

The immunomodulatory capacity of ADO was verified *in vitro*. In brief, $2x10^5$ cells/mL MNCs were cultured in RPMI 1640 medium plus 10% human serum-supplemented or not with ADO (100 µM) for 2h. Cells were further activated using the TLR7/TLR8 agonist CL097 (5 µg/mL) (*In vivo*gen), used as a viral mimetic, for additional 22h. After stimulation, the supernatants from the cultures were stored at -80°C.

Cytokines measurement

Commercial ELISA kits were used to measure IL-6, TNF-α, and IL-10 (R&D Systems) production in culture supernatants, according to the manufacturer's protocols. The absorbance was measured at 450 nm with a microplate reader ELx800 (BioTek).

Statistical analysis

Comparisons between patients and healthy controls were performed with the One-way ANOVA test or Mann-Whitney U test, while for comparisons between paired baseline and stimulated conditions within the same group the Wilcoxon signed-rank test was applied. The Spearman test was used for the correlation analysis. The level of significance considered was $p \leq 0.05$.

Results

Impaired expression of nucleotidases is associated with inflammatory responses in COVID-19

Although CD39 and CD73 are widely studied in immune cells, several nucleotidases are involved in the extracellular metabolism of purines and hydrolysis of ATP into ADO. Herein, we detected the gene expression of ENPP1, ENPP2, ENPP3, ENTPD1 (CD39), ENTPD5, and NT5E (CD73) in the whole blood of COVID-19 patients. As shown in Figure 1A, there is a significant reduction in the expression of *ENPP1*, *ENPP2*, *ENPP3*, and *NT5E* in the blood of patients with severe COVID-19 when compared to HDs and a lower expression of *ENPP2* and *ENPP3* when compared to mild hospitalized cases. Interestingly, the impaired gene expression of these enzymes is negatively correlated to plasmatic levels of C-reactive protein (Figure 1B) and the neutrophil-to-lymphocyte ratio (Supplementary Figure 2), two inflammatory markers of the disease (30, 31), which is in agreement with the idea that the reduced expression of ectonucleotidases is at least in part accountable for the inflammatory status of COVID-19. In accordance with this data, there is a higher concentration of plasmatic ATP in patients with COVID-19 when compared to HDs, independent of disease severity (Figure 1C). At the same time, COVID-19 patients had lower plasma levels of ADO, indicating that the purinergic degradation pathway and ADO production could be compromised in the disease.

Altered frequencies of CD39+ and CD73+T and B lymphocytes compromise the hydrolysis of extracellular ATP in COVID-19

As the expression of ectonucleotidases varies among leukocytic populations (32–34), we further analyzed the

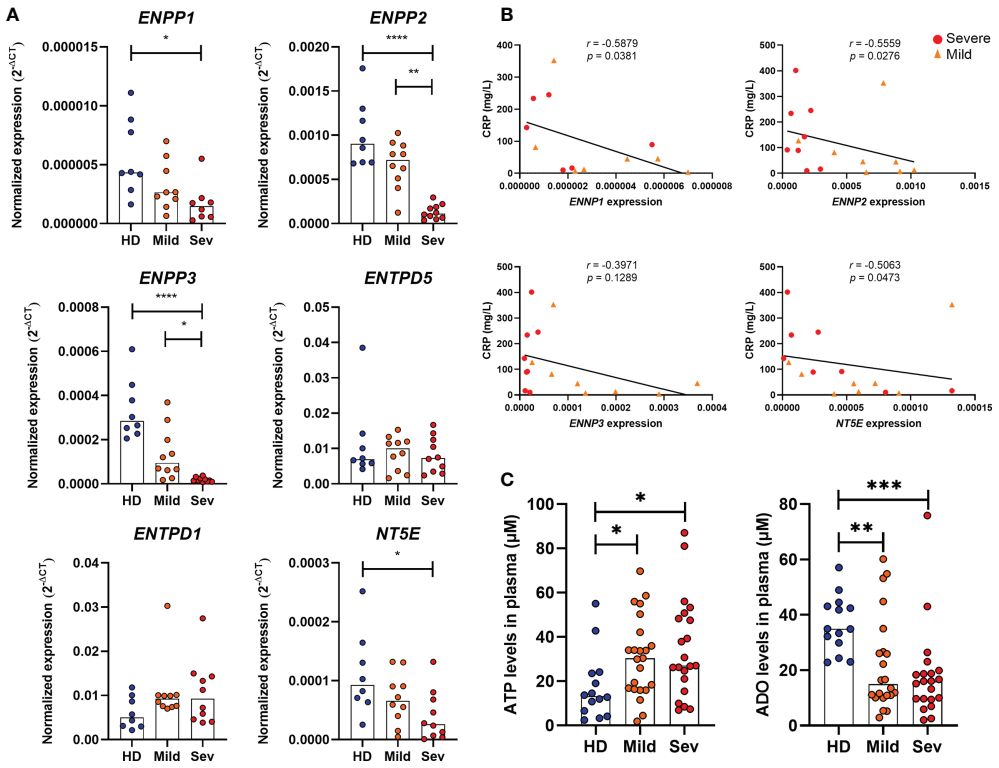

FIGURE 1
Altered expression of nucleotidases and purinergic composition in the blood of COVID-19 patients. **(A)** Gene expression of nucleotidases ENPP1, ENPP2, ENPP3, ENTPD5, ENTPD1 (CD39) and NT5E (CD73) in whole blood of healthy donors (n=8) and COVID-19 patients (Mild hospitalized, n=10; Severe, n=10). **(B)** Negative correlation between the expression of nucleotidases and blood levels of C-reactive protein (CRP) in COVID-19 patients. **(C)** Plasma levels of ATP and ADO in healthy donors (n=14) and COVID-19 patients (Mild hospitalized, n=23; Severe, n=21). Data are shown as the median. One-way ANOVA test: *p<0.05, **p<0.01, ***p<0.001, ****p<0.0001. Spearman's correlation test was used to determine the correlation coefficient (r) and the significance (p<0.05). Blue dots indicate healthy donors (HD) whereas orange and red dots indicate hospitalized patients with mild and severe (Sev) COVID-19, respectively.

presence of CD39 and CD73 in specific cell types by flow cytometry. It has already been reported that under healthy conditions CD39 is largely expressed on B cells and monocytes, followed by CD4+ T cells and, less significantly, by CD8+ T and NK cells (35). Despite the considerable expression of CD39 in monocytes, we did not observe significant changes in the frequency of CD14+CD39+ cells in SARS-CoV-2 infected individuals (Supplementary Figure 3). However, there is an increase in the frequency of CD4+CD39+ and CD8+CD39+ T cells with greater expression of CD39 in patients with severe COVID-19 (Figures 2A, B), indicating the prevalence of activated T cells or even regulatory T cells in infected subjects.

On the other hand, CD73 expression is reduced in both, CD4+ and CD8+ T cells, in COVID-19 patients (Figures 2A, B), corroborating with previous studies (20). Indeed, while T cell activation leads to upregulation of CD39, it also results in the loss of CD73 from the cell membrane which can remain enzymatically active as a soluble protein. To access if the reduced expression of CD73 in lymphocytes of COVID-19 patients is due to its shedding from the cellular membrane, we quantified soluble CD73 (sCD73) in plasma. As can be seen in Figure 2D, there are no differences in the plasma levels of sCD73 between HDs and COVID-19 patients.

While mostly human CD4+ and CD8+ T cells can either express CD39 or CD73, B lymphocytes are usually double-positive for these enzymes and, therefore, play a significant role in the generation of ADO from ATP (36). Interestingly, there is a reduction in the expression of CD39 and CD73 in B cells from COVID-19 patients and the CD19+CD39+CD73+ population is diminished in patients regardless of the disease status (Figure 2C).

We further asked if the modified expression of nucleotidases in leukocytes would be a direct effect of viral exposure. Therefore, we reanalyzed single-cell RNA-sequencing data from PBMCs of healthy donors exposed *in vitro* to SARS-CoV-2, as described by Kazmierski et al. (28). Overall, no significant modulation in the expression of *ENPP1*, *ENPP2*, *ENPP3*, *ENTPD1*, and *NT5E* was found in B cells, CD4+ T cells, and CD8+ T cells when they were incubated with SARS-CoV-2 for 24h (Figure 2E). Although limited to isolated PBMCs, these data indicate that the altered expression of ectonucleotidases observed in COVID-19 patients is more

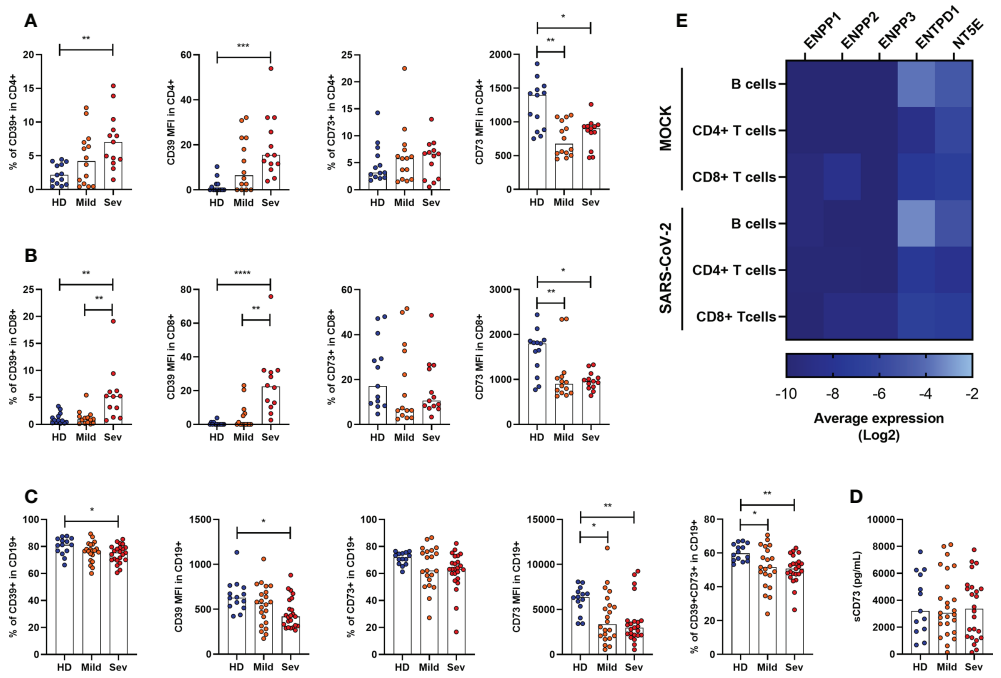

FIGURE 2
Altered frequency of CD39+ and CD73+ leucocytes in the blood of COVID-19 patients. Frequency and expression of CD39 and CD73 in **(A)** CD4+ T cells, **(B)** CD8+ T cells and **(C)** CD19+ cells from healthy donors (n=14) and COVID-19 patients (Mild hospitalized, n=14-21; Severe, n=12-24) based on the percentage of positive cells and the median of fluorescence (MFI) values. **(D)** Concentration of plasmatic CD73 from healthy donors (n=13) and COVID-19 patients (Mild hospitalized, n=25; Severe, n=24). **(E)** Heatmap of average gene expression values for ENPP1, ENPP2, ENPP3, ENTPD1, and NT5E in B cells, CD4+ T cells, and CD8+ T cells exposed or not to SARS-CoV-2. One-way ANOVA test: *p<0.05, **p<0.01, ***p<0.001, ****p<0.0001. Blue dots indicate healthy donors (HD) whereas orange and red dots indicate hospitalized patients with mild and severe (Sev) COVID-19, respectively.

likely to be induced by the immune response triggered by SARS-CoV-2 than the virus itself.

Considering that B cells play a crucial role in controlling purinergic-dependent immune responses due to the high expression of CD39 and CD73, the reduction of CD19+CD39+CD73+ cells could directly impact ADO availability. To verify if these phenotypic changes would compromise the consumption of ATP, ADP, and AMP, B cells were isolated from severely ill patients with COVID-19 and HDs and incubated with ATP (500 μM) for various periods. As expected, B cells from subjects infected with SARS-CoV-2 converted less ATP into ADP and produced less ADO when compared with those from HDs (Figure 3), indicating an impaired capacity of hydrolyzing ATP in B cells from patients with severe COVID-19.

ADO signaling is compromised in COVID-19 patients

ADO signals *via* receptors A_1R, $A_{2A}R$, $A_{2B}R$, and A_3R, and it has been reported that alterations in the expression of these receptors may directly influence the inflammatory response in some pathologies (37, 38). Therefore, we have also investigated the expression of ADO receptors in whole blood samples from COVID-19 patients. Our data indicate a significant reduction of *ADORA2A* gene expression in the whole blood of patients critically ill with COVID-19 (Figure 4A). Cell-type flow cytometry analysis additionally suggests that all four ADO receptors are less expressed in both, granulocytes and lymphocytes of COVID-19 patients in a severity-dependent manner (Figure 4B).

Upon ADO binding, $A_{2A}R$ and $A_{2B}R$ couple with the GαS protein and lead to an increase of intracellular cAMP and PKA activity (12, 39). To explore if this signaling pathway is affected during acute COVID-19, we accessed PKA activation in MNCs from patients and HDs. Our findings indicate that MNCs from COVID-19 patients have, indeed, reduced PKA activity rates under ATP or ADO stimulation when compared to HDs cells (Figure 4C). Together, these results indicate that not only the generation of ADO from ATP is compromised during COVID-19 but the ADO signaling pathway as well.

Inhibition of inflammatory responses by ADO

In order to investigate whether lower availability of ADO could contribute to the pro-inflammatory profile of COVID-19,

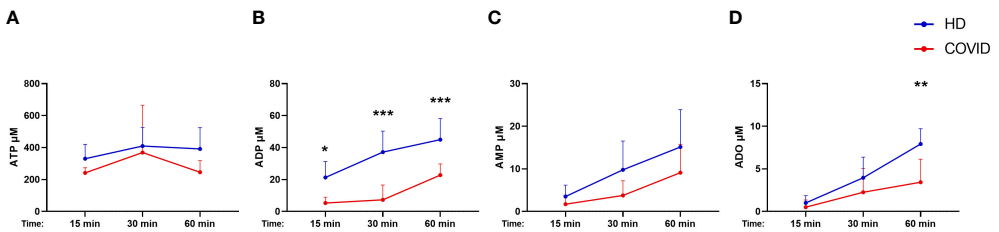

FIGURE 3
Decreased hydrolysis of ATP by COVID-19 patients' B cells. Isolated B cells from healthy donors (n=7) and COVID-19 patients (Severe, n=6) were incubated with 500 µM of ATP for 15, 30, and 60 minutes. Consumption of ATP **(A)** and production of ADP **(B)**, AMP **(C)**, and ADO **(D)** was accessed. Data shown as mean with SD. Two-way ANOVA with Bonferroni's post-test for multiple comparisons: *p<0.05, **p<0.01, ***p<0.001. Blue lines indicate healthy donors (HD) whereas red lines indicate patients with severe (Sev) COVID-19.

MNCs from patients with severe COVID-19 and HDs were cultured with a TLR7/TLR8 agonist (CL097, imidazoquinoline-derived compound) under the presence or absence of ADO. This agonist was chosen as an attempt to mimic innate immune responses triggered during SARS-CoV-2 recognition by MNCs (40). The immunomodulatory effect of ADO was measured by the production of cytokines in the culture supernatants. As shown in Figure 5A, incubation with the TLR7/TLR8 agonist induces the production of TNF-α and IL-6 in cells from HDs and COVID-19 patients. Interestingly, in the presence of ADO, this inflammatory response is partially controlled, suggesting a potential anti-inflammatory effect of ADO. Consistent with these findings, we noticed that ADO itself triggers the production of the anti-inflammatory cytokine IL-10 in MNCs from COVID-19 patients and HDs (Figure 5B), indicating a possible mechanism by which ADO suppresses the production of inflammatory molecules. Taken together, these data suggest that although the ADO signaling pathway is compromised in COVID-19, this nucleotide can still trigger the production of IL-10 and partially suppress inflammatory responses.

Discussion

ATP dephosphorylation into ADO mediated by ectonucleotidases is a key regulatory mechanism of immune responses, promoting the shift from ATP-driven inflammation to immunosuppression induced by ADO (41). Given the pronounced inflammatory characteristics of severe COVID-19 and the role of purinergic signaling in immunosuppression, alterations in the metabolism of extracellular nucleotides could contribute to the immunopathogenesis of the disease. Herein, we demonstrate that impaired expression of nucleotidases and lower ADO concentration in the blood is associated with a worse prognosis of COVID-19, while *in vitro* administration of exogenous ADO helps to prevent inflammatory responses in the leukocytes of patients.

Expression profiles of ectonucleotidases can be modified under pathological conditions. Higher expression of CD39 in lymphocytes, for example, has been reported in solid tumors and chronic viral infection by HIV and HCV, and more recently during acute infection by SARS-CoV-2 (21, 42, 43). Induction of CD39 expression occurs upon cellular activation and is regulated by hypoxia, oxidative stress, and inflammatory cytokines such as IL-6 and TNF-α (41, 44–46), which are frequently increased in COVID-19 patients (47–50). Although higher expression of CD39 in T cells from COVID-19 patients might indicate a possible mechanism to counterbalance the inflammatory responses *via* consumption of ATP, its expression in B cells, the major leukocyte population that expresses CD39, is diminished.

The compromised expression of *ENPP1*, *ENPP2*, *ENPP3*, and *NT5E* (CD73) in the peripheral blood of COVID-19 patients shown here, negatively correlates to plasma levels of the inflammatory marker CRP and the neutrophil-to-lymphocyte ratio, supporting the hypothesis of a direct contribution of the purinergic metabolism to the pathogenesis of the disease. In accordance with our findings, Ahmadi et al. reported that loss of CD73 expression in CD8+ T and NKT cells of COVID-19 patients negatively correlates with serum levels of ferritin, another inflammatory marker of the disease (20). It is important to mention, though, that gene expression analysis in whole blood of COVID-19 patients should be interpreted with caution due to the mono-lymphopenia associated with the disease (51, 52). In this context, it is hard to distinguish whether the altered gene expression results from transcriptional events or whether it is a consequence of the imbalance proportion of lymphocytes and monocytes that express such enzymes in the blood of patients. In any case, reduced expression of nucleotidases in peripheral blood may be possibly responsible for the lower concentrations of ADO in the plasma of COVID-19 patients shown here.

Deep and cell-specific analysis evidence that the surface expression of CD73 is impaired in CD4+ T cells and CD8+ T cells in patients with COVID-19, corroborating previously published data (20, 21). In addition, we verified, for the first time, lower expression of CD73 also in CD19+ B cells. Loss of

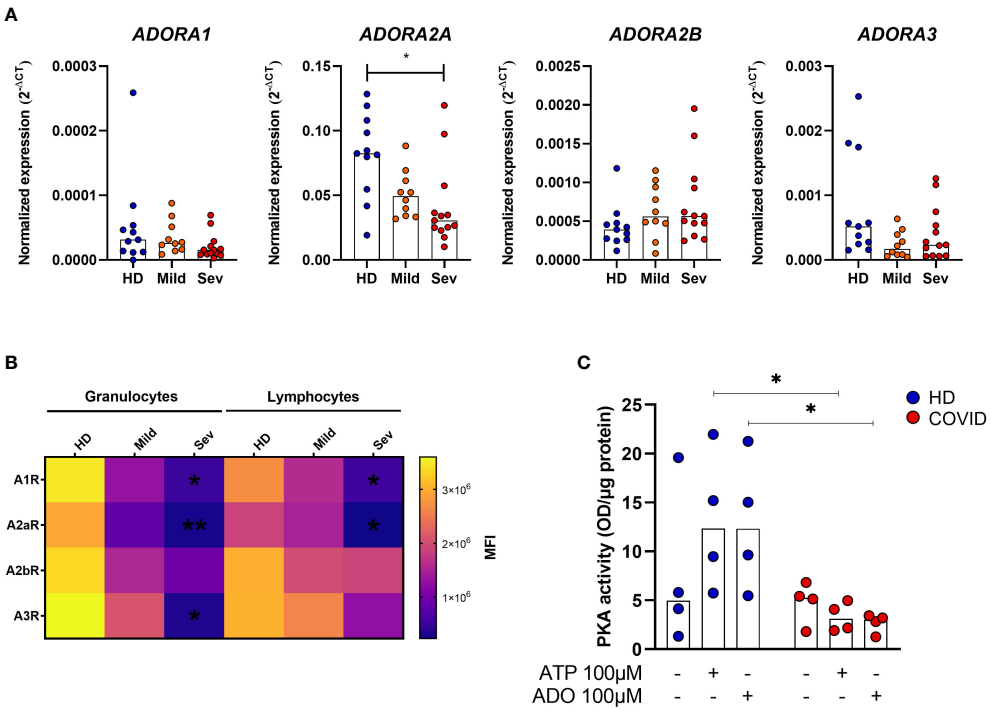

FIGURE 4
Impaired ADO signaling in COVID-19 patients. **(A)** Gene expression of ADORA1, ADORA2A, ADORA2B, and ADORA3 in whole blood of healthy donors (n=11) and COVID-19 patients (Mild hospitalized, n=10; Severe, n=13). Data presented as median. One-way ANOVA test: *p<0.05. **(B)** Heatmap of A_1R, $A_{2A}R$, $A_{2B}R$, and A_3R MFI values expression in lymphocytes and granulocytes of healthy donors (n=6) and COVID-19 patients (Mild hospitalized, n=4; Severe, n=8) based on the median of fluorescence (MFI) values. Data presented as mean. One-way ANOVA test: *p<0.05, **p<0.01. **(C)** MNCs from healthy donors (n=4) and COVID-19 patients (n=4) were incubated with ATP (100 µM) or ADO (100 µM) for 30 minutes. The PKA activity is shown. Data presented as median. Mann-Whitney U test: *p<0.05 (HD vs. COVID-19). Blue dots indicate healthy donors (HD) whereas orange and red dots indicate hospitalized patients with mild and severe (Sev) COVID-19, respectively.

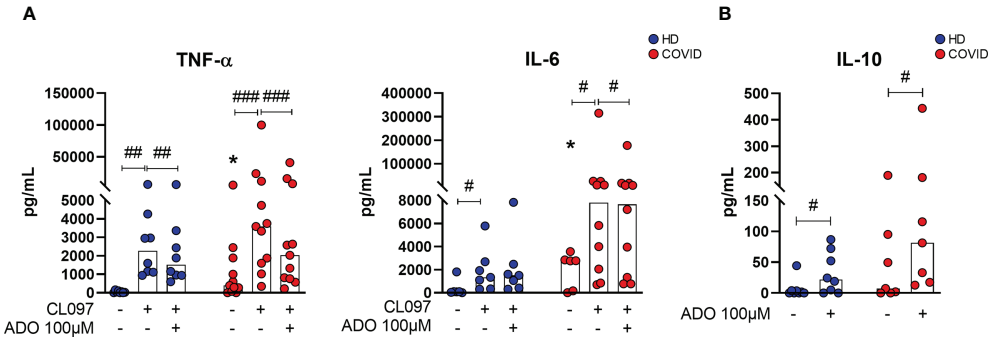

FIGURE 5
ADO prevents cellular activation triggered by TLRs and induces anti-inflammatory responses. **(A)** MNCs from healthy donors (n=8) and COVID-19 patients (n=11) were incubated with ADO (100 µM) for 2 hours followed by activation with TLR7/8 agonist. Cytokine production in the supernatant after 24h is shown. **(B)** MNCs from healthy donors (n=8) and COVID-19 patients (n=7) were incubated with ADO (100 µM) for 24 hours and IL-10 production in the supernatant after 24h was accessed. Data are shown as the median. Wilcoxon signed-rank test: $^{\#}$p<0.05; $^{\#\#}$p<0.01, $^{\#\#\#}$p<0.001 (between different treatments). Mann-Whitney U test: *p<0.05 (HD vs. COVID-19). Blue dots indicate healthy donors (HD) whereas red dots indicate patients with COVID-19.

surface CD73 can be explained by alterations at the transcriptional level or also by the shedding of the enzyme from the cell membrane upon cellular activation (53). Complementary, our single-cell RNA-sequencing data analysis from PBMCs exposed to SARS-CoV-2 indicate that the expression of nucleotidases is not likely to be directly affected by the virus (Figure 2E). However, it has been shown that incubation with plasma from COVID-19 patients inhibits the expression of CD73 in lymphocytes from HDs (21), suggesting the contribution of soluble factors in these alterations besides the virus itself. Moreover, matrix metalloproteinase (MMP-9), which is released by neutrophils during acute lung damage and is elevated in COVID-19 patients' blood (54, 55), can cleave CD73 from the cellular membrane generating a soluble protein (56, 57). In our cohort, however, no differences regarding soluble CD73 in the plasma of COVID-19 patients and HDs were observed (Figure 2D). Regardless of the specific mechanism behind this alteration has not been elucidated in detail here, loss of CD73 could contribute to the maintenance of the effector function of T cells by preventing ADO-mediated immunosuppression (53, 57). In support of our findings, lymphocyte activation markers such as CD38, CD69, and CD44 are highly expressed on CD4+ and CD8+ T cells of COVID-19 patients (58), and CD73 absence in CD8+ T cells induces granzyme production in these individuals (20).

Different from other lymphocytes, the majority of B cells express CD39 and CD73, contributing significantly to the generation of ADO and inhibiting proliferation and cytokine production in T cells (36). Herein we evidence that B cells from patients with severe COVID-19, which have lower expression of CD39 and CD73, show an impaired capacity to hydrolyze ATP. Similar results were already reported in patients infected with HIV and HBV, where the compromised generation of ADO is claimed to favor inflammatory responses and immune activation (15, 16, 59). Therefore, we have evidences to support the hypothesis that the marked reduction of CD39+CD73+ B cells, together with the impaired expression of CD73 in T cells and the lack of other nucleotidases in the blood, lead to the lower concentrations of plasmatic ADO in COVID-19 patients and might exacerbate innate immune activation. In addition, the absence of CD73 and defective activation of the ADO downstream PKA-mediated phosphorylation of activation-induced deaminase (AID) impairs immunoglobulin class switching in human B cells (60, 61). Whether these alterations compromise humoral responses in COVID-19 patients remains uncertain.

Like us, others have suggested that increased systemic levels of ATP are likely to be involved in the immunopathogenesis of COVID-19 (62, 63), possibly as consequence of the altered expression of nucleotidases. Indeed, the accumulation of ATP has been shown the trigger inflammatory responses such as the activation of the inflammasome pathway (64, 65). Interestingly, there is a higher activation of the NLR family PYRIN domain containing-3, NLRP3, inflammasome in COVID patients (66, 67). In addition, extracellular ATP can contribute to lung local inflammation by recruiting eosinophils, dendritic cells, and neutrophils via $P2Y_2$ receptor (68–70), implying that imbalanced metabolization of this nucleotide could directly contribute to the immunopathogenesis of COVID-19.

Apart from the defective hydrolysis of ATP, ADO signaling itself is apparently compromised in COVID-19, where lower expression of ADO receptors and reduced activity of PKA were observed. Mechanistically, activation of the cAMP/PKA pathway *via* ADO receptors inhibits the production of TNF-α, IFN-γ, and IL-2 and T cell proliferation (71, 72). At the same time, ADO receptor signaling, more specific $A_{2A}R$ and $A_{2B}R$, has been shown to trigger IL-10 production via CREB activation (73–75). Therefore, the compromised generation of ADO by leukocytes, especially B cells, associated with impaired signaling mediated by ADO receptors could exacerbate inflammatory responses systemically.

Although ADO signaling is compromised in leukocytes of severe COVID-19 patients, we verified that *in vitro* treatment can attenuate the production of TNF-α and IL-6 in CMNs after activation. Both cytokines are increased in the blood of COVID-19 patients (76). In fact, it has been reported that ADO reduces NF-κB activation in T cells and monocytes of COVID-19 patients *in vitro* (21), and the administration of an A2aR agonist attenuated the production of pro-inflammatory cytokines in SARS-CoV-2 mice infection model (77). Moreover, preliminary data suggest that inhaled ADO reduces the levels of CRP in the blood while improving oxygenation rates and reduces hospitalization time in patients with COVID-19 (78, 79). Here we observed that, at the dose used, extracellular ADO can partially overcome the impaired expression of its receptors and imbalanced induction of PKA activity (Figures 4, 5), attenuating inflammatory responses. It is important to mention though that co-treatment with other cAMP inducers, such as the neuropeptide PACAP (80), could result in a more pronounced immunosuppressant effect. Taken together, these findings evidence the potential of ADO as a therapeutic strategy to overcome the exacerbated inflammatory responses in COVID-19.

In summary, our findings indicate that alterations in the purinergic signaling contribute, at least in part, to the immune activation and worse prognosis in acute COVID-19 and reveal the therapeutic potential of ADO-mediated responses in this disease. Whether these alterations persist in recovered patients or impact the development of post-COVID-19 syndrome remains to be elucidated.

Data availability statement

The authors acknowledge that the data presented in this study must be deposited and made publicly available in an acceptable repository, prior to publication. Frontiers cannot accept a manuscript that does not adhere to our open data policies.

Ethics statement

The studies involving human participants were reviewed and approved by the Ethics Committee of the HC-FMUSP (no. 30800520.7.0000.0068-2020) and the procedures were conducted following the Declaration of Helsinki. The patients/participants provided their written informed consent to participate in this study.

Author contributions

AP and MS developed the overall study design, analysis, and manuscript writing. AP, RC, LMO, contributed to data generation and analysis. AP, FT, contributed to the sample processing and data generation. RA, JS, and TG helped to design and execute the chromatography experiments; C. provided the laboratory for patient's sample manipulation. JK and CG provided single-cell data and performed the analysis; AT, TY, VA, GB recruited and approached patients. FF, AB, and HU helped to design experiments, discussed hypotheses and edited the manuscript. AD provided tools for proper work development. MS directed the study; and all authors reviewed the manuscript.

Funding

This work was supported by the Laboratory of Dermatology and Immunodeficiencies (LIM-56), the São Paulo Research Foundation (FAPESP) grant numbers 2020/13148-0 and 2018/07366-4, the Coordenação de Aperfeiçoamento de Pessoal de Nível Superior (CAPES) grant number 88887.503842/2020-00 and the National Council for Scientific and Technological Development (CNPq).

Conflict of interest

The authors declare that the research was conducted in the absence of any commercial or financial relationships that could be construed as a potential conflict of interest.

Publisher's note

All claims expressed in this article are solely those of the authors and do not necessarily represent those of their affiliated organizations, or those of the publisher, the editors and the reviewers. Any product that may be evaluated in this article, or claim that may be made by its manufacturer, is not guaranteed or endorsed by the publisher.

Supplementary material

The Supplementary Material for this article can be found online at: https://www.frontiersin.org/articles/10.3389/fimmu.2022.1012027/full#supplementary-material

References

1. Merad M, Martin JC. Pathological inflammation in patients with COVID-19: a key role for monocytes and macrophages. *Nat Rev Immunol* (2020) 20(6):355–62. doi: 10.1038/s41577-020-0331-4

2. Lai CC, Ko WC, Lee PI, Jean SS, Hsueh PR. Extra-respiratory manifestations of COVID-19. *Int J Antimicrob Agents* (2020) 56(2):106024. doi: 10.1016/j.ijantimicag.2020.106024

3. Chen G, Wu D, Guo W, Cao Y, Huang D, Wang H, et al. Clinical and immunological features of severe and moderate coronavirus disease 2019. *J Clin Invest* (2020) 130(5):2620–9. doi: 10.1172/JCI137244

4. Puelles VG, Lütgehetmann M, Lindenmeyer MT, Sperhake JP, Wong MN, Allweiss L, et al. Multiorgan and renal tropism of SARS-CoV-2. *N Engl J Med* (2020) 383(6):590–2. doi: 10.1056/NEJMc2011400

5. Darby M, Kuzmiski JB, Panenka W, Feighan D, MacVicar BA. ATP released from astrocytes during swelling activates chloride channels. *J Neurophysiol* (2003) 89(4):1870–7. doi: 10.1152/jn.00510.2002

6. Corriden R, Insel PA. Basal release of ATP: an autocrine-paracrine mechanism for cell regulation. *Sci Signal* (2010) 3(104):re1. doi: 10.1126/scisignal.3104re1

7. Taruno A. ATP release channels. *Int J Mol Sci* (2018) 19(3):808. doi: 10.3390/ijms19030808

8. Ralevic V, Burnstock G. Receptors for purines and pyrimidines. *Pharmacol Rev* (1998) 50(3):413–92. doi: 10.1007/978-3-642-28863-0_5

9. Allard B, Allard D, Buisseret L, Stagg J. The adenosine pathway in immuno-oncology. *Nat Rev Clin Oncol* (2020) 17(10):611–29. doi: 10.1038/s41571-020-0382-2

10. Haskó G, Cronstein BN. Adenosine: an endogenous regulator of innate immunity. *Trends Immunol* (2004) 25(1):33–9. doi: 10.1016/j.it.2003.11.003

11. Zimmermann H, Zebisch M, Sträter N. Cellular function and molecular structure of ecto-nucleotidases. *Purinergic Signal* (2012) 8(3):437–502. doi: 10.1007/s11302-012-9309-4

12. Haskó G, Linden J, Cronstein B, Pacher P. Adenosine receptors: therapeutic aspects for inflammatory and immune diseases. *Nat Rev Drug Discov* (2008) 7(9):759–70. doi: 10.1038/nrd2638

13. Haskó G, Cronstein B. Regulation of inflammation by adenosine. *Front Immunol* (2013) 4:85. doi: 10.3389/fimmu.2013.00085

14. de Sousa Palmeira PH, Gois BM, Guerra-Gomes IC, Peixoto RF, de Sousa Dias CN, Araújo JMG, et al. Downregulation of CD73 on CD4+ T cells from patients with chronic chikungunya infection. *Hum Immunol* (2022) 83(4):306–318. doi: 10.1016/j.humimm.2022.01.006

15. Zhou SN, Zhang N, Liu HH, Xia P, Zhang C, Song JW, et al. Skewed CD39/CD73/adenosine pathway contributes to b-cell hyperactivation and disease progression in patients with chronic hepatitis b. *Gastroenterol Rep (Oxf)* (2021) 9(1):49–58. doi: 10.1093/gastro/goaa048

16. Chang W-X, Huang H-H, Huang L, Shi J-J, Jiao Y-M, Zhang C, et al. Skewed CD39/CD73/adenosine pathway in b cells is associated with innate immune hyperactivation in chronic HIV-1 infection. *Trans Med Commun* (2019) 9(1):49–58. doi: 10.1186/s41231-019-0033-8

17. Eberhardt N, Bergero G, Mazzocco Mariotta YL, Aoki MP. Purinergic modulation of the immune response to infections. *Purinergic Signal* (2022) 18(1):93–113. doi: 10.1007/s11302-021-09838-y

18. Zhang C, He H, Wang L, Zhang N, Huang H, Xiong Q, et al. Virus-triggered ATP release limits viral replication through facilitating IFN-β production in a P2X7-dependent manner. *J Immunol* (2017) 199(4):1372–81. doi: 10.4049/jimmunol.1700187

19. Demaria O, Carvelli J, Batista L, Thibult ML, Morel A, André P, et al. Identification of druggable inhibitory immune checkpoints on natural killer cells in COVID-19. *Cell Mol Immunol* (2020) 17(9):995–7. doi: 10.1038/s41423-020-0493-9

20. Ahmadi P, Hartjen P, Kohsar M, Kummer S, Schmiedel S, Bockmann JH, et al. Defining the CD39/CD73 axis in SARS-CoV-2 infection: The CD73. *Cells* (2020) 9(8):1750. doi: 10.3390/cells9081750

21. Dorneles GP, Teixeira PC, da Silva IM, Schipper LL, Santana Filho PC, Rodrigues Junior LC, et al. Alterations in CD39/CD73 axis of T cells associated with COVID-19 severity. *J Cell Physiol* (2022) 237(8):3394–407. doi: 10.1002/jcp.30805

22. Romão PR, Teixeira PC, Schipper L, da Silva I, Santana Filho P, Júnior LCR, et al. Viral load is associated with mitochondrial dysfunction and altered monocyte phenotype in acute severe SARS-CoV-2 infection. *Int Immunopharmacol* (2022) 108:108697. doi: 10.1016/j.intimp.2022.108697

23. WHO. *COVID-19 therapeutic trial synopsis*. (Switzerland:World Health Organization) (2020).

24. Zhou Y, Yang Q, Chi J, Dong B, Lv W, Shen L, et al. Comorbidities and the risk of severe or fatal outcomes associated with coronavirus disease 2019: A systematic review and meta-analysis. *Int J Infect Dis* (2020) 99:47–56. doi: 10.1016/j.ijid.2020.07.029

25. Liu B, Spokes P, He W, Kaldor J. High risk groups for severe COVID-19 in a whole of population cohort in Australia. *BMC Infect Dis* (2021) 21(1):685. doi: 10.1186/s12879-021-06378-z

26. Livak KJ, Schmittgen TD. Analysis of relative gene expression data using real-time quantitative PCR and the 2(-delta delta C(T)) method. *Methods* (2001) 25 (4):402–8. doi: 10.1006/meth.2001.1262

27. Voelter W, Zech K, Arnold P, Ludwig G. Determination of selected pyrimidines, purines and their metabolites in serum and urine by reversed-phase ion-pair chromatography. *J Chromatogr* (1980) 199:345–54. doi: 10.1016/s0021-9673(01)91386-x

28. Kazmierski J, Friedmann K, Postmus D, Fischer C, Jansen J, Richter A, et al. Non-productive exposure of PBMCs to SARS-CoV-2 induces cell-intrinsic innate immunity responses. *bioRxiv* (2022) 18(8):e10961. doi: 10.1101/2022.02.15.480527

29. Butler A, Hoffman P, Smibert P, Papalexi E, Satija R. Integrating single-cell transcriptomic data across different conditions, technologies, and species. *Nat Biotechnol* (2018) 36(5):411–20. doi: 10.1038/nbt.4096

30. Marimuthu AK, Anandhan M, Sundararajan L, Chandrasekaran J, Ramakrishnan B. Utility of various inflammatory markers in predicting outcomes of hospitalized patients with COVID-19 pneumonia: A single-center experience. *Lung India* (2021) 38(5):448–53. doi: 10.4103/lungindia.lungindia_935_20

31. Samprathi M, Jayashree M. Biomarkers in COVID-19: An up-To-Date review. *Front Pediatr* (2020) 8:607647. doi: 10.3389/fped.2020.607647

32. Clayton A, Al-Taei S, Webber J, Mason MD, Tabi Z. Cancer exosomes express CD39 and CD73, which suppress T cells through adenosine production. *J Immunol* (2011) 187(2):676–83. doi: 10.4049/jimmunol.1003884

33. Zacca ER, Amezcua Vesely MC, Ferrero PV, Acosta CDV, Ponce NE, Bossio SN, et al. B cells from patients with rheumatoid arthritis show conserved CD39-mediated regulatory function and increased CD39 expression after positive response to therapy. *J Mol Biol* (2021) 433(1):166687. doi: 10.1016/j.jmb.2020.10.021

34. de Leve S, Wirsdörfer F, Jendrossek V. Targeting the immunomodulatory CD73/Adenosine system to improve the therapeutic gain of radiotherapy. *Front Immunol* (2019) 10:698. doi: 10.3389/fimmu.2019.00698

35. Savio LEB, Leite-Aguiar R, Alves VS, Coutinho-Silva R, Wyse ATS. Purinergic signaling in the modulation of redox biology. *Redox Biol* (2021) 47:102137. doi: 10.1016/j.redox.2021.102137

36. Saze Z, Schuler PJ, Hong CS, Cheng D, Jackson EK, Whiteside TL. Adenosine production by human b cells and b cell-mediated suppression of activated T cells. *Blood* (2013) 122(1):9–18. doi: 10.1182/blood-2013-02-482406

37. Ohta A, Sitkovsky M. Role of G-protein-coupled adenosine receptors in downregulation of inflammation and protection from tissue damage. *Nature* (2001) 414(6866):916–20. doi: 10.1038/414916a

38. Flögel U, Burghoff S, van Lent PL, Temme S, Galbarz L, Ding Z, et al. Selective activation of adenosine A2A receptors on immune cells by a CD73-dependent prodrug suppresses joint inflammation in experimental rheumatoid arthritis. *Sci Transl Med* (2012) 4(146):146ra108. doi: 10.1126/scitranslmed.3003717

39. Németh ZH, Leibovich SJ, Deitch EA, Sperlágh B, Virág L, Vizi ES, et al. Adenosine stimulates CREB activation in macrophages *via* a p38 MAPK-mediated mechanism. *Biochem Biophys Res Commun* (2003) 312(4):883–8. doi: 10.1016/j.bbrc.2003.11.006

40. Salvi V, Nguyen HO, Sozio F, Schioppa T, Laffranchi M, Scapini P, et al. SARS-CoV-2-associated ssRNAs activate inflammation and immunity *via* TLR7/8. *BioRxiv* (2021) 6(18):e150542. doi: 10.1101/2021.04.15.439839

41. Antonioli L, Pacher P, Vizi ES, Haskó G. CD39 and CD73 in immunity and inflammation. *Trends Mol Med* (2013) 19(6):355–67. doi: 10.1016/j.molmed.2013.03.005

42. Bastid J, Cottalorda-Regairaz A, Alberici G, Bonnefoy N, Eliaou JF, Bensussan A. ENTPD1/CD39 is a promising therapeutic target in oncology. *Oncogene* (2013) 32(14):1743–51. doi: 10.1038/onc.2012.269

43. Gupta PK, Godec J, Wolski D, Adland E, Yates K, Pauken KE, et al. CD39 expression identifies terminally exhausted CD8+ T cells. *PloS Pathog* (2015) 11(10): e1005177. doi: 10.1371/journal.ppat.1005177

44. Zheng Y, Li Y, Tang B, Zhao Q, Wang D, Liu Y, et al. IL-6-induced CD39 expression on tumor-infiltrating NK cells predicts poor prognosis in esophageal squamous cell carcinoma. *Cancer Immunol Immunother* (2020) 69(11):2371–80. doi: 10.1007/s00262-020-02629-1

45. Raczkowski F, Rissiek A, Ricklefs I, Heiss K, Schumacher V, Wundenberg K, et al. CD39 is upregulated during activation of mouse and human T cells and attenuates the immune response to listeria monocytogenes. *PloS One* (2018) 13(5): e0197151. doi: 10.1371/journal.pone.0197151

46. Shevchenko I, Mathes A, Groth C, Karakhanova S, Müller V, Utikal J, et al. Enhanced expression of CD39 and CD73 on T cells in the regulation of anti-tumor immune responses. *Oncoimmunology* (2020) 9(1):1744946. doi: 10.1080/2162402X.2020.1744946

47. Huang C, Wang Y, Li X, Ren L, Zhao J, Hu Y, et al. Clinical features of patients infected with 2019 novel coronavirus in wuhan, China. *Lancet* (2020) 395 (10223):497–506. doi: 10.1016/S0140-6736(20)30183-5

48. Rubin EJ, Longo DL, Baden LR. Interleukin-6 receptor inhibition in covid-19 - cooling the inflammatory soup. *N Engl J Med* (2021) 384(16):1564–5. doi: 10.1056/NEJMe2103108

49. Cecchini R, Cecchini AL. SARS-CoV-2 infection pathogenesis is related to oxidative stress as a response to aggression. *Med Hypotheses* (2020) 143:110102. doi: 10.1016/j.mehy.2020.110102

50. Laforge M, Elbim C, Frère C, Hémadi M, Massaad C, Nuss P, et al. Tissue damage from neutrophil-induced oxidative stress in COVID-19. *Nat Rev Immunol* (2020) 20(9):515–6. doi: 10.1038/s41577-020-0407-1

51. Cao X. COVID-19: immunopathology and its implications for therapy. *Nat Rev Immunol* (2020) 20(5):269–70. doi: 10.1038/s41577-020-0308-3

52. Liu K, Chen Y, Lin R, Han K. Clinical features of COVID-19 in elderly patients: A comparison with young and middle-aged patients. *J Infect* (2020) 80(6): e14–8. doi: 10.1016/j.jinf.2020.03.005

53. Schneider E, Rissiek A, Winzer R, Puig B, Rissiek B, Haag F, et al. Generation and function of non-cell-bound CD73 in inflammation. *Front Immunol* (2019) 10:1729. doi: 10.3389/fimmu.2019.01729

54. Avila-Mesquita CD, Couto AES, Campos LCB, Vasconcelos TF, Michelon-Barbosa J, Corsi CAC, et al. MMP-2 and MMP-9 levels in plasma are altered and associated with mortality in COVID-19 patients. *BioMed Pharmacother* (2021) 142:112067. doi: 10.1016/j.biopha.2021.112067

55. Gelzo M, Cacciapuoti S, Pinchera B, De Rosa A, Cernera G, Scialò F, et al. Matrix metalloproteinases (MMP) 3 and 9 as biomarkers of severity in COVID-19 patients. *Sci Rep* (2022) 12(1):1212. doi: 10.1038/s41598-021-04677-8

56. Davey A, McAuley DF, O'Kane CM. Matrix metalloproteinases in acute lung injury: mediators of injury and drivers of repair. *Eur Respir J* (2011) 38 (4):959–70. doi: 10.1183/09031936.00032111

57. Zhang W, Zhou S, Liu G, Kong F, Chen S, Yan H. Multiple steps determine CD73 shedding from RPE: lipid raft localization, ARA1 interaction, and MMP-9 up-regulation. *Purinergic Signal* (2018) 14(4):443–57. doi: 10.1007/s11302-018-9628-1

58. Zhou Y, Fu B, Zheng X, Wang D, Zhao C, Qi Y, et al. Aberrant pathogenic GM-CSF + T cells and inflammatory CD14 + CD16 + monocytes in severe pulmonary syndrome patients of a new coronavirus. *biorxiv* (2020) 7(6):998–1002. doi: 10.1101/2020.02.12.945576

59. Kim ES, Ackermann C, Tóth I, Dierks P, Eberhard JM, Wroblewski R, et al. Down-regulation of CD73 on b cells of patients with viremic HIV correlates with b cell activation and disease progression. *J Leukoc Biol* (2017) 101(5):1263–71. doi: 10.1189/jlb.5A0816-346R

60. Schena F, Volpi S, Faliti CE, Penco F, Santi S, Proietti M, et al. Dependence of immunoglobulin class switch recombination in b cells on vesicular release of ATP and CD73 ectonucleotidase activity. *Cell Rep* (2013) 3(6):1824–31. doi: 10.1016/j.celrep.2013.05.022

61. Basu U, Chaudhuri J, Alpert C, Dutt S, Ranganath S, Li G, et al. The AID antibody diversification enzyme is regulated by protein kinase a phosphorylation. *Nature* (2005) 438(7067):508–11. doi: 10.1038/nature04255

62. da Silva GB, Manica D, da Silva AP, Kosvoski GC, Hanauer M, Assmann CE, et al. High levels of extracellular ATP lead to different inflammatory responses in COVID-19 patients according to the severity. *J Mol Med (Berl)* (2022) 100 (4):645–63. doi: 10.1007/s00109-022-02185-4

63. Díaz-García E, García-Tovar S, Alfaro E, Zamarrón E, Mangas A, Galera R, et al. Role of CD39 in COVID-19 severity: Dysregulation of purinergic signaling and thromboinflammation. *Front Immunol* (2022) 13:847894. doi: 10.3389/fimmu.2022.847894

64. Pétrilli V, Dostert C, Muruve DA, Tschopp J. The inflammasome: a danger sensing complex triggering innate immunity. *Curr Opin Immunol* (2007) 19 (6):615–22. doi: 10.1016/j.coi.2007.09.002

65. Muñoz-Planillo R, Kuffa P, Martínez-Colón G, Smith BL, Rajendiran TM, Núñez G. K^+ efflux is the common trigger of NLRP3 inflammasome activation by bacterial toxins and particulate matter. *Immunity* (2013) 38(6):1142–53. doi: 10.1016/j.immuni.2013.05.016

66. Ferreira AC, Soares VC, de Azevedo-Quintanilha IG, Dias SDSG, Fintelman-Rodrigues N, Sacramento CQ, et al. SARS-CoV-2 engages inflammasome and pyroptosis in human primary monocytes. *Cell Death Discov* (2021) 7(1):43. doi: 10.1038/s41420-021-00428-w

67. Rodrigues TS, de Sá KSG, Ishimoto AY, Becerra A, Oliveira S, Almeida L, et al. Inflammasomes are activated in response to SARS-CoV-2 infection and are associated with COVID-19 severity in patients. *J Exp Med* (2021) 218(3): e20201707. doi: 10.1084/jem.20201707

68. Idzko M, Dichmann S, Panther E, Ferrari D, Herouy Y, Virchow C, et al. Functional characterization of P2Y and P2X receptors in human eosinophils. *J Cell Physiol* (2001) 188(3):329–36. doi: 10.1002/jcp.1129

69. Idzko M, Dichmann S, Ferrari D, Di Virgilio F, la Sala A, Girolomoni G, et al. Nucleotides induce chemotaxis and actin polymerization in immature but not mature human dendritic cells *via* activation of pertussis toxin-sensitive P2y receptors. *Blood* (2002) 100(3):925–32. doi: 10.1182/blood.v100.3.925

70. Chen Y, Corriden R, Inoue Y, Yip L, Hashiguchi N, Zinkernagel A, et al. ATP release guides neutrophil chemotaxis *via* P2Y2 and A3 receptors. *Science* (2006) 314(5806):1792–5. doi: 10.1126/science.1132559

71. Lappas CM, Sullivan GW, Linden J. Adenosine A2A agonists in development for the treatment of inflammation. *Expert Opin Investig Drugs* (2005) 14(7):797–806. doi: 10.1517/13543784.14.7.797

72. Erdmann AA, Gao ZG, Jung U, Foley J, Borenstein T, Jacobson KA, et al. Activation of Th1 and Tc1 cell adenosine A2A receptors directly inhibits IL-2 secretion *in vitro* and IL-2-driven expansion in vivo. *Blood* (2005) 105(12):4707–14. doi: 10.1182/blood-2004-04-1407

73. Csóka B, Németh ZH, Virág L, Gergely P, Leibovich SJ, Pacher P, et al. A2A adenosine receptors and C/EBPbeta are crucially required for IL-10 production by macrophages exposed to escherichia coli. *Blood* (2007) 110(7):2685–95. doi: 10.1182/blood-2007-01-065870

74. Koscsó B, Csóka B, Selmeczy Z, Himer L, Pacher P, Virág L, et al. Adenosine augments IL-10 production by microglial cells through an A2B adenosine receptor-mediated process. *J Immunol* (2012) 188(1):445–53. doi: 10.4049/jimmunol.1101224

75. Németh ZH, Lutz CS, Csóka B, Deitch EA, Leibovich SJ, Gause WC, et al. Adenosine augments IL-10 production by macrophages through an A2B receptor-mediated posttranscriptional mechanism. *J Immunol* (2005) 175(12):8260–70. doi: 10.4049/jimmunol.175.12.8260

76. Del Valle DM, Kim-Schulze S, Huang HH, Beckmann ND, Nirenberg S, Wang B, et al. An inflammatory cytokine signature predicts COVID-19 severity and survival. *Nat Med* (2020) 26(10):1636–43. doi: 10.1038/s41591-020-1051-9

77. Mann BJ, Chhabra P, Ma M, Brovero SG, Jones MK, Linden J, et al. Adenosine A2A receptor (A2AR) agonists improve survival in K28-hACE2 mice following SARS CoV-2 infection. *bioRxiv* (2022). doi: 10.1101/2022.02.25.481997

78. Correale P, Caracciolo M, Bilotta F, Conte M, Cuzzola M, Falcone C, et al. Therapeutic effects of adenosine in high flow 21% oxygen aereosol in patients with Covid19-pneumonia. *PloS One* (2020) 15(10):e0239692. doi: 10.1371/journal.pone.0239692

79. Caracciolo M, Correale P, Mangano C, Foti G, Falcone C, Macheda S, et al. Efficacy and effect of inhaled adenosine treatment in hospitalized COVID-19 patients. *Front Immunol* (2021) 12:613070. doi: 10.3389/fimmu.2021.613070

80. Guirland C, Buck KB, Gibney JA, DiCicco-Bloom E, Zheng JQ. Direct cAMP signaling through G-protein-coupled receptors mediates growth cone attraction induced by pituitary adenylate cyclase-activating polypeptide. *J Neurosci* (2003) 23(6):2274–83. doi: 10.1523/JNEUROSCI.23-06-02274.2003

frontiers | Frontiers in Immunology

TYPE Original Research
PUBLISHED 07 October 2022
DOI 10.3389/fimmu.2022.1034379

OPEN ACCESS

EDITED BY
Juan Pablo de Rivero Vaccari,
University of Miami, United States

REVIEWED BY
Laurence Corash,
Cerus, United States
Silvano Wendel,
Hospital Sirio Libanes, Brazil

*CORRESPONDENCE
Fabrice Cognasse
fabrice.cognasse@efs.sante.fr

SPECIALTY SECTION
This article was submitted to Inflammation, a section of the journal Frontiers in Immunology

RECEIVED 01 September 2022
ACCEPTED 20 September 2022
PUBLISHED 07 October 2022

CITATION
Cognasse F, Hamzeh-Cognasse H, Duchez A-C, Shurko N, Eyraud M-A, Arthaud C-A, Prier A, Heestermans M, Hequet O, Bonneaudeau B, Rochette-Eribon S, Teyssier F, Barlet-Excoffier V, Chavarin P, Legrand D, Richard P, Morel P, Mooney N and Tiberghien P (2022) Inflammatory profile of convalescent plasma to treat COVID: impact of amotosalen/UVA pathogen reduction technology. *Front. Immunol.* 13:1034379. doi: 10.3389/fimmu.2022.1034379

Inflammatory profile of convalescent plasma to treat COVID: Impact of amotosalen/UVA pathogen reduction technology

Fabrice Cognasse[1,2]*, Hind Hamzeh-Cognasse[2], Anne-Claire Duchez[1,2], Natalia Shurko[3], Marie-Ange Eyraud[1,2], Charles-Antoine Arthaud[1,2], Amélie Prier[1,2], Marco Heestermans[1,2], Olivier Hequet[1,4], Brigitte Bonneaudeau[5], Sandrine Rochette-Eribon[1], Françoise Teyssier[1], Valérie Barlet-Excoffier[1], Patricia Chavarin[1], Dominique Legrand[1], Pascale Richard[5], Pascal Morel[5,6], Nuala Mooney[7] and Pierre Tiberghien[5,6]

[1]Etablissement Français du Sang Auvergne-Rhône-Alpes, Saint-Étienne, France, [2]Université Jean Monnet, Mines Saint-Étienne, INSERM (Institut National de la Santé et de la Recherche Médicale), U 1059 Sainbiose, (SAnté INgéniérie BIOlogie St-Etienne), Saint-Étienne, France, [3]Institute of Blood Pathology and Transfusion Medicine NAMS (National Academy of Medical Sciences) of Ukraine, Lviv, Ukraine, [4]CIRI, International Center for Infectiology Research, INSERM (Institut National de la Santé et de la Recherche Médicale) U1111, Université de Lyon, Lyon, France, [5]Etablissement Français du Sang, La Plaine St Denis, France, [6]UMR (Unité mixte de recherche) RIGHT U1098, INSERM, Etablissement Français du Sang, Université de Franche-Comté, Besançon, France, [7]Human Immunology, Pathophysiology and Immunotherapy, INSERM (Institut National de la Santé et de la Recherche Médicale) U976, Paris, France

Blood products in therapeutic transfusion are now commonly acknowledged to contain biologically active constituents during the processes of preparation. In the midst of a worldwide COVID-19 pandemic, preliminary evidence suggests that convalescent plasma may lessen the severity of COVID-19 if administered early in the disease, particularly in patients with profound B-cell lymphopenia and prolonged COVID-19 symptoms. This study examined the influence of photochemical Pathogen Reduction Treatment (PRT) using amotosalen-HCl and UVA light in comparison with untreated control convalescent plasma (n= 72 – paired samples) - cFFP, regarding soluble inflammatory factors: sCD40L, IFN-alpha, IFN-beta, IFN-gamma, IL-1 beta, IL-6, IL-8, IL-10, IL-18, TNF-alpha and *ex-vivo* inflammatory bioactivity on endothelial cells. We didn't observe significant modulation of the majority of inflammatory soluble factors (8 of 10 molecules tested) pre- or post-PRT. We noted that IL-8 concentrations were significantly decreased in cFFP with PRT, whereas the IL-18 concentration was increased by PRT. In contrast, endothelial cell release of IL-6 was similar whether cFFP was pre-treated with or without PRT. Expression of CD54 and CD31 in the presence of cFFP

were similar to control levels, and both were significant decreased in when cFFP had been pre-treated by PRT. It will be interesting to continue investigations of IL-18 and IL-8, and the physiopathological effect of PRT- treated convalescent plasma and in clinical trials. But overall, it appears that cFFP post-PRT were not excessively pro-inflammatory. Further research, including a careful clinical evaluation of CCP-treated patients, will be required to thoroughly define the clinical relevance of these findings.

KEYWORDS

COVID-19, convalescent plasma, inflammation, cytokine, endothelial cell

Introduction

In order to improve the survival of COVID-19 patients with extreme acute respiratory syndromes of viral etiology, convalescent plasma therapy, *i.e.* passive polyclonal antibody administration to provide immediate immunity has been used (1). Patients who have recovered from COVID-19 and have a high plasma titer of neutralizing antibody may be a valuable source of convalescent plasma. Nevertheless, a therapeutic strategy in COVID-19 has not yet been tested regarding the balance between possible clinical advantages and the risks of convalescent blood product transfusion. Moreover, the potential association between the effectiveness of convalescent plasma and the inflammatory characteristics of this plasma has never been established, to our knowledge. Cytokines and/or chemokines are potent modulators of many immune response characteristics including inflammation. Such molecules are major inflammatory response effectors and regulators, which influence immune cell function (2). Inflammatory cytokines/chemokines also interfere with coagulation by fostering a pro-coagulant state that maintains inflammation (3). Plasma transfusion can modulate innate immune responses; however, the immunomodulatory capacity of various plasma products is little understood. Considering that most previous immune modulation research centered on red blood cell products or platelet concentrates linked to transfusion, even less is known about the immunomodulatory effects of plasma products (4, 5).

Although not completely understood, the pathological mechanisms underlying lung injury following the transfusion of Fresh Frozen Plasma (FFP) are thought to result from an inflammatory response involving neutrophil infiltration into the lungs and elevated interleukin (IL)-8 and IL-1 pulmonary levels, as observed in TRALI patients (6, 7). Several studies have shown that pathogen reduction technologies reduced the potential risk of transfusion-transmitted infections (8, 9), still, to our knowledge, convalescent plasma (cFFP) and the inflammatory properties of this plasma have not been investigated. Therefore, in the perspective of a therapeutic strategy in COVID-19, it is essential to characterize precisely the pro-inflammatory content and ability of plasmas that will be transfused to patients, in addition to determining the neutralizing antibody capacity of these plasmas.

Material and methods

Donor recruitment and sample collection

Convalescent patients eligible for plasma donation were asked to undergo plasma apheresis, as described recently (10). In France, plasma collection is recommended no earlier than 14 to 28 days after symptom resolution and plasma for transfusion currently undergoes pathogen reduction or quarantine. Once treated and qualified, plasma was cryopreserved (in 200–250 ml units) and made available for clinical use. Anti–SARS-CoV-2 antibody content was assessed in each donation, with a requirement for a SARS-CoV-2 seroneutralization titer of ≥ 40 and/or an immunoglobulin G (IgG) enzyme-linked immunosorbent assay (EUROIMMUN, Bussy-Saint-Martin, France) ratio > 5.6 (11). cFFP (n=72) units were produced in one regional center of the National Blood Service (EFS Auvergne-Rhône-Alpes). cFFP were collected from anonymous regular blood donors who had accepted, after receiving specific information, that their blood samples be used for research purposes and had signed a consent form approved by the regulatory authorities. Written informed consent was obtained from all the patients or their trusted persons. Data collection from the PLASMACOV cohort was approved by the French national ethics committee (2020-A00728-31) (12, 13). Apheresis was carried out using a plasma collection system (Auto-C or Aurora, Fresenius Kabi, BadHomburg, Germany) containing the anticoagulant Citrate Dextrose Solution (ACD, Macopharma, Tourcoing, France). After a leukofiltration step, a sample (2 mL) of each unit of convalescent plasma without pathogen reduction

technology (PRT - INTERCEPT Blood System - Cerus Corp, Concord, CA) was aliquoted. A 2 mL sample of the same cFFP that met treatment criteria for amotosalen/UVA-PRT was used for pathogen reduction according to the manufacturers instructions (14). Before and after PRT treatment, samples of each cFFP were stored at -80°C before use.

Soluble inflammatory factor assays in cFFP

Levels of various soluble inflammatory factors (sCD40 Ligand, IFN-alpha, IFN-beta, IFN-gamma, IL-1 beta, IL-6, IL-8, IL-10, IL-18, and TNF-alpha) were quantified in cFFP with or without PRT using Luminex Technology, according to the manufacturer's instructions (Bio-Techne, Minneapolis, US). Absorbance at 450 nm was determined using an enzyme-linked immunosorbent assay reader (Magellan Sunrise software, Tecan Group Ltd., Lyon, France).

EA.hy926: Endothelial cell culture

EA.hy926 is a permanent cell line derived by fusing human umbilical vein endothelial cells (HUVEC) with the cell line A549 (15). The EA.hy926 cell line was obtained from the American Type Culture Collection (ATCC, Manassas, Virginia, USA). EA.hy926 was cultured as described (16) in 6-well and 96-well plates in order to obtain approximately 10^6 cells/ml. The cell number was quantified with a TC10 Automated Cell Counter (Bio-Rad, Marnes-la-Coquette, France). Cells were grown until confluent then passaged with 0.25% trypsin (Sigma-Aldrich, Saint-Quentin-Fallavier, France).

Stimulation of EA.hy926

EA.hy926 endothelial cells were cultured in 6- ($1x10^6$ cells/well) or 96-well plates ($5x10^4$cells/well) and grown for 48 hours to reach confluence prior to the experiment. Confluent endothelial monolayers were washed and incubated for 24 hours at 37°C and underwent the following treatments: control wells were incubated with DMEM only, test wells with convalescent FFP with or without PRT diluted at 1/5 in DMEM, and positive control wells were stimulated by recombinant human TNF-alpha (PeproTech, Neuilly-sur-Seine, France) at a final concentration of 100 pg/ml. After 24 hours of incubation, supernatants were recovered and frozen at -80°C. After washing in phosphate buffered saline (PBS), the cells were centrifuged for 5 minutes at 300 g and 22°C. The EA.hy926 Endothelial cells pellets were resuspended in 1% paraformaldehyde in PBS for 30 minutes and then washed. The fixed cells were resuspended in PBS for further analyses as described below.

Flow cytometry analyses

The surface phenotype of EA.hy926 endothelial cells was determined by flow cytometry. Cells were fixed as described above. Direct labelling was performed for the following markers: endoglin/CD105 (BD Biosciences, Le Pont de Claix, France), ICAM-1/CD54 (BD Biosciences, Le Pont de Claix, France), and Platelet endothelial cell adhesion molecule PECAM1/CD31 (BD Biosciences, Le Pont de Claix, France). The cells were incubated for 30 minutes with antibodies. In all experiments, background labelling was assessed using the relevant fluorochrome-conjugated mouse IgG isotype control (BD Biosciences, Le Pont de Claix, France). Cells were centrifuged at 300 g for 5 minutes at 22°C then washed in PBS. Data acquisition was performed using a Guava easyCyte HT Flow Cytometer (Merck Millipore, Molsheim, France) and analysis carried out using the Incyte program. At least 10,000 events were collected for each sample.

Endothelial cell IL-6 quantification

The production of soluble cytokines in culture supernatants of EA.hy926 Endothelial cells both stimulated and not stimulated by convalescent plasma or not was measured using the specific enzyme-linked immunosorbent assays (ELISA). Interleukin-6 levels (DuoSet) were measured by commercial ELISA kit (DuoSet - R&D Systems, Lille, France) according to the manufacturer's instructions. Absorbance at 450 nm was determined with an ELISA reader (Magellan Sunrise software, Tecan Group Ltd., Lyon, France).

Statistical analysis

The data was not normally distributed. The results were presented as scatter dot plots and red lines show the median of raw data. Statistical analysis was performed using paired t-tests (GraphPad™, La Jolla, CA). Statistically significant differences required a p value < 0.05 (*p<0.05, **p<0.01, ***p<0.001). Group comparisons were made using a one-way analysis of variance (ANOVA) followed by a Kruskal-Wallis test and a Dunn's post-test. The two-tailed t-test and Mann-Whitney test were used to compare two groups (GraphPad Software, La Jolla, California, USA).

Results and discussion

Contents of sCD40 Ligand (A), IFN-alpha (B), IFN-beta (C), IFN-gamma (D), IL-1 beta (E), IL-6 (F), IL-10 (G) and TNF-alpha (H) in cFFP with PRT were not significantly different ($P > 0.05$) from untreated FFP (without PRT) (Table 1) - (Figures 1A–H), contrary to IL-8 (Figure 1I) and IL-18 (Figure 1J). Although the values are relatively low, we observed a significantly higher concentration of IL-8 in convalescent FFP without PRT compared to with PRT, respectively 0.9501 ± 2.012 vs. 0.4664 ± 2.203 pg/mL, this may indicate a less inflammatory plasma preparation after PRT treatment. In contrast, a significantly higher concentration of IL-18 is observed in convalescent FFP with PRT compared to without PRT; 258.1 ± 127.5 pg/mL vs. 207.6 ± 96.25 pg/mL respectively).

One limit of this study concerns the high cytokine profile heterogeneity. Interpretation of cytokine data in such studies is frequently made by comparing the mean levels in several experimental conditions. Our data show that the mean and median values are different. Outliers affect the mean value of the data but have little effect on the median or mode of a given set of data. Analysis of the outlier cFFPs with or without PRT could be interesting, particularly in a clinical context. Finally, clinical aspects were less detailed in our study but efficacy of Convalescent Plasma to Treat COVID-19 Patients, a Nested Trial in the CORIMUNO-19 Cohort (CORIPLASM) (NCT04345991) is under analysis.

Production of IL-6 by endothelial cells has been widely documented in pro-inflammatory environments. We therefore examined Il-6 release after endothelial cell activation with cFFP. We did not observe any PRT-related modulation of IL-6 release (n=72), in contrast to IL-6 levels activated by TNF-α stimulation (n=12) (Figure 2A).

To further evaluate the effect of cFFP with or without PRT treatment (n=72) on endothelial cells, plasma was added to EA.hy926 cell cultures and membrane expression of adhesion molecules was then evaluated. The percentage expression of CD105 (data not shown) was unchanged in the presence of cFFP with or without PRT treatment or by recombinant human TNF-α at a final concentration of 100 pg/ml (n=12).

CD54 (Figure 2B) and CD31 (Figure 2C) two crucial endothelial cell adhesion molecules, that are implicated in endothelial permeability, and transendothelial leukocyte migration had similar expression levels as in controls. We did not observe significant modulation of CD54 in the presence of cFFP with or without PRT treatment compared to unstimulated EA.hy926 cells. However, expression of CD31 was significantly increased in the presence of cFFP with or without PRT treatment compared to unstimulated EA.hy926 cells, respectively $p=0.207$ and $p<0.0001$ (Figure 2C). Furthermore, both CD54 and CD31 expression were significantly decreased by exposure to cFFP that had undergone PRT treatment (Figure 2C). As expected, TNF-α stimulation reduced the expression of PECAM-1 (CD31). This molecule is highly implicated in the process of trans-endothelial-migration [reviewed in (17) and (18)]. Moreover, as previously reported, TNF-α stimulation increased the expression of ICAM (CD54) (19) (Figures 2B, C). Biological response modifiers (BRMs), such as anti-microparticles, lipids, and cytokines/chemokines, and particularly sCD40L, have been linked to inflammatory Serious Adverse Reactions (SARs), such as Transfusion-related acute lung injury (TRALI). sCD40L is a platelet-derived proinflammatory mediator that accumulates during platelet concentrate or FFP storage. Because COVID-19 patients are more likely to develop Acute Respiratory Distress Syndrome (ARDS), the absence of significant modulation of sCD40L in cFFP with PRT was reassuring.

Treatment of cFFP by PRT clearly increased levels of the pro-inflammatory cytokine IL-18. Serum IL-18 levels in healthy subjects ranged from 80 to 120 pg/mL (20). An increase of IL-18 concentration has been observed in the serum of i) adult and pediatric patients with Crohn's disease (21) (in the order of 400 pg/mL), ii) patients with coronary artery disease (22, 23) (in the range of 70 to 300 pg/mL) an iii) patients with ARDS (in the order of 600 pg/mL), and correlated with severity score and death (24). In the light of these studies, clinical research will be performed to evaluate the transfusion efficacy related to the transfusion of convalescent or non-convalescent plasma as a therapeutic support in ARDS patients.

In the context of COVID-19, Zachary B Zalinger et al. suggested that inflammasome signaling is largely protective in murine coronavirus infection, largely due to the pro-inflammatory effects of IL-18 (25). However, another report noted significantly elevated levels of IL-18 in the plasma of COVID-19 patients (26). The levels of other inflammatory cytokines/chemokines IL-1b, IL-1RA, IL-6, IL-8, IL-18 and TNFα were not higher in critically ill patients with COVID-19 than in critically ill patients admitted for ARDS or sepsis (27). Finally, although high concentrations of cytokines/chemokines have been widely described in COVID-19 patients, the vast majority (including IL-6, IL-10, IL-18, CTACK and IFN-γ) do not appear to be prognostic, as they do not always differentiate between moderate and severe cases (28). In a model of the immune cell interaction between DC and B cells in COVID-19 patients, IL-18 was found to be critical for antibody production by B cells, suggesting its importance in recovery (29). It will be interesting to see whether IL-18 present in convalescent plasma correlates with plasma titers of neutralizing antibody.

Convalescent plasma from recovered COVID-19 patients contain neutralizing antibodies against the spike protein of SARS CoV-2, which may benefit severely sick COVID-19 patients by neutralizing the virus and halting its replication in the host. Early administration of high-titer convalescent plasma against SARS-CoV-2 to mildly ill infected older adults reduced the progression of Covid-19. The use of inflammatory convalescent plasma to treat COVID-19 may be an interesting approach that has not yet been fully studied and may potentially increase the efficacy of transfusion.

The concentration of IL-8 in convalescent plasma with or without PRT treatment was low, with a median of 0 [0-15.40] and 0.32 [0-11.80] pg/mL respectively. In healthy subjects, the

TABLE 1 Descriptive statistic of database.

		Number of values	Minimum (pg/mL)	25% Percentile (pg/mL)	Median (pg/mL)	75% Percentile (pg/mL)	Maximum (pg/mL)	Range (pg/mL)	Mean (pg/mL)	Std. Deviation	Std. Error of Mean	Lower 95% CI of mean	Upper 95% CI of mean	Coefficient of variation
sCD40 Ligand	cFFP w PRT	72	0	0	108.5	198.9	1655	1655	**172.3**	256.3	30.2	112.1	232.6	148.7%
	cFFP w/o PRT	72	0	18.65	67.57	126.2	848	848	**112.3**	165.5	19.51	73.36	151.2	147.4%
IFN-alpha	cFFP w PRT	72	0	0	0	0.91	57.41	57.41	**1.692**	7.23	0.852	-0.0066	3.391	427.2%
	cFFP w/o PRT	72	0	0	0	0	30.38	30.38	**0.985**	4.396	0.518	-0.0478	2.018	446.2%
IFN-beta	cFFP w PRT	72	0	0	0	0	0.66	0.66	**0.0366**	0.152	0.017	0.0008	0.0724	415.2%
	cFFP w/o PRT	72	0	0	0	0	1.41	1,41	**0,0195**	0,166	0,019	-0,0194	0,0586	848,5%
IFN-gamma	cFFP w PRT	72	0	0	0	0,83	169,9	169,9	**13,86**	38,02	4,48	4,924	22,79	274,3%
	cFFP w/o PRT	72	0	0	0	0	90,79	90,79	**7,057**	19,51	2,299	2,473	11,64	276,4%
IL-1 beta	cFFP w PRT	72	0	0	0	0	33	33	**0,857**	4,422	0,521	-0,1821	1,896	516,0%
	cFFP w/o PRT	72	0	0	0	0	24,21	24,21	**0,757**	3,435	0,404	-0,0494	1,565	453,3%
IL-6	cFFP w PRT	72	0	0	0,1	1,168	4,28	4,28	**0,627**	0,943	0,111	0,4063	0,8495	150,2%
	cFFP w/o PRT	72	0	0	0	0,26	4,68	4,68	**0,413**	0,973	0,114	0,1844	0,6417	235,6%
IL-10	cFFP w PRT	72	0	0	0	0	18,03	18,03	**0,567**	2,425	0,285	-0.0018	1.138	427.0%
	cFFP w/o PRT	72	0	0	0	0	7.05	7.05	**0.418**	1.114	0.131	0.1571	0.6804	265.9%
TNF-alpha	cFFP w PRT	72	0	0	0	0.68	13.08	13.08	**0.776**	2.181	0.257	0.2638	1.289	280.9%
	cFFP w/o PRT	72	0	0	0.18	0.73	9.71	9.71	**0.779**	1.895	0.223	0.3343	1.225	243.1%
IL-8	cFFP w PRT	72	0	0	0	0	15.4	15.4	**0.466**	2.203	0.259	-0.0512	0.9841	472.3%
	cFFP w/o PRT	72	0	0	0.32	0.79	11.8	11.8	**0.950**	2.012	0.237	0.4773	1.423	211.8%
IL-18	cFFP w PRT	72	18.51	185.2	223.8	306.3	953.9	935.4	**258.1**	127.5	15.03	228.1	288	49.40%
	cFFP w/o PRT	72	30.51	155.5	184.5	240.6	726	695.5	**207.6**	96.25	11.34	185	230.2	46.36%

The Mean (pg/mL), a more significant variable is represented by the bold values.

10.3389/fimmu.2022.1034379

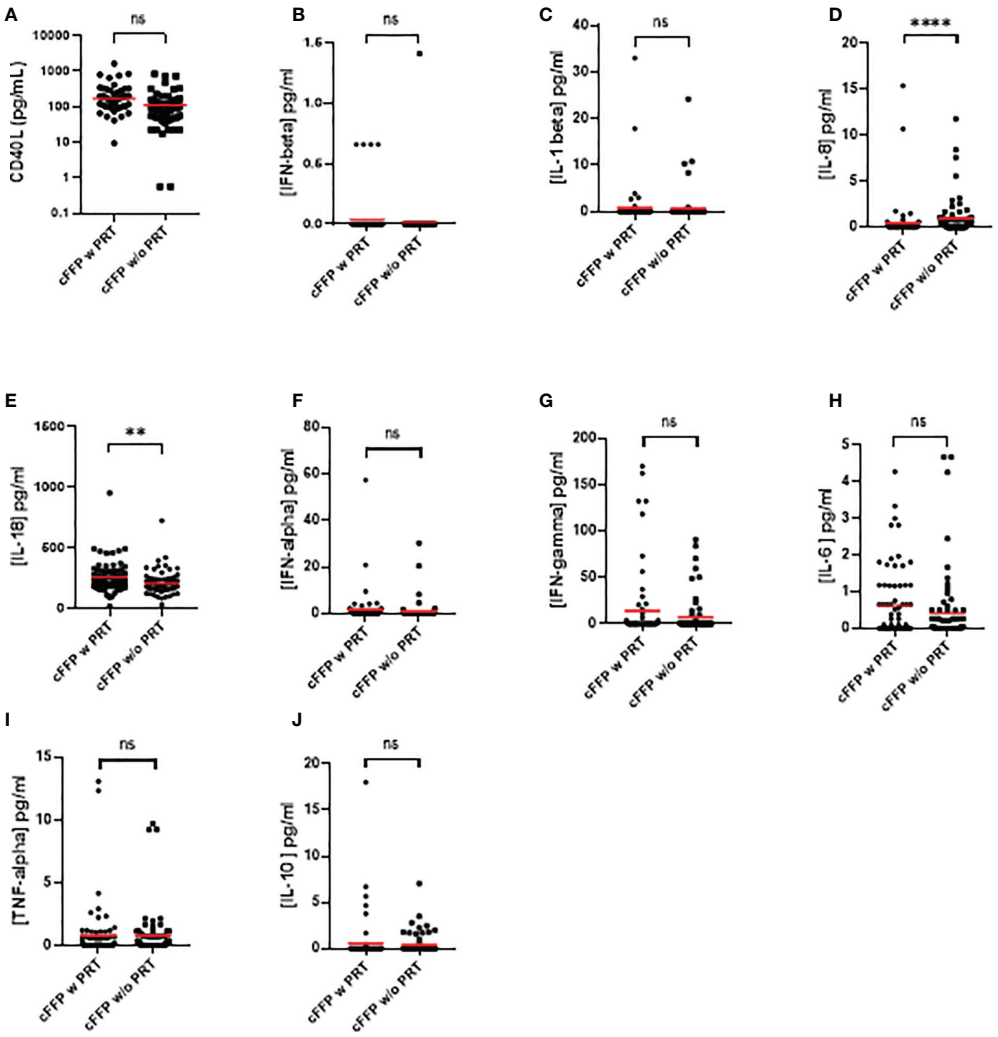

FIGURE 1
Quantification of soluble sCD40 Ligand **(A)**, IFN-alpha **(B)**, IFN-beta **(C)**, IFN-gamma **(D)**, IL-1 beta **(E)**, IL-6 **(F)**, IL-10 **(G)**, TNF-alpha **(H)**, IL-8 **(I)**, and IL-18 **(J)** in convalescent FFP (cFFP) with or without PRT. The concentration of soluble inflammatory factors was quantified by Luminex technology. Values shown are deducted from background levels. Data (Scatter plot and mean; n = 72 for each group. Significance between samples was assessed using a paired sample. P values < 0.05 were considered to be significant (ns, not significant; ** < 0.01; **** < 0.0001).

median serum IL-8 level was 87.45 pg/mL (5–7500), which exceeded the normal range (< 62 pg/mL) and indicated an increase in serum IL-8 level.

Anil Bagri et al. (30) measured the level of cytokines in CCP and the impact of Amotosalen/UVA pathogen reduction treatment (A/UVA-PRT), and compared Pre-PRT and Post-PRT levels using a highly sensitive and specific Luminex-based multiplexed cytokine panel. Concerning the common soluble inflammatory factors, TNF alpha, IL-6, IL-10, we did not observe significant modulation pre-PRT or post-PRT. Overall, Anil Bagri et al. (30) did not observe significant modulation of cytokines studied (in agreement with our study) including GM-CSF, Interleukin (IL)-2, IL-3, IL-4, IL-5, IL-7 and IL-17. We have reported similar results concerning sCD40 Ligand, IFN-alpha, IFN-beta, IFN-gamma, IL-1 beta, IL-6, IL-10 and TNF-alpha in cFFP with or without PRT. However, Anil Bagri et al. reported that PRT reduced the levels of all three pro-inflammatory cytokines (MIP-1β p, MCP-1 and IL-1β p), this is in keeping with our results concerning IL-8 (30).

There are several potential explanations for the higher IL-18 concentration detected in PRT cFFP i) the soluble IL-18Rα complex is composed of the soluble forms of the IL-18Rα and IL-18Rβ chains and binds IL-18. We can't exclude that PRT cFFP could decrease the cFFP concentration of the soluble IL-18R resulting in increased detection of free IL-18; ii) The sequestration of IL-18 by its soluble decoy receptor IL-18-Binding Protein (IL-18BP) is critical to the regulation of IL-18 activity and a similar mechanism could result in a decreased concentration of IL-18-BP in PRT cFFP leading to detection of higher levels of free IL-18. Finally, upon

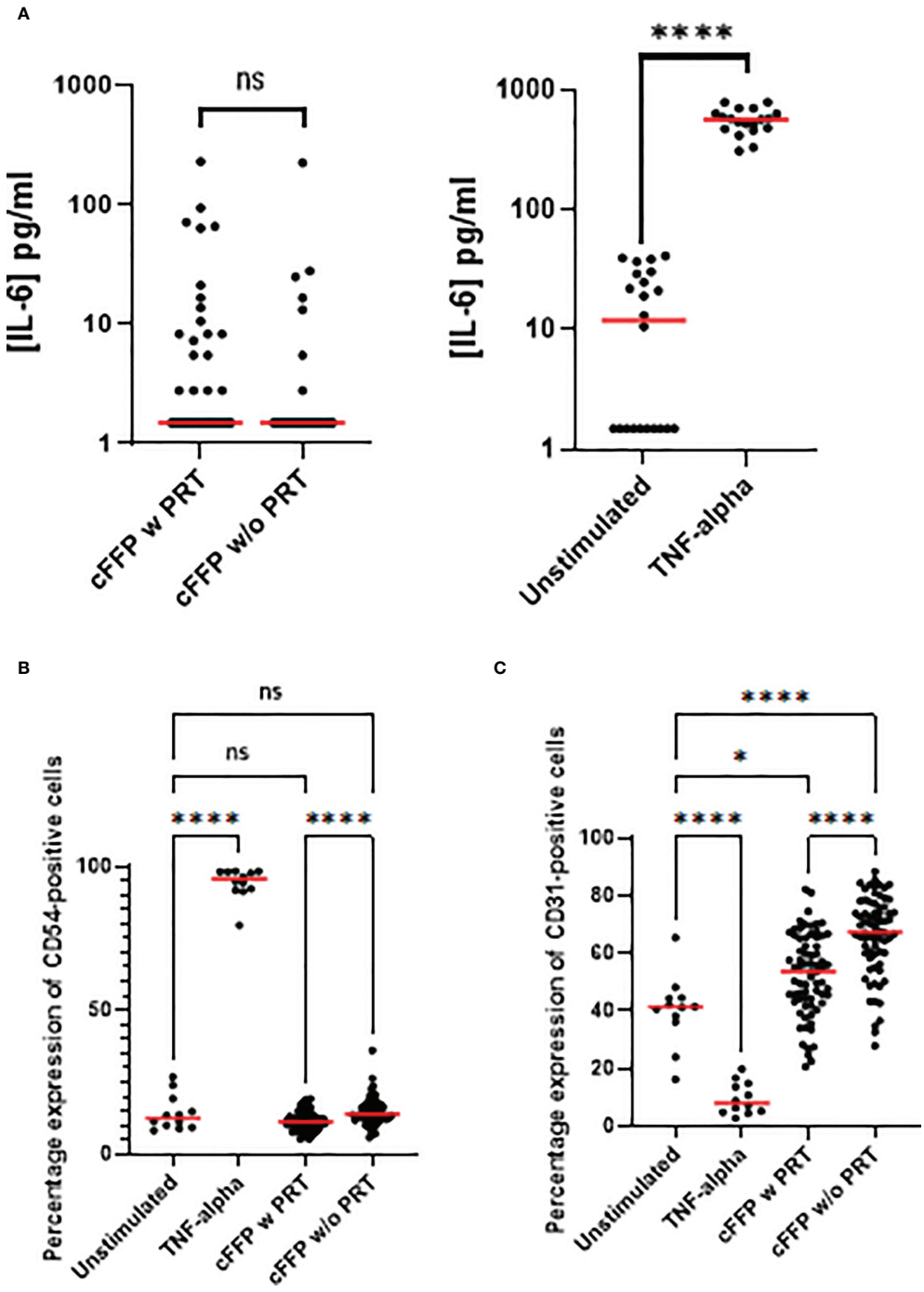

FIGURE 2
Endothelial cells (EA.hy926 cells) activation focusing on IL-6 release and on membrane expression. EA.hy926 cells were stimulated with convalescent FFP (cFFP) with (n = 72) - considered as the gold standard - or without PRT (n = 72). EA.hy926 cells were stimulated with negative and positive controls. TNF-α stimulation was considered the positive control (n = 18) and unstimulated EA.hy926 cells were viewed as the negative control (n = 19). Bioactivity in EA.hy926 endothelial cells was measured with IL-6 release **(A)**, with or without stimulation. Bioactivity in EA.hy926 endothelial cells was measured with FCM focusing on membrane expression of CD54 **(B)** and CD31 **(C)** with or without stimulation. Scatter dot plots represent the data, and the red line denotes the median of raw data. Statistical analyses were performed using one-way Anova with multiple comparisons (P-values<0.05 were considered significant; * < 0.05; **** < 0.0001).

exposure to UV radiation, both precursors (pro-IL-18) are cleaved by caspase-1. Caspase-1plays a major role in the cleavage of the IL-18 precursor, and we cannot exclude that PRT does not increase caspase-1 activity resulting in a higher IL-18 concentration in PRT cFFP.

Cytokines/chemokines have been considered individually and we can't exclude synergistic, antagonistic and additive effects also, the modulation of cytokine/chemokine concentration between the two conditions was noted but this was not reflected in their bioactivity on endothelial cells. IL-18 concentration was significantly elevated in cFFP PRT compared to cFFP w/o PRT, but this concentration is very low compared to that in serum samples from patients with COVID-19. Hospitalized. COVID-19 patients had higher IL-18 levels compared to healthy subjects (103 pg/mL vs. 310 pg/mL). Moreover, in the same report, the authors demonstrated that serum IL-18 concentrations are remarkably increased in patients with COVID-19 and correlated with other inflammatory markers and disease severity (31).

Moreover, this study examined whether convalescent plasma with or without PRT treatment modified the endothelial bioactivity. Concerning the EA.hy926 cell line, we did not observe any significant modulation of IL-6 release after activation with convalescent plasma with or without PRT treatment. Although CD54 expression in the presence of cFFP (with or without PRT treatment) remained close to control levels, expression was significantly decreased in the presence of cFFP pre-treated by PRT treatment. In contrast, CD31 expression was higher in endothelial cells treated by cFFP, importantly PRT treatment decreased the CD31 expression. Modulation of CD54 and/or CD31 may have important consequences because both CD54 have well-documented roles in the process of trans-endothelial-migration. This process has been intensely studied. Endothelial cell membrane CD54 has a role early in the transendothelial migration (TEM) of polymorphonuclear neutrophils and accumulates below the leukocyte in response to interactions with LFA-1 on the leukocyte. As TEM begins, ICAM-1 surrounds the leukocyte as it transmigrates. CD31 localizes both in the endothelial border and in Lateral Border recycling compartments LBRC and in the steady state 30% of total PECAM-1 is estimated to be within the LBRC. Endothelial CD31 is implicated in two critical and related signaling events in transmigration, by engaging in homotypic interactions with the leukocyte followed by a transient intracellular Ca^{++} increase. Disruption of CD31-CD31 homophilic interactions blocks both TEM and recycling of the LBRC and limitation of either of signaling event restricts TEM of neutrophils and/or monocytes. Therefore, the modification of CD54 and/or CD31 expression by PRT is likely to decrease both early and late stages of leukocyte binding and migration across the endothelial membrane and may thereby reduce inflammation.

Because some debate persists on the broad implementation of PRT regardless of consensus, it is crucial to continue investigations on both the physiopathology of intercept treated-blood products and post marketing clinical trials.

Data availability statement

The raw data supporting the conclusions of this article will be made available by the authors, without undue reservation.

Ethics statement

Data collection from the PLASMACOV cohort was approved by the French national ethics committee (2020-A00728-31). The patients/participants provided their written informed consent to participate in this study.

Author contributions

CF and HH-C made the study hypothesis, wrote the manuscript, designed the protocol and trained personnel in blood banks. PM, NM, NS, and PT contributed to the writing of the manuscript. FC, HH-C, A-CD, NS, M-AE, C-AA, AP, MH, OH, BB, SR-E, FT, VB-E, PC, DL, PR, NM and PT collected samples, did the experiments and statistical analyses, and co-wrote the manuscript. All authors contributed to the article and approved the submitted version.

Funding

This work was supported by grants from the French National Blood Service – EFS (Grant APR), France and the Association "Les Amis de Rémi" Savigneux, France.

Acknowledgments

We would like to thank the medical staff and personnel of the Etablissement Français du Sang Auvergne-Rhone-Alpes, Saint-Etienne, France for technical support throughout our studies. We thank the blood donors for taking part in this study.

Conflict of interest

The authors declare that the research was conducted in the absence of any commercial or financial relationships that could be construed as a potential conflict of interest.

Publisher's note

References

1. Casadevall A, Pirofski LA. The convalescent sera option for containing COVID-19. *J Clin Invest* (2020) 130(4):1545–48. doi: 10.1172/jci138003

2. Casadevall A, Pirofski LA. Antibody-mediated regulation of cellular immunity and the inflammatory response. *Trends Immunol* (2003) 24(9):474–8. doi: 10.1016/s1471-4906(03)00228-x

3. Levi M, van der Poll T. Coagulation and sepsis. *Thromb Res* (2017) 149:38–44. doi: 10.1016/j.thromres.2016.11.007

4. Hod EA, Spitalnik SL. Stored red blood cell transfusions: Iron, inflammation, immunity, and infection. *Transfusion clinique biologique J la Societe francaise transfusion sanguine* (2012) 19(3):84–9. doi: 10.1016/j.tracli.2012.04.001

5. Sut C, Tariket S, Aubron C, Aloui C, Hamzeh-Cognasse H, Berthelot P, et al. The non-hemostatic aspects of transfused platelets. *Front Med* (2018) 5:42. doi: 10.3389/fmed.2018.00042

6. Toy P, Gajic O, Bacchetti P, Looney MR, Gropper MA, Hubmayr R, et al. Transfusion-related acute lung injury: incidence and risk factors. *Blood* (2012) 119 (7):1757–67. doi: 10.1182/blood-2011-08-370932

7. Vlaar AP, Hofstra JJ, Determann RM, Veelo DP, Paulus F, Levi M, et al. Transfusion-related acute lung injury in cardiac surgery patients is characterized by pulmonary inflammation and coagulopathy: a prospective nested case-control study. *Crit Care Med* (2012) 40(10):2813–20. doi: 10.1097/CCM.0b013e31825b8e20

8. Herbrecht R, Ojeda-Uribe M, Kientz D, Fohrer C, Bohbot A, Hinschberger O, et al. Characterization of efficacy and safety of pathogen inactivated and quarantine plasma in routine use for treatment of acquired immune thrombotic thrombocytopenic purpura. *Vox sanguinis* (2018) 113:459–67. doi: 10.1111/vox.12663

9. Saadah NH, van Hout FMA, Schipperus MR, le Cessie S, Middelburg RA, Wiersum-Osselton JC, et al. Comparing transfusion reaction rates for various plasma types: a systematic review and meta-analysis/regression. *Transfusion* (2017) 57(9):2104–14. doi: 10.1111/trf.14245

10. Tiberghien P, de Lamballerie X, Morel P, Gallian P, Lacombe K, Yazdanpanah Y. Collecting and evaluating convalescent plasma for COVID-19 treatment: why and how? *Vox Sanguinis* (2020) 115(6):488–94. doi: 10.1111/vox.12926

11. Hueso T, Pouderoux C, Péré H, Beaumont AL, Raillon LA, Ader F, et al. Convalescent plasma therapy for b-cell-depleted patients with protracted COVID-19. *Blood* (2020) 136(20):2290–5. doi: 10.1182/blood.2020008423

12. ANSM. *COVID-19 : L'ANSM modifie les conditions d'utilisation de plasma de personnes convalescentes* (2022). Available at: https://ansm.sante.fr/actualites/covid-19-lansm-modifie-les-conditions-dutilisation-de-plasma-de-personnes-convalescentes.

13. ANSM. *COVID-19: L'ANSM encadre le recours possible à l'utilisation de plasma de personnes convalescentes pour des patients ne pouvant être inclus dans les essais cliniques-point d'information* (2020). Available at: https://www.ansm.sante.fr/S-informer/Points-d-information-Points-d-information/COVID-19-L-ANSM-encadre-le-recours-possible-a-l-utilisation-de-plasma-de-personnes-convalescentes-pour-des-patients-ne-pouvant-etre-inclus-dans-les-essais-cliniques-Point-d-information.

14. Lanteri MC, Santa-Maria F, Laughhunn A, Girard YA, Picard-Maureau M, Payrat JM, et al. Inactivation of a broad spectrum of viruses and parasites by photochemical treatment of plasma and platelets using amotosalen and ultraviolet a light. *Transfusion* (2020) 60(6):1319–31. doi: 10.1111/trf.15807

15. Edgell CJ, McDonald CC, Graham JB. Permanent cell line expressing human factor VIII-related antigen established by hybridization. *Proc Natl Acad Sci USA* (1983) 80(12):3734–7. doi: 10.1073/pnas.80.12.3734

16. Sut C, Hamzeh-Cognasse H, Arthaud CA, Eyraud MA, Chettab K, Dumontet C, et al. Platelet concentrate supernatants alter endothelial cell mRNA and protein expression patterns as a function of storage length. *Transfusion* (2018) 58(11):2635–44. doi: 10.1111/trf.14973

17. Muller WA. Transendothelial migration: unifying principles from the endothelial perspective. *Immunol Rev* (2016) 273(1):61–75. doi: 10.1111/imr.12443

18. Woodfin A, Voisin MB, Nourshargh S. PECAM-1: a multi-functional molecule in inflammation and vascular biology. *Arterioscler Thromb Vasc Biol* (2007) 27(12):2514–23. doi: 10.1161/atvbaha.107.151456

19. Bui TM, Wiesolek HL, Sumagin R. ICAM-1: A master regulator of cellular responses in inflammation, injury resolution, and tumorigenesis. *J Leukoc Biol* (2020) 108(3):787–99. doi: 10.1002/jlb.2mr0220-549r

20. Novick D, Schwartsburd B, Pinkus R, Suissa D, Belzer I, Sthoeger Z, et al. A novel IL-18BP ELISA shows elevated serum IL-18BP in sepsis and extensive decrease of free IL-18. *Cytokine* (2001) 14(6):334–42. doi: 10.1006/cyto.2001.0914

21. Leach ST, Messina I, Lemberg DA, Novick D, Rubenstein M, Day AS. Local and systemic interleukin-18 and interleukin-18-binding protein in children with inflammatory bowel disease. *Inflammation Bowel Dis* (2008) 14(1):68–74. doi: 10.1002/ibd.20272

22. Chapman CM, McQuillan BM, Beilby JP, Thompson PL, Hung J. Interleukin-18 levels are not associated with subclinical carotid atherosclerosis in a community population. the Perth carotid ultrasound disease assessment study (CUDAS). *Atherosclerosis* (2006) 189(2):414–9. doi: 10.1016/j.atherosclerosis.2005.12.026

23. Zirlik A, Abdullah SM, Gerdes N, MacFarlane L, Schönbeck U, Khera A, et al. Interleukin-18, the metabolic syndrome, and subclinical atherosclerosis: results from the Dallas heart study. *Arterioscler Thromb Vasc Biol* (2007) 27 (9):2043–9. doi: 10.1161/atvbaha.107.149484

24. Dolinay T, Kim YS, Howrylak J, Hunninghake GM, An CH, Fredenburgh L, et al. Inflammasome-regulated cytokines are critical mediators of acute lung injury. *Am J Respir Crit Care Med* (2012) 185(11):1225–34. doi: 10.1164/rccm.201201-0003OC

25. Zalinger ZB, Elliott R, Weiss SR. Role of the inflammasome-related cytokines il-1 and il-18 during infection with murine coronavirus. *J Neurovirol* (2017) 23(6):845–54. doi: 10.1007/s13365-017-0574-4

26. Jamilloux Y, Henry T, Belot A, Viel S, Fauter M, El Jammal T, et al. Should we stimulate or suppress immune responses in COVID-19? cytokine and anti-cytokine interventions. *Autoimmun Rev* (2020) 19(7):102567. doi: 10.1016/j.autrev.2020.102567

27. Wilson JG, Simpson LJ, Ferreira A-M, Rustagi A, Roque J, Asuni A, et al. Cytokine profile in plasma of severe COVID-19 does not differ from ARDS and sepsis. *JCI Insight* (2020) 5(17):e140289. doi: 10.1101/2020.05.15.20103549

28. Yang Y, Shen C, Li J, Yuan J, Yang M, Wang F, et al. Exuberant elevation of IP-10, MCP-3 and IL-1ra during SARS-CoV-2 infection is associated with disease severity and fatal outcome. *medRxiv* (2020) doi: 10.1101/2020.03.02.20029975

29. Wen W, Su W, Tang H, Le W, Zhang X, Zheng Y, et al. Immune cell profiling of COVID-19 patients in the recovery stage by single-cell sequencing. *Cell Discovery* (2020) 6:31. doi: 10.1038/s41421-020-0168-9

30. Bagri A, de Assis RR, Tsai CT, Simmons G, Mei ZW, Von Goetz M, et al. Antibody profiles in COVID-19 convalescent plasma prepared with amotosalen/UVA pathogen reduction treatment. *Transfusion* (2022) 62(3):570–83. doi: 10.1111/trf.16819

31. Satış H, Özger HS, Aysert Yıldız P, Hızel K, Gulbahar Ö., Erbaş G, et al. Prognostic value of interleukin-18 and its association with other inflammatory markers and disease severity in COVID-19. *Cytokine* (2021) 137:155302. doi: 10.1016/j.cyto.2020.155302

frontiers | Frontiers in Immunology

TYPE Original Research
PUBLISHED 01 November 2022
DOI 10.3389/fimmu.2022.1022750

OPEN ACCESS

EDITED BY
Gilles Kaplanski,
Assistance Publique Hôpitaux de Marseille, France

REVIEWED BY
Kai Kisand,
University of Tartu, Estonia
Johan Van Weyenbergh,
KU Leuven, Belgium

*CORRESPONDENCE
Fabienne Venet
fabienne.venet@chu-lyon.fr

SPECIALTY SECTION
This article was submitted to Inflammation, a section of the journal Frontiers in Immunology

RECEIVED 18 August 2022
ACCEPTED 11 October 2022
PUBLISHED 01 November 2022

CITATION
Tardiveau C, Monneret G, Lukaszewicz A-C, Cheynet V, Cerrato E, Imhoff K, Peronnet E, Bodinier M, Kreitmann L, Blein S, Llitjos J-F, Conti F, Gossez M, Buisson M, Yonis H, Cour M, Argaud L, Delignette M-C, Wallet F, Dailler F, Monard C, Brengel-Pesce K, Venet F and the RICO study group (2022) A 9-mRNA signature measured from whole blood by a prototype PCR panel predicts 28-day mortality upon admission of critically ill COVID-19 patients. *Front. Immunol.* 13:1022750. doi: 10.3389/fimmu.2022.1022750

A 9-mRNA signature measured from whole blood by a prototype PCR panel predicts 28-day mortality upon admission of critically ill COVID-19 patients

Claire Tardiveau[1,2], Guillaume Monneret[1,3], Anne-Claire Lukaszewicz[1,4], Valérie Cheynet[1,2], Elisabeth Cerrato[1,2], Katia Imhoff[1,2], Estelle Peronnet[1,2], Maxime Bodinier[1,2], Louis Kreitmann[1,2], Sophie Blein[1,2], Jean-François Llitjos[1,2,4], Filippo Conti[1,3], Morgane Gossez[3,5], Marielle Buisson[6], Hodane Yonis[7], Martin Cour[8], Laurent Argaud[8], Marie-Charlotte Delignette[9], Florent Wallet[10], Frederic Dailler[11], Céline Monard[4], Karen Brengel-Pesce[1,2], Fabienne Venet[3,5]* and the RICO study group

[1]Joint Research Unit HCL-bioMérieux, Equipe d'Accueil (EA) 7426 "Pathophysiology of Injury-Induced Immunosuppression" (Université Claude Bernard Lyon 1 – Hospices Civils de Lyon, bioMérieux), Lyon, France, [2]Open Innovation and Partnerships (OIP), bioMérieux Société Anonyme (S.A.), Lyon, France, [3]Immunology Laboratory, Edouard Herriot Hospital – Hospices Civils de Lyon, Lyon, France, [4]Anaesthesia and Critical Care Medicine Department, Hospices Civils de Lyon, Edouard Herriot Hospital, Lyon, France, [5]Centre International de Recherche en Infectiologie (CIRI), INSERM U1111, CNRS, UMR5308, Ecole Normale supérieure de Lyon, Université Claude Bernard-Lyon 1, Lyon, France, [6]Centre d'Investigation Clinique de Lyon (CIC 1407 Inserm), Hospices Civils de Lyon, Lyon, France, [7]Medical Intensive Care Department, Hospices Civils de Lyon, Croix-Rousse Hospital, Lyon, France, [8]Medical Intensive Care Department, Hospices Civils de Lyon, Edouard Herriot Hospital, Lyon, France, [9]Anaesthesia and Critical Care Medicine Department, Hospices Civils de Lyon, Croix-Rousse Hospital, Lyon, France, [10]Medical Intensive Care Department, Hospices Civils de Lyon, Lyon sud Hospital, Pierre-Bénite, France, [11]Neurological Anesthesiology and Intensive Care Department, Hospices Civils de Lyon, Pierre Wertheimer Hospital, Lyon, France

Immune responses affiliated with COVID-19 severity have been characterized and associated with deleterious outcomes. These approaches were mainly based on research tools not usable in routine clinical practice at the bedside. We observed that a multiplex transcriptomic panel prototype termed Immune Profiling Panel (IPP) could capture the dysregulation of immune responses of ICU COVID-19 patients at admission. Nine transcripts were associated with mortality in univariate analysis and this 9-mRNA signature remained significantly associated with mortality in a multivariate analysis that included age, SOFA and Charlson scores. Using a machine learning model with these 9 mRNA, we could predict the 28-day survival status with an Area Under the Receiver Operating Curve (AUROC) of 0.764. Interestingly, adding patients' age

10.3389/fimmu.2022.1022750

to the model resulted in increased performance to predict the 28-day mortality (AUROC reaching 0.839). This prototype IPP demonstrated that such a tool, upon clinical/analytical validation and clearance by regulatory agencies could be used in clinical routine settings to quickly identify patients with higher risk of death requiring thus early aggressive intensive care.

KEYWORDS

transcriptomic multiplex tool, SARS-CoV-2 infection, immune response, 28-day mortality prediction, personalized medicine

1 Introduction

The current pandemic of coronavirus disease-2019 (COVID-19) caused by severe acute respiratory syndrome-related coronavirus 2 (SARS-CoV-2) has infected over 589 million patients with more than 6 million deaths worldwide as of August 2022. Disease severity is highly variable, with the vast majority of patients remaining asymptomatic or demonstrating minimal to mild symptoms such as fever, cough and shortness of breath. Nonetheless, it was reported that 5 to 10% of patients require intensive care due to rapid progression (9 to 12 days) toward acute respiratory distress syndrome (ARDS) requiring ICU (intensive care unit) admission and invasive mechanical ventilation (1, 2).

The immune response has been demonstrated to play a key role in the physiopathology of COVID-19. In the most severe phenotype, patients present a complex immune profile that evolves over time (3, 4). At ICU admission, their immune response is mostly characterized by altered immuno-inflammatory responses with inadequate response of type I interferons signaling and downregulation of IFN-stimulated genes (ISGs), increased cytokines levels (both pro- and anti-inflammatory), marked lymphopenia, elevated immature myeloid cells, and decreased monocyte HLA-DR (mHLA-DR). Those alterations were hypothesized to lead to microthrombosis and tissue injury, eventually resulting in ARDS, multiorgan failure and death (5). During the pandemic, many exploratory non-hypothesis-driven studies have been conducted for deciphering the immune processes. As a whole, these studies used mixed various flow approaches (spectral flow, multicolor flow, time of flight mass spectrometry), transcriptomic strategies (transcriptomic signatures, single-cell RNA-seq), functional testing, and multiplex measurement of soluble mediators. Results were mostly analyzed though multi-data/–omic approaches. While providing crucial information on COVID-19 pathophysiology, these approaches were mainly based on clinical research tools that are, due to several limitations (i.e., time consuming, lack of standardization, poorly reproducible between cohorts or costly), not usable in clinical routine at the patients' bedside or central lab.

A prototype multiplex transcriptomic tool used on the BIOFIRE® FILMARRAY® System allows whole blood assessment of mRNA of several genes involved in various aspects of the immune response (6, 7). Thus, this Immune Profiling Panel (IPP) gene set could potentially contribute to better decipher the complex immune status of severe COVID-19 patients when admitted to ICU. Here, we investigated this transcriptomic prototype device in a large cohort of critically ill COVID-19 patients. We found that a set of 9-mRNA immune-related markers was capable in predicting 28-day mortality and providing relevant information about immune dysregulations.

2 Material and methods

2.1 Subject details

2.1.1 RICO cohort

RICO (REA-IMMUNO-COVID) is an ongoing prospective observational clinical study. In this ancillary study, 309 patients were enrolled between August 2020 and August 2021 in five ICUs of university-affiliated hospitals (Hospices Civils de Lyon, Lyon, France). They all presented pulmonary infection with SARS-CoV-2. Results on this cohort have been published previously (8). Briefly, inclusion criteria were (1) man or woman ≥ 18 years of age (2), hospitalization in ICU for SARS-CoV-2 respiratory infection (3), first hospitalization in ICU (4), positive diagnosis of SARS-CoV-2 infection carried out by PCR or by another approved method in at least one respiratory sample (5), blood sampling in the first 24h after admission to ICU (Day 0) feasible and (6) patient or next of kin who has been informed of the terms of the study and has not objected to participating. Exclusion criteria were pregnancy, institutionalized patients and inability to obtain informed consent. In the present work, IPP was tested at Day 0. Patients were 65.0 years old [IQR, 57.0-72.0] and presented a disparate distribution of males and females (68/32).

The RICO study protocol was approved by ethics committee (Comité de Protection des Personnes Ile de France 1 – N°IRB/IORG #: IORG0009918) under agreement number 2020-A01079-

30. This clinical study was registered at ClinicalTrials.gov (NCT04392401). The committee waived the need for written informed consent because the study was observational, with a low risk to patients, and no specific procedure, other than routine blood sampling, was required. The RICO cohort comply with the Declaration of Helsinki, principles of Good Clinical Practice and the French personal data protection act.

2.1.2 Healthy donors

Concomitantly, blood samples from 49 healthy volunteers were independently obtained from EFS (Etablissement Français du Sang, Lyon, France). Briefly, healthy donors were 40 years old [IQR, 27-54] and were heterogeneously distributed between males and females (73/27). Samples were collected in April 2020 and November 2021.

We used the Etablissement Français du Sang standardized procedures for blood donation and followed provisions of articles R.1243–49 and the French public health code to obtain written non-opposition to the use of donated blood for research purposes from healthy volunteers. The blood donors' personal data were deidentified before transfer to our research laboratory.

2.2 Method details

2.2.1 Transcriptome analysis

Whole blood was collected in PAXgene™ tubes following the manufacturer's guidelines. Briefly, samples were left for 2 hours at room temperature in contact with reagents in the tubes before being transferred to -20°C for at least 24 hours and stored at -80°C. Samples were run on the BIOFIRE® FILMARRAY® TORCH (BioFire Diagnostics®, USA) using the prototype IPP gene set. Results were delivered in less than an hour and normalized expression values of markers were computed and used for the analyses.

2.2.2 Immunological markers measurements

CD3+ T cells count was performed on an automated volumetric flow cytometer (Aquios CL, Beckman Coulter). Standardized mHLA-DR values (AB/C, antibodies bound per cell) were obtained by flow cytometry (Navios, Beckman Coulter) with HLA-DR Quantibrite reagents (Becton Dickinson) as previously described (8).

2.3 Statistical analysis

The study cohort was split randomly in a 70/30 manner to obtain two datasets balanced on three parameters: age, sex and mortality. This resulted in a dataset of 216 patients used for machine learning training purposes and an independent test set of 93 patients used for performances validation. For datasets description, qualitative data were reported as counts and frequencies and quantitative data were reported as median [IQR range]. Clinical characteristics were compared with non-parametric Mann-Whitney-Wilcoxon test for continuous variables and a Fisher's exact test or chi-squared test (as appropriate) for categorical variables. The level of significance was set at 5% two-sided tests. Statistical analyses were performed with R software version 3.6.2. Data were centered and scaled to perform non-supervised principal components analysis using FactoMineR package (version 2.4). Genes that were significantly associated with 28-day mortality in a univariate logistic regression model were used to build multivariate models for prediction of the 28-day survival status. Trained models were logistic regression with L1 (Lasso), L2 (Ridge) and mixed (ElasticNet) regularization, Partial Least Squares-discriminant (PLS) analysis and Support Vector Machines with linear kernels (linear SVM) using CARET package (version 6.0-84). To compensate the imbalanced repartition of mortality in our datasets, the Synthetic Minority Oversampling Technique (SMOTE) was applied for hyper parameters tuning (9). Models hyper parameters were chosen corresponding to the largest mean Area Under Precision Recall Curve (AUPRC) value among test folds from repeated cross-validation (k-fold=5, number of repeats=10) in the RICO training cohort (10) as sensitivity and Positive Predictive Values (PPV) are parameters of interest. Briefly, among the 5 machine learning algorithm evaluated, the hyper parameters selected were as follow, Lasso (α=1, λ=0.031), Ridge (α=0, λ=0.556), ElasticNet (α=0.35, λ=0.37), PLS (ncomp=1) and linear SVM (C=0.367). AUPRC and their bootstrap 95% confidence interval was obtained using PRROC (version 1.3.1) and boot (version 1.3-28) packages. Number of bootstrap resamples has been set to N=1000. Variables relative importance in the linear SVM model was calculated using the FIRM method from vip package (version 0.3.2) (11). Area Under the ROC Curve (AUROC) and bootstrap 95% confidence interval and diagnostic performances (sensitivity, specificity, positive and negative predictive values and F1 score) at optimal cut-offs for the 9-mRNA panel as well as others individual parameters were obtained considering respective Youden values from cutpointr package (version 1.1.1) defined on training dataset and then applied on test dataset values. The F1 score (harmonic mean of recall and precision) was used as model accuracy measure due to unbalanced data. The survival probability rendered by the linear SVM machine learning model with the 9 genes significantly associated with 28-day mortality was tested in a multivariate logistic regression analysis with confounding clinical factors found to be significantly associated to 28-day mortality in the univariate analysis (i.e. age, Charlson and SOFA scores). The SAPS II score was excluded from the analysis as age and severity were captured by age and SOFA score. As the number of events of interest in the combined train and test cohorts was 52; the inclusion of three confounding factors in such multivariate analysis appeared appropriate.

10.3389/fimmu.2022.1022750

3 Results

3.1 Clinical characteristics at ICU admission

Patient characteristics (whole, training and test cohorts) are shown in Table 1. A total of 309 patients were hospitalized in 5 hospitals in Lyon between August 2020 and August 2021. Briefly and as previously reported, we observed that 70% of patients were male. Overall, patient characteristics were similar to those described in previously published cohorts of critically ill COVID-19 patients. Patients were admitted to the Intensive Care Unit (ICU) with a median of 9 days after presentation of the first symptoms [IQR, 6.0-11.0]. They presented comorbidities as assessed by their Charlson score. Among these comorbidities, diabetes was preponderant (31%). As reported worldwide, patients presented a high median BMI (kg/m3) of 29.1 [IQR, 26.1-33.2]. In terms of severity of the disease, patients presented a decreased PaO2/FiO2 (mmHg) with a median of 97.5 [IQR: 74.3-146.5], elevated SOFA [median: 2.0; IQR: 1.0-5.0] and SAPS II scores [median: 30.0; IQR: 23.5-39.0]. At admission, 17.2% patients required invasive mechanical ventilation. All patients were under systemic corticoid therapy upon or at admission (6mg dexamethasone daily). Patients spent a median 18 days [IQR, 11.0-31.8] in the hospital among which 8 days [IQR, 4.0-17.0] were spent in the ICU. About a third developed secondary infections. Most of these were pneumopathies (87/99) among which 16 were fungal infections. Lastly, among the 309 patients, 52 (17%) died by day 28.

3.2 Cellular immunology and IPP transcriptomic profile

As previously reported, mHLA-DR was decreased with a median of 8950 AB/C [IQR, 6655.5-12173.5] in comparison with references values (> 13 500 AB/C) and patients presented with severe lymphopenia with a median T cell count of 325 cells/µL [IQR, 228.0-505.5] compared to reference values > 1000 cells/µL (13, 14).

Non-supervised clustering using principal component analysis (PCA) on the 26 IPP mRNA transcripts resulted in clear distinct clusters between the 309 critically ill COVID-19 patients at admission and 49 healthy donors (Figure 1A). The IPP gene set revealed significant changes in inflammation and cellular-associated transcriptomic markers in COVID-19 patients when compared with healthy volunteers. *CD74, CIITA, CD3D* and *IL7R* were downregulated in critically ill COVID-19 patients (Figure 1B) in accordance with the occurrence of altered monocyte and T lymphocyte responses. Pro- and anti-inflammatory responses (e.g. *IL1RN, IL10, IL1R2* and *IP10*) were both upregulated in patients (Figure 1B). In contrast, we observed that *IFNG* and *TNF* mRNA levels were lower in patients than in healthy donors. Overall, these first results indicated that the IPP gene set provided relevant information recapitulating immune dysregulation known in COVID-19 critically ill patients, in line with the vast literature previously published on this population.

3.3 Association with 28-day mortality

We further investigated the association between IPP markers and the 28-day mortality. A logistic regression univariate analysis was performed on the training dataset composed of 216 patients, we identified 9 genes that were significantly associated with 28-day mortality (Table 2), namely *ADGRE3, C3AR1, CD177, CD74, CIITA, IL10, IL1R2, OAS2* and *TDRD9*. Among those, *ADGRE3, CD74* and *CIITA* were significantly downregulated in non-survivors when compared to survivors, while all other markers were upregulated in non-survivors. Among cellular parameters, only CD3 T cells count was significantly associated with 28-day mortality in a logistic regression model (p=0.031). Descriptive boxplots of the 9 genes that compose the panel along with clinical scores and age regarding with 28-day survival status are presented in Figure 2. Consistent with the existing literature, age, SOFA, SAPS II and Charlson scores were significantly associated with mortality in univariate analysis.

This 9-mRNA signature was then used in five different machine learning models to predict the 28-day survival status in the training dataset. We selected the best performing machine learning model based on the area under the precision-recall curve (Table 3). We found that the linear support vector machine learning model presented the best AUPRC (0.431) and second best AUROC (0.744). We then tested the tuned models on the test dataset (93 patients) to confirm results obtained in training dataset. The AUPRC calculated was 0.431 while the AUROC reached 0.764 (Table 3). The ROC curves generated on the training and test datasets are shown in Figure 3. Overall, results from the test dataset confirm the robustness of those obtained on the training dataset to predict mortality. The 9-mRNA signature was further tested in a logistic regression multivariate analysis with the following confounding factors: age, SOFA score and Charlson score. The signature remained significantly associated with 28-day mortality with an odds ratio per interquartile range of 3.78 (Table 4).

In order to test the added value of a 9-mRNA signature, we then examined individual 28-day mortality prediction performance of each mRNA in the signature set as well as age, SOFA and SAPS II scores, and T cell count using logistic regression models. We found that the 9-mRNA signature presented the best AUPRC (and AUROC) when compared to all other individual parameters. Using the Youden threshold, we calculated the sensitivity, specificity, positive predictive value, negative predictive value and F1 score for each parameter (Table 5). Not surprisingly, we found that age was also well

10.3389/fimmu.2022.1022750

TABLE 1 Clinical characteristics of critically ill patients with COVID-19.

	All patients (n = 309)	Training			Test		
		28-day survivors (n = 179)	28-day non survivors (n = 37)	*p* value	28-day survivors (n = 78)	28-day non survivors (n = 15)	*p* value
Demographics							
Age - years	65.0 [57.0-72.0]	64.0 [55.0-70.0]	71.0 [69.0-78.0]	**<0.001**	64.5 [55.0-70.0]	72.0 [68.0-76.0]	**<0.001**
Male gender – *n (%)*	210 (68.0%)	119 (66.5%)	28 (75.7%)	0.369	52 (66.7%)	11 (73.3%)	0.767
Body mass index - kg/m²	29.1 [26.1-33.2]	29.1 [25.7-33.1]	29.6 [27.33-33.0]	0.674	28.7 [26.1-33.4]	30.1 [28.0-33.2]	0.335
BMI > 30 – *n (%)*	128 (43.7%)	75 (43.9%)	15 (46.9%)	0.903	30 (40.0%)	8 (53.3%)	0.504
Comorbidities							
Diabetes: none - *n (%)*	213 (69%)	131 (73.2%)	18 (48.7%)	**0.001**	55 (70.5%)	9 (60.0%)	0.534
Diabetes: with damage - *n (%)*	15 (4.9%)	6 (3.4%)	6 (16.2%)		3 (3.9%)	0 (0.0%)	
Diabetes: w/o organic damage - *n (%)*	81 (26.2%)	42 (23.4%)	13 (35.1%)		20 (25.6%)	6 (40.0%)	
Charlson Score - points	1.0 [0.0-2.0]	1.0 [0.0-1.0]	2.0 [1.0-4.0]	**<0.001**	0.5 [0.0-1.0]	1.0 [1.0-2.0]	**0.043**
Clinical severity at admission							
Delay between symptoms and ICU admission - days	9.0 [6.0-11.0]	9.0 [7.0-12.0]	7.5 [5.0-9.8]	**0.013**	9.0 [6.8-10.3]	6.0 [5.5-9.0]	**0.041**
ARDS at admission – *n (%)*	72 (23.8%)	41 (23.3%)	11 (30.6%)	0.478	13 (17.1%)	7 (46.7%)	**0.029**
SOFA Score - points	2.0 [1.0-5.0]	2.0 [0.0-5.0]	4.0 [2.0-6.0]	**0.008**	2.0 [0.3-3.0]	3.0 [1.5-7.5]	0.068
SAPS II Score - points	30.0 [23.5-39.0]	30.0 [23.0-38.8]	39.0 [33.0-47.0]	**<0.001**	27.5 [21.0-34.0]	32.0 [26.8-41.3]	0.086
PaO2/FIO2 - mmHg	97.5 [74.3-146.5]	95.0 [77.5-146.0]	82.0 [70.5-147.8]	0.376	98.0 [89.0-149.0]	104.5 [93.8-128.3]	0.844
pH	7.45 [7.42-7.49]	7.46 [7.42-7.49]	7.44 [7.40-7.49]	0.591	7.46 [7.43-7.49]	7.47 [7.40-7.49]	0.769
Lactate - mmol/L	1.65 [1.30-2.00]	1.70 [1.37-2.02]	1.90 [1.40-2.20]	0.326	1.50 [1.30-1.90]	1.40 [1.30-1.80]	0.785
Organ support							
Invasive mechanical ventilation at Day 0 – *n (%)*	53 (17.2%)	29 (16.2%)	10 (27%)	0.186	9 (11.5%)	5 (33.3%)	**0.046**
Vasoactive drugs - *n (%)*	35 (11.4%)	19 (10.7%)	8 (21.6%)	0.120	6 (7.7%)	2 (13.3%)	0.611
Renal replacement therapy - *n (%)*	31 (10.0%)	13 (7.3%)	11 (29.7%)	**<0.001**	4 (5.1%)	3 (20.0%)	0.080
Follow-up							
MV duration - days	14.0 [7.0-27.3]	17.0 [7.0-34.0]	12.0 [7.0-20.0]	0.110	22.5 [11.3-30.8]	12.0 [6.5-15.5]	**0.030**
ICU length of stay - days	8.0 [4.0-17.0]	8.0 [3.0-16.0]	12.0 [8.0-19.0]	**0.017**	8.0 [5.0-16.8]	11.0 [5.5-15.5]	0.871
Hospital length of stay - days	18.0 [11.0-31.8]	18.0 [10.0-36.5]	15.0 [9.0-21.0]	**0.024**	20.5 [13.0-34.8]	14.0 [7.5-18.5]	**0.014**
28-day mortality - *n (%)*	52 (16.8%)	0 (0%)	37 (100%)	**<0.001**	0 (0%)	15 (100%)	**<0.001**
90-day mortality - *n (%)*	66 (21.9%)	12 (6.8%)	37 (100%)	**<0.001**	2 (2.7%)	15 (100%)	**<0.001**
ICU-acquired infections – *n (%)*	99 (33.1%)	55 (31.6%)	19 (54.3%)	**0.018**	15 (20.0%)	10 (66.7%)	**<0.001**
ICU-acquired pneumopathies - *n (% IAI)*	87/99 (87.9%)	48/55 (87.3%)	18/19 (94.7%)	0.366	12/15 (80.0%)	9/10 (90.0%)	0.504

(Continued)

TABLE 1 Continued

	All patients (n = 309)	Training			Test		
		28-day survivors (n = 179)	28-day non survivors (n = 37)	*p* value	28-day survivors (n = 78)	28-day non survivors (n = 15)	*p* value
Immunological parameters at admission							
mHLA-DR – AB/C	8950.0 [6655.5-12173.5]	9246.0 [6770.0-12827.0]	7377.5 [4760.8-11413.0]	**0.029**	8939.0 [6859.8-11038.8	8967.0 [7551.5-11118.0]	0.810
CD3 T cells – absolute count	325.0 [228.0-505.5]	326.0 [236.5-506.0]	303.0 [200.0-400.0]	0.056	326.0 [218.0-515.0]	500.0 [251.0-555.5]	0.583

Medians and interquartile ranges [Q1-Q3] are shown for continuous variables or numbers and percentages are presented for categorical variables. COVID-19 patients were separated in two groups based on their 28-day survival status after admission. Sequential organ failure (SOFA) and simplified acute physiology II (SAPS II) scores were calculated during the first 24 hours after admission. Acute respiratory distress at admission was based on the Berlin definition (12). Data were compared using the nonparametric Mann-Whitney-Wilcoxon test for continuous variables or the chi-square/Fisher exact test for categorical variables.
p values ≤ 0.05 are highlighted in bold.

associated with 28-day mortality, which is consistent with numerous observations made since the beginning of the pandemic. Based on this, we next investigated whether a machine learning model including age and the 9-mRNA signature could be more informative to predict 28-day mortality. Using the same previous methodology, we found that the linear support vector machine learning model composed of the 9 genes and age was the best to predict 28-day mortality with an AUPRC of 0.539 (AUROC = 0.839) in the training dataset. The test dataset provided similar results, i.e., an AUPRC of 0.532 (AUROC = 0.839) (Figure 4A). Results from the two models (i.e., with and without age) are depicted in Figure 4B.

4 Discussion

Clinical presentation of COVID-19 ranges from asymptomatic, mild infection to severe cases with acute respiratory distress syndrome, respiratory failure and, ultimately, death. It is now well established that immune alterations play a pivotal role in determining the severity of the disease course (15). Finding effective patient-tailored care management for COVID-19 patients that take into account their immune status is key to lessening the clinical burden and improve prognosis (16). Different approaches have been used to characterize the immune status in COVID-19 patients at the protein (circulating cytokines and/or other biomarkers), cellular (characterization of the immune subsets and functionality) or RNA levels (bulk/single-cell RNA-seq in whole blood, respiratory fluids) (3, 5, 17–19). Many groups over the past 2 years have worked on the identification of risk factors for severe disease progression in order to identify patients at high-risk of evolving towards a severe outcome. Among illustrative examples, in a study combining ~50 clinical features and ~200 high-dimensionality immunological features, Mathew et al. previously reported three distinct immunotypes associated with COVID-19 severity (20). In an extensive immune assessment study combining cellular data accessed by flow cytometry, soluble immune markers (multiplex cytokine analysis), RNA expressions (Nanostring) and serology (ELISA), Laing et al. identified a core peripheral blood immune signature in COVID-19 patients, which could identify settings of immunopathology, correlate with disease severity and anticipate clinical progression (4). In another elegant work, Abers et al. established that longitudinal trajectories of 11 immune-based circulating biomarkers were substantially associated with mortality when increased (10) or decreased (1) providing additional evidence that immune-based biomarkers may provide an early warning of COVID-19 outcome (21). Transcriptomic approaches have shown that they could discriminate between distinct physio-pathological states of the COVID-19 (e.g paucisymptomatic, mild/moderate and severe) (22). Recently, a 6-gene signature was identified to predict COVID-19 mortality based on cohort explorative approaches (23).

However, to date, none is implemented in the standard bundle of care of patients. The IPP prototype tool measures immune-related markers that were pragmatically selected based on their known-documented function or prognostic significance with the aim to assess the immune status of sepsis patients in a multi-dimensional way (7), recently it was demonstrated to predict 30-day mortality in patients with sepsis (24). In addition, technically speaking, the IPP prototype device could be used with its dedicated measurement platform to provide results in less than an hour from whole blood. When compared to other devices used for transcriptomic analyses, the IPP tool presents with several advantages, as it does not require any specific technicity. It is easy to use as it works with whole blood directly instead of extracted RNAs. Thus, the IPP prototype device presents the potential, in the future, to be used as a very appropriate and practical tool for implementation at the bedside.

In this study, we showed that IPP captured immune response dysregulations induced by SARS-CoV-2 infection. For examples, monocyte alterations (CD74, CIITA mRNA), lymphopenia (CD3, IL7R mRNA), increased anti-inflammatory response (IL10, IL1RN mRNA), altered IFN response (OAS2, IFNG mRNA) were observed.

Most importantly, from this whole blood multiplex mRNA assessment, we reported that the IPP prototype resulted in

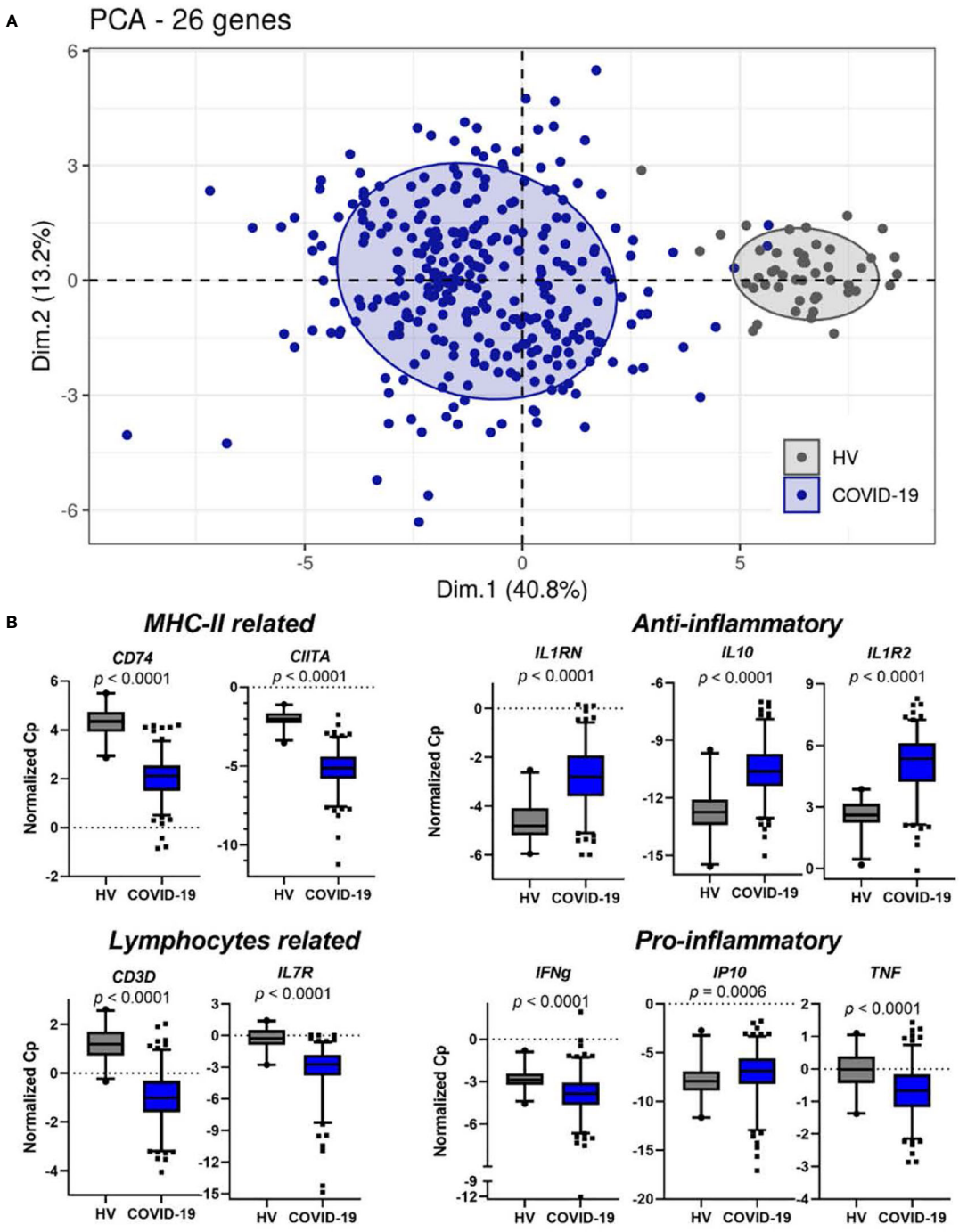

FIGURE 1
IPP markers distinguish healthy donors from critically ill COVID-19 patients and are associated with immunological parameters. **(A)** Non-supervised PCA on IPP markers measured at admission (Day 0) in critically ill COVID-19 patients (n=309) and healthy donors (n=49). **(B)** Boxplots representation of the expression of IPP markers related to immunological parameters. p values were computed with a Mann-Whitney-Wilcoxon test. Whiskers indicate the 2.5 and 97.5 percentiles.

prediction of 28-day survival with a sensitivity of 0.667 and specificity of 0.808. We found that 9 genes associated with 28-day mortality and using machine learning approaches. This 9-mRNA signature could be used to predict 28-day survival status. Among them, some were already known and described in the literature for their role in pathophysiology and/or association with mortality such as IL10, CD74, CTIIA, IL1R2, CD177 and C3AR1 (22, 25–28). For example, increased expressions of IL10,

10.3389/fimmu.2022.1022750

TABLE 2 Association between IPP transcriptomic, immune, clinical or demographical parameters and 28-day survival status: univariate analyses.

	OR_{IQR} [95% CI]	IQR	*p* value
ADGRE3	0.66 [0.45-0.93]	1.17	**0.021**
C3AR1	2.02 [1.20-3.55]	1.90	**0.010**
CD177	1.76 [1.10-2.94]	2.69	**0.022**
CD74	0.56 [0.34-0.88]	1.08	**0.014**
CIITA	0.54 [0.33-0.82]	1.41	**0.005**
IL10	2.88 [1.72-5.01]	1.67	**< 0.001**
IL1R2	2.82 [1.15-3.39]	1.84	**0.016**
OAS2	1.82 [1.02-3.31]	2.43	**0.045**
TDRD9	1.86 [1.15-3.11]	1.60	**0.014**
mHLA-DR [antibody/cell]	0.97 [0.67-1.30]	6246	0.856
CD3 T Cells [cells/µL]	0.56 [0.31-0.90]	258.5	**0.031**
SOFA Score	1.50 [1.04-2.15]	4	**0.029**
SAPS II Score	1.65 [1.17-2.33]	16	**0.004**
Charlson Score	1.62 [1.14-2.42]	2	**0.017**
Age	4.95 [2.62-10.17]	15.25	**< 0.001**

Two hundred and sixteen critically ill patients were included in the training set. One hundred and seventy-nine patients survived up until Day 28 and thirty-seven died. The association between 28-day survival status and transcriptomic IPP parameters, classical immune, clinical or demographical parameters were performed by implementing univariate logistic regression models. To allow comparison between models, odds ratios calculated for each parameter were normalized to an increment from first to third quartile (inter quartile range odd ratios, OR_{IQR}). p values ≤ 0.05 are highlighted in bold.

IL1R2 mRNA and decreased expression of CD74 and CIITA mRNA were described in monocytes of progressive COVID-19 patients compared with stable patients suggesting the acquisition of a regulatory phenotype by myeloid cells. In the same study, increased expression of IL1R2 was also observed in neutrophils (29). Regarding neutrophils, the increased expressions of CD177, IL1R2 and S100A9 in our study agree with the existing literature, which points towards the induction of a dysregulated neutrophil function in COVID-19 patients with increased NET production that aggravates the pathophysiology of COVID-19. Similarly, increased mRNA expression of IL10 was reported in regulatory T cells of severe COVID-19 patients suggesting a defective adaptive immune response (30). Saichi et al. reported that antigen-presenting cells from severe COVID-19 patients presented with defects in several antiviral processes among which a downregulation of MHC class II related genes was observed in both monocytes and dendritic cells (31). Thus, while we cannot discriminate the cell specific mRNA deregulation in our study, we believe that the current results are consistent with the literature and thus that the fully automated IPP transcriptomic solution can capture immune deregulation induced by COVID-19 in the most severe patients.

In addition, we observed that OAS2 was also associated with mortality and its expression level at admission was informative to build our 9-mRNA model. OAS2 is an interferon stimulated gene involved in interferon response, it was previously reported to be associated with COVID-19 severity (32). Nonetheless, the current literature is conflicting regarding the OAS2 role in the pathophysiology of COVID-19. Indeed, on the one hand, a haplotype in the region containing OAS2 has been described to be protective against severe COVID-19 (33). on the other hand, transcriptomic levels of OAS2 in PBMCs were found to be upregulated in severe cases of COVID-19 (34, 35). TDRD9 and ADGRE3 were chosen since they have been previously demonstrated to be part of the SRS1 signature in sepsis (36). In agreement, although their precise role in pathophysiology remains to be further explored, both mRNAs were found to be associated with 28-day mortality in COVID-19 critically ill patients.

Most importantly, beyond the individual predictive value of the 9 mRNAs, their combination, based on machine learning models, was found to be a robust indicator of 28-day mortality within an AUROC of 0.764. Previous studies have demonstrated that various combinations of clinical and biochemical parameters could be used to predict mortality in COVID-19 patients. In a work by Halasz et al., a machine learning approach that used 6 clinical and biochemical features resulted in mortality prediction with an AUROC of 0.78 [0.74-0.84] (37). Zhao et al. presented a model using 7 clinical and biochemical variables which resulted in mortality prediction with AUROC of 0.83 [0.73-0.92] consistent with our results (38). Using machine learning algorithms with an input of 21 clinical or biochemical variables, Banoei et al. presented an in-hospital mortality prediction with AUROC of 0.91-0.95 (39). Thus, we acknowledge that our transcriptomic-only based approach yields predictive metrics that are in the same ranges of other published approaches. However, we propose the use of a tool

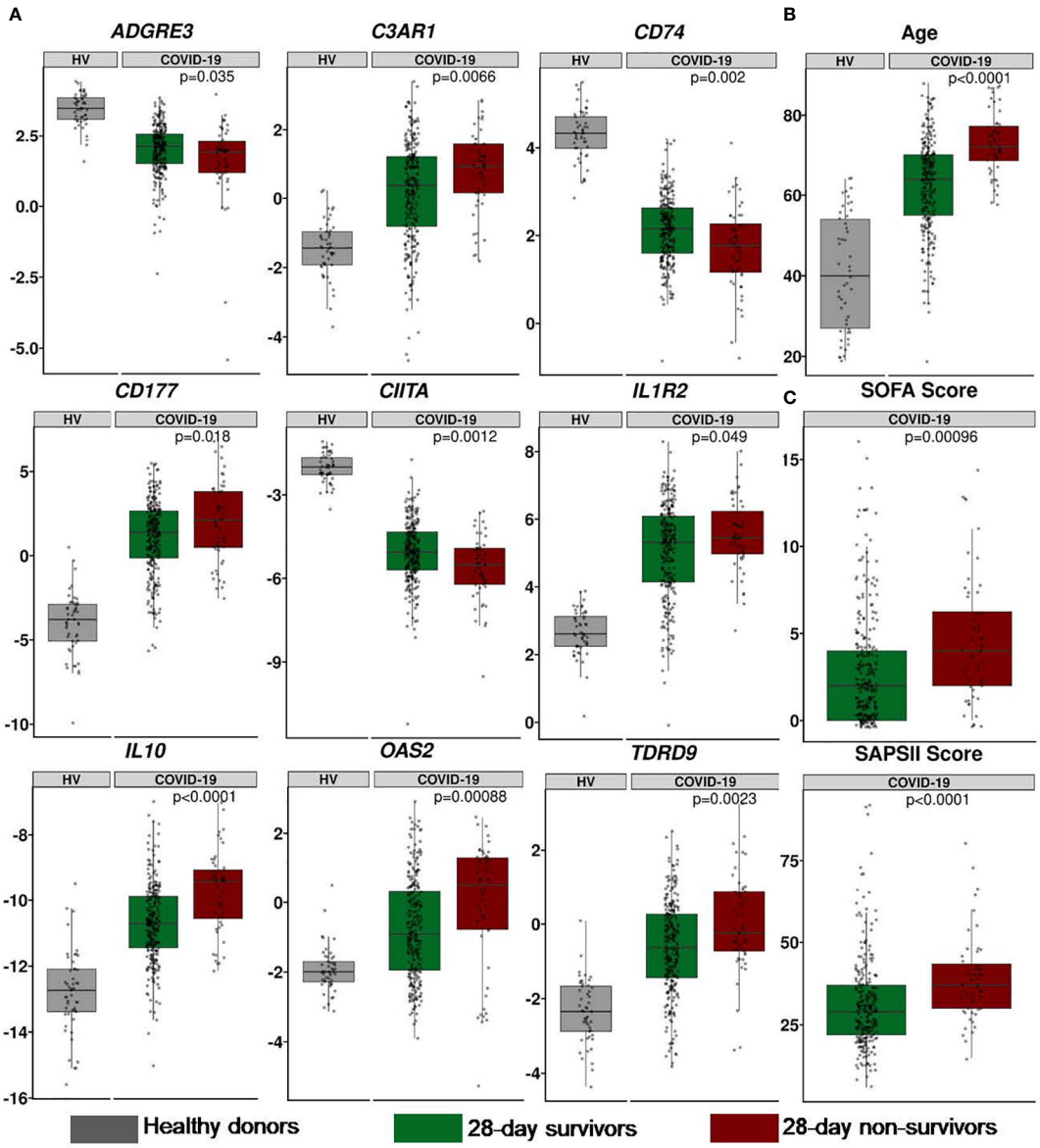

FIGURE 2
Description of IPP 9-mRNA and clinical parameters in the RICO cohort of 309 critically ill COVID-19 patients. **(A)** Expression of IPP markers (values are presented as normalized Cp). **(B)** Age (years). **(C)** Clinical scores. All parameters are presented at admission between 28-day survivors (green) and non-survivors (red). When relevant, reference values of healthy donors are presented in grey. The p-value were generated using a Mann-Whitney-Wilcoxon test between survivors and non-survivors.

that captures the immune profile of a patient directly through processing blood samples without added laborious hands-on time and resource. In regard, none of the elegant transcriptomic-based machine learning models which were previously described to predict mortality in COVID-19 (21, 23) can be easily implemented at the patient´s bedside due to constraints with RNAs processing and standardization of the measures. Similarly, while demographic parameters such as age or clinical parameters such as the SOFA score can readily be obtained at patient admission, some other variables used to build models in the literature are not so easily accessed. Going further, with regards to risk factors largely described in COVID-19 and observed in our study, adding age in the model improved mortality prediction with an AUROC of 0.84. Implementation of the IPP prototype device, that could be considered for use in clinical routine, may help in rapidly identifying patients at higher risk of death in order to provide early aggressive intensive care.

TABLE 3 Summary of the performance of the five different machine learning models on the training and test datasets.

ML Models	$AUROC_{training}$[95% CI]	$AUPRC_{training}$[95% CI]	$AUROC_{test}$[95% CI]	$AUPRC_{test}$[95% CI]
Elastic Net	0.715 [0.575-0.844]	0.361 [0.243-0.524]	0.721 [0.493-0.938]	0.380 [0.171-0.662]
Ridge	0.737 [0.612-0.859]	0.406 [0.257-0.584]	0.751 [0.575-0.927]	0.326 [0.164-0.558]
Lasso	0.754 [0.630-0.874]	0.402 [0.256-0.576]	0.748 [0.554-0.932]	0.346 [0.168-0.620]
PLS	0.732 [0.605-0.853]	0.406 [0.256-0.579]	0.744 [0.567-0.924]	0.312 [0.156-0.566]
svmLin	**0.744 [0.600-0.881]**	**0.431 [0.278-0.610]**	**0.764 [0.536-0.960]**	**0.431 [0.214-0.720]**

Area Under the Receiver Operating Characteristics Curves and Area Under the Precision Recall Curves with their respective 95% confidence intervals calculated for 5 different machine learning models on the training and test datasets to predict 28-day survival.
Performances of the best model are highlighted in bold.

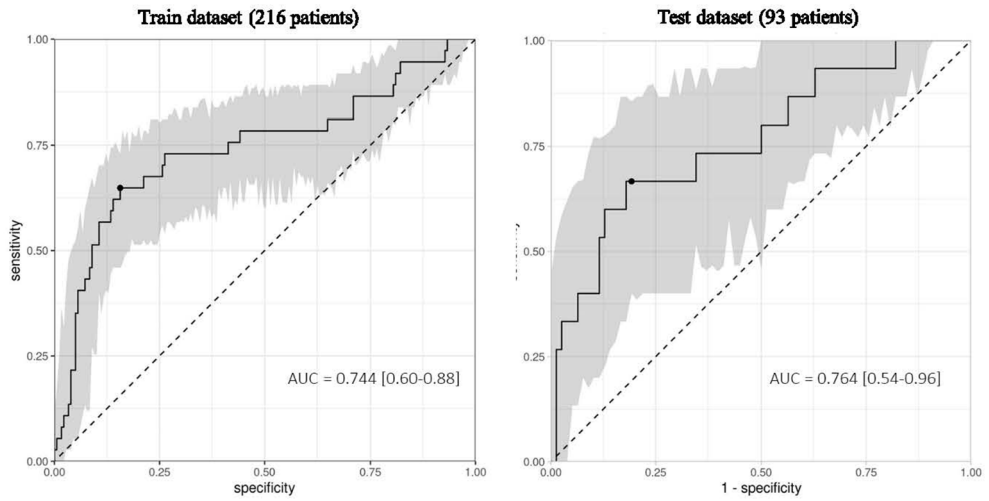

FIGURE 3
IPP markers measured at admission predict 28-day mortality in critically ill COVID-19 patients. Area Under the Receiver Operating Characteristics curve (AUC) calculated on the training dataset of 216 patients and the independent test set of 93 critically ill COVID-19 patients using the 9-mRNA panel at their admission in the ICU. The 95% confidence interval (grey) was calculated using bootstrap with 1000 repetitions.

TABLE 4 Association between 9-mRNA signature, clinical or demographical parameters and 28-day survival status: multivariate analysis.

	OR_{IQR} [95% CI]	IQR	*p* value
9-mRNA signature	3.78 [2.22-6.73]	0.26	< **0.001**
SOFA Score	1.34 [0.90-2.03]	4	0.151
Charlson Score	1.37 [1.04-1.81]	2	**0.015**
Age	5.11 [2.82-9.96]	15	< **0.001**

Three hundred and nine critically ill patients were included. Fifty two patients died by Day 28. The association between 28-day survival status and the 9-mRNA signature and clinical and demographical parameters was evaluated by implementing multivariate logistic regression models with the following confounding factors: age, SOFA score and Charlson score. To allow comparison between models, odds ratios calculated for each parameter were normalized to an increment from first to third quartile (inter quartile range odd ratios, OR_{IQR}). p values ≤ 0.05 are highlighted in bold.

TABLE 5 Indicators of 28-day survival prediction performance of individual transcripts and the 9-mRNA panel along with age, CD3 T cells count, SOFA and SAPS II scores at admission.

Parameters	$AUROC_{Test}$	$AUPRC_{Test}$	Sensitivity	Specificity	PPV	NPV	F1 Score
9-mRNA signature	**0.764**	**0.431**	**0.667**	**0.808**	**0.400**	**0.926**	**0.500**
Age	0.763	0.429	0.733	0.667	0.297	0.929	0.423
CD177	0.606	0.352	0.467	0.705	0.233	0.873	0.311
IL10	0.717	0.351	0.533	0.872	0.444	0.907	0.485
SOFA Score	0.647	0.339	0.533	0.654	0.229	0.879	0.320
OAS2	0.305	0.270	0.067	0.949	0.200	0.841	0.100
TDRD9	0.668	0.266	0.667	0.513	0.208	0.889	0.317
SAPSII Score	0.645	0.222	0.500	0.718	0.241	0.889	0.326
#CD3 T cells	0.455	0.180	0.467	0.338	0.121	0.765	0.192
C3AR1	0.578	0.172	0.600	0.590	0.220	0.885	0.321
IL1R2	0.541	0.160	0.800	0.346	0.190	0.900	0.308
CD74	0.697	0.133	0.400	0.833	0.316	0.878	0.353
ADGRE3	0.594	0.126	0.667	0.487	0.200	0.884	0.308
CIITA	0.644	0.118	0.400	0.782	0.261	0.871	0.316

Parameters are presented by descending Area Under the Precision Recall Curve (AUPRC) values. Values superior to 0.75 for Area Under the Receiver Operating Characteristics curve (AUC) and 0.4 for AUPRC are underlined.
Prediction performances of 9-mRNA signature are highlighted in bold.

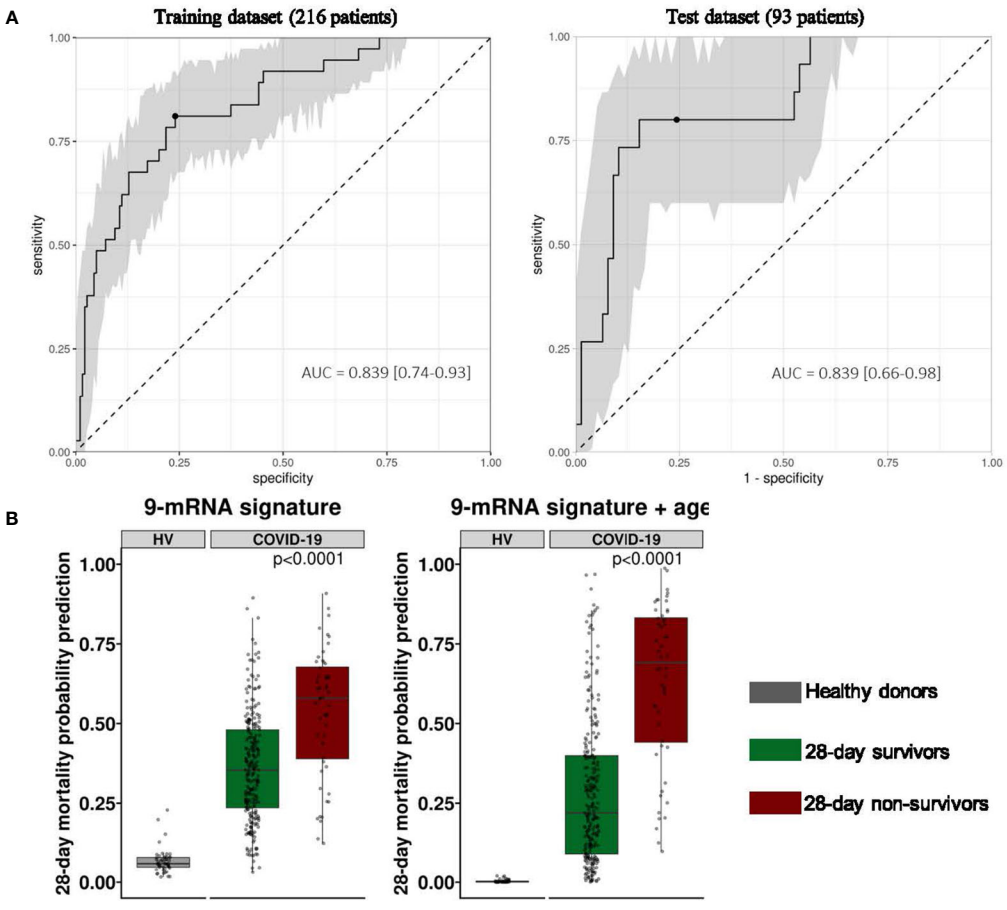

FIGURE 4
Performance of the 9-mRNA signature combined with age to predict 28-day survival status in critically ill COVID-19 patients at ICU admission. **(A)** Area Under the Receiver Operating Characteristics curve (AUC) calculated on the training dataset of 216 patients and the independent test set of 93 critically ill COVID-19 patients using the 9-mRNA panel along with the age at their admission in ICU. The 95% confidence interval (grey) is calculated using bootstrap with 1000 repetitions. **(B)** Probability of 28-day mortality from linear SVM model trained on 9-gene panel (left) and 9-gene panel combined with age (right) on the entire cohort (n=309) of patients and healthy donors (n=49). p-values were generated using a Mann-Whitney-Wilcoxon test between survivors and non-survivors.

Although patients were enrolled in 5 different ICU in university hospitals (multi-center study), all ICUs are located within the same city (Lyon, France). This constitutes the main limitation of this study. Results need thus to be confirmed in cohorts from other cities/countries.

In conclusion, we showed that the multiplex transcriptomic panel prototype termed Immune Profiling Panel (IPP) could capture the dysregulation of immune responses of ICU COVID-19 patients at admission. Nine transcripts were associated with mortality in univariate analysis and this 9-mRNA signature remained significantly associated with mortality in a multivariate analysis including usual clinical confounders. Upon clinical/analytical validation and clearance by regulatory agencies, such fully automated and standardized immune monitoring tool could be used in clinical routine settings to quickly identify patients with higher risk of death requiring thus early aggressive intensive care.

Data availability statement

The original contributions presented in the study are included in the article/Supplementary Material. Further inquiries can be directed to the corresponding author.

Ethics statement

The studies involving human participants were reviewed and approved by Comité de Protection des Personnes Ile de France 1 – N°IRB/IORG #: IORG0009918. The patients/participants provided their written informed consent to participate in this study.

Author contributions

GM, KB-P, and FV conceived the study, supervised the work and the analysis of all data. CT performed the majority of experiments and analyzed the data. VC, EP, MBu, and EC performed part of the IPP experiments. KI, MBo, and SB assisted with statistics and machine leaning analyses. A-CL, MBu, HY, MC, LA, M-CD, FW, FD, and CM helped for samples and data collection. A-CL, LK, and J-FL provided clinical inputs. FC and MG assisted with investigation. CT wrote the manuscript with inputs from GM. All authors discussed the results and commented on the manuscript. All authors contributed to the article and approved the submitted version.

Funding

This work was supported by funds from the Hospices Civils de Lyon, Fondation HCL and Claude Bernard Lyon 1 University/Région Auvergne Rhône-Alpes and by bioMérieux. The funder was not involved in the study design, collection, analysis, interpretation of data, the writing of this article or the decision to submit it for publication.

Conflict of interest

CT, VC, EC, KI, KB-P, EP, MBo, LK, SB, and J-FL, are bioMérieux's employees. EP, GM, and FV are co-inventors in patent applications covering the following markers: CX3CR1, CD127, IL10 and S100A9. bioFire – a bioMérieux company - holds patents on the technology. This does not alter the authors' adherence to all the policies on sharing data and materials.

The remaining authors declare that the research was conducted in the absence of any commercial or financial relationships that could be construed as a potential conflict of interest.

Publisher's note

References

1. Huang C, Wang Y, Li X, Ren L, Zhao J, Hu Y, et al. Clinical features of patients infected with 2019 novel coronavirus in wuhan, China. *Lancet* (2020) 395:497–506. doi: 10.1016/s0140-6736(20)30183-5

2. Salje H, Kiem CT, Lefrancq N, Courtejoie N, Bosetti P, Paireau J, et al. Estimating the burden of SARS-CoV-2 in France. *Science* (2020) 369:208–11. doi: 10.1126/science.abc3517

3. Ong EZ, Chan YFZ, Leong WY, Lee NMY, Kalimuddin S, Mohideen SMH, et al. A dynamic immune response shapes COVID-19 progression. *Cell Host Microbe* (2020) 27:879–82.e2. doi: 10.1016/j.chom.2020.03.021

4. Laing AG, Lorenc A, del BIdM, Das A, Fish M, Monin L, et al. A dynamic COVID-19 immune signature includes associations with poor prognosis. *Nat Med* (2020) 26:1623–35. doi: 10.1038/s41591-020-1038-6

5. Hadjadj J, Yatim N, Barnabei L, Corneau A, Boussier J, Smith N, et al. Impaired type I interferon activity and inflammatory responses in severe COVID-19 patients. *Science* (2020) 369:718–24. doi: 10.1126/science.abc6027

6. Tawfik DM, Lankelma JM, Vachot L, Cerrato E, Pachot A, Wiersinga WJ, et al. Comparison of host immune responses to LPS in human using an immune profiling panel, *in vivo* endotoxemia versus ex vivo stimulation. *Sci Rep-uk* (2020) 10:9918. doi: 10.1038/s41598-020-66695-2

7. Tawfik DM, Vachot L, Bocquet A, Venet F, Rimmelé T, Monneret G, et al. Immune profiling panel: A proof-of-Concept study of a new multiplex molecular tool to assess the immune status of critically ill patients. *J Infect Dis* (2020) 222:S84–95. doi: 10.1093/infdis/jiaa248

8. Venet F, Cour M, Rimmelé T, Viel S, Yonis H, Coudereau R, et al. Longitudinal assessment of IFN-I activity and immune profile in critically ill COVID-19 patients with acute respiratory distress syndrome. *Crit Care* (2021) 25:140. doi: 10.1186/s13054-021-03558-w

9. Chawla NV, Bowyer KW, Hall LO, Kegelmeyer WP. SMOTE: Synthetic minority over-sampling technique. *J Artif Int Res* (2002) 16:321–57. doi: 10.48550/arXiv.1106.1813

10. Ozenne B, Subtil F, Maucort-Boulch D. The precision–recall curve overcame the optimism of the receiver operating characteristic curve in rare diseases. *J Clin Epidemiol* (2015) 68:855–9. doi: 10.1016/j.jclinepi.2015.02.010

11. Greenwell BM, Boehmke BC, McCarthy AJ. A simple and effective model-based variable importance measure. *Arxiv* (2018). doi: 10.48550/arxiv.1805.04755

12. Force ADT, Ranieri VM, Rubenfeld GD, Thompson BT, Ferguson ND, Caldwell E, et al. Acute respiratory distress syndrome: The Berlin definition. *JAMA* (2012) 307:2526–33. doi: 10.1001/jama.2012.5669

13. Weiskopf D, Schmitz KS, Raadsen MP, Grifoni A, Okba NMA, Endeman H, et al. Phenotype and kinetics of SARS-CoV-2–specific T cells in COVID-19 patients with acute respiratory distress syndrome. *Sci Immunol* (2020) 5: eabd2071. doi: 10.1126/sciimmunol.abd2071

14. Venet F, Textoris J, Blein S, Rol M-L, Bodinier M, Canard B, et al. Immune profiling demonstrates a common immune signature of delayed acquired immunodeficiency in patients with various etiologies of severe injury*. *Crit Care Med* (2022) 50:565–75. doi: 10.1097/ccm.0000000000005270

15. Lucas C, Wong P, Klein J, Castro TBR, Silva J, Sundaram M, et al. Longitudinal analyses reveal immunological misfiring in severe COVID-19. *Nature* (2020) 584:463–9. doi: 10.1038/s41586-020-2588-y

16. Group RC, Horby P, Lim WS, Emberson JR, Mafham M, Bell JL, et al. Dexamethasone in hospitalized patients with covid-19. *New Engl J Med* (2020) 384:693–704. doi: 10.1056/nejmoa2021436

17. Valle DMD, Kim-Schulze S, Huang H-H, Beckmann ND, Nirenberg S, Wang B, et al. An inflammatory cytokine signature predicts COVID-19 severity and survival. *Nat Med* (2020) 26:1636–43. doi: 10.1038/s41591-020-1051-9

18. Kwan PKW, Cross GB, Naftalin CM, Ahidjo BA, Mok CK, Fanusi F, et al. A blood RNA transcriptome signature for COVID-19. *BMC Med Genomics* (2021) 14:155. doi: 10.1186/s12920-021-01006-w

19. Su Y, Chen D, Yuan D, Lausted C, Choi J, Dai CL, et al. Multi-omics resolves a sharp disease-state shift between mild and moderate COVID-19. *Cell* (2020) 183:1479–95.e20. doi: 10.1016/j.cell.2020.10.037

20. Mathew D, Giles JR, Baxter AE, Oldridge DA, Greenplate AR, Wu JE, et al. Deep immune profiling of COVID-19 patients reveals distinct immunotypes with therapeutic implications. *Science* (2020) 369:eabc8511. doi: 10.1126/science.abc8511

21. Abers MS, Delmonte OM, Ricotta EE, Fintzi J, Fink DL, de JAAA, et al. An immune-based biomarker signature is associated with mortality in COVID-19 patients. *JCI Insight* (2020) 6:e144455. doi: 10.1172/jci.insight.144455

22. Wilk AJ, Rustagi A, Zhao NQ, Roque J, Martínez-Colón GJ, McKechnie JL, et al. A single-cell atlas of the peripheral immune response in patients with severe COVID-19. *Nat Med* (2020) 26:1070–6. doi: 10.1038/s41591-020-0944-y

23. Buturovic L, Zheng H, Tang B, Lai K, Kuan WS, Gillett M, et al. A 6-mRNA host response classifier in whole blood predicts outcomes in COVID-19 and other acute viral infections. *Sci Rep-uk* (2022) 12:889. doi: 10.1038/s41598-021-04509-9

24. Kreitmann L, Bodinier M, Fleurie A, Imhoff K, Cazalis M-A, Peronnet E, et al. Mortality prediction in sepsis with an immune-related transcriptomics signature: A multi-cohort analysis. *Front Med* (2022) 9:930043. doi: 10.3389/fmed.2022.930043

25. Silvin A, Chapuis N, Dunsmore G, Goubet A-G, Dubuisson A, Derosa L, et al. Elevated calprotectin and abnormal myeloid cell subsets discriminate severe from mild COVID-19. *Cell* (2020) 182:1401–18.e18. doi: 10.1016/j.cell.2020.08.002

26. Lévy Y, Wiedemann A, Hejblum BP, Durand M, Lefebvre C, Surénaud M, et al. CD177, a specific marker of neutrophil activation, is associated with coronavirus disease 2019 severity and death. *Iscience* (2021) 24:102711. doi: 10.1016/j.isci.2021.102711

27. Sweeney TE, Shidham A, Wong HR, Khatri P. A comprehensive time-course–based multicohort analysis of sepsis and sterile inflammation reveals a robust diagnostic gene set. *Sci Transl Med* (2015) 7:287ra71. doi: 10.1126/scitranslmed.aaa5993

28. Cazalis M-A, Friggeri A, Cavé L, Demaret J, Barbalat V, Cerrato E, et al. Decreased HLA-DR antigen-associated invariant chain (CD74) mRNA expression predicts mortality after septic shock. *Crit Care* (2013) 17:R287. doi: 10.1186/cc13150

29. Unterman A, Sumida TS, Nouri N, Yan X, Zhao AY, Gasque V, et al. Single-cell multi-omics reveals dyssynchrony of the innate and adaptive immune system in progressive COVID-19. *Nat Commun* (2022) 13:440. doi: 10.1038/s41467-021-27716-4

30. Neumann J, Prezzemolo T, Vanderbeke L, Roca CP, Gerbaux M, Janssens S, et al. Increased IL-10-producing regulatory T cells are characteristic of severe cases of COVID-19. *Clin Transl Immunol* (2020) 9:e1204. doi: 10.1002/cti2.1204

31. Saichi M, Ladjemi MZ, Korniotis S, Rousseau C, Hamou ZA, Massenet-Regad L, et al. Single-cell RNA sequencing of blood antigen-presenting cells in severe COVID-19 reveals multi-process defects in antiviral immunity. *Nat Cell Biol* (2021) 23:538–51. doi: 10.1038/s41556-021-00681-2

32. Consortium Co-19 MBAt (COMBAT), DJ A, Ai Z, Ainsworth M, Allan C, Allcock A, et al. A blood atlas of COVID-19 defines hallmarks of disease severity and specificity. *Cell* (2022) 185:916–38.e58. doi: 10.1016/j.cell.2022.01.012

33. Zeberg H, Pääbo S. A genomic region associated with protection against severe COVID-19 is inherited from neandertals. *Proc Natl Acad Sci* (2021) 118: e2026309118. doi: 10.1073/pnas.2026309118

34. Li Y, Renner DM, Comar CE, Whelan JN, Reyes HM, Cardenas-Diaz FL, et al. SARS-CoV-2 induces double-stranded RNA-mediated innate immune responses in respiratory epithelial-derived cells and cardiomyocytes. *Proc Natl Acad Sci* (2021) 118:e2022643118. doi: 10.1073/pnas.2022643118

35. Shaath H, Vishnubalaji R, Elkord E, Alajez NM. Single-cell transcriptome analysis highlights a role for neutrophils and inflammatory macrophages in the pathogenesis of severe COVID-19. *Cells* (2020) 9:2374. doi: 10.3390/cells9112374

36. Davenport EE, Burnham KL, Radhakrishnan J, Humburg P, Hutton P, Mills TC, et al. Genomic landscape of the individual host response and outcomes in sepsis: a prospective cohort study. *Lancet Respir Med* (2016) 4:259–71. doi: 10.1016/s2213-2600(16)00046-1

37. Halasz G, Sperti M, Villani M, Michelucci U, Agostoni P, Biagi A, et al. A machine learning approach for mortality prediction in COVID-19 pneumonia: Development and evaluation of the piacenza score. *J Med Internet Res* (2021) 23: e29058. doi: 10.2196/29058

38. Zhao Z, Chen A, Hou W, Graham JM, Li H, Richman PS, et al. Prediction model and risk scores of ICU admission and mortality in COVID-19. *PLoS One* (2020) 15:e0236618. doi: 10.1371/journal.pone.0236618

39. Banoei MM, Dinparastisaleh R, Zadeh AV, Mirsaeidi M. Machine-learning-based COVID-19 mortality prediction model and identification of patients at low and high risk of dying. *Crit Care* (2021) 25:328. doi: 10.1186/s13054-021-03749-5

frontiers | Frontiers in Immunology

TYPE Original Research
PUBLISHED 04 November 2022
DOI 10.3389/fimmu.2022.1028613

OPEN ACCESS

EDITED BY
Pietro Ghezzi,
University of Urbino Carlo Bo, Italy

REVIEWED BY
Talita Glaser,
University of São Paulo, Brazil
Suchitra Kamle,
Brown University, United States

*CORRESPONDENCE
Satoshi Kanazawa
kanas@med.nagoya-cu.ac.jp

SPECIALTY SECTION
This article was submitted to Inflammation, a section of the journal Frontiers in Immunology

RECEIVED 26 August 2022
ACCEPTED 14 October 2022
PUBLISHED 04 November 2022

CITATION
Miura Y, Ohkubo H, Nakano A, Bourke JE and Kanazawa S (2022) Pathophysiological conditions induced by SARS-CoV-2 infection reduce ACE2 expression in the lung. *Front. Immunol.* 13:1028613. doi: 10.3389/fimmu.2022.1028613

Pathophysiological conditions induced by SARS-CoV-2 infection reduce ACE2 expression in the lung

Yoko Miura[1], Hirotsugu Ohkubo[2], Akiko Nakano[2], Jane E. Bourke[3] and Satoshi Kanazawa[1*]

[1]Department of Neurodevelopmental Disorder Genetics, Nagoya City University Graduate School of Medical Sciences, Nagoya, Japan, [2]Department of Respiratory Medicine, Allergy and Clinical Immunology, Nagoya City University Graduate School of Medical Sciences, Nagoya, Japan, [3]Department of Pharmacology, Biomedicine Discovery Institute, Monash University, Clayton, VA, Australia

SARS-CoV-2 infection causes a variety of physiological responses in the lung, and understanding how the expression of SARS-CoV-2 receptor, angiotensin-converting enzyme 2 (ACE2), and its proteolytic activator, transmembrane serine protease 2 (TMPRSS2), are affected in patients with underlying disease such as interstitial pneumonia will be important in considering COVID-19 progression. We examined the expression of ACE2 and TMPRSS2 in an induced usual interstitial pneumonia (iUIP) mouse model and patients with IPF as well as the changes in whole-lung ACE2 and TMPRSS2 expression under physiological conditions caused by viral infection. Histopathological and biochemical characteristics were analyzed using human specimens from patients with IPF and precision-cut lung slices (PCLS) from iUIP mouse model showing UIP with honeycombing and severe fibrosis after non-specific interstitial pneumonia. ACE2 expression decreased with acute lung inflammation and increased in the abnormal lung epithelium of the iUIP mouse model. ACE2 is also expressed in metaplastic epithelial cells. Poly(I:C), interferons, and cytokines associated with fibrosis decreased ACE2 expression in PCLS in the iUIP model. Hypoxia also decreases ACE2 *via* HIF1α in PCLS. Antifibrotic agent, nintedanib attenuates ACE2 expression in invasive epithelial cells. Patients with IPF are at a higher risk of SARS-CoV-2 infection due to the high expression of ACE2. However, ACE2 and TMPRSS2 expression is decreased by immune intermediaries, including interferons and cytokines that are associated with viral infection and upon administration of antifibrotic agents, suggesting that most of the viral infection-induced pathophysiological responses aid the development of resistance against SARS-CoV-2 infection.

KEYWORDS

angiotensin converting enzyme 2 (ACE2), idiopathic pulmonary fibrosis (IPF), SARS-CoV-2, precision-cut lung slices (PCLS), transmembrane protease, serine 2 (TMPRSS2)

Introduction

A limited number of type II alveolar epithelial (AECII) and ciliated cells in pulmonary bronchi express angiotensin-converting enzyme 2 (ACE2). The transmission of severe acute respiratory syndrome coronavirus 2 (SARS-CoV-2) involves ACE2, leading to coronavirus disease-19 (COVID-19) (1, 2). ACE2 catalyzes the conversion of the vasoconstrictor angiotensin II to the vasodilation peptide angiotensin 1–7. The imbalance between vasoconstriction and vasodilation through altered ACE2 expression is associated with hypertension and chronic pulmonary diseases such as idiopathic pulmonary fibrosis (IPF) (3–5). ACE2 regulates ACE-induced fibrosis in a reciprocal manner (6, 7). Transmembrane serine protease 2 (TMPRSS2), which proteolytically activates the SARS-CoV-2 spike protein, is also expressed in AECII and type I alveolar epithelial (AECI) and ciliated cells (8). TMPRSS2 cooperates with the internalization of SARS-CoV-2 into lung epithelial cells.

SARS-CoV-2 infection induces disease-associated bias in type 1-helper T cells. Interferon (IFN)-γ-producing T cells are a major source of various cytokines and chemokines, including IFNs (9). Considering the early pathogenesis of COVID-19, lung epithelial cells produce IFNs upon SARS-CoV-2 infection and subsequently induce the production of IFN-stimulated genes (ISGs) (2, 10). IFNs and poly(I:C) induce ACE2 in human upper airway basal and nasal epithelial cells (2, 11) in lung cancer cells but not in primary human differentiated bronchial cells (12). Interleukin (IL)-4 and IFN-γ/tumor necrosis factor (TNF)-α reduced *Ace2* expression in Vero E6 cells, resulting in decreased SARS-CoV infection; thus, genetic regulation of ACE2 *via* cytokines appears to be cell type-dependent (13). A marked increase in ACE2 expression in patients with IPF predicts severe SARS-CoV-2 infection. ACE2 deficiency exacerbates bleomycin-induced lung fibrosis in mice and reduces inflammatory cytokines such as IL-6 and TNF-α (14, 15). ACE2 overexpression suppresses collagen production *via* hypoxia and attenuates pulmonary fibrosis (PF) formation (16). ACE2 inhibits cancer cell migration by reducing the activities of matrix metalloprotease (MMP) 2 and MMP9 (17). In addition, ACE and vascular endothelial growth factor A levels were also reduced *via* the angiotensin II type 1 receptor. ACE2 is protective against acute and chronic lung failure and fibrosis under hypoxic conditions (3). The COVID-19 cytokine storm, which results from the rapid production of pro-inflammatory cytokines such as IL-6, TNF-α, and IFN-γ, is correlated with an unfavorable outcome with immune dysregulation (18). Decreasing IFN-γ-producing T-cells appears to be critical for antibody production (9). As RNA viral infection sensor, toll-like receptors (TLRs) such as TLR3 and TLR7 were activated during SARS-CoV-2 infection (19). Poly(I:C) together with TGF-β induces MMP9 production *via* TLR3 (20, 21). IL-6 acts as a pro-fibrotic factor and stimulates collagen production in various cells, including fibroblasts, whereas IFN-γ causes a reduction in collagens and fibronectin as an antifibrotic agent (22, 23). Viral infection is a risk factor for exacerbating interstitial lung disease (ILD) (24). Worse outcomes have been reported in patients with COVID-19 and other underlying diseases (25, 26). As antifibrotic therapies for ILD or progressive fibrosing interstitial lung disease, pirfenidone and nintedanib are effective but have different pharmacological actions. Nintedanib has shown efficacy in the treatment of COVID-19 (27). These agents may be effective in the treatment of post-COVID lung fibrosis (28).

We developed an induced usual interstitial pneumonia (iUIP) mouse model (29). Bimodal fibrosis was also observed in this model. Primary fibrosis with severe acute inflammation was observed at weeks 2–4 during the non-specific interstitial pneumonia (NSIP) stage after BMS induction wherein bleomycin was mixed with an equal volume of microbubbles before sonoporation. Secondary fibrosis occurs at weeks 10–14 after BMS induction (UIP stage). Metaplastic epithelial conversion and honeycomb formation were observed at the UIP stage. Most metaplastic cells express secretoglobin family 1A member 1 (*Scgb1a1*), but not keratin 5 (*Krt5*). These cells produce a laminin-degrading product (γ2 proteolytic fragment, γ2PF) by disrupting the basement membrane and acquiring invasive properties (30). These invasive cells are distinct from lineage-negative epithelial stem/progenitor or basal cells, or hyperplastic AECII (31). The iUIP model is based on D1CC×D1BC transgenic mice, which develop inflammatory arthritis followed by ILD after immunization with low doses of arthritogenic antigen, hereafter termed the induced rheumatoid arthritis-associated interstitial lung disease (iRA-ILD) mouse model. The major histopathological features in the iRA-ILD model were similar to those of NSIP with inflammation, but with milder epithelial abnormalities than those in iUIP mice (32). The antifibrotic agent nintedanib ameliorated fibrosis and reduced the number of invasive epithelial cells.

Precision-lung cut slices (PCLS), an *ex vivo* tissue culture using lung sections, have been applied to various translational analyses (33). This technique was originally developed to analyze bronchoconstriction-induced effectors and has been applied to the evaluation of chemical toxicity (34). More recently, the lungs from conventional bleomycin-induced IPF models and human specimens have been used to evaluate fibrosis and the effects of therapeutic agents (35, 36). PCLS from bleomycin-treated animals were used to evaluate the therapeutic targets of IPF (37).

In this study, we examined the expression levels of ACE2 and TMPRSS2 in patients with IPF and iUIP mouse. We also investigated the effects of SARS-CoV-2 infection on various physiological conditions induced by IFNs, fibrosis-related cytokines, poly(I:C)-induced viral infection mimicry and hypoxia, using *ex vivo* cultures of PCLS from iUIP mice. Finally, we examined whether antifibrotic agents altered ACE2 expression in iUIP mice.

10.3389/fimmu.2022.1028613

Materials and methods

Mice details and pirfenidone and nintedanib administration protocol

D1CC×D1BC tg mice bred on a DBA/1J background were housed in a pathogen-free animal care facility at Nagoya City University Medical School in accordance with institutional guidelines (38). iUIP mice were administered pirfenidone (3.6 mg/mouse/day, n = 8), nintedanib (1.8 mg/mouse/day, n = 10), or the vehicle (sterilized 0.5% of methylcellulose, Fujifilm-Wako, Tokyo, Japan, n = 9) orally daily from 6–14 weeks after BMS treatment.

BMS induction protocol

Bleomycin (0.512 mg/mL in normal saline, Nippon Kayaku) was mixed with an equal volume of microbubbles (Ultrasound Contrast Agent SV-25, NepaGene) and administered *via* the i.t. route using a spray nebulizer (40 μl/mouse, 1.28 mg/kg body weight, Natsume), prior to sonoporation on the chest by 1.0 W/cm^2 for 1 min (Sonitron GTS Sonoporation System, NepaGene, BMS induction). IP induction was monitored by measuring serum SP-D levels.

Induction of inflammatory arthritis in iRA-ILD mouse model

Inflammatory polyarthritis followed by interstitial lung disease was induced as previously described (32). Briefly, mice were anesthetized with isoflurane and immunized with bColII (0.01 mg/mouse) with an equal volume of complete (1^{st}) and incomplete (2^{nd}–5^{th}) Freund's adjuvant. The first immunization was administered at 8–10 weeks after birth. Mice were monitored using joint scoring.

Human specimens

We analyzed lung biopsy specimens from three patients with IPF at Nagoya City University Graduate School of Medical Sciences. Lung controls were obtained from US Biomax (Derwood, MD, USA). The clinical features are presented in Supplementary Table 1.

In situ hybridization

Lungs were harvested at 0, 2, and 14 weeks after BMS induction for iUIP and at 43 weeks after the 1^{st} bColII immunization for RA-ILD, fixed overnight in 4% paraformaldehyde diluted in PBS, and embedded in paraffin before 2 μm thick sections were cut. *In situ* hybridization for *Scgb1a1, Sftpc, Krt5, Ace2*, and *Tmprss2* was performed using the RNAscope Multiplex Fluorescent Reagent Kit v2 (Advanced Cell Diagnostics, Newark, CA, USA) according to the manufacturer's instructions.

Immunohistochemistry

For mouse lung immunohistochemistry, the deparaffinized sections were stained with the following primary antibodies: rabbit anti-E-cadherin and rabbit anti- MMP7 (Cell Signaling Technology, Danvers, MA, USA), rabbit anti-SP-C (Hycult Biotech, Uden, Netherlands), and ACE-2 (R&D Systems, Minneapolis, MN, USA). For human lung immunohistochemistry, deparaffinized sections were stained with the following primary antibodies: rabbit anti-E-cadherin (Cell Signaling Technology), rabbit anti-proSP-C (Merck, Darmstadt, Germany), rabbit anti-ACE-2 (R&D Systems), and mouse anti-Laminin γ2 N-terminal fragment (γ2pf, Funakoshi, Tokyo, Japan). Histofine simple stain mouse MAX-PO secondary antibodies (Nichirei, Tokyo, Japan) and the Opal multiplex fluorescent immunohistochemistry system (Akoya Biosciences, Marlborough, MA, USA) were used according to the manufacturer's protocol. All the images were captured using a fluorescence microscope (BZ-X710; Keyence, Osaka, Japan). To calculate the percentage of $Ace2^+$ cells in E-cadherin$^+$ bronchioles or invasive epithelial cells from the UIP lungs of four mice, five images (200× magnification) were captured and the percentage of Ace2 positive cells was calculated by ImageJ Fiji.

PCLS preparation

Fresh lungs were isolated from iUIP and control mice under sterile conditions. Lungs were filled with 2% of low-melting agarose in HBSS (agarose: Sigma-Aldrich, Steinheim, Germany; HBSS; Thermo Fisher Sciences, Waltham, MA, USA; agarose solution was preincubated at 45°C before use). The whole carcass was chilled at 4°C for 10 min to allow gelling of the agarose. Each lobe was dissected and embedded in the 2% of low-melting agarose. The embedded lung was cut to a thickness of 300 μm using a vibratome (Compresstome ^{TM} VF-300 OZ, Precisionary, Natick, MA, USA). Approximately 60 slices were collected from each mouse. All PCLS were cultured in DMEM/F12 (Sigma-Aldrich) media supplemented with 0.1% fetal bovine serum, 100 U/mL penicillin, 100 μg/mL streptomycin, and 2.5 μg/mL amphotericin for 24 h and frozen with CELLBANKER 1 (Zynogen Pharma, Fukushima, Japan) before use.

Ex vivo culture of PCLS

Ex vivo culture of PCLS was performed at 37°C in 5% CO_2 for 96 h in the case of poly(I:C) and/or IFNs and for 120 h in the case of fibrosis cocktail. IFN-γ (100 ng/ml, Fujifilm-Wako), IFN-α2 (100 ng/ml, R&D Systems), and Poly(I:C) (10 ng/ml, Tocris, Bristol, UK) were used to simulate RNA virus infections, such as SARS-CoV-2. The fibrosis cocktail consisted of 10 ng/ml platelet-derived growth factor (PDGF)-BB (Fujifilm-Wako), 10 ng/mL TNF-α (Fujifilm-Wako), 5 ng/mL transforming growth factor-β (TGF-β) (R&D systems), and 5 μM lysophosphatidic acid (LPA) (Focus Biomolecules, Plymouth Meeting, PA) and was replenished at 48 and 96 h (35). The O_2 concentrations for hypoxia and physioxia were used as 2 and 5%, respectively (39, 40). PCLSs were incubated under hypoxia, physioxia, and normaxia (21% O_2) for 12, 24 and 48 h with or without Roxadustat (50 μM, Cayman, MI, USA) in hypoxia chamber (SV-140A, Blast, Tokyo).

Western blot

The following primary antibodies were used: goat anti-ACE-2 (R&D Systems) and rabbit anti-β-actin (Proteintech Group, Tokyo, Japan). ECL™ anti-rabbit IgG (GE Healthcare, Uppsala, Sweden) or anti-goat IgG (R&D Systems) horseradish peroxidase-linked antibodies were used as the secondary antibodies. Each signal was detected using ImmunoStar Zeta or ImmunoStar LD (Fujifilm Wako) and Amersham Imager 600 series (GE Healthcare). Statistical analysis of the expression levels of each protein was performed using ImageJ Fiji (41). All actual western blotting data are in Supplementary Figure 1.

Quantitative PCR analysis

Total RNA was extracted using the RNeasy Mini Kit (Qiagen, Hilden, Germany) for lung tissues and ReliaPrep RNA Tissue Miniprep System (Promega, Madison, WI, USA) for PCLS samples according to the manufacturer's instructions. For qPCR, cDNA was synthesized using ReverTra Ace qPCR RT Master Mix with gDNA Remover (TOYOBO, Osaka, Japan). qPCR was performed using the PrimeTime Gene Expression Master Mix (Integrated DNA Technologies, Coralville, IA, USA). The relative expression of each gene was determined by an internal control using *Hprt* for each sample.

Statistical analyzes

The results are shown as mean ± standard error (SE). Differences between non-instillation (0 w) or vehicle, and the other groups were evaluated by one-way analysis of variance (ANOVA) followed by Student's *t* test or Dunnett's test for parametric data (Prism9, GraphPad). In the pirfenidone and nintedanib administration studies, statistical significance among data at UIP phase (14 weeks), 0 weeks, and at the time of drug administration were evaluated using one-way ANOVA followed by Dunnett's test for parametric data (Prism9, GraphPad). Values of $P < 0.05$ were considered statistically significant.

Results

ACE2 is expressed in invasive epithelial cells of iUIP mouse

SARS-CoV-2 binds to ACE2, which is specifically expressed in AECII in the lungs. To assess the alteration of ACE2 in interstitial pneumonia, we performed *in situ* hybridization using the iUIP mouse model. In iUIP mice, bimodal fibrosis consisted of pulmonary fibrosis with inflammation (an NSIP stage, most sampling at week 2 after intratracheal instillation of bleomycin) and chronic fibrosis with less inflammation (a UIP stage, most sampling at week 14 after intratracheal instillation of bleomycin). The expression of ACE2 was limited mainly to surfactant protein C (*Sftpc*)$^+$ AECII and bronchioles, such as ciliated cells (Figure 1A). The number of *Ace2*$^+$/*Sftpc*$^+$ cells decreased at the NSIP stage, and most *Ace2*$^+$ cells were excluded from hyperplastic AECII (3). At the UIP stage, *Ace2* expression increased dramatically and was distinguished from most cells expressing *Sftpc* alone (Figure 1A-3 and -4). Next, we examined the expression of *Tmprss2* at both stages. While the expression of *Tmprss2* was weak at week 0 and the NSIP stage, the levels of *Tmprss2* and *Ace2* increased in *Scgb1a1*$^+$ invasive epithelial cells at the UIP stage (Figure 1B). Honeycomb-forming epithelial cells expressed *Tmprss2* and *Ace2*, but some cells expressed *Tmprss2* alone (Figure 1B, white arrow). The expression of *Ace2* was also observed in invasive epithelial cells found in the iRA-ILD mouse model (Figure 1B). Some of these invasive epithelial cells expressed E-cadherin, MMP7, and ACE2, even at the protein level, at UIP stage (Figure 1C). Hyperplastic AECII, honeycomb structure, and E-cadherin$^+$ invasive epithelial cells are typical pathologies of the UIP stage. Expression of the ACE2 protein was detected in honeycomb-forming epithelial cells and hyperplastic areas (Figure 1D). Approximately 20% of E-cadherin-positive cells expressed Ace2 (Figure 1E). Thus, aberrantly expressed-Ace2 was widely distributed throughout the lungs at this stage. *Krt5*$^+$ basaloid cells are adjacent to invasive *Scgb1a1*$^+$ ones. We examined whether *Ace2* expression was excluded from *Krt5*$^+$ basaloid cells. *Ace2* expression was not detected in *Krt5*$^+$ basaloid cells (Figure 1F).

10.3389/fimmu.2022.1028613

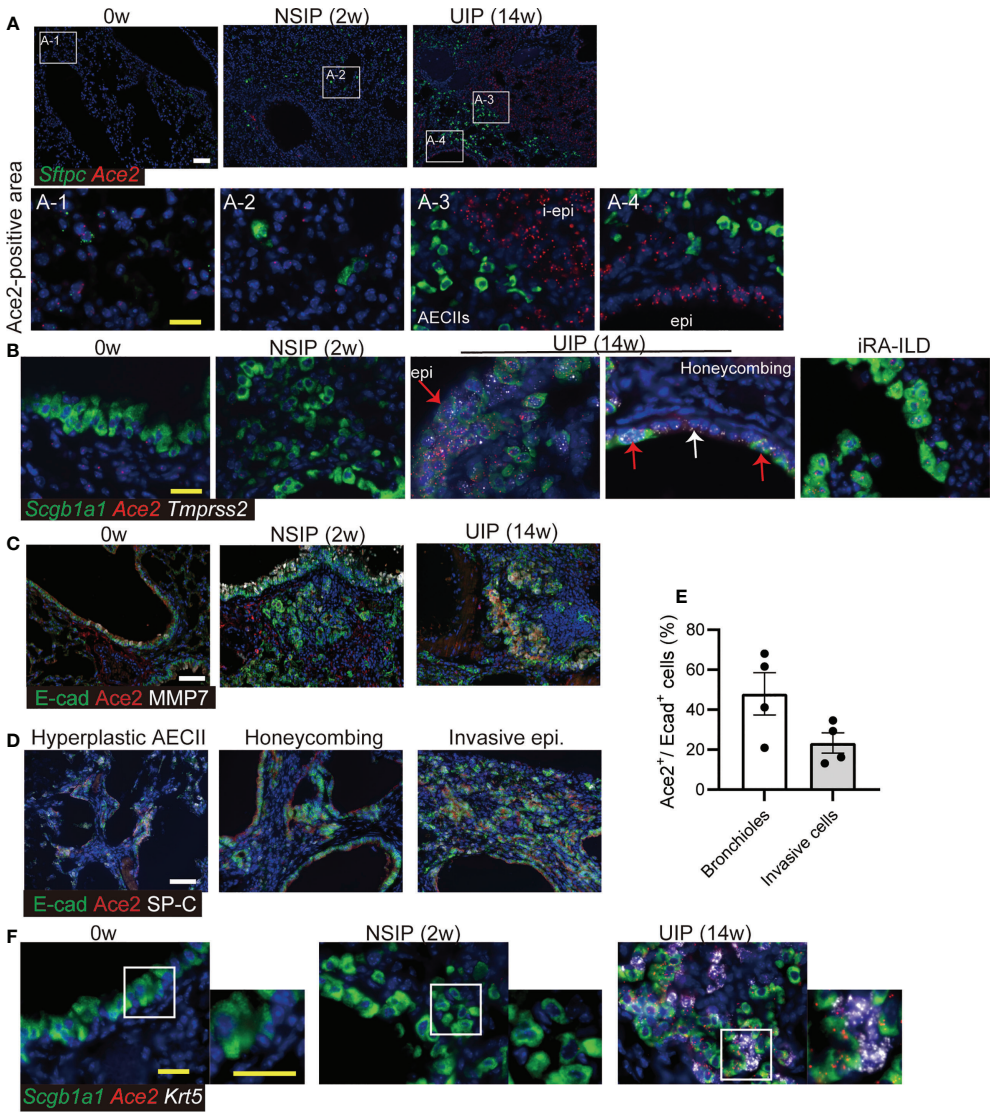

FIGURE 1
Ace2 expresses in AECII and epithelial cells with abnormalities. **(A)** *In situ* hybridization of *Sftpc* (green) and *Ace2* (red), **(B)** *Scgb1a1* (green), *Ace2* (red), and *Tmprss2* (white) in the lungs at week 0, the NSIP (2w), the UIP (14w) stages, and iRA-ILD. Red arrows indicate epithelial cells expressing *Scgb1a1*, *Ace2*, and *Tmprss2*. The white arrow indicates the inner cells of the honeycomb structure that express only *Tmprss2*. A-1 to-4 are enlarged images. **(C)** Immunohistochemical staining for E-cadherin (E-cad, green), ACE2 (red), and MMP7 (white) at week 0, the NSIP, and the UIP stages. **(D)** Immunohistochemical staining for E-cadherin (green), ACE2 (red), and SP-C (white) in the areas of hyperplastic AECII, honeycombing, and invasive epithelial cells at the UIP stage. **(E)** Percentage of $Ace2^+$ cells in E-$cadherin^+$ bronchioles or invasive cells at the UIP stage. Data are presented as mean ± SE of five images. **(F)** *in situ* hybridization of *Scgb1a1* (green), *Ace2* (red), and *Krt5* (white) in the bronchiolar epithelium at week 0, the NSIP, and the UIP stages. Scale bars indicate 50 μm (white) and 20 μm (yellow).

ACE2 expression is low at the NSIP stage and high at the UIP stage

Next, qPCR was performed for *Ace2*, *Tmprss2*, and *Il6* expression in whole-lung extracts of the iUIP model. *Ace2* and *Tmprss2* expression decreased at the NSIP stage (Figures 2A, B). On the other hand, *Ace2* expression increased at the UIP stage more than week 0. In contrast, *Il6* expression was inversely correlated with, rather than coincident with, *Ace2* expression (Figures 2A–C). The expression of *Ifng* increased after bleomycin induction (Figure 2D); however, the expression of *Ifna2* was not detected in qPCR (data not shown). The lungs at the UIP stage of the iUIP mice were studied under hypoxia. Endothelin-1 (*Edn1*) and angiotensin-converting enzyme (*Ace*), which act as a counterpart of vasoregulatory ACE2, were tested; *Edn1* showed no increase either NSIP or UIP stage, whereas *Ace*

10.3389/fimmu.2022.1028613

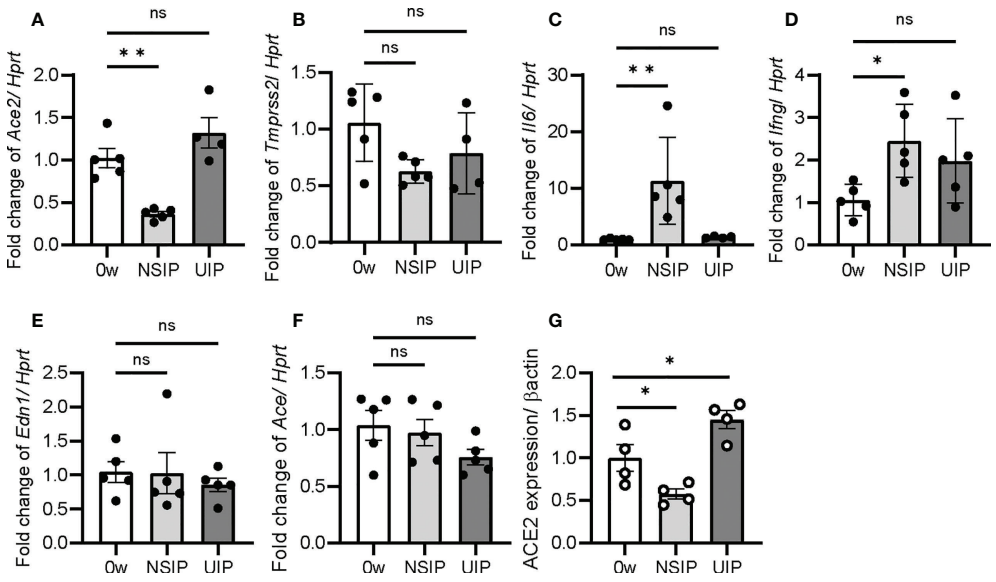

FIGURE 2
Ace2 expression was increased at UIP stage. The expression of *Ace2, Tmprss2, Il6, Ifng, Edn1,* and *Ace* was determined by qPCR in the whole lung extract **(A–F)** and western blotting for ACE2 expression **(G)**. Data are presented at week 0 as the controls and at the NSIP, and the UIP stages. *Hprt* and β-actin were used as the internal controls for qPCR and western blotting, respectively. Data are presented as mean ± SE of four to five mice at each stage. Asterisks indicate **P* < 0.05, ***P* <0.01, compared with week 0. "ns" is not statistically significant.

decreased slightly at the UIP stage (Figures 2E, F). At the UIP stage, increased Ace2 expression was confirmed at the protein level (Figure 2G).

ACE2 expression is elevated in IPF

Squamous metaplasia is often observed in patients with PF. These metaplastic epithelia were localized in the bronchioles, including honeycombing, and diffused into the lungs (Figure 3A). Since ACE2 expression was elevated in invasive epithelial cells at the UIP stage of the mouse model, we investigated whether ACE2 expression was observed in the bronchiolar epithelium with abnormalities in patients with IPF by qPCR. Most of these cells expressed ACE2, E-cadherin, and SP-C (Figure 3B). In contrast, SP-C-positive AECII expressed only ACE2 in the normal regions of the same specimens and in the control. Bronchiolar epithelial cells that acquire invasiveness feature increased laminin-5 expression, which is prognostically significant for lung cancer, and high levels of ACE2 expression have been reported in squamous carcinoma tissues (17). Thus, we examined whether γ2pf, as a cancer marker, is related to invasiveness and colocalizes with ACE2-positive cells in patients with IPF. A small number of ACE2/E-cadherin-positive diffused cells expressed γ2pf, suggesting that most of the ACE2-positive cells were not malignant (Figure 3C).

Poly(I:C) and IFNs mixture reduced *Ace2* expression

Ex vivo cultures of PCLS from iUIP mice were used to assess the biological response of whole lung tissue to extracellular effectors. The effects of poly(I:C) alone (mimicking SARS-CoV-2 infection) and poly(I:C)/IFN-α2 and -γ mixtures (as IFNs production after virus infection) in PCLS were examined by qPCR (Figure 4A). Poly(I:C) significantly increased *Ifng* expression at the UIP stage but not in *Ifna2* (Figures 4B, C). The combination of poly(I:C) and IFNs mixture produced more IFN-γ. Lungs from the UIP stage were susceptible to poly(I:C) treatment. These effectors enhanced *Il6* expression; however, there were no differences between the UIP stage and controls (Figure 4D). The antifibrotic effects of IFNs have been well studied. Indeed, poly(I:C) alone increased *Mmp9* expression, but an additional IFN mixture downregulated *Mmp9* expression (Figure 4E). Additionally, *Col1a1* expression was strongly downregulated (Figure 4F). Under these conditions, poly(I:C) alone did not alter *Ace2* expression, and the combination of poly

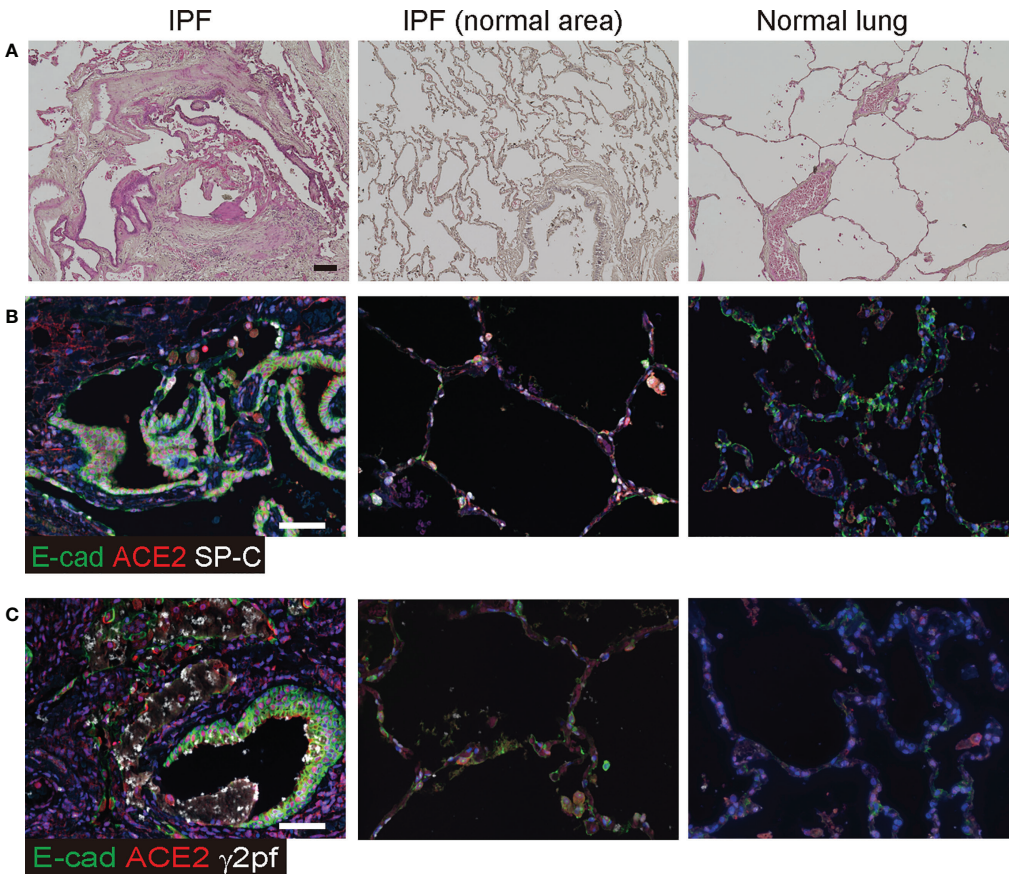

FIGURE 3
ACE2 was detected in epithelial cells of patients with IPF. **(A)** Histopathology of human normal lung and IPF lung. Specimens were stained with hematoxylin and eosin. **(B)** Immunohistochemical staining for E-cadherin (green), ACE2 (red), and SP-C (white) in the honeycombing region and normal area of IPF lung or the control. **(C)** Immunohistochemical staining for E-cadherin (green), ACE2 (red), and γ2PF (white) in squamous hyperplasia and the control area. Scale bars indicate 50 μm (black or white).

(I:C) and IFNs did not increase *Ace2* expression (Figure 4G). The expression of *Tmprss2* was not altered (Figure 4H). These data suggest that *Ace2* gene expression is regulated independently of viral infection and the subsequent cytokine storm.

Fibrosis cocktail decreased *Ace2* expression

The PCLS is also a useful tool for assessing the severity of fibrosis. In a previous study, a mixture of TNF-α, TGF-β, PDGF-BB, and LPA was used as a fibrosis cocktail to enhance *Col1a1* expression in PCLS (Figures 5A, B) (35). We examined whether *Ace2* expression is altered under fibrotic conditions in PCLS. In the murine PCLS system, the fibrosis cocktail enhanced *Col1a1* and *Acta2* expression at the UIP stage compared with that of the controls. The findings from this experiment suggests that UIP lungs are more susceptible to the fibrosis cocktail than that of normal lungs, even though *Il6* was the same in both samples (Figures 5B–D). Under these conditions, both *Ace2* and *Tmprss2* were downregulated by fibrosis cocktail treatment (Figures 5E, F). Next, we examined the effects of exposure to a mixture of poly(I:C) and IFNs and subsequent treatment with a fibrosis cocktail (Figure 5G). This sequential exposure had no effect on the decreased expression of *Ace2* and *Tmprss2* (Figures 5H, I).

Hypoxia decreased *Ace2* expression

The overall lung condition in the UIP stage was relatively hypoxic (Supplementary Figure 2). Therefore, we examined whether hypoxia (2% O_2) or physioxia (5% O_2) alters the expression of *Ace2* in PCLS (Figure 6A). Hypoxia decreased *Ace2* expression at 24 and 48 h (Figure 6B). In contrast, *Tmprss2* expression was increased after 48 h of hypoxia (Figure 6C).

10.3389/fimmu.2022.1028613

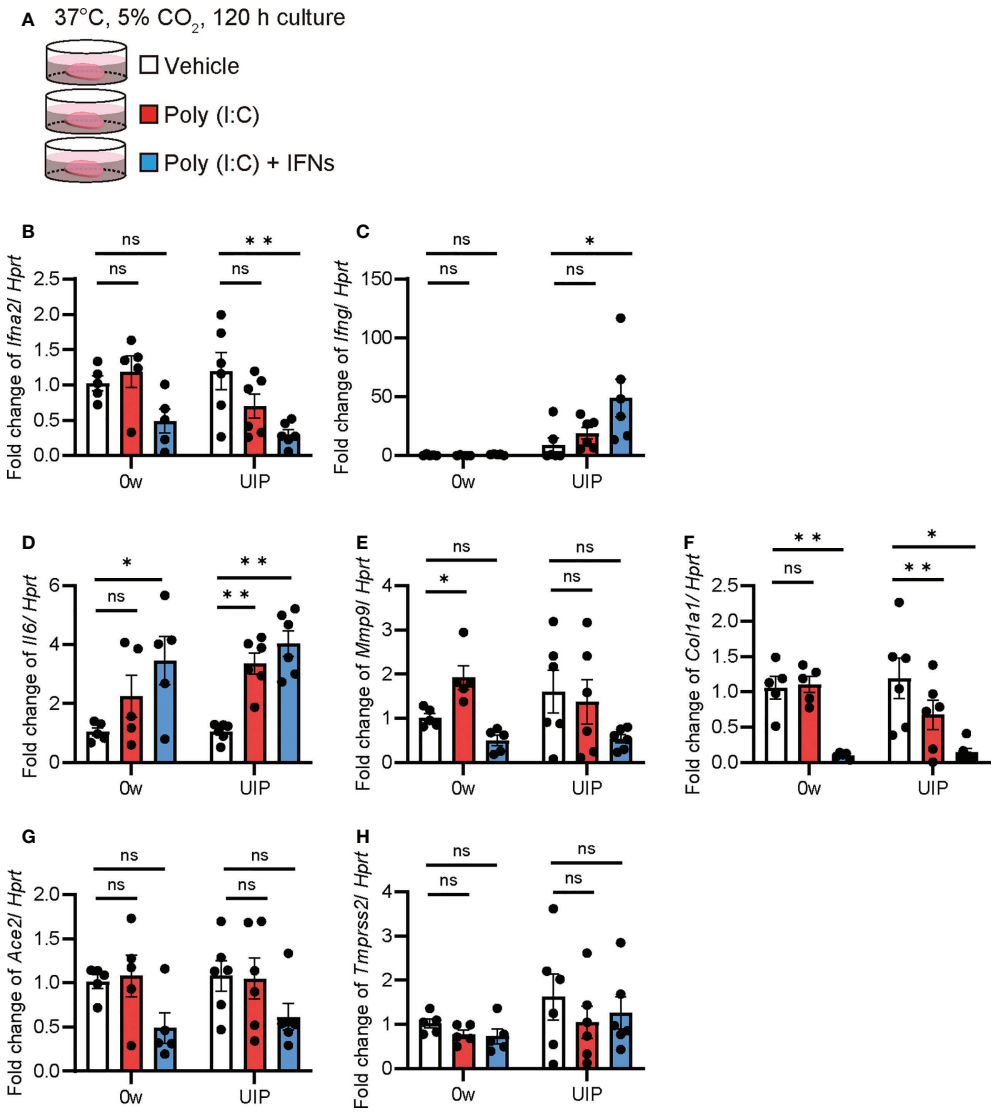

FIGURE 4
Poly(I:C) and the combination of poly(I:C) and INFs decreased *Ace2* expression in *ex vivo* culture using PCLS qPCRs using *ex vivo* culture of PCLS treated with poly(I:C) and the combination of poly(I:C) and IFNs were performed. **(A)** Schematic diagram of the protocol using poly(I:C) and a combination of poly(I:C) and INFs in PCLS. **(B–H)** Fold changes in expression levels of each gene, *Ifna2* **(B)**, *Ifng* **(C)**, *Il6* **(D)**, *Mmp9* **(E)**, *Col1a1* **(F)**, *Ace2* **(G)**, and *Tmprss2* **(H)** at week 0 and the UIP stage. *Hprt* expression was used as an internal control for qPCR. Each bar represents the control (vehicle, white bar), poly(I:C) alone (red bars), poly(I:C), and the combination of poly(I:C) and IFNs (blue bars), respectively. Each mRNA was prepared from PCLS samples from each stage of the iUIP mouse model. Data are presented as mean ± SE of five to six mice. Asterisks indicate $*P < 0.05$, $**P < 0.01$, compared with week 0. "ns" is not statistically significant.

Under these conditions, *Edn1* increased in a less oxygen-concentration-dependent manner (Figure 6D). Expression levels of Hif1a and Gapdh were increased under hypoxia (Supplementary Figures 3A, C). The hypoxia-inducible factor roxadustat inhibits prolyl hydroxylase (PHD), which stabilizes hypoxia inducible factor 1 subunit α (HIF1α) and induces gene transcription *via* HIF1α (Figure 6E). Thus, even under normoxia, roxadustat decreased *Ace2* expression but had no effect on *Tmprss2* (Figure 6F, G). Because roxadustat inhibits *Ace* and *End1*, it activates HIF1α but may have some side effects on gene regulation in the whole lung, including PCLS (Supplementary Figures 4A, C).

10.3389/fimmu.2022.1028613

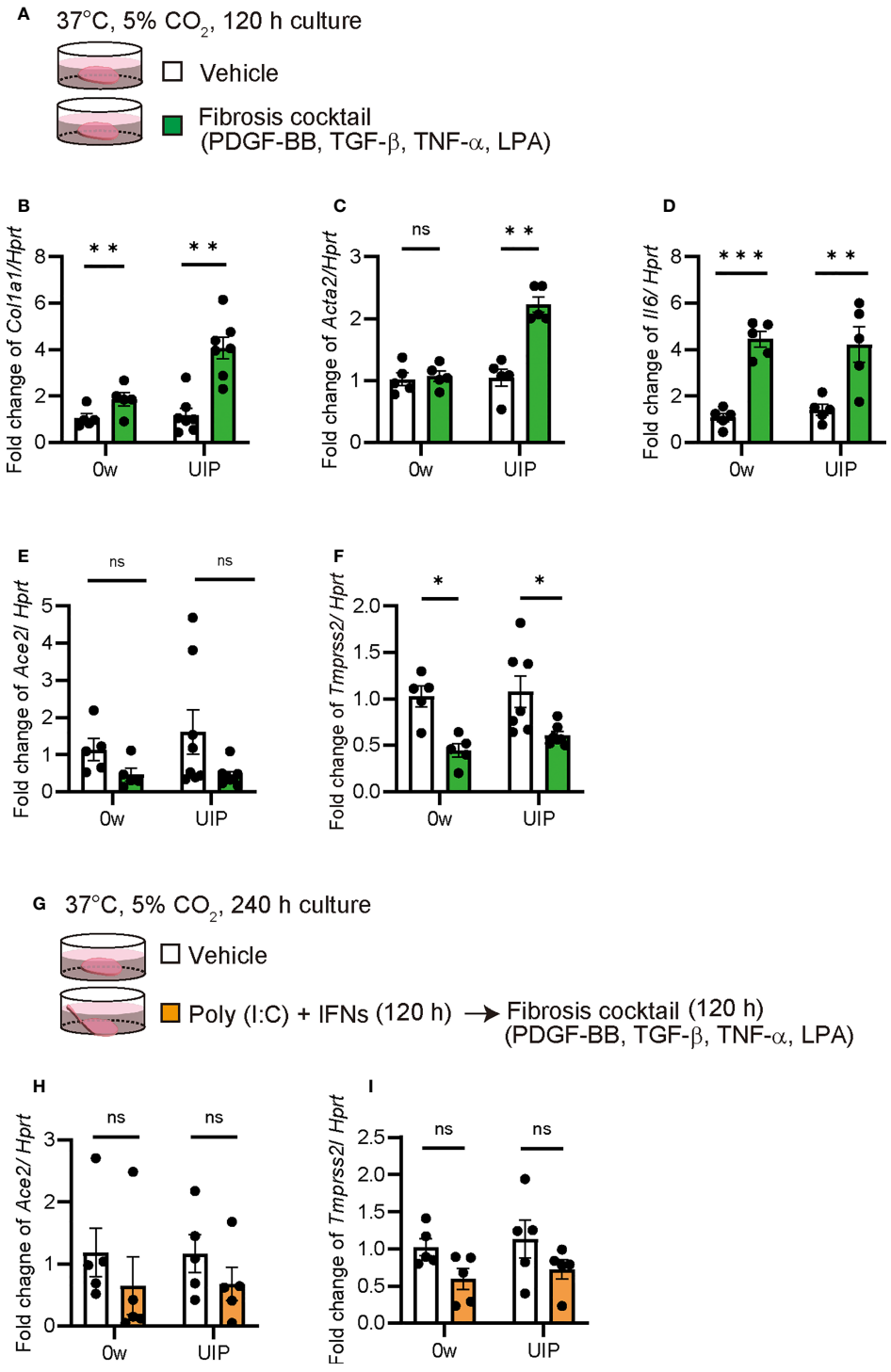

FIGURE 5
Fibrosis cocktail decreased *Ace2* and *Tmprss2* expression qPCRs using *ex vivo* culture of PCLS treated with fibrosis cocktail were performed. **(A)** Schematic diagram of the protocol for using a fibrosis cocktail in PCLS. **(B–F)** Fold changes in the expression levels of each gene, *Col1a1* **(B)**, *Acta2* **(C)**, *Il6* **(D)**, *Ace2* **(E)**, and *Tmprss2* **(F)** at week 0 and the UIP stage. **(G)** Schematic diagram of the protocol using a fibrosis cocktail following the combination of poly(I:C) and IFNs in PCLS. **(H, I)** Fold changes in the expression levels of *Ace2* **(H)** and *Tmprss2* **(I)**. *Hprt* expression was used as an internal control for qPCR. Each bar represents the vehicle (white bars) or fibrosis cocktail (green or orange bars). Each mRNA was prepared from PCLS samples from each stage of the iUIP mouse model. Data are presented as mean ± SE of five or seven mice. Asterisks indicate $*P < 0.05$, $**P < 0.01$, $***P < 0.001$, compared with week 0. "ns" is not statistically significant.

10.3389/fimmu.2022.1028613

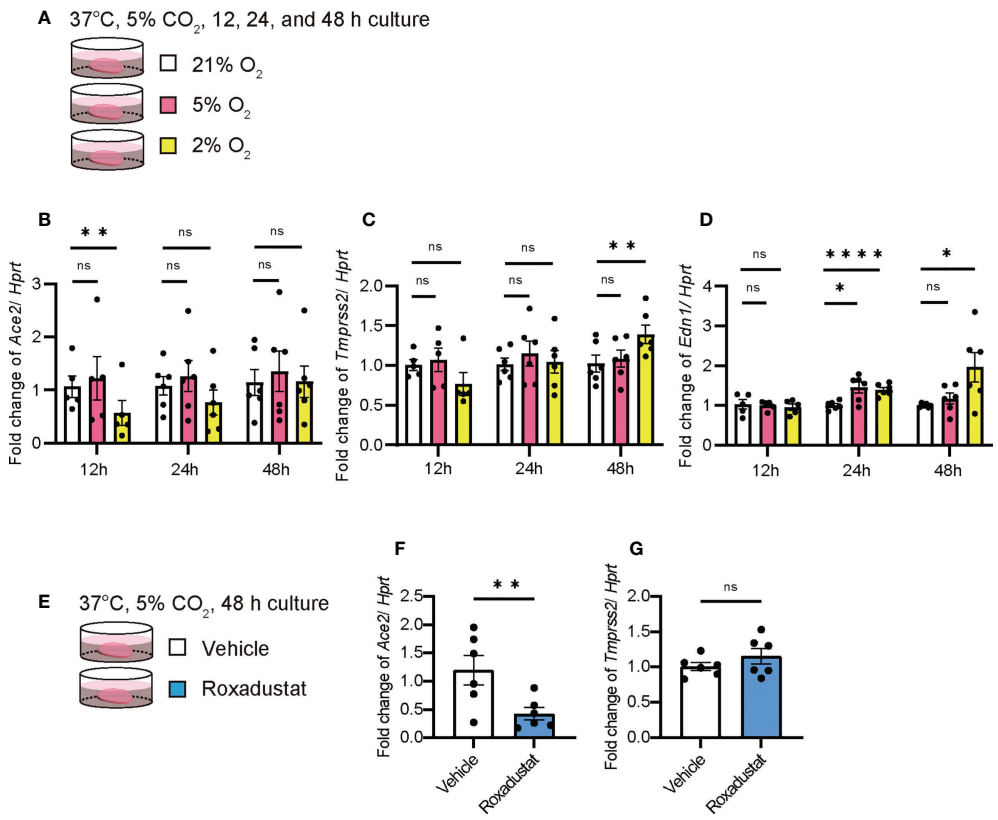

FIGURE 6
Hypoxia decreased Ace2 expression qPCRs using *ex vivo* culture of PCLS at week 0 under hypoxia were performed. **(A)** Schematic diagram of protocol in PCLS under normoxia (21%), physioxia (5%), and hypoxia (2%). **(B–D)** Fold changes in the expression levels of each gene, *Ace2* **(B)**, *Tmprss2* **(C)**, and *Edn1* **(D)**. **(E)** Schematic diagram of the protocol using roxadustat, which is an HIF-α prolyl hydroxylase inhibitor, under normoxia in PCLS. **(F–G)** Fold changes in the expression levels of *Ace2* **(F)** and *Tmprss2* **(G)**. *Hprt* expression was used as an internal control for qPCR. Each bar represents vehicle (white bars) and roxadustat (blue bars). Each mRNA was prepared from the PCLS samples after 12, 24, and 48 h of treatment. Data are presented as mean ± SE of five to six mice. Asterisks indicate *$P < 0.05$, **$P < 0.01$, and ****$P < 0.0001$ compared with week 0. "ns" is not statistically significant.

Antifibrotic agent, nintedanib decreased *Ace2* expression

iUIP mice were treated with the antifibrotic agents pirfenidone and nintedanib, and levels of ACE2 in whole lungs were compared by western blotting, qPCR, and *in situ* hybridization (Figure 7A, schematic diagram of pirfenidone or nintedanib treatment). Nintedanib and pirfenidone treatment decreased type I collagen expression (Figures 7B, C, and western blotting photos in Figure 2E). ACE2 expression was reduced with nintedanib treatment but not with pirfenidone (Figures 7D, E, 2E). This nintedanib-induced decrease in *Ace2* expression was also confirmed at the mRNA level (Figure 7F). In contrast, *Ace* expression was reduced at the UIP stage, suggesting that nintedanib restored the pulmonary blood pressure (Figure 7G). Nintedanib did not affect the expression of *Tmprss2* (Figure 7H). Since Ace2 expression was increased in invasive epithelial cells at the UIP stage, we examined whether nintedanib reduced *Ace2* expression in these cells using *in situ* hybridization. Nintedanib reduced *Ace2* expression but not *Tmprss2* expression (Figure 7I).

Discussion

We investigated whether patients with IPF are more susceptible to SARS-CoV-2 infection and whether subsequent virus-induced interferons and cytokines affected levels of ACE2 and TMPRSS2. ACE2 expression decreased with acute inflammation in the lung; however, it increased in the pulmonary epithelium with abnormalities in the iUIP mouse model. A similar pathological feature has been observed in patients with IPF. The combination of poly(I:C) and IFNs weakly decreased *Ace2* expression and did not alter *Tmprss2* expression in PCLS of the iUIP mouse model. Fibrosis-related cytokines suppress TMPRSS2 and elevate ACE2 expression.

10.3389/fimmu.2022.1028613

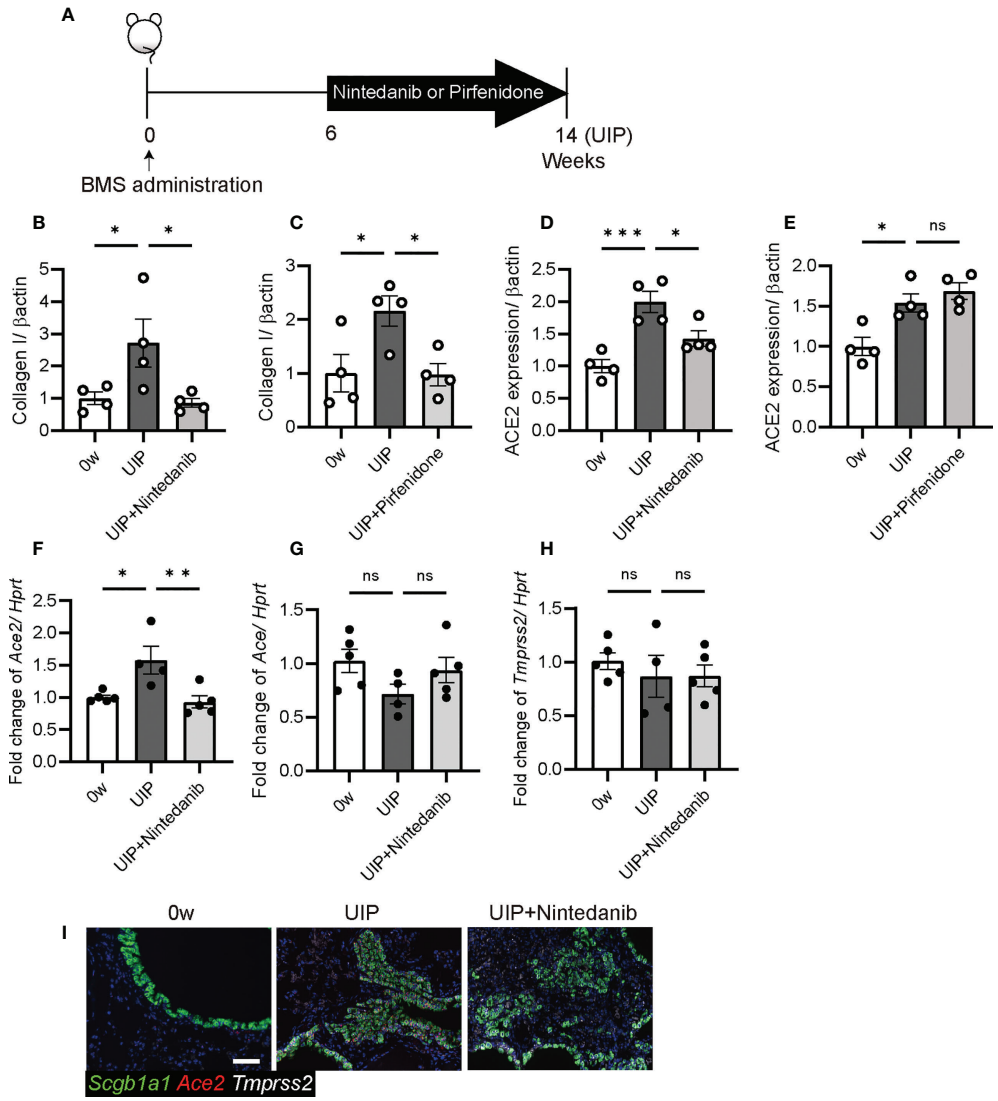

FIGURE 7
Nintedanib attenuated the degree of *Ace2* and *Ace* expression **(A)** Schematic diagram of protocol for the oral administration of nintedanib or pirfenidone. Both treatments were started from six weeks after BMS administration and were carried out daily for next eight weeks. **(B–E)** Western blotting was performed using protein extracts from each lung at week 0, the UIP stage, and the UIP stage with nintedanib (UIP+nintedanib) or pirfenidone (UIP+pirfenidone) treatments. **(B, C)** Nintedanib **(B)** and pirfenidone **(C)** decreased the expression of type I collagen at the UIP stage. **(D, E)** Nintedanib **(D)** decreased the expression of ACE2, whereas pirfenidone did not **(E)**. Expression data from western blotting were normalized to β-actin expression levels. **(F–H)** qPCR were performed using whole lungs from each mouse. Fold changes in expression levels of *Ace2* **(F)**, *Ace* **(G)**, and *Tmprss2* **(H)**. *Hprt* expression was used as an internal control of qPCR. **(I)** *in situ* hybridization of *Scgb1a1* (green), *Ace2* (red), and *Tmprss2* (white) in the lungs from each mouse at week 0, the UIP stage, and the UIP+nintedanib. Data are presented as mean ± SE averaged over 4-5 mice. Asterisks indicate **P* < 0.05, ***P* <0.01, and ****P* <0.001 compared with week 0. "ns" is not statistically significant.

Thus, SARS-CoV-2 infection enhances host defense, leading to suppression of viral entry into pulmonary epithelial cells. Nintedanib also suppress the expression of ACE2 in invasive epithelial cells during the UIP stage. However, it did not alter TMPRSS2 expression.

Notably, the level of ACE2 in a conventional bleomycin mouse model was controversial in previous studies (3, 4). In most cases, upregulation of ACE2 is observed in isolated epithelial cells or cell lines, such as lung cancer cells (12). However, consistent with the data on overexpression and loss of function of ACE2, we concluded that acute inflammatory conditions, such as the NSIP stage, induced the downregulation of ACE2 expression (Figure 2). In contrast, in chronic diseases such as IPF, pulmonary hypertension is present due to decreased pulmonary vascularity and decreased cytokines/chemokines in the lung, which may upregulate ACE2 expression. As a result,

vasodilation may be enhanced in patients with IPF. Severe capillary dysplasia is observed at the UIP stage of the iUIP mouse model (29). Hypoxia immediately induces ACE2 expression *via* a HIF-1α-independent pathway (42). The Subsequent HIF-1α expression increased ACE expression and reduced ACE2 expression by angiotensin II. Rather, hypoxia downregulated *Ace2* expression immediately in PCLS (Figure 6). These events suggests that normoxia is rather persistent in the whole lung of IPF because of the elevated expression of ACE2 but downregulated ACE (Figures 1, 2). Furthermore, ACE2 works in opposition to ACE and may lead to vasodilation from vasoconstriction, either locally or throughout the lung, to ameliorate pulmonary hypertension due to poor angiogenesis (29, 43). In contrast, infection with SARS-CoV-2 results in the downregulation of ACE2, both by the production of the infection itself and by the subsequent production of cytokines and chemokines. This event abrogated the beneficial changes in the increased ACE2 expression in IPF, even though it reduced the number of SARS-CoV-2 receptors.

Previous studies have suggested that IFNs might increase ACE2 expression and render lung epithelial cells more infectious. Interestingly, poly(I:C) or a mixture of Poly(I:C) and IFNs (IFN-α2 and IFN-γ) significantly induced *Ifng* at UIP stage, but not at week 0. Even under presumed autocrine/paracrine-mediated positive feedback by IFN-γ, *Ace2* expression was not induced, suggesting that IFN-γ and IFN-α2 have no potential to induce *Ace2* in PCLSs. *Col1a1* was also dramatically reduced by poly(I:C) and IFNs. Activation of TRL3 by poly(I:C) and subsequent IFNs functioned as an antifibrotic agent in the whole lung. Poly(I:C) and IFNs simultaneously enhanced *Il6* expression. Therefore, IFN treatment may lead to a therapeutic approach as an anti-fibrosis agent if it can block the function of *de novo* IL-6; otherwise, it is less effective (44). Focusing on inflammation, we can see that IL-6 and ACE2 are reciprocal; however, further investigation is needed. These data suggest that SARS-CoV-2 is unlikely to spread *via* elevated ACE2 expression to promote viral entry into lungs after infection. Under such conditions, these factors exert an antifibrotic effect, at least for short periods of time, such as during acute inflammation. Recently, *deltaACE2*, a truncated form of ACE2 without a binding site for SARS-CoV-2 and enzymatic activity, was identified only in primates (45). Canonical ACE2 is not an IFN-stimulated gene (46). No activation of IFN or OAS-RNase L was observed in alveolar type 2-derived pluripotent stem cells by SARS-CoV-2 infection (47). In contrast, mimicking SARS-CoV-2 infection with poly(I:C) induced the expression of both IFNs and IL-6, which appeared to be similar to the situation in virus-infected lungs. Under these conditions, the effect of IFNs overcomes the fibrotic condition induced by *Il6* (Figure 4). In fact, IFN-γ suppresses *Col1a2* and *Col1a1* expression (48). Since PCLS could respond to fibrosis cocktails and induce *Il6* and *Col1a1*, we concluded that viral infections, such as SARS-CoV-2, strongly suppress fibrosis (Figure 5). Therefore, after SARS-CoV-2 infection, under normal conditions, at least two phases function: an antifibrotic effect by IFNs and a hypoinfectious state for SARS-CoV-2 due to decreased ACE2 expression.

Post-COVID-19, reducing the incidence of pulmonary fibrosis has become an urgent global issue. It will be interesting to determine the effects of pirfenidone and nintedanib in this regard. In the mouse model, there were no obvious changes after pirfenidone treatment, but nintedanib decreased *Ace2* and increased *Ace* expression (Figure 6). This suggests a beneficial change in drug treatment for the disease. On the other hand, note that in the RA-ILD mouse model, there was no significant differences in gene expression with nintedanib treatment (49). Thus, nintedanib treatment induced a balanced host response to blood pressure in the lungs.

Using PCLS, we investigated the effect of viral infection on the entire lung. These results suggest that SARS-CoV-2 infection cannot directly and extensively promote viral entry into lung cells. Rather, severe capillary dysplasia is observed during the UIP stage of IPF, and ACE2 expression may increase to compensate for hypertension in the lungs. Thus, the decrease in ACE2 under viral infection may cause vasoconstriction rather than vasodilation, which may strain the blood vessels, especially capillaries. These results suggest that the lungs are resistant to further infection after the initial SARS-CoV-2 infection. However, SARS-CoV-2 infection may adversely affect blood vessels by reducing the expression of ACE2.

Data availability statement

The raw data supporting the conclusions of this article will be made available by the authors, without undue reservation.

Ethics statement

The studies involving human participants were reviewed and approved by The ethics board of the Nagoya City University Graduate School of Medicinal Sciences. The patients/participants provided their written informed consent to participate in this study. The animal study was reviewed and approved by The Committee on the Ethics of Animal Experiments of Nagoya City University.

Author contributions

YM and SK contributed to study design and the manuscript preparation. YM and AN performed immune-histopathology, *in situ* hybridization, and WB. JB contributed to study PCLS. AN and HO contributed to clinical management, patient recruitment and data analysis. All authors contributed to the article and approved the submitted version.

Funding

This research was supported by grants-in aid from the Ministry of Education, Culture, Sports, Science and Technology (MEXT)/JSPS KAKENHI Grant Number JP 17K16055 (YM), The Nitto Foundation 2020 (YM), GSK Japan Research Grant 2018 (YM), and a personal donation by T. Furuya (SK), a Project Grant from the National Health and Medical Research Council Australia Grant Number APP1165690 and APP1187755 (JB), and by JST START University Ecosystem Promotion Type (Supporting Creation of Startup Ecosystem in Startup Cities), Grant Number JPMJST2183, Japan. The funders were not involved in the study design, collection, analysis, interpretation of data, the writing of this article or the decision to submit it for publication.

Acknowledgments

We thank A. Nitatouge, T. Takenaka, Y. Chochi, S. Ogawa helping us with all aspects of this all. We would like to thank Editage (www.editage.com) for English language editing.

Conflict of interest

The authors declare that the research was conducted in the absence of any commercial of financial relationships that could be construed as a potential conflict of interest.

Publisher's note

All claims expressed in this article are solely those of the authors and do not necessarily represent those of their affiliated organizations, or those of the publisher, the editors and the reviewers. Any product that may be evaluated in this article, or claim that may be made by its manufacturer, is not guaranteed or endorsed by the publisher.

Supplementary material

The Supplementary Material for this article can be found online at: https://www.frontiersin.org/articles/10.3389/fimmu.2022.1028613/full#supplementary-material

References

1. Hoffmann M, Kleine-Weber H, Schroeder S, Kruger N, Herrler T, Erichsen S, et al. SARS-CoV-2 cell entry depends on ACE2 and TMPRSS2 and is blocked by a clinically proven protease inhibitor. *Cell* (2020) 181(2):271–80.e8. doi: 10.1016/j.cell.2020.02.052

2. Ziegler CGK, Allon SJ, Nyquist SK, Mbano IM, Miao VN, Tzouanas CN, et al. SARS-CoV-2 receptor ACE2 is an interferon-stimulated gene in human airway epithelial cells and is detected in specific cell subsets across tissues. *Cell* (2020) 181(5):1016–35.e19. doi: 10.1016/j.cell.2020.04.035

3. Li X, Molina-Molina M, Abdul-Hafez A, Uhal V, Xaubet A, Uhal BD. Angiotensin converting enzyme-2 is protective but downregulated in human and experimental lung fibrosis. *Am J Physiol Lung Cell Mol Physiol* (2008) 295(1):L178–85. doi: 10.1152/ajplung.00009.2008

4. Li HH, Liu CC, Hsu TW, Lin JH, Hsu JW, Li AF, et al. Upregulation of ACE2 and TMPRSS2 by particulate matter and idiopathic pulmonary fibrosis: A potential role in severe COVID-19. *Part Fibre Toxicol* (2021) 18(1):11. doi: 10.1186/s12989-021-00404-3

5. Bui LT, Winters NI, Chung M-I, Joseph C, Gutierrez AJ, Habermann AC, et al. Chronic lung diseases are associated with gene expression programs favoring SARS-CoV-2 entry and severity. *Nat Commun* (2021) 12(1):4314. doi: 10.1038/s41467-021-24467-0

6. Wang L, Wang Y, Yang T, Guo Y, Sun T. Angiotensin-converting enzyme 2 attenuates bleomycin-induced lung fibrosis in mice. *Cell Physiol Biochem* (2015) 36(2):697–711. doi: 10.1159/000430131

7. Simoes ESAC, Teixeira MM. ACE inhibition, ACE2 and angiotensin-(1-7) axis in kidney and cardiac inflammation and fibrosis. *Pharmacol Res* (2016) 107:154–62. doi: 10.1016/j.phrs.2016.03.018

8. Bestle D, Heindl MR, Limburg H, Van Lam van T, Pilgram O, Moulton H, et al. TMPRSS2 and furin are both essential for proteolytic activation of SARS-CoV-2 in human airway cells. *Life Sci Alliance* (2020) 3(9):e202000786. doi: 10.26508/lsa.202000786

9. Zuo J, Dowell AC, Pearce H, Verma K, Long HM, Begum J, et al. Robust SARS-CoV-2-specific T cell immunity is maintained at 6 months following primary infection. *Nat Immunol* (2021) 22(5):620–6. doi: 10.1038/s41590-021-00902-8

10. Tay MZ, Poh CM, Renia L, MacAry PA, Ng LFP. The trinity of COVID-19: Immunity, inflammation and intervention. *Nat Rev Immunol* (2020) 20(6):363–74. doi: 10.1038/s41577-020-0311-8

11. Salka K, Abutaleb K, Chorvinsky E, Thiruvengadam G, Arroyo M, Gomez JL, et al. IFN stimulates ACE2 expression in pediatric airway epithelial cells. *Am J Respir Cell Mol Biol* (2021) 64(4):515–8. doi: 10.1165/rcmb.2020-0352LE

12. Busnadiego I, Fernbach S, Pohl MO, Karakus U, Huber M, Trkola A, et al. Antiviral activity of type I, II, and III interferons counterbalances ACE2 inducibility and restricts SARS-CoV-2. *mBio* (2020) 11(5):e01928-20. doi: 10.1128/mBio.01928-20

13. de Lang A, Osterhaus AD, Haagmans BL. Interferon-gamma and interleukin-4 downregulate expression of the SARS coronavirus receptor ACE2 in vero E6 cells. *Virology* (2006) 353(2):474–81. doi: 10.1016/j.virol.2006.06.011

14. Rey-Parra GJ, Vadivel A, Coltan L, Hall A, Eaton F, Schuster M, et al. Angiotensin converting enzyme 2 abrogates bleomycin-induced lung injury. *J Mol Med (Berl)* (2012) 90(6):637–47. doi: 10.1007/s00109-012-0859-2

15. Imai Y, Kuba K, Rao S, Huan Y, Guo F, Guan B, et al. Angiotensin-converting enzyme 2 protects from severe acute lung failure. *Nature* (2005) 436(7047):112–6. doi: 10.1038/nature03712

16. Grobe JL, Der Sarkissian S, Stewart JM, Meszaros JG, Raizada MK, Katovich MJ. ACE2 overexpression inhibits hypoxia-induced collagen production by cardiac fibroblasts. *Clin Sci (Lond)* (2007) 113(8):357–64. doi: 10.1042/CS20070160

17. Feng Y, Wan H, Liu J, Zhang R, Ma Q, Han B, et al. The angiotensin-converting enzyme 2 in tumor growth and tumor-associated angiogenesis in non-small cell lung cancer. *Oncol Rep* (2010) 23(4):941–8. doi: 10.3892/or_00000718

18. Pedersen SF, Ho YC. SARS-CoV-2: A storm is raging. *J Clin Invest* (2020) 130(5):2202–5. doi: 10.1172/JCI137647

19. Bortolotti D, Gentili V, Rizzo S, Schiuma G, Beltrami S, Strazzabosco G, et al. TLR3 and TLR7 RNA sensor activation during SARS-CoV-2 infection. *Microorganisms* (2021) 9(9):1820. doi: 10.3390/microorganisms9091820

20. Ritter M, Mennerich D, Weith A, Seither P. Characterization of toll-like receptors in primary lung epithelial cells: Strong impact of the TLR3 ligand poly(I:C) on the regulation of toll-like receptors, adaptor proteins and inflammatory response. *J Inflammation (Lond)* (2005) 2:16. doi: 10.1186/1476-9255-2-16

21. Royer PJ, Henrio K, Pain M, Loy J, Roux A, Tissot A, et al. TLR3 promotes MMP-9 production in primary human airway epithelial cells through wnt/beta-catenin signaling. *Respir Res* (2017) 18(1):208. doi: 10.1186/s12931-017-0690-y

22. She YX, Yu QY, Tang XX. Role of interleukins in the pathogenesis of pulmonary fibrosis. *Cell Death Discovery* (2021) 7(1):52. doi: 10.1038/s41420-021-00437-9

23. Vu TN, Chen X, Foda HD, Smaldone GC, Hasaneen NA. Interferon-gamma enhances the antifibrotic effects of pirfenidone by attenuating IPF lung fibroblast activation and differentiation. *Respir Res* (2019) 20(1):206. doi: 10.1186/s12931-019-1171-2

24. Azadeh N, Limper AH, Carmona EM, Ryu JH. The role of infection in interstitial lung diseases: A review. *Chest* (2017) 152(4):842–52. doi: 10.1016/j.chest.2017.03.033

25. Esposito AJ, Menon AA, Ghosh AJ, Putman RK, Fredenburgh LE, El-Chemaly SY, et al. Increased odds of death for patients with interstitial lung disease and COVID-19: A case-control study. *Am J Respir Crit Care Med* (2020) 202 (12):1710–3. doi: 10.1164/rccm.202006-2441LE

26. Huang H, Zhang M, Chen C, Zhang H, Wei Y, Tian J, et al. Clinical characteristics of COVID-19 in patients with preexisting ILD: A retrospective study in a single center in wuhan, China. *J Med Virol* (2020) 92(11):2742–50. doi: 10.1002/jmv.26174

27. Umemura Y, Mitsuyama Y, Minami K, Nishida T, Watanabe A, Okada N, et al. Efficacy and safety of nintedanib for pulmonary fibrosis in severe pneumonia induced by COVID-19: An interventional study. *Int J Infect Dis* (2021) 108:454–60. doi: 10.1016/j.ijid.2021.05.055

28. Mohammadi A, Balan I, Yadav S, Matos WF, Kharawala A, Gaddam M, et al. Post-COVID-19 pulmonary fibrosis. *Cureus* (2022) 14(3):e22770. doi: 10.7759/cureus.22770

29. Miura Y, Lam M, Bourke JE, Kanazawa S. Bimodal fibrosis in a novel mouse model of bleomycin-induced usual interstitial pneumonia. *Life Sci Alliance* (2022) 5 (1):e202101059. doi: 10.26508/lsa.202101059

30. Miyazaki K, Oyanagi J, Sugino A, Sato H, Yokose T, Nakayama H, et al. Highly sensitive detection of invasive lung cancer cells by novel antibody against amino-terminal domain of laminin gamma2 chain. *Cancer Sci* (2016) 107 (12):1909–18. doi: 10.1111/cas.13089

31. Vaughan AE, Brumwell AN, Xi Y, Gotts JE, Brownfield DG, Treutlein B, et al. Lineage-negative progenitors mobilize to regenerate lung epithelium after major injury. *Nature* (2015) 517(7536):621–5. doi: 10.1038/nature14112

32. Miura Y, Ohkubo H, Niimi A, Kanazawa S. Suppression of epithelial abnormalities by nintedanib in induced-rheumatoid arthritis-associated interstitial lung disease mouse model. *ERJ Open Res* (2021) 7(4):00345. doi: 10.1183/23120541.00345-2021

33. Alsafadi HN, Uhl FE, Pineda RH, Bailey KE, Rojas M, Wagner DE, et al. Applications and approaches for three-dimensional precision-cut lung slices. disease modeling and drug discovery. *Am J Respir Cell Mol Biol* (2020) 62 (6):681–91. doi: 10.1165/rcmb.2019-0276TR

34. Lauenstein L, Switalla S, Prenzler F, Seehase S, Pfennig O, Forster C, et al. Assessment of immunotoxicity induced by chemicals in human precision-cut lung slices (PCLS). *Toxicol In Vitro* (2014) 28(4):588–99. doi: 10.1016/j.tiv.2013.12.016

35. Alsafadi HN, Staab-Weijnitz CA, Lehmann M, Lindner M, Peschel B, Konigshoff M, et al. An ex vivo model to induce early fibrosis-like changes in human precision-cut lung slices. *Am J Physiol Lung Cell Mol Physiol* (2017) 312(6): L896–902. doi: 10.1152/ajplung.00084.2017

36. Roach KM, Castells E, Dixon K, Mason S, Elliott G, Marshall H, et al. Evaluation of pirfenidone and nintedanib in a human lung model of fibrogenesis. *Front Pharmacol* (2021) 12:679388. doi: 10.3389/fphar.2021.679388

37. Cedilak M, Banjanac M, Belamaric D, Paravic Radicevic A, Faraho I, Ilic K, et al. Precision-cut lung slices from bleomycin treated animals as a model for testing potential therapies for idiopathic pulmonary fibrosis. *Pulm Pharmacol Ther* (2019) 55:75–83. doi: 10.1016/j.pupt.2019.02.005

38. Kanazawa S, Ota S, Sekine C, Tada T, Otsuka T, Okamoto T, et al. Aberrant MHC class II expression in mouse joints leads to arthritis with extraarticular manifestations similar to rheumatoid arthritis. *Proc Natl Acad Sci U.S.A.* (2006) 103(39):14465–70. doi: 10.1073/pnas.0606450103

39. Carreau A, El Hafny-Rahbi B, Matejuk A, Grillon C, Kieda C. Why is the partial oxygen pressure of human tissues a crucial parameter? small molecules and hypoxia. *J Cell Mol Med* (2011) 15(6):1239–53. doi: 10.1111/j.1582-4934.2011.01258.x

40. Le QT, Chen E, Salim A, Cao H, Kong CS, Whyte R, et al. An evaluation of tumor oxygenation and gene expression in patients with early stage non-small cell lung cancers. *Clin Cancer Res* (2006) 12(5):1507–14. doi: 10.1158/1078-0432.CCR-05-2049

41. Schindelin J, Arganda-Carreras I, Frise E, Kaynig V, Longair M, Pietzsch T, et al. Fiji: An open-source platform for biological-image analysis. *Nat Methods* (2012) 9(7):676–82. doi: 10.1038/nmeth.2019

42. Zhang R, Wu Y, Zhao M, Liu C, Zhou L, Shen S, et al. Role of HIF-1alpha in the regulation ACE and ACE2 expression in hypoxic human pulmonary artery smooth muscle cells. *Am J Physiol Lung Cell Mol Physiol* (2009) 297(4):L631–40. doi: 10.1152/ajplung.90415.2008

43. Shenoy V, Qi Y, Katovich MJ, Raizada MK. ACE2, a promising therapeutic target for pulmonary hypertension. *Curr Opin Pharmacol* (2011) 11(2):150–5. doi: 10.1016/j.coph.2010.12.002

44. Raghu G, Brown KK, Bradford WZ, Starko K, Noble PW, Schwartz DA, et al. A placebo-controlled trial of interferon gamma-1b in patients with idiopathic pulmonary fibrosis. *N Engl J Med* (2004) 350(2):125–33. doi: 10.1056/NEJMoa030511

45. Onabajo OO, Banday AR, Stanifer ML, Yan W, Obajemu A, Santer DM, et al. Interferons and viruses induce a novel truncated ACE2 isoform and not the full-length SARS-CoV-2 receptor. *Nat Genet* (2020) 52(12):1283–93. doi: 10.1038/s41588-020-00731-9

46. Ng KW, Attig J, Bolland W, Young GR, Major J, Wrobel AG, et al. Tissue-specific and interferon-inducible expression of nonfunctional ACE2 through endogenous retroelement co-option. *Nat Genet* (2020) 52(12):1294–302. doi: 10.1038/s41588-020-00732-8

47. Li Y, Renner DM, Comar CE, Whelan JN, Reyes HM, Cardenas-Diaz FL, et al. SARS-CoV-2 induces double-stranded RNA-mediated innate immune responses in respiratory epithelial-derived cells and cardiomyocytes. *Proc Natl Acad Sci U.S.A.* (2021) 118(16):e2022643118. doi: 10.1073/pnas.2022643118

48. Buttner C, Skupin A, Rieber EP. Transcriptional activation of the type I collagen genes COL1A1 and COL1A2 in fibroblasts by interleukin-4: analysis of the functional collagen promoter sequences. *J Cell Physiol* (2004) 198(2):248–58. doi: 10.1002/jcp.10395

49. Mikami S, Miura Y, Kondo S, Sakai K, Nishimura H, Kyoyama H, et al. Nintedanib induces gene expression changes in the lung of induced-rheumatoid arthritis-associated interstitial lung disease mice. *PloS One* (2022) 17(6):e0270056. doi: 10.1371/journal.pone.0270056

frontiers | Frontiers in Immunology

TYPE Original Research
PUBLISHED 15 December 2022
DOI 10.3389/fimmu.2022.1070379

OPEN ACCESS

EDITED BY
Fabrice Cognasse,
INSERM U1059 SAnté INgéniérie BIOlogie, France

REVIEWED BY
Antonio d'Amati,
University of Bari Aldo Moro, Italy
Sergio Iván Valdés-Ferrer,
Instituto Nacional de Ciencias Médicas y Nutrición Salvador Zubirán (INCMNSZ), Mexico

*CORRESPONDENCE
Nino Stocchetti
nino.stocchetti@policlinico.mi.it
Maria Sessa
msessa@asst-pg23.it
Elisa R. Zanier
elisa.zanier@marionegri.it

SPECIALTY SECTION
This article was submitted to Inflammation, a section of the journal Frontiers in Immunology

RECEIVED 14 October 2022
ACCEPTED 02 December 2022
PUBLISHED 15 December 2022

CITATION
Bonetto V, Pasetto L, Lisi I, Carbonara M, Zangari R, Ferrari E, Punzi V, Luotti S, Bottino N, Biagianti B, Moglia C, Fuda G, Gualtierotti R, Blasi F, Canetta C, Montano N, Tettamanti M, Camera G, Grimoldi M, Negro G, Rifino N, Calvo A, Brambilla P, Biroli F, Bandera A, Nobili A, Stocchetti N, Sessa M and Zanier ER (2022) Markers of blood-brain barrier disruption increase early and persistently in COVID-19 patients with neurological manifestations. *Front. Immunol.* 13:1070379. doi: 10.3389/fimmu.2022.1070379

Markers of blood-brain barrier disruption increase early and persistently in COVID-19 patients with neurological manifestations

Valentina Bonetto[1], Laura Pasetto[1], Ilaria Lisi[1], Marco Carbonara[2], Rosalia Zangari[3], Erica Ferrari[4], Veronica Punzi[4], Silvia Luotti[1], Nicola Bottino[2], Bruno Biagianti[4], Cristina Moglia[5,6], Giuseppe Fuda[5], Roberta Gualtierotti[2], Francesco Blasi[2,4], Ciro Canetta[2], Nicola Montano[2], Mauro Tettamanti[1], Giorgia Camera[7], Maria Grimoldi[7], Giulia Negro[8], Nicola Rifino[9], Andrea Calvo[5,6], Paolo Brambilla[2,4], Francesco Biroli[3], Alessandra Bandera[2,4], Alessandro Nobili[1], Nino Stocchetti[2,4]*, Maria Sessa[7]* and Elisa R. Zanier[1]*

[1]Istituto di Ricerche Farmacologiche Mario Negri IRCCS, Milan, Italy, [2]Fondazione IRCCS Ca' Granda Ospedale Maggiore Policlinico, Milan, Italy, [3]FROM Research Foundation, Papa Giovanni XXIII Hospital, Bergamo, Italy, [4]Department of Pathophysiology and Transplantation, University of Milan, Milan, Italy, [5]"Rita Levi Montalcini", Department of Neuroscience, University of Turin, Turin, Italy, [6]AOU Città della Salute e della Scienza Hospital, Turin, Italy, [7]Department of Neurology, Papa Giovanni XXIII Hospital, ASST Papa Giovanni XXIII, Bergamo, Italy, [8]Neurology Section, School of Medicine and Surgery, University of Milano-Bicocca, Monza, Italy, [9]Division of Neurology, University of Milano-Bicocca, Milan, Italy

Background: Coronavirus disease 2019 (COVID-19) caused by SARS-CoV-2 infection is associated with disorders affecting the peripheral and the central nervous system. A high number of patients develop post-COVID-19 syndrome with the persistence of a large spectrum of symptoms, including neurological, beyond 4 weeks after infection. Several potential mechanisms in the acute phase have been hypothesized, including damage of the blood-brain-barrier (BBB). We tested weather markers of BBB damage in association with markers of brain injury and systemic inflammation may help in identifying a blood signature for disease severity and neurological complications.

Methods: Blood biomarkers of BBB disruption (MMP-9, GFAP), neuronal damage (NFL) and systemic inflammation (PPIA, IL-10, TNFα) were measured in two COVID-19 patient cohorts with high disease severity (ICUCovid; n=79) and with neurological complications (NeuroCovid; n=78), and in two control groups free from COVID-19 history, healthy subjects (n=20) and patients with amyotrophic lateral sclerosis (ALS; n=51). Samples from COVID-19 patients were collected during the first and the second wave of COVID-19 pandemic in

10.3389/fimmu.2022.1070379

Lombardy, Italy. Evaluations were done at acute and chronic phases of the COVID-19 infection.

Results: Blood biomarkers of BBB disruption and neuronal damage are high in COVID-19 patients with levels similar to or higher than ALS. NeuroCovid patients display lower levels of the cytokine storm inducer PPIA but higher levels of MMP-9 than ICUCovid patients. There was evidence of different temporal dynamics in ICUCovid compared to NeuroCovid patients with PPIA and IL-10 showing the highest levels in ICUCovid patients at acute phase. On the contrary, MMP-9 was higher at acute phase in NeuroCovid patients, with a severity dependency in the long-term. We also found a clear severity dependency of NFL and GFAP levels, with deceased patients showing the highest levels.

Discussion: The overall picture points to an increased risk for neurological complications in association with high levels of biomarkers of BBB disruption. Our observations may provide hints for therapeutic approaches mitigating BBB disruption to reduce the neurological damage in the acute phase and potential dysfunction in the long-term.

KEYWORDS

COVID-19, neurological damages, blood-brain barrier, inflammation, blood biomarkers, critical care

Introduction

SARS-CoV-2 infection is associated with neurological symptoms and complications that range from headache, anosmia and dysgeusia, to severe complications such as cerebrovascular events, encephalopathy, Guillain-Barré syndrome, and dementia-like syndrome (1). In addition, many COVID-19 patients develop a 'post-COVID-19 syndrome' defined as the persistence of a wide spectrum of symptoms beyond four weeks after infection (2). In symptomatic COVID-19 patients, a community-based study with over half a million people in the UK estimated that about one in three experienced at least one persistent symptom for 12 weeks or more (3). In a population-based study in Lombardy, the post-COVID-19 condition was associated with death, rehospitalization and use of health resources (4). Long-term neuropsychological impairments such as executive, attentional and memory deficits, are reported even after mild infection (5). While the exact causes of post-COVID-19 syndrome remain largely elusive, the prevalence of associated neurological symptoms with an increased risk of anxiety and depression at 16-month follow-up (6) suggests a brain origin (7, 8).

There is neurochemical evidence of neuronal injury in patients with COVID-19 (9, 10), with reports of a severity-dependent increase of neurofilament light chain (NFL) at 4-month follow-up, further supporting ongoing brain injury even weeks and months after acute infection (11). Not surprisingly, the neurological complications are associated with worse functional outcome, particularly in older subjects and those with comorbidities (12).

Hypotheses of pathogenic processes implicated in acute and delayed brain injury following a SARS-CoV-2 infection include: i) viral invasion, ii) bioenergy failure, iii) autoimmunity, and iv) innate neuroimmune responses (13). In all these processes the blood-brain barrier (BBB), which maintains the specialized microenvironment of the neural tissue by regulating the trafficking of substances between the blood and brain compartments, has a central role.

Brain endothelial cells are the primary unit in close association with pericytes and astrocytes (14). Pericytes, which are key cells in maintaining and supporting vascular homeostasis and barrier function (15), are also the main source of matrix metalloproteinase 9 (MMP-9) (16, 17). Inflammatory stimuli very rapidly activate MMP-9 at the pericyte somata, leading to degradation of the underlying tight junction complexes. Thus, MMP-9 can act as a toxic culprit of BBB disruption after acute (18, 19) and neurodegenerative diseases (20). Peptidyl prolyl cis-trans isomerase A (PPIA), also known as cyclophilin A, acts as an activator of MMP-9 (21, 22) through binding to its CD147 receptor, which in addition has been proposed as an alternative route for SARS-CoV-2 infection (23).

Mechanistically, it has been demonstrated that the severe COVID-19-related cytokine storm is induced by a "spike protein-CD147-PPIA signaling axis" (24). *In vivo* experiments using a preclinical mouse model indicated that an anti-CD147 antibody inhibited the cytokine storm of SARS-CoV-2 (24).

Astrocytic end-feet containing glial fibrillary acidic protein (GFAP) are an essential component of the BBB. High blood GFAP is a marker of structural damage in the acute phase of brain injury and a severity-dependent increase has been detected in COVID-19 patients (11, 25). These data highlight PPIA, MMP-9, and GFAP as key disease biomarkers, so their measurement in association with NFL, an established marker of brain injury, may help identify a blood signature for disease severity and neurological complications in COVID-19 patients (NeuroCovid).

We identified significant effects associated with SARS-CoV-2 infection in COVID-19 patients, with NeuroCovid subjects showing the highest levels of biomarkers associated with BBB disruption, while patients in the intensive care unit (ICUCovid) had higher levels of inflammatory response biomarkers.

Materials and methods

Study approval

The study was approved by the ethics committees of the clinical centers involved: Fondazione IRCCS Ca' Granda Ospedale Maggiore Policlinico, Milano (approval #868_2020, 28.10.2020), ASST Papa Giovanni XXIII, Bergamo (approval #123/20, 14.05.2020). Written consent was obtained from patients themselves or their legal representatives when they lacked capacity to consent. Wherever possible, informed consent was collected verbally. However, in most cases, due to the patient's inability to provide informed consent or to collect it in compliance with the contagion prevention measures, the principle of secondary use of data was used in accordance with art. 28, paragraph 2, letter b) of the November 20, 2017 law, no. 167, included in the legislative decree 196/03 of art. 110-bis.

Study populations

Two COVID-19 populations, referred to as ICUCovid and NeuroCovid, were recruited between February 2020 and February 2021. All participants received a positive PCR test for SARS-CoV-2 RNA on nasopharyngeal swab. Control groups free from COVID-19 history were patients with amyotrophic lateral sclerosis and a healthy population. Their main demographic and clinical characteristics are reported in Table 1.

ICUCovid

All patients admitted to the ICU, Rianimazione 1 Fiera Milano COVID-19 (Fondazione IRCCS Ca' Granda Ospedale Maggiore Policlinico, Milan, Italy) were screened for eligibility. Inclusion criteria for this study population were: i) signed informed consent and ii) >18 years of age. Exclusion criteria were: i) known previous neurological conditions; ii) more than 48h in another ICU before admission; iii) pregnancy. Out of 296 screened patients, 79 were recruited for the study.

NeuroCovid

Patients admitted to the COVID-19 wards (ASST Papa Giovanni XXIII, Bergamo, Italy) with neurological manifestations confirmed by a neurological consultation/

TABLE 1 Demographic and clinical characteristics of the patient cohorts.

Characteristics	ICUCovid	NeuroCovid	ALS	Healthy
N	79	78	51	20
Age at sampling, years, median (IQR)	65 (58–70)	61 (53-71)	67 (62-71)	61 (58-63)
Sex (% males)	77%	73%	51%	35%
Hospitalization, days, median (IQR)	17 (10-28)	29 (10-51)	–	–
Mortality (% deceased)	34%	16%	–	–
PaO_2/FIO_2 ratio, median (IQR)	131 (93-180)	–	–	–
ALSFRS-R[1] at sampling, median (IQR)	–	–	33 (22-38)	–

[1]ALSFRS-R: Revised Amyotrophic Lateral Sclerosis Functional Rating Scale.

neurophysiological assessment/neuroradiologic investigation were recruited. Patients' samples had been collected in an observational study on neurological manifestations in COVID-19 patients approved by the local Ethics Committee (257/2020, 13/5/2020) (26). The neurological diagnoses in this cohort are summarized in Table 2 and included peripheral neuropathies (33% of patients), encephalopathies/encephalitis (33%) and cerebrovascular disorders (23%). Inclusion criteria were: i) signed informed consent; ii) > 18 years of age; iii) cognitive or neurological symptoms presenting during COVID-19 hospitalization, for which a neurological consultation/neurophysiological assessment/neuroradiologic investigation was required; iv) blood samples available. Of the 137 NeuroCovid patients, 78 fitted these criteria and their samples were included in the study. Patients were stratified based on clinical outcome: discharged fully recovered (moderate), discharged with sequalae (severe), and deceased (dead).

ALS patients and healthy controls

Informed written consent was obtained from all subjects involved and the study was approved by the ethics committee of Azienda Ospedaliero Universitaria Città della Salute e della Scienza, Turin. Healthy subjects and ALS patients had no COVID-19 history. The diagnosis of ALS was based on a detailed medical history and physical examination and confirmed by electrophysiological evaluation. Inclusion criteria for ALS patients were: i) >18 years old; ii) diagnosis of definite, probable or laboratory-supported probable ALS, according to revised El Escorial criteria. Exclusion criteria were: i) diabetes or severe inflammatory conditions; ii) active malignancy; iii) pregnancy or breast-feeding. ALS patients served as positive controls for severe neurodegeneration.

TABLE 2 Case definition for NeuroCovid cohort.

NeuroCovid total patients (N)	78
Neurological complications	N (%)
Cerebrovascular disorders[1]	*18 (23)*
Ischemic stroke	13
Hemorrhagic stroke	4
Transient ischemic attack	1
Peripheral neuropathies	*26 (33)*
Guillain Barrè Syndrome[2]	26
Encephalopathies/Encephalites[3]	*26 (33)*
Miscellaneous	*8 (10)*
Epilepsy	4
Myelopathy	1
Syncope	1
Movement disorder Headache	1 1

[1]As defined by Sacco et al. (27)
[2]As defined by Sejvar et al. (28)
[3]As defined by Quist-Paulsen et al. (29)

Study design

The study design is summarized in Figure 1. Two COVID-19 populations and ALS and healthy control groups were included (see *Study Populations* above). In the ICUCovid cohort, blood samples were drawn acutely at ICU admission (T0) and after 7 (T7) and 14 (T14) days. Clinical data were collected throughout the ICU stay and CT scans were done every two weeks when feasible. For the NeuroCovid cohort, the blood samples had initially been collected for clinical and not experimental purposes, so the samples available did not precisely match those collected in the ICUCovid cohort; therefore, we retrieved available samples from week 1 to week 2 in the ward (acute: T0-T14) and from longer timepoints (long-term: T15-T90). Clinical data were retrieved from medical records. Blood samples and clinical analyses were then done at the Istituto di Ricerche Farmacologiche Mario Negri IRCCS.

Biomarker analysis

Bloods were processed at the contributing centers and plasma samples were aliquoted, cryopreserved at -80°C and shipped to the Istituto di Ricerche Farmacologiche Mario Negri IRCCS for biomarker analyses. Levels of NFL, GFAP, IL-10 and TNFα were measured using commercially available single molecule array assay kits on an SR-X Analyzer (Neuro 2-Plex B (#103520), interleukin-10 (IL-10) (#101643) and tumor necrosis factor (TNFα) (#101580) advantage kits) as described by the manufacturer (Quanterix, Billerica, MA). A single batch of reagents was used for each analyte. MMP-9 was measured with an AlphaLISA kit for the human protein (#AL3138, PerkinElmer). AlphaLISA signals were measured using an Ensight Multimode Plate Reader (PerkinElmer). PPIA was measured with an ELISA for the human protein (#RD191329200R, BioVendor).

Other laboratory data

Clinical and outcome data were retrieved from medical records for all patients.

Statistical analysis

For each variable the differences between experimental groups were analysed by a Mann Whitney test or Kruskall-Wallis test, followed by Dunn's *post-hoc* tests. Two-way ANOVA for repeated measures followed by Sidak's *post-hoc*

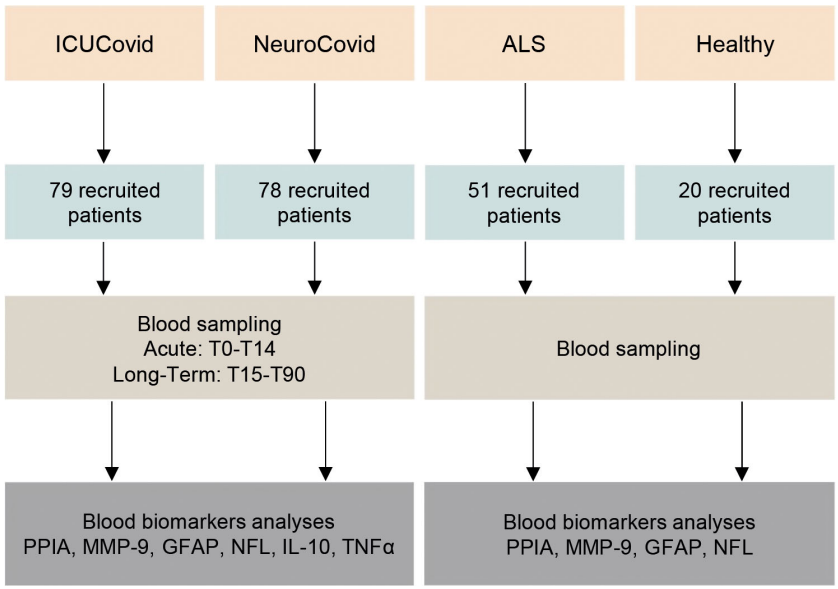

FIGURE 1
Schematic workflow for the biomarker characterization in two cohorts of COVID-19 patients and two cohorts of controls (ALS and healthy). The two cohorts of COVID-19 patients analyzed in the study are COVID-19 patients admitted to the ICU ward Rianimazione 1 Fiera Milano COVID-19 (ICUCovid; n=79) and to COVID-19 wards ASST Papa Giovanni XXIII, Bergamo, with neurological complications (NeuroCovid; n=78). Blood samples were drawn acutely at ICU admission and after 7-14 days (T0-T14), and in the long-term between 15 and 90 days in the ward (T15-T90). Plasma samples were isolated and then analyzed for PPIA, MMP-9, GFAP, NFL, IL-10 and TNFα biomarkers. Control groups were ALS patients (n=51) and healthy subjects (n=20). Plasma samples were isolated and then analyzed for PPIA, MMP-9, GFAP and NFL.

test was used to analyse biomarkers in ICUCovid patients. *P* values below 0.05 were considered significant. Prism 8.0 (GraphPad Software Inc., San Diego, CA) was used.

Data availability

All data produced in the present study are available upon reasonable request to the authors.

Results

Blood biomarkers of BBB disruption and neuronal damage are high in COVID-19 patients with levels similar to or higher than in a severe neurodegenerative disease

PPIA, an inducer of MMP-9 (22) and cytokine storm (24), showed the highest levels in ICUCovid patients (Figure 2A), while MMP-9, which is strictly related to BBB disruption, is highest in NeuroCovid patients (Figure 2B). Both PPIA and MMP-9 in hospitalized COVID-19 patients are substantially higher than ALS patients, characterized by severe neurodegeneration, and healthy controls (Figures 2A, B). Plasma concentrations of GFAP were also high, irrespective of the neurological complications compared to healthy controls and were equal to or higher than the levels in ALS patients (Figure 2C). NFL has similar behavior, with the highest levels in NeuroCovid significantly higher than in ICUCovid patients (Figure 2D). These data suggest a clear neurological implication and call for a granular description of biomarker changes in these patient cohorts in relation to time and severity.

NeuroCovid patients have lower levels of the cytokine storm inducer PPIA but higher levels of BBB disruption markers

We characterized the severity-dependent changes and temporal dynamics of PPIA, MMP-9, GFAP and NFL in ICUCovid and NeuroCovid patients. In the acute phase, ICUCovid patients had higher PPIA levels than NeuroCovid patients (Figure 3A). Among ICUCovid patients, a slight temporal increase was observed in the deceased group, leading to higher PPIA levels at 14 days than in alive patients (T14, Figure 3B). NeuroCovid patients showed no severity dependency in the acute and the longer phases (Figures 3C, D). In the acute phase, ICUCovid patients had lower MMP-9 levels than NeuroCovid patients (Figure 3E). In the ICUCovid cohort,

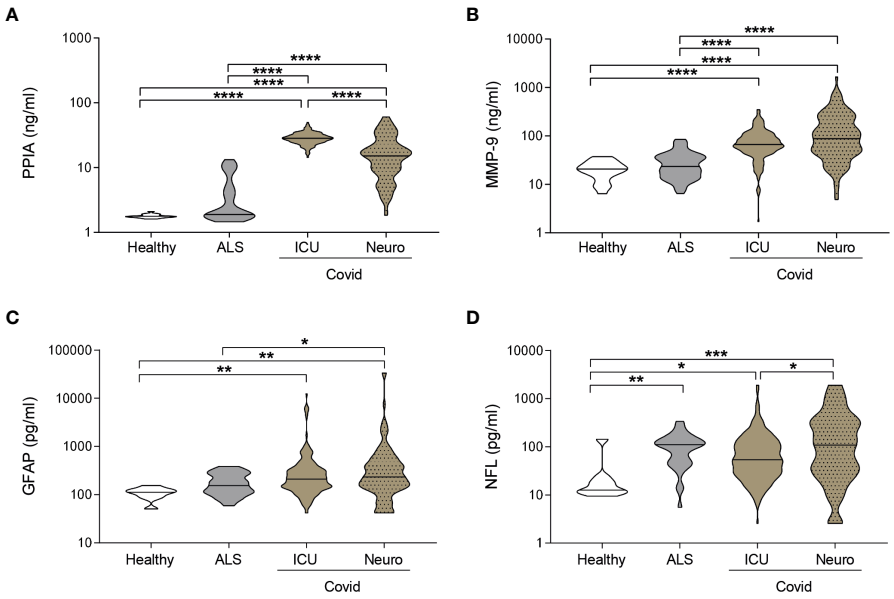

FIGURE 2
Biomarkers comparison between COVID-19 and a neurodegenerative disorder. **(A-D)** PPIA **(A)**, MMP-9 **(B)**, GFAP **(C)**, and NFL **(D)** concentrations were measured in plasma samples from ICUCovid patients (ICU n=79), NeuroCovid patients (n=78), ALS patients (PPIA n=50; MMP-9 n=51; GFAP and NFL n=34); and healthy controls (PPIA n=18; MMP-9 n=20; GFAP and NFL n=9). Violin plots indicate median, variability and probability density of biomarker concentrations. **(A, B, D)** Kruskal-Wallis, $p < 0.0001$; **(C)** Kruskal-Wallis, $p = 0.0003$. **(A-D)** *$p < 0.05$, **$p < 0.01$, ***$p < 0.001$, ****$p < 0.0001$ by Kruskal-Wallis, Dunn's *post hoc* test.

there was a slight decrease over the first two weeks in alive patients, leading to significantly lower levels on day 14 compared to deceased patients (T14, Figure 3F). In the NeuroCovid cohort, MMP-9 levels were similarly high in alive and deceased patients in the acute phase, while in the longer term they showed severity dependency (Figures 3G, H).

In the acute phase, GFAP levels did not differ between groups (Figure 4A). The longitudinal trajectories in ICUCovid patients showed an increase only in deceased patients, with the highest difference at admission (T0, Figure 4B). NeuroCovid patients displayed a high heterogeneity in GFAP levels in the acute phase (Figure 4A). This is due to GFAP severity dependency, significant in the acute phase and as a tendency in the long-term (Figures 4C, D).

In the acute phase, ICUCovid patients showed NFL levels like NeuroCovid patients (Figure 4E). The trajectories of live and death ICUCovid cohorts highlight a steep increase in NLF levels over the first two weeks, reaching the highest value for deceased patients at 14 days from ICU admission (T14, Figure 4F). While in the acute phase live and dead NeuroCovid patients have similar NFL levels (Figure 4G), in the long-term NFL levels showed a clear severity dependency (Figure 4H).

Inflammatory markers of systemic immune response, including IL-10 and TNFα, were also measured. In the acute phase, IL-10 levels were highest in ICUCovid compared to NeuroCovid patients (Figure 5A), with a clear increase in ICUCovid deceased patients at day 14 (T14, Figure 5B). Within the NeuroCovid cohort, IL-10 levels were similar in alive and deceased patients (Figure 5C). In the long-term, however, severity dependency was observed (Figure 5D).

In the acute phase, TNFα levels did not differ between ICUCovid and NeuroCovid patients (Figure 5E) and within ICUCovid cohort there were no temporal changes in alive and deceased patients up to day 14 (T14, Figure 5F). In the NeuroCovid cohort, acute TNFα levels were similar in alive and deceased patients (Figure 5G). In the long-term, however, NeuroCovid patients showed a significant severity dependency (Figure 5H).

Discussion

This study examined the effects of SARS-CoV-2 infection on blood biomarkers of BBB disruption, neuronal damage and systemic inflammation by longitudinally monitoring two patient cohorts of COVID-19, with increasing disease severity and neurological complications. Blood biomarkers of BBB disruption were elevated in COVID-19 patients with levels comparable to or even higher than in ALS patients, pointing to neurological implications over a range of disease severities.

There was evidence of different temporal dynamics in ICUCovid compared to NeuroCovid patients with PPIA, the potent activator of the cytokine storm and MMP-9 inducer, and

10.3389/fimmu.2022.1070379

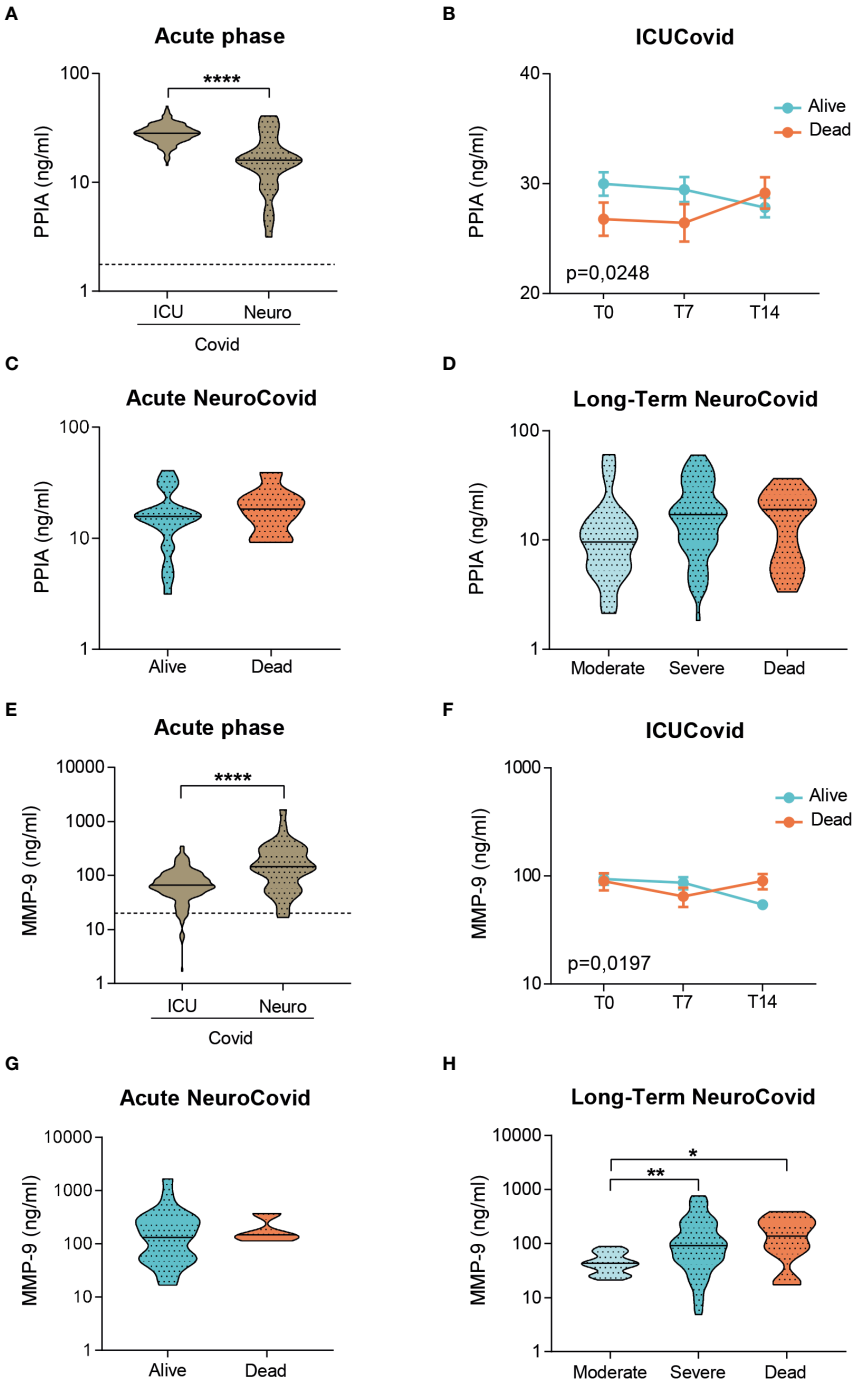

FIGURE 3
Analysis of PPIA and MMP-9 in plasma of two cohorts of COVID-19 patients. **(A-H)** PPIA **(A-D)** and MMP-9 **(E-H)** concentrations were measured respectively by ELISA and AlphaLISA technology in plasma samples from two cohorts of COVID-19 patients. **(A, E)** Violin plots indicate the median, variability and probability density of PPIA **(A)** and MMP-9 **(E)** at acute phase, in ICUCovid (n=79) and NeuroCovid samples (n=31). Dotted line indicates the mean level of healthy controls. **(A, E)** Mann Whitney, ****p< 0.0001. **(B, F)** The concentrations of PPIA **(B)** and MMP-9 **(F)** were measured in ICUCovid patients over time, at ICU admission (T0) and after 7 (T7) and 14 days (T14). ICUCovid patients were stratified as alive (n=32) and dead (n=14). Data (mean ± SEM) indicate biomarker concentrations. **(B)** Two-way ANOVA for repeated measures, p = 0.0248; **(F)** two-way ANOVA for repeated measures, p = 0.0197. **(C, G)** The concentrations of PPIA **(C)** and MMP-9 **(G)** were measured at acute phase, in samples from NeuroCovid patients, stratified as alive (n=23) and dead (n=8). Violin plots indicate median, variability and probability density of biomarker concentrations. **(C)** Mann Whitney, p = 0.3966; **(G)** Mann Whitney, p = 0.5498. **(D, H)** The concentrations of PPIA **(D)** and MMP-9 **(H)** in the long-term, in samples from NeuroCovid patients, stratified as moderate (n=18), severe (n=42) and dead (n=8). Violin plots indicate median, variability and probability density of biomarker concentrations. **(D)** Kruskal-Wallis, p = 0.1175. **(H)** Kruskal-Wallis, p = 0.0048; *p < 0.05, **p < 0.01 by Kruskal-Wallis, Dunn's *post hoc* test.

10.3389/fimmu.2022.1070379

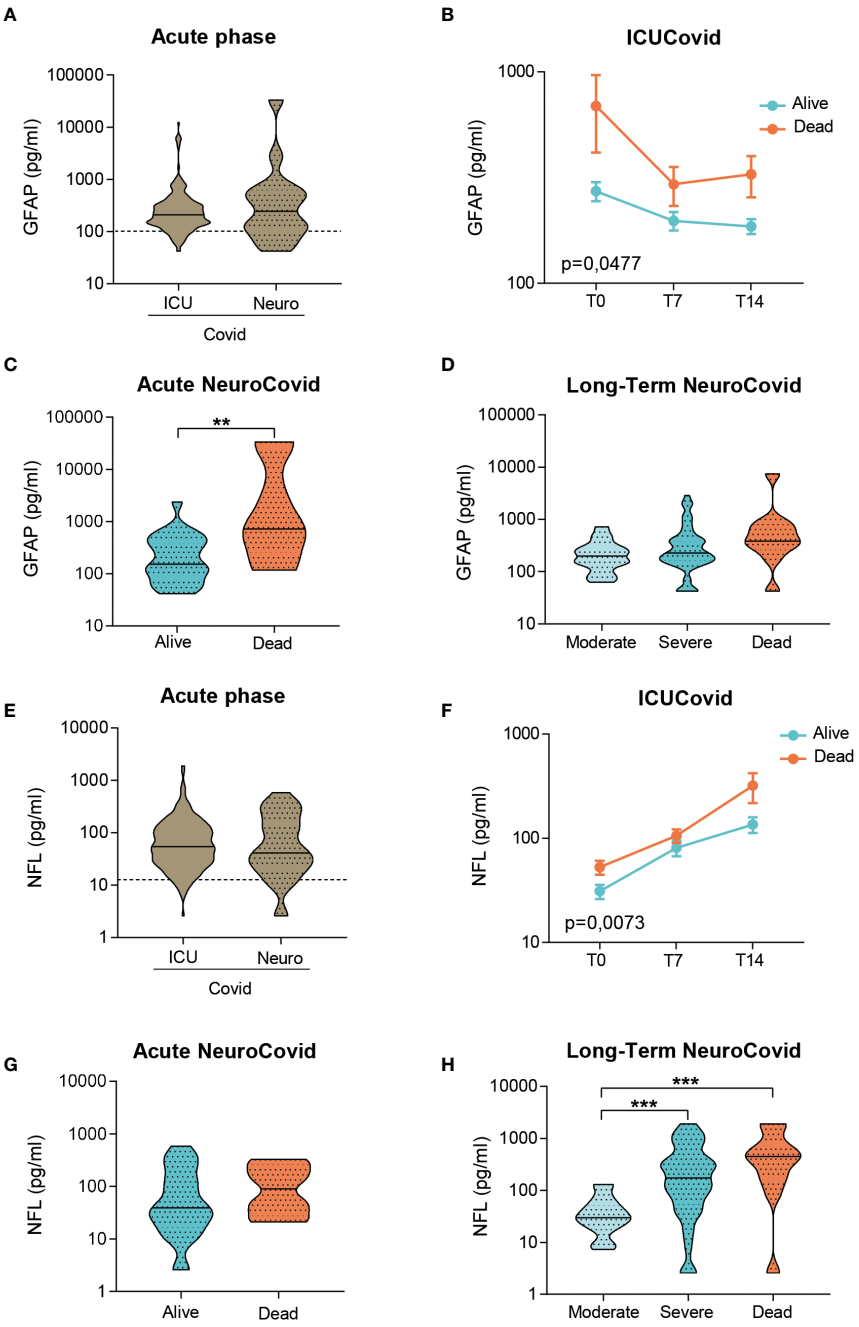

FIGURE 4
Analysis of GFAP and NFL in plasma of two cohorts of COVID-19 patients. **(A-H)** GFAP **(A-D)** and NFL **(E-H)** concentrations were measured by Simoa technology in plasma samples from two cohorts of COVID-19 patients. **(A, E)** Violin plots represent the median, variability and probability density of GFAP **(A)** and NFL **(E)** at acute phase, in ICUCovid (n=79) and NeuroCovid samples (n=31). Dotted line indicates the mean level of healthy controls. **(A)** Mann Whitney, p = 0.7910; **(E)** Mann Whitney, p = 0.7054. **(B, F)** The concentrations of GFAP **(B)** and NFL **(F)** were measured in ICUCovid patients over time, at ICU admission (T0) and after 7 (T7) and 14 days (T14). ICUCovid patients were stratified as alive (n=32) and dead (n=14). Data (mean ± SEM) indicate biomarker concentrations. **(B)** Two-way ANOVA for repeated measures, p = 0.0477; **p < 0.005 alive versus dead at T0 by Sidak's *post hoc* test; **(F)** Two-way ANOVA for repeated measures, p = 0.0073; ***p < 0.001 alive versus dead at T14 by Sidak's *post hoc* test. **(C, G)** The concentrations of GFAP **(C)** and NFL **(G)** were measured at acute phase, in samples from NeuroCovid patients, stratified as alive (n=23) and dead (n=8). Violin plots indicate median, variability and probability density of biomarker concentrations. **(C)** Mann Whitney, **p = 0.0088; **(G)** Mann Whitney, p = 0.2868. **(D, H)** The concentrations of GFAP **(D)** and NFL **(H)** in long-term samples from NeuroCovid patients, stratified as moderate (n=18), severe (n=42) and dead (n=8). Violin plots indicate median, variability and probability density of biomarker concentrations. **(D)** Kruskal-Wallis, p = 0.0570; **(H)** Kruskal-Wallis, p < 0.0001. ***p < 0.001 by Dunn's *post hoc* test.

IL-10, the master regulator of immunity to infection, with the highest levels in ICUCovid patients in the acute phase (Figure 6). In contrast, MMP-9 was significantly higher in the acute phase in NeuroCovid patients, with severity dependency in the longer term. In line with previous findings, we found also clear severity dependency of NFL and GFAP levels with the highest levels in deceased patients, and severe NeuroCovid patients showing a tendency to maintain higher values than moderate patients in the longer term.

PPIA is a foldase and a molecular chaperone with multiple functions and substrates, including viral proteins essential for coronavirus replication (30). PPIA is a major target of redox regulation in activated lymphocytes (31, 32). Under stress conditions PPIA is secreted extracellularly by several types of cells, including pericytes, vascular smooth muscle cells and macrophages, behaving as a pro-inflammatory cytokine, with potent chemotactic activity toward leukocytes (21, 33, 34). Through the interaction with its CD147 receptor, in a NF-κB-dependent pathway, PPIA is an inducer of MMP-9 and of pro-inflammatory cytokines and chemokines (22, 35). High levels of PPIA have been seen in biofluids of several conditions associated with inflammation, including neurological and cardiovascular diseases (22, 36). Interestingly, high plasma concentrations of PPIA have also recently been reported in COVID-19 patients with mechanistic evidence for its involvement in the induction of the cytokine storm by activating CD147 (24).

A growing body of clinical data suggests that the cytokine storm is associated with COVID-19 severity, ICU admission, and is a crucial cause of death (37). In agreement with this, our ICUCovid patients had PPIA concentrations substantially higher than NeuroCovid patients. Also noteworthy is the extremely high PPIA plasma concentration in all COVID-19 patients. This may be linked to its up-regulation upon interaction of SARS-CoV-2 with CD147, as observed in animal models (24), and may favor viral replication (30, 38). Similarly, MMP-9 was very high in all COVID-19 patients. However, NeuroCovid patients had the highest levels of MMP-9 in the acute phase, with persistent high levels in most severe patients in the long-term. MMP-9 is a metalloproteinase with a wide substrate spectrum and is an important mechanism for fine-tuning cellular processes, but if aberrantly activated it is a key factor in BBB disruption and neuronal damage, by degrading tight junction proteins and laminin (18–20). MMP-9 can be induced by inflammatory signaling cascades with CD147 acting as the major upstream inducer in the CNS (39). CD147 is highly expressed in the brain capillary endothelium and various sub-regions of the brain (40). Brain pericytes are the main source of MMP-9 at the neurovascular unit and it is rapidly released in response to inflammatory stimuli (16, 17). It has also been demonstrated *in vitro* and *in vivo* that SARS-CoV-2 can infect the brain microvascular endothelial cells and cross the BBB by MMP-9-mediated disruption of basement membrane (41). Therefore, one can hypothesize that a local, early high MMP-9 concentration at the neurovascular unit in NeuroCovid patients, rather than extensive systemic inflammation as in ICUCovid patients, may be responsible for the BBB disruption that triggers neurological complications following SARS-CoV-2 infection.

Astrocytic end feet cover more than 99% of the neurovascular surface and directly affect BBB permeability (42). GFAP is a highly expressed protein of the CNS, almost exclusively in astrocytes. In neuropathological conditions, GFAP is released into the bloodstream either by direct venous drainage or through a compromised BBB (43). Blood GFAP can therefore serve as a useful biomarker and prognostic tool for numerous neurological conditions (25).

While classically considered a marker of astrogliosis, the presence of glial-derived proteins in peripheral body fluids has been suggested as indicating BBB disruption in acute CNS injury (44). In the case of traumatic brain injury, it has been recently suggested that high blood GFAP concentrations might reflect damage to astrocytic end feet enveloping the BBB, thus releasing GFAP directly into the blood when the BBB is injured (45). Elevated GFAP plasma levels have been reported in COVID-19 patients (10, 45) and were in line with neuropathological data indicating post-mortem evidence of BBB disruption and gliosis (46). In accordance with this, here we report high GFAP levels in a severity-dependent manner, with significantly higher levels at acute timepoints in deceased patients. GFAP only tended to be higher in NeuroCovid patients than in ICUCovid patients. However, the NeuroCovid cohort included several patients with Guillain-Barré syndrome in which blood-nerve-barrier (BNB) disruption is a key step (47). BNB lacks astrocytes and glia limitans, so the detection of barrier damage through GFAP in these cases is underestimated. Maladaptive microglia and monocyte activation may also exert a detrimental effect on BBB function and integrity in COVID-19 (14). Interestingly, a recent publication has shown that microglia–derived chemokine MCP-1 (also known as CCL2) seems to have a major role in neocortex neuroinflammation and BBB disruption in a mouse model of autoimmune encephalomyelitis (48). Moreover, high blood MCP-1 levels have been associated with disease severity and mortality in COVID-19 (49). Although not measured in our study, longitudinal analyses of MCP-1 in plasma and CSF of COVID-19 patients and correlation with neurological symptoms will shed light on this aspect in future studies.

NFL is an established marker of axonal injury (50). Although axonal degeneration is not a specific feature of ALS, NFL is considered its most characteristic biomarker since its concentration is higher than in any other neurological disease (51, 52). This may be because neurofilaments are abundantly expressed in the large myelinated axons involved in the degenerative process, which is particularly fast and severe in ALS compared to other diseases. The only other condition in which the NFL plasma concentration is as high as in ALS is HIV-associated dementia (HAD) (53). Interestingly, it seems that HIV-related CNS degeneration starts during primary infection

10.3389/fimmu.2022.1070379

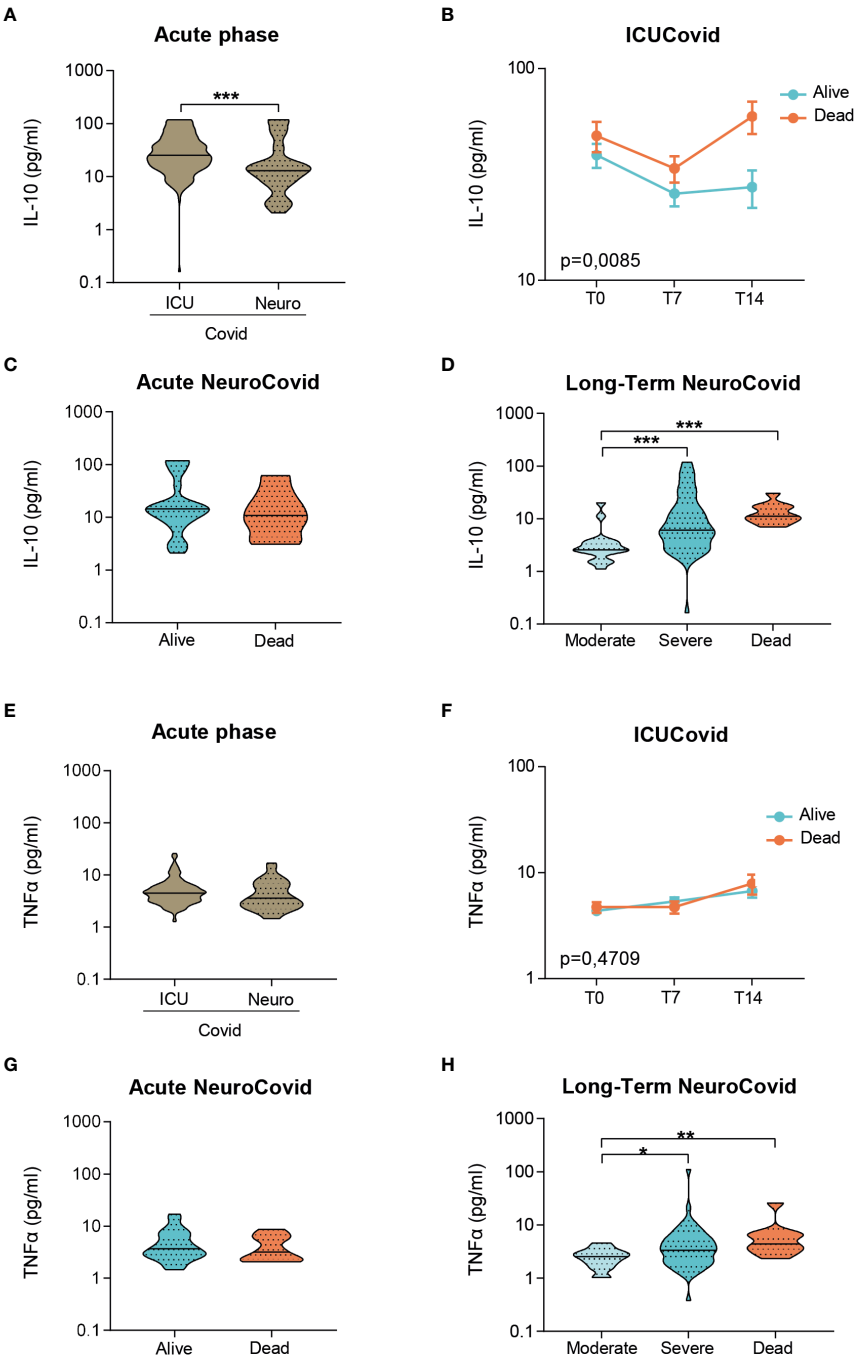

FIGURE 5
IL-10 and TNFα in plasma of two cohorts of COVID-19 patients. **(A-H)** IL-10 **(A-D)** and TNFα **(E-H)** concentrations were measured by Simoa technology in plasma from two cohorts of COVID-19 patients. **(A, E)** Violin plots of IL-10 **(A)** and TNFα **(E)** in the acute phase, in ICUCovid (n=79) and NeuroCovid samples (n=31). **(A)** Mann Whitney, ***p < 0.001. **(E)** Mann Whitney, p = 0.085. **(B, F)** IL-10 **(B)** and TNFα **(F)** were measured in ICUCovid patients at ICU admission (T0) and after 7 (T7) and 14 days (T14). ICUCovid patients were stratified as alive (n=32) or dead (n=14). Data (mean ± SEM) indicate biomarker concentrations. **(B)** Two-way ANOVA for repeated measures, p < 0.01 for cohort factor; **p < 0.005 alive versus dead at T14 by Sidak's *post hoc* test. **(F)** Two-way ANOVA for repeated measures, p = 0.4709. **(C, G)** IL-10 **(C)** and TNFα **(G)** were measured in the acute phase in samples from NeuroCovid patients, stratified as alive (n=23) or dead (n=8). **(C)** Mann Whitney, p = 0.6652; **(G)** Mann Whitney, p = 0.5498. **(D, H)** The concentrations of IL-10 **(D)** and TNFα **(H)** at a longer time, in samples from NeuroCovid patients, stratified as moderate (n=18), severe (n=42) or dead (n=8). **(D)** Kruskal-Wallis, p < 0.0001; ***p < 0.001 by Kruskal-Wallis, Dunn's *post hoc* test. **(H)** Kruskal-Wallis, p < 0.01; *p < 0.05, **p < 0.01 by Kruskal-Wallis, Dunn's *post hoc* test.

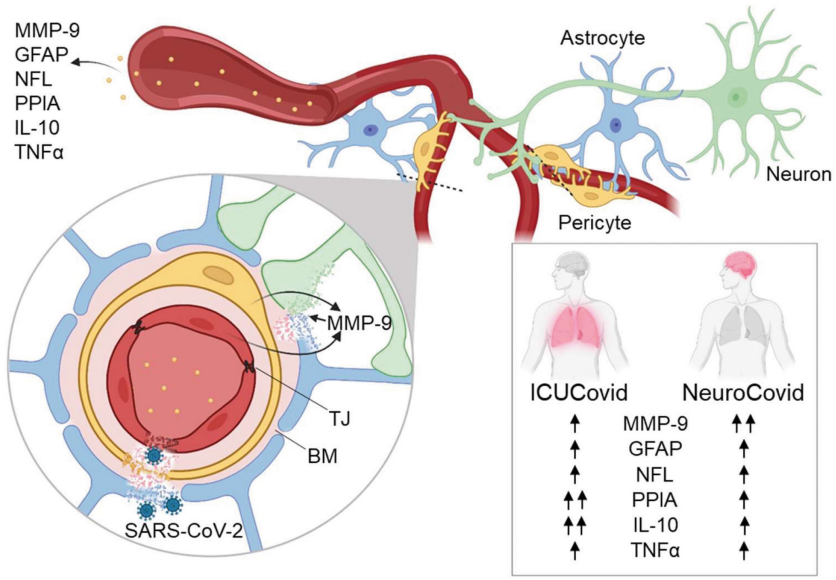

FIGURE 6
Highlights of the results. The effect of SARS-CoV-2 infection on blood biomarkers of BBB disruption (MMP-9, GFAP), neuronal damage (NFL) and systemic inflammation (PPIA, IL-10, TNFα) was measured in patient cohorts with high disease severity (ICUCovid) and with neurological complications (NeuroCovid). There were higher levels of PPIA and IL-10 in ICU compared to NeuroCovid patients, while MMP-9 was significantly higher in NeuroCovid patients. Over-activation of MMP-9 may lead to degradation of tight junctions (TJ), basement membrane (BM) and laminin, implying BBB disruption, penetration of SARS-CoV-2 into the brain and neuronal damage. Blood biomarkers of BBB disruption and neuronal damage were elevated in all COVID-19 patients suggesting potential neurological dysfunctions in the long-term, over a range of disease severities. Figure created with BioRender.com.

and continues during subsequent stages of the disease. However, CSF NFL levels in primary infection are associated with CNS immune activation and BBB disruption but are not accompanied by high CSF total tau and low amyloid beta peptides, as in subjects with HAD (54). This indicates that this early neuronal injury is less severe and/or involves a different mechanism and can in fact be halted by antiretroviral therapy (55). Plasma NFL levels were high in all COVID-19 patients, with NeuroCovid patients reaching the same high levels as in HAD (53). Although the overall picture points to an increased risk for neurological dysfunctions in the long-term, the mechanism and extent to which acute axonal damage, in combination with systemic inflammation and BBB disruption, can predispose to neurodegeneration calls for further investigation.

Our observations may provide hints for a preventive approach. Should further evidence confirm that the neuronal damage found is secondary to, or exacerbated by, BBB disruption, therapies reducing BBB damage could serve as a valuable aid in attenuating the neurological damage in the acute phase and potential dysfunction in the longer term. Interestingly, MMP-9 stands as a druggable target since a set of potent MMPs inhibitors are already available for clinical use (56), furthermore drugs targeting the PPIA-CD147-MMP-9 signaling pathway are also under investigation. A PPIA inhibitor, cyclosporine A (CsA), a well-known immunosuppressive drug, and Meplazumab, an anti-CD147 monoclonal antibody, are being assessed in clinical trials up to phase 2/3 (NCT05113784) for the treatment of severe COVID-19 (57). There are some indications from observational studies of milder COVID-19 and lower mortality in solid organ transplant recipients and autoimmune disease patients under CsA treatment (58). Last, there is evidence that Annexin A1, an endogenous molecule endowed with resolving/protecting action on tight junctions, may have therapeutic potential in restoring cerebrovascular damage and BBB disruption in neurodegenerative diseases and metabolic disorders (59). Indeed, human recombinant annexin A1 has been recently shown to restore BBB integrity and reduce the expression and activity of MMP-9 in brain microvessels when administered in an experimental model of metabolic diabetic disorder (60). Thus, also Annexin A1 could be a therapeutic avenue for COVID-19 to explore in future studies.

There are limitations in this study that should be highlighted. First, neurocognitive assessment in these cohorts of patients was not performed, thus the question as to whether BBB biomarker changes may predict late cognitive dysfunction is still open and should be addressed in future studies. 13% NeuroCOVID patients had a known history of mild cognitive

impairment possibly contributing to the altered neurologic state observed in the acute phase. However, in these patients acute NFL levels were comparable to or even lower than the other patients in the NeuroCovid group, making it unlikely that an already altered CNS homeostasis was the cause of the biomarker changes. Notably, in the ICU cohort there were no patients with pre-existing neurological conditions thus reinforcing the finding that COVID-19 *per se* may induce markers of BBB disruption and neurological damage. Last, patients in our study were recruited before the vaccination campaign. Although there is increasing evidence that COVID-19 vaccination may have a protective effect against the post-COVID-19 syndrome (61, 62), this aspect has not been fully explored, calling for follow-up studies to monitor distinct long-term consequences in vaccinated and non-vaccinated subjects.

Despite these caveats, our study may provide hints for upcoming therapeutic approaches for COVID-19 mitigating at the same time BBB disruption and neurodegeneration to reduce the neurological damage in the acute phase and potential dysfunction in the long-term.

Data availability statement

The original contributions presented in the study are included in the article. Further inquiries can be directed to the corresponding authors.

Ethics statement

The studies involving human participants were reviewed and approved by the ethics committees of the clinical centers involved: Fondazione IRCCS Ca' Granda Ospedale Maggiore Policlinico, Milano (approval #868_2020, 28.10.2020), ASST Papa Giovanni XXIII, Bergamo (approval #123/20, 14.05.2020). The patients/participants provided their written informed consent to participate in this study.

Author contributions

VB, NS, MS, EZ: Drafting/revision of the manuscript, major role in the acquisition of data, study concept and design, analysis and interpretation of data. LP, IL: Drafting/revision of the manuscript, major role in the acquisition of data, analysis and interpretation of data. MC, NB: Drafting/revision of the manuscript, study concept and design. RZ, EF, VP, SL, GC, MG, NR, AC, CM: Drafting/revision of the manuscript, major role in the acquisition of data. BB, GF, RG, FBl, CC, NM, MT, PB, FBi, AB, AN: Drafting/revision of the manuscript. All authors contributed to the article and approved the submitted version.

Funding

The study was supported by project TreXUno, by the 2020-1366 Regione Lombardia, Cariplo e Fondazione Umberto Veronesi, project DigiCovid, and by EU funding within the MUR PNRR - NextGenerationEU Extended Partnership Program on Emerging Infectious Diseases (Project no. PE00000007, INF-ACT). The authors declare that this study also received funding from Brembo S.p.A (Curno, Bergamo, Italy). The funder was not involved in the study design, collection, analysis, interpretation of data, the writing of this article or the decision to submit it for publication.

Acknowledgments

We would like to thank the "COVID-19 NETWORK" WORKING GROUP. Fondazione IRCCS Ca' Granda Ospedale Maggiore Policlinico. Scientific Direction: Silvano Bosari, Luigia Scudeller, Giuliana Fusetti, Laura Rusconi, Silvia Dell'Orto; Department of Transfusion Medicine and Hematology (Biobank): Daniele Prati, Luca Valenti, Silvia Giovannelli, Maria Manunta, Giuseppe Lamorte, Francesca Ferarri; Infectious Diseases Unit: Andrea Gori, Alessandra Bandera, Antonio Muscatello, Davide Mangioni, Laura Alagna, Giorgio Bozzi, Andrea Lombardi, Riccardo Ungaro, Giuseppe Ancona, Gianluca Zuglian, Matteo Bolis, Nathalie Iannotti, Serena Ludovisi, Agnese Comelli, Giulia Renisi, Simona Biscarini, Valeria Castelli, Emanuele Palomba, Marco Fava, Valeria Fortina, Carlo Alberto Peri, Paola Saltini, Giulia Viero, Teresa Itri, Valentina Ferroni,Valeria Pastore,Roberta Massafra, Arianna Liparoti,Toussaint Muheberimana, Alessandro Giommi, Rosaria Bianco, Rafaela Montalvao De Azevedo, Grazia Eliana Chitani; Angelo Bianchi Bonomi Hemophilia and Thrombosis Center and Fondazione Luigi Villa: Flora Peyvandi, Roberta Gualtierotti, Barbara Ferrari, Raffaella Rossio, Nadia Boasi, Erica Pagliaro, Costanza Massimo, Michele De Caro, Andrea Giachi; UOC Internal Medicine, Immunology and Allergology: Nicola Montano, Barbara Vigone, Chiara Bellocchi, Angelica Carandina, Elisa Fiorelli, Valerie Melli, Eleonora Tobaldini; Respiratory Unit and Cystic Fibrosis Adult Center: Francesco Blasi, Stefano Aliberti, Maura Spotti,Leonardo Terranova, Sofia Misuraca, Alice D'Adda, Silvia Della Fiore, Marta Di Pasquale, Marco Mantero Martina Contarini, Margherita Ori, Letizia Morlacchi, Valeria Rossetti, Andrea Gramegna, Maria Pappalettera, Mirta Cavallini, Agata Buscemi; Cardiology Unit: Marco Vicenzi, Irena Rota.

Emergency Unit: Giorgio Costantino, Monica Solbiati, Ludovico Furlan, Marta Mancarella, Giulia Colombo, Giorgio Colombo, Alice Fanin, Mariele Passarella; Acute Internal Medicine: Valter Monzani, Ciro Canetta, Angelo Rovellini, Laura Barbetta, Filippo Billi, Christian Folli, Silvia Accordino; Rare Diseases Center: Diletta Maira, Cinzia Maria Hu, Irene Motta, Natalia Scaramellini; General Medicine and Metabolic Diseases: Anna Ludovica Fracanzani, Rosa Lombardi, Annalisa Cespiati; Geriatric Unit: Matteo Cesari,Tiziano Lucchi,Marco Proietti, Laura Calcaterra, Clara Mandelli, Carlotta Coppola, Arturo Cerizza. Intensive Care Unit: Antonio Maria Pesenti, Giacomo Grasselli, Alessandro Galazzi. Istituto di Ricerche Farmacologiche Mario Negri IRCCS: Alessandro Nobili, Mauro Tettamanti, Igor Monti, Alessia Antonella Galbussera.

Conflict of interest

The authors declare that the research was conducted in the absence of any commercial or financial relationships that could be construed as a potential conflict of interest.

Publisher's note

References

1. Ren AL, Digby RJ, Needham EJ. Neurological update: COVID-19. *J Neurol* (2021) 268:4379–87. doi: 10.1007/s00415-021-10581-y

2. Mehandru S, Merad M. Pathological sequelae of long-haul COVID. *Nat Immunol* (2022) 23:194–202. doi: 10.1038/s41590-021-01104-y

3. Whitaker M, Elliott J, Chadeau-Hyam M, Riley S, Darzi A, Cooke G, et al. Persistent COVID-19 symptoms in a community study of 606,434 people in England. *Nat Commun* (2022) 13:1957. doi: 10.1038/s41467-022-29521-z

4. Mannucci PM, Nobili A, Tettamanti M, D'Avanzo B, Galbussera AA, Remuzzi G, et al. Impact of the post-COVID-19 condition on health care after the first disease wave in Lombardy. *J Intern Med* (2022) 292(3):450–62. doi: 10.1111/joim.13493

5. Voruz P, Allali G, Benzakour L, Nuber-Champier A, Thomasson M, Jacot I, et al. Long COVID neuropsychological deficits after severe, moderate or mild infection. *Clinical and Translational Neuroscience* (2022) 6(2):9. doi: 10.3390/ctn6020009

6. Magnúsdóttir I, Lovik A, Unnarsdóttir AB, McCartney D, Ask H, Kõiv K, et al. Acute COVID-19 severity and mental health morbidity trajectories in patient populations of six nations: an observational study. *Lancet Public Health* (2022) 7: e406–16. doi: 10.1016/S2468-2667(22)00042-1

7. Zayet S, Zahra H, Royer P-Y, Tipirdamaz C, Mercier J, Gendrin V, et al. Post-COVID-19 syndrome: Nine months after SARS-CoV-2 infection in a cohort of 354 patients: Data from the first wave of COVID-19 in nord franche-comté hospital, France. *Microorganisms* (2021) 9(8):1719. doi: 10.3390/microorganisms9081719

8. Malik P, Patel K, Pinto C, Jaiswal R, Tirupathi R, Pillai S, et al. Post-acute COVID-19 syndrome (PCS) and health-related quality of life (HRQoL)-a systematic review and meta-analysis. *J Med Virol* (2022) 94:253–62. doi: 10.1002/jmv.27309

9. Aamodt AH, Høgestøl EA, Popperud TH, Holter JC, Dyrhol-Riise AM, Tonby K, et al. Blood neurofilament light concentration at admittance: a potential prognostic marker in COVID-19. *J Neurol* (2021) 268:3574–83. doi: 10.1007/s00415-021-10517-6

10. Kanberg N, Ashton NJ, Andersson L-M, Yilmaz A, Lindh M, Nilsson S, et al. Neurochemical evidence of astrocytic and neuronal injury commonly found in COVID-19. *Neurology* (2020) 95:e1754–9. doi: 10.1212/WNL.0000000000010111

11. Needham EJ, Ren AL, Digby RJ, Norton EJ, Ebrahimi S, Outtrim JG, et al. Brain injury in COVID-19 is associated with dysregulated innate and adaptive immune responses. *Brain* (2022) 145(11):4097–107. doi: 10.1093/brain/awac321

12. Beghi E, Helbok R, Ozturk S, Karadas O, Lisnic V, Grosu O, et al. Short- and long-term outcome and predictors in an international cohort of patients with neuro-COVID-19. *Eur J Neurol* (2022) 29:1663–84. doi: 10.1111/ene.15293

13. Balcom EF, Nath A, Power C. Acute and chronic neurological disorders in COVID-19: potential mechanisms of disease. *Brain* (2021) 144:3576–88. doi: 10.1093/brain/awab302

14. Erickson MA, Rhea EM, Knopp RC, Banks WA. Interactions of SARS-CoV-2 with the blood-brain barrier. *Int J Mol Sci* (2021) 22(5):2681. doi: 10.3390/ijms22052681

15. Butsabong T, Felippe M, Campagnolo P, Maringer K. The emerging role of perivascular cells (pericytes) in viral pathogenesis. *J Gen Virol* (2021) 102 (8):001634. doi: 10.1099/jgv.0.001634

16. Underly RG, Levy M, Hartmann DA, Grant RI, Watson AN, Shih AY. Pericytes as inducers of rapid, matrix metalloproteinase-9-Dependent capillary damage during ischemia. *J Neurosci* (2017) 37:129–40. doi: 10.1523/JNEUROSCI.2891-16.2016

17. Takata F, Dohgu S, Matsumoto J, Takahashi H, Machida T, Wakigawa T, et al. Brain pericytes among cells constituting the blood-brain barrier are highly sensitive to tumor necrosis factor-α, releasing matrix metalloproteinase-9 and migrating. *vitro. J Neuroinflamm* (2011) 8:106. doi: 10.1186/1742-2094-8-106

18. Yang Y, Estrada EY, Thompson JF, Liu W, Rosenberg GA. Matrix metalloproteinase-mediated disruption of tight junction proteins in cerebral vessels is reversed by synthetic matrix metalloproteinase inhibitor in focal ischemia in rat. *J Cereb Blood Flow Metab* (2007) 27:697–709. doi: 10.1038/sj.jcbfm.9600375

19. Barr TL, Latour LL, Lee K-Y, Schaewe TJ, Luby M, Chang GS, et al. Blood-brain barrier disruption in humans is independently associated with increased matrix metalloproteinase-9. *Stroke* (2010) 41:e123–128. doi: 10.1161/STROKEAHA.109.570515

20. Weekman EM, Wilcock DM. Matrix metalloproteinase in blood-brain barrier breakdown in dementia. *J Alzheimers Dis* (2016) 49:893–903. doi: 10.3233/JAD-150759

21. Bell RD, Winkler EA, Singh I, Sagare AP, Deane R, Wu Z, et al. Apolipoprotein e controls cerebrovascular integrity *via* cyclophilin a. *Nature* (2012) 485:512–6. doi: 10.1038/nature11087

22. Pasetto L, Pozzi S, Castelnovo M, Basso M, Estevez AG, Fumagalli S, et al. Targeting extracellular cyclophilin a reduces neuroinflammation and extends survival in a mouse model of amyotrophic lateral sclerosis. *J Neurosci* (2017) 37:1413–27. doi: 10.1523/JNEUROSCI.2462-16.2016

23. Wang K, Chen W, Zhang Z, Deng Y, Lian J-Q, Du P, et al. CD147-spike protein is a novel route for SARS-CoV-2 infection to host cells. *Signal Trans Target Ther* (2020) 5:283. doi: 10.1038/s41392-020-00426-x

24. Geng J, Chen L, Yuan Y, Wang K, Wang Y, Qin C, et al. CD147 antibody specifically and effectively inhibits infection and cytokine storm of SARS-CoV-2 and its variants delta, alpha, beta, and gamma. *Signal Trans Target Ther* (2021) 6:347. doi: 10.1038/s41392-021-00760-8

25. Abdelhak A, Foschi M, Abu-Rumeileh S, Yue JK, D'Anna L, Huss A, et al. Blood GFAP as an emerging biomarker in brain and spinal cord disorders. *Nat Rev Neurol* (2022) 18:158–72. doi: 10.1038/s41582-021-00616-3

26. Rifino N, Censori B, Agazzi E, Alimonti D, Bonito V, Camera G, et al. Neurologic manifestations in 1760 COVID-19 patients admitted to papa Giovanni XXIII hospital, bergamo, Italy. *J Neurol* (2021) 268:2331–8. doi: 10.1007/s00415-020-10251-5

27. Sacco RL, Kasner SE, Broderick JP, Caplan LR, Connors JJB, Culebras A, et al. An updated definition of stroke for the 21st century: a statement for healthcare professionals from the American heart Association/American

stroke association. *Stroke* (2013) 44:2064–89. doi: 10.1161/STR.0b013e318296aeca

28. Sejvar JJ, Kohl KS, Gidudu J, Amato A, Bakshi N, Baxter R, et al. Guillain-Barré Syndrome and Fisher syndrome: case definitions and guidelines for collection, analysis, and presentation of immunization safety data. *Vaccine* (2011) 29:599–612. doi: 10.1016/j.vaccine.2010.06.003

29. Quist-Paulsen E, Kran A-MB, Lindland ES, Ellefsen K, Sandvik L, Dunlop O, et al. To what extent can clinical characteristics be used to distinguish encephalitis from encephalopathy of other causes? results from a prospective observational study. *BMC Infect Dis* (2019) 19:80. doi: 10.1186/s12879-018-3570-2

30. Pfefferle S, Schöpf J, Kögl M, Friedel CC, Müller MA, Carbajo-Lozoya J, et al. The SARS-coronavirus-host interactome: identification of cyclophilins as target for pan-coronavirus inhibitors. *PloS Pathog* (2011) 7:e1002331. doi: 10.1371/journal.ppat.1002331

31. Ghezzi P, Casagrande S, Massignan T, Basso M, Bellacchio E, Mollica L, et al. Redox regulation of cyclophilin a by glutathionylation. *Proteomics* (2006) 6:817–25. doi: 10.1002/pmic.200500177

32. Fratelli M, Demol H, Puype M, Casagrande S, Eberini I, Salmona M, et al. Identification by redox proteomics of glutathionylated proteins in oxidatively stressed human T lymphocytes. *Proc Natl Acad Sci U.S.A.* (2002) 99:3505–10. doi: 10.1073/pnas.052592699

33. Sherry B, Yarlett N, Strupp A, Cerami A. Identification of cyclophilin as a proinflammatory secretory product of lipopolysaccharide-activated macrophages. *Proc Natl Acad Sci U.S.A.* (1992) 89:3511–5. doi: 10.1073/pnas.89.8.3511

34. Satoh K, Nigro P, Matoba T, O'Dell MR, Cui Z, Shi X, et al. Cyclophilin a enhances vascular oxidative stress and the development of angiotensin II-induced aortic aneurysms. *Nat Med* (2009) 15:649–56. doi: 10.1038/nm.1958

35. Kim H, Kim WJ, Jeon ST, Koh EM, Cha HS, Ahn KS, et al. Cyclophilin a may contribute to the inflammatory processes in rheumatoid arthritis through induction of matrix degrading enzymes and inflammatory cytokines from macrophages. *Clin Immunol* (2005) 116:217–24. doi: 10.1016/j.clim.2005.05.004

36. Nigro P, Pompilio G, Capogrossi MC. Cyclophilin a: a key player for human disease. *Cell Death Dis* (2013) 4:e888. doi: 10.1038/cddis.2013.410

37. Liu QQ, Cheng A, Wang Y, Li H, Hu L, Zhao X, et al. Cytokines and their relationship with the severity and prognosis of coronavirus disease 2019 (COVID-19): a retrospective cohort study. *BMJ Open* (2020) 10:e041471. doi: 10.1136/bmjopen-2020-041471

38. Softic L, Brillet R, Berry F, Ahnou N, Nevers Q, Morin-Dewaele M, et al. Inhibition of SARS-CoV-2 infection by the cyclophilin inhibitor alisporivir (Debio 025). *Antimicrob Agents Chemother* (2020) 64(7):e00876-20. doi: 10.1128/AAC.00876-20

39. Kaushik DK, Hahn JN, Yong VW. EMMPRIN, an upstream regulator of MMPs, in CNS biology. *Matrix Biol* (2015) 44–46:138–46. doi: 10.1016/j.matbio.2015.01.018

40. Fan QW, Yuasa S, Kuno N, Senda T, Kobayashi M, Muramatsu T, et al. Expression of basigin, a member of the immunoglobulin superfamily, in the mouse central nervous system. *Neurosci Res* (1998) 30:53–63. doi: 10.1016/S0168-0102(97)00119-3

41. Zhang L, Zhou L, Bao L, Liu J, Zhu H, Lv Q, et al. SARS-CoV-2 crosses the blood-brain barrier accompanied with basement membrane disruption without tight junctions alteration. *Signal Trans Target Ther* (2021) 6:337. doi: 10.1038/s41392-021-00719-9

42. Abbott NJ. Astrocyte-endothelial interactions and blood-brain barrier permeability. *J Anat* (2002) 200:629–38. doi: 10.1046/j.1469-7580.2002.00064.x

43. Yang Z, Wang KKW. Glial fibrillary acidic protein: from intermediate filament assembly and gliosis to neurobiomarker. *Trends Neurosci* (2015) 38:364–74. doi: 10.1016/j.tins.2015.04.003

44. Janigro D, Mondello S, Posti JP, Unden J. GFAP and S100B: What you always wanted to know and never dared to ask. *Front Neurol* (2022) 13:835597. doi: 10.3389/fneur.2022.835597

45. Graham NSN, Zimmerman KA, Moro F, Heslegrave A, Maillard SA, Bernini A, et al. Axonal marker neurofilament light predicts long-term outcomes and progressive neurodegeneration after traumatic brain injury. *Sci Transl Med* (2021), 13(613):eabg9922. doi: 10.1126/scitranslmed.abg9922

46. Lee M-H, Perl DP, Nair G, Li W, Maric D, Murray H, et al. Microvascular injury in the brains of patients with covid-19. *N Engl J Med* (2021) 384:481–3. doi: 10.1056/NEJMc2033369

47. Kanda T. Biology of the blood-nerve barrier and its alteration in immune mediated neuropathies. *J Neurol Neurosurg Psychiatry* (2013) 84:208–12. doi: 10.1136/jnnp-2012-302312

48. Errede M, Annese T, Petrosino V, Longo G, Girolamo F, de Trizio I, et al. Microglia-derived CCL2 has a prime role in neocortex neuroinflammation. *Fluids Barriers CNS* (2022) 19:68. doi: 10.1186/s12987-022-00365-5

49. Huang C, Wang Y, Li X, Ren L, Zhao J, Hu Y, et al. Clinical features of patients infected with 2019 novel coronavirus in wuhan, China. *Lancet* (2020) 395:497–506. doi: 10.1016/S0140-6736(20)30183-5

50. Gaetani L, Blennow K, Calabresi P, Di Filippo M, Parnetti L, Zetterberg H. Neurofilament light chain as a biomarker in neurological disorders. *J Neurol Neurosurg Psychiatry* (2019) 90:870–81. doi: 10.1136/jnnp-2018-320106

51. Verde F, Steinacker P, Weishaupt JH, Kassubek J, Oeckl P, Halbgebauer S, et al. Neurofilament light chain in serum for the diagnosis of amyotrophic lateral sclerosis. *J Neurol Neurosurg Psychiatry* (2019) 90:157–64. doi: 10.1136/jnnp-2018-318704

52. Falzone YM, Domi T, Mandelli A, Pozzi L, Schito P, Russo T, et al. Integrated evaluation of a panel of neurochemical biomarkers to optimize diagnosis and prognosis in amyotrophic lateral sclerosis. *Eur J Neurol* (2022) 29(7):1930–9. doi: 10.1111/ene.15321

53. Gisslén M, Price RW, Andreasson U, Norgren N, Nilsson S, Hagberg L, et al. Plasma concentration of the neurofilament light protein (NFL) is a biomarker of CNS injury in HIV infection: A cross-sectional study. *EBioMedicine* (2016) 3:135–40. doi: 10.1016/j.ebiom.2015.11.036

54. Peterson J, Gisslen M, Zetterberg H, Fuchs D, Shacklett BL, Hagberg L, et al. Cerebrospinal fluid (CSF) neuronal biomarkers across the spectrum of HIV infection: hierarchy of injury and detection. *PloS One* (2014) 9:e116081. doi: 10.1371/journal.pone.0116081

55. Yilmaz A, Blennow K, Hagberg L, Nilsson S, Price RW, Schouten J, et al. Neurofilament light chain protein as a marker of neuronal injury: review of its use in HIV-1 infection and reference values for HIV-negative controls. *Expert Rev Mol Diagn* (2017) 17:761–70. doi: 10.1080/14737159.2017.1341313

56. Mondal S, Adhikari N, Banerjee S, Amin SA, Jha T. Matrix metalloproteinase-9 (MMP-9) and its inhibitors in cancer: A minireview. *Eur J Med Chem* (2020) 194:112260. doi: 10.1016/j.ejmech.2020.112260

57. Bian H, Zheng Z-H, Wei D, Wen A, Zhang Z, Lian J-Q, et al. Safety and efficacy of meplazumab in healthy volunteers and COVID-19 patients: a randomized phase 1 and an exploratory phase 2 trial. *Signal Trans Target Ther* (2021) 6:194. doi: 10.1038/s41392-021-00603-6

58. Rodriguez-Cubillo B, de la Higuera MAM, Lucena R, Franci EV, Hurtado M, Romero NC, et al. Should cyclosporine be useful in renal transplant recipients affected by SARS-CoV-2? *Am J Transplant* (2020) 20:3173–81. doi: 10.1111/ajt.16141

59. McArthur S, Loiola RA, Maggioli E, Errede M, Virgintino D, Solito E. The restorative role of annexin A1 at the blood–brain barrier. *Fluids Barriers CNS* (2016) 13:17. doi: 10.1186/s12987-016-0043-0

60. Sheikh MH, Errede M, d'Amati A, Khan NQ, Fanti S, Loiola RA, et al. Impact of metabolic disorders on the structural, functional, and immunological integrity of the blood-brain barrier: Therapeutic avenues. *FASEB J* (2022) 36(1):e22107. doi: 10.1096/fj.202101297R

61. Azzolini E, Levi R, Sarti R, Pozzi C, Mollura M, Mantovani A, et al. Association between BNT162b2 vaccination and long COVID after infections not requiring hospitalization in health care workers. *JAMA* (2022) 328:676. doi: 10.1001/jama.2022.11691

62. Notarte KI, Catahay JA, Velasco JV, Pastrana A, Ver AT, Pangilinan FC, et al. Impact of COVID-19 vaccination on the risk of developing long-COVID and on existing long-COVID symptoms: A systematic review. *eClinicalMedicine* (2022) 53:101624. doi: 10.1016/j.eclinm.2022.101624

frontiers | Frontiers in Immunology

TYPE Case Report
PUBLISHED 23 February 2023
DOI 10.3389/fimmu.2023.1125960

OPEN ACCESS

EDITED BY
Pietro Ghezzi,
University of Urbino Carlo Bo, Italy

REVIEWED BY
Anna Starshinova,
Saint Petersburg State University, Russia
Snezana Zivancevic-Simonovic,
University of Kragujevac, Serbia

*CORRESPONDENCE
Mark R. Gillrie
mark.gillrie@ucalgary.ca

†These authors share first authorship

SPECIALTY SECTION
This article was submitted to Inflammation, a section of the journal Frontiers in Immunology

RECEIVED 16 December 2022
ACCEPTED 06 February 2023
PUBLISHED 23 February 2023

CITATION
Gillrie MR, Rosin N, Sinha S, Kang H, Farias R, Nguyen A, Volek K, Mah J, Mahe E, Fritzler MJ, Yipp BG and Biernaskie J (2023) Case report: Immune profiling links neutrophil and plasmablast dysregulation to microvascular damage in post-COVID-19 Multisystem Inflammatory Syndrome in Adults (MIS-A). *Front. Immunol.* 14:1125960. doi: 10.3389/fimmu.2023.1125960

Case report: Immune profiling links neutrophil and plasmablast dysregulation to microvascular damage in post-COVID-19 Multisystem Inflammatory Syndrome in Adults (MIS-A)

Mark R. Gillrie[1,2,3*†], Nicole Rosin[4†], Sarthak Sinha[4], Hellen Kang[1], Raquel Farias[5], Angela Nguyen[5], Kelsie Volek[1], Jordan Mah[3], Etienne Mahe[6], Marvin J. Fritzler[3,7], Bryan G. Yipp[2,5] and Jeff Biernaskie[4,8,9,10]

[1]Department of Microbiology, Immunology and Infectious Diseases, Cumming School of Medicine, University of Calgary, Calgary, AB, Canada, [2]Snyder Institute for Chronic Diseases, Cumming School of Medicine, University of Calgary, Calgary, AB, Canada, [3]Department of Medicine, Cumming School of Medicine, University of Calgary, Calgary, AB, Canada, [4]Department of Comparative Biology and Experimental Medicine, Faculty of Veterinary Medicine, University of Calgary, Calgary, AB, Canada, [5]Department of Critical Care Medicine, Cumming School of Medicine, University of Calgary, Calgary, AB, Canada, [6]Department of Pathology & Laboratory Medicine, Cumming School of Medicine, University of Calgary, Calgary, AB, Canada, [7]Department of Biochemistry and Molecular Biology, Cumming School of Medicine, University of Calgary, Calgary, AB, Canada, [8]Hotchkiss Brain Institute, University of Calgary, Calgary, AB, Canada, [9]Alberta Children's Hospital Research Institute, University of Calgary, Calgary, AB, Canada, [10]Department of Surgery, University of Calgary, Calgary, AB, Canada

Despite surviving a SARS-CoV-2 infection, some individuals experience an intense post-infectious Multisystem Inflammatory Syndrome (MIS) of uncertain etiology. Children with this syndrome (MIS-C) can experience a Kawasaki-like disease, but mechanisms in adults (MIS-A) are not clearly defined. Here we utilize a deep phenotyping approach to examine immunologic responses in an individual with MIS-A. Results are contextualized to healthy, convalescent, and acute COVID-19 patients. The findings reveal systemic inflammatory changes involving novel neutrophil and B-cell subsets, autoantibodies, complement, and hypercoagulability that are linked to systemic vascular dysfunction. This deep patient profiling generates new mechanistic insight into this rare clinical entity and provides potential insight into other post-infectious syndromes.

KEYWORDS

MIS-A, COVID-19, immunophenotyping, neutrophil, plasmablast, immune dysfunction, microvascular damage, case report

Introduction

Despite low incidence of severe acute COVID-19 in healthy younger individuals, they are not completely spared. The most notable post-COVID-19 disease is referred to as Multisystem Inflammatory Syndrome in Children (MIS-C) characterized by an intense inflammatory disease affecting the heart, skin, and mucosal surfaces with onset weeks after primary infection (1, 2). A similar syndrome has been reported in case series of post-COVID-19 adults with marked multiorgan dysfunction including cardiac failure that spares the lungs, referred to as MIS-A (3). Five criteria have been proposed to define this condition (3) with updated criteria by the US CDC (4) and ongoing surveillance revealing hundreds of cases globally (5). Unlike the substantial body of literature on primary SARS-Cov2 infection, there is limited understanding of the mechanisms for late complications of COVID-19 in adults such as MIS-A. Little is known about the pathophysiology of MIS-A, but candidate pathways include cytokine storm, immune cell dysregulation, autoantibody production, vascular dysfunction, and immunothrombosis (6–10). The aim of the current study is to profile the immune response of a patient with MIS-A to reveal unique molecular and cellular mechanisms underlying this rare condition.

Post-COVID-19 MIS-A case report

A 38-year-old unvaccinated South Asian male presented to a tertiary care hospital complaining of a 4-day history of fever, abdominal pain, and diarrhea. The patient was previously healthy and had no known relevant family or psychosocial history. On exam he was noted to have a macular blanching skin rash on his torso and proximal extremities, bilateral non-purulent conjunctivitis, sore throat, and prominent non-exertional chest pressure associated with progressive shortness of breath (Figure 1A). In the emergency department he was febrile, hypotensive due to cardiogenic shock, and started on vasopressors to maintain systolic blood pressure and was eventually transferred to the Cardiac Care Unit (CCU) for cardiac support (Figure 1A, Supplementary Table 1).

Twenty-five days prior to presentation, the patient had several days of cough and sore throat without any other respiratory symptoms. Both the patient and household family members tested positive for SARS-CoV2 by RT-PCR of nasopharyngeal swabs. These symptoms had completely resolved for more than two weeks prior to the most recent presentation.

Initial laboratory investigations on admission revealed elevated inflammatory, renal, hepatic, and coagulation dysfunction markers (Supplementary Table 1). An echocardiogram showed severe biventricular heart failure. An initial chest Computed Tomography (CT) scan using a pulmonary embolism protocol was negative with remarkably normal lungs (Figure 1A). A SARS-CoV2 NP RT-PCR test was low positive (Ct-value >30) with the remainder of the respiratory viral pathogen panel negative. SARS-CoV2 serology to spike RBD and N proteins was strongly positive. The patient was presumptively diagnosed with myocarditis and potential acute coronary syndrome while being investigated for sepsis. He was started on aspirin, enoxaparin, and broad-spectrum antibiotics in consultation with cardiology and infectious diseases clinical teams.

While in CCU, he was slowly weaned off vasopressors but developed worsening leukocytosis with neutrophilia, renal failure with evidence of a procoagulant state (increased D-Dimer), further elevated inflammatory (C-reactive protein) and cardiac dysfunction (NT-proBNP and troponin) markers. He had continued diarrhea and severe abdominal pain leading to escalation of his antimicrobial therapy to meropenem. The rest of his infectious and autoimmune disease workups were negative aside from evidence of complement activation (low C3/C4 levels) (Supplementary Table 1). CT imaging of his head, neck, chest, and abdomen were normal. Eventually while still in CCU he had an indium white blood scan that did not show any active infection or inflammation (Supplementary Figure 1).

Given the constellation of extra-pulmonary systems involvement without respiratory disease, recent resolved SARS-CoV2 infection, and positive serology, he was diagnosed with COVID-19-associated MIS-A meeting all published criteria for the condition (3, 4). Antibiotics were stopped and 6mg of oral dexamethasone daily for 5 days was started. A repeat echocardiogram prior to discharge showed normal right and left ventricular function which was corroborated by cardiac MRI showing no signs of myocarditis (Supplementary Figure 1). The patient was discharged after 15 days, 10 of which were in the CCU.

Materials and methods

See supplemental Materials and Methods.

Results

MIS-A deep immune profiling

To better contextualize our findings, we compared both acute and convalescent blood samples from our MIS-A patient to three age-matched healthy and convalescent COVID-19 controls at similar time frames post infection (Supplementary Table 2 and Figure 1B, see Supplemental Materials and Methods) using a published precision medicine approach (11).

We first set out to establish the presence of 'cytokine storm' mediators reflecting a state of systemic inflammation. Analysis of >75 cytokines and soluble receptors highlighted 5-fold elevated levels of sCD25R, CTACK, I-309, IL-10 and IP-10 (CXCL10) in acute MIS-A as compared to healthy and convalescent controls (Figure 1C), the latter of which has been implicated in MIS-C (7). Our results contrast those in severe COVID-19 where IL-6, MCP-2 (CCL2), G-/GM-CSF, and IFN-γ are often high (12). Additionally, we found elevated circulating calprotectin (S100A8/9, MIS-A = 298 picogram/mL, all controls <14pg/mL) an 'alarmin' associated with neutrophils that has been found elevated in severe COVID-19 (13) and MIS-C patients (6).

10.3389/fimmu.2023.1125960

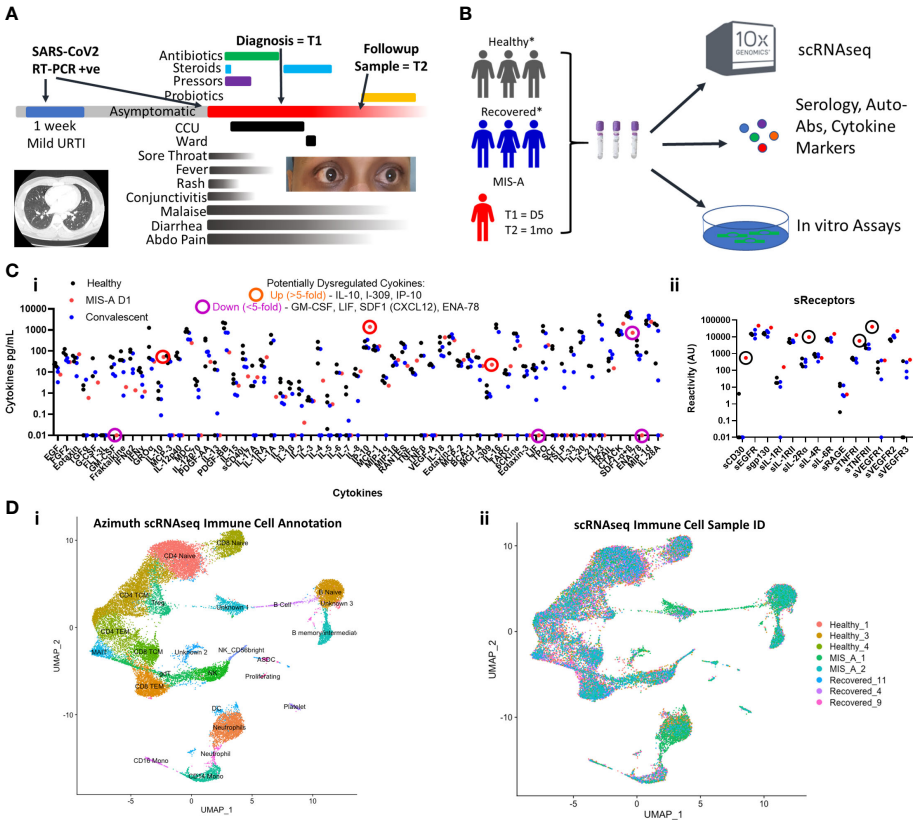

FIGURE 1
COVID-19 associated Multisystem Inflammatory Syndrome of Adults (MIS-A) is associated with critical illness, cytokine dysregulation and altered immune cell landscape. **(A)** MIS-A case outlining timeline of prior mild COVID-19 upper respiratory tract infection (URTI) and subsequent presentation of critical illness due to MIS-A with symptoms, treatments, and investigational sampling times (T=1 and T=2) highlighted. **(B)** A multi-disciplinary pre-existing COVID-19 investigational approach was utilized to investigate immune responses in this rare syndrome with relevant healthy and recovered COVID-19 controls. **(C)** Multiplex cytokine arrays (i) defined upregulated and down regulated cytokines, notably IL-10 and IP-10, and soluble cytokine receptors (ii) including sCD25 (IL2αR) as key markers of cytokine storm. **(D)** Single cell RNA seq (scRNAseq) immune cell annotation using the Azimuth database (i) with identification of cellular source (ii) identifying increased B cell and neutrophil populations in MIS-A.

scRNAseq reveals emergence of neutrophil and B cell subpopulations during MIS-A

We next utilized single-cell RNA sequencing (scRNAseq) to further delineate circulating immune cell alterations in MIS-A compared to healthy and COVID-19 convalescent controls (11). This revealed notable decreases in total numbers of T, NK, and mononuclear cells but increases in neutrophil and B-cell populations during acute MIS-A (Figures 1D). Global transcriptional changes during admission demonstrated differences in B cell, naïve CD4 T cells, and neutrophil populations which, aside from some sustained abnormalities in neutrophils, were largely resolved by day 30 in MIS-A (Supplementary Figure 3).

Neutrophil counts were strikingly elevated in MIS-A with increased immature neutrophil populations in clinical blood counts (Figure 2A). Consistent with this, peripheral blood smears demonstrated a large percentage of neutrophil progenitor cells including 'band' forms with features of metamyelocytes, and neutrophils with 'toxic changes' suggestive of activation and phagocytosis (Figures 2A, B and S4) not typically seen healthy individuals. scRNAseq analysis of total neutrophil populations revealed elevated markers of immaturity (MMP9), B cells (e.g. MZB1, Immunoglobulins, XBP1) and inflammation (CD177, CST7) (Figures 2D and S5). Unsupervised clustering of neutrophils from all scRNAseq samples identified six ('0-5') neutrophil subpopulations expressing common markers FCGR3B and CSF3R (Figures 2C–D). Clusters 0,1,5 were shared by all clinical groups but predominantly represented by healthy and convalescent patients (Figure 2C). In contrast, cluster 2-4 neutrophils were exclusive to MIS-A with 2 and 3 co-expressing immature neutrophil (MMP9), activation (CD177), and B cell markers (IGHA1 and XBP1) while cluster 4 had greater expression of IFN stimulated genes (ISGs) including IFIT2 and IFIT3 yet did not map to our previously identified PMN populations in severe COVID-19 (Figures 2D and S5, 6) (11).

We also found decreased total lymphocyte numbers during acute MIS-A but morphologically increased large granular lymphocytes (also known as 'activated' or 'atypical' lymphocytes) (Figures 3A, B and S7) which are rare in healthy controls. These

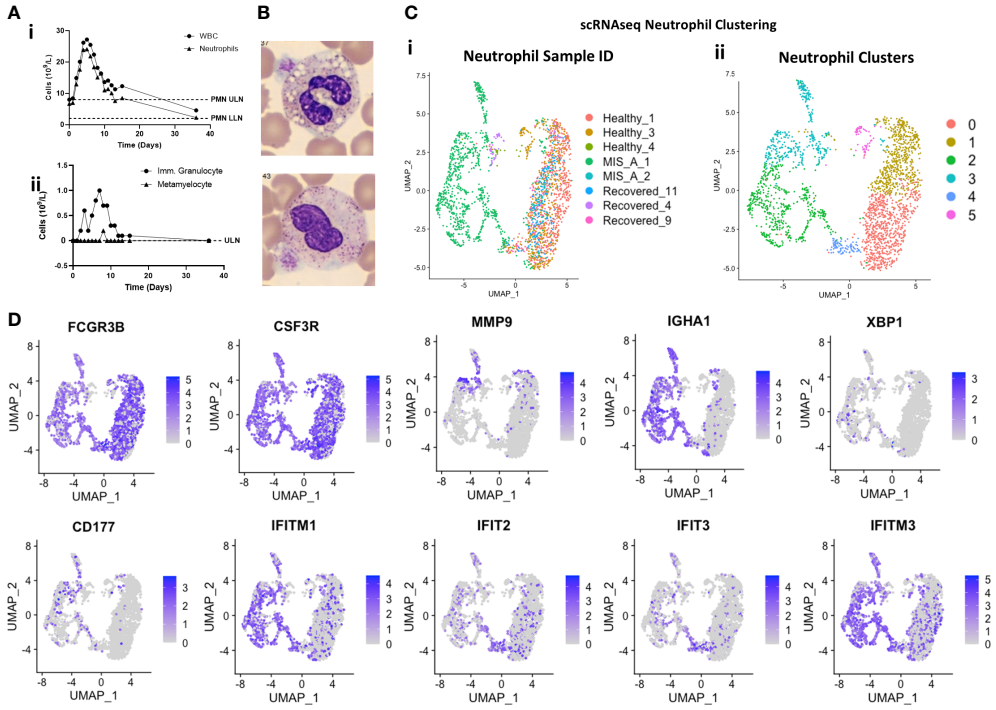

FIGURE 2
Immature, B-cell like, and 'IFN' neutrophil subpopulations emerge in MIS-A. **(A)** Total peripheral blood neutrophil (PMN) counts (i) transiently increase in MIS-A with concurrent increases in immature neutrophil populations (ii). **(B)** Morphologic assessment demonstrates 'toxic' changes in neutrophils with increased vacuolization and cytoplasmic irregularities (i) plus immature 'band' forms (ii). **(C)** scRNAseq analysis of all neutrophils identifies increases in neutrophils in MIS-A (i) with increases seen in three (2-4) of six (0-5) neutrophil subpopulations (ii). **(D)** Neutrophil mRNA expression by scRNAseq of classical neutrophil markers (FCGR3B, CSF3R), immature neutrophils (MMP9), B cells (IGHA1, XBP1), neutrophil activation (CD177), and interferon (IFN) stimulated genes (IFITM1 and 3, IFIT2-3).

atypical lymphocytes stained largely negative for T/NKT cell marker CD3 but positive for plasma/plasmablast (PB) markers CD79a and SDC1/CD138 (Figure 3C). Using scRNAseq we found typical B-cell populations in all groups but unique PB populations in MIS-A (Figures 3D and S8–10). PB subpopulations have been linked with rapid expansion, short survival (<1-2 weeks), and potentially damaging autoantibody production in human diseases including COVID-19 (14–16). Initially we noted three unique PB subpopulations by scRNAseq two of which were unique to MIS-A (Supplementary Figure 8). However, during scRNAseq quality control steps, we noticed that MIS-A uniquely had higher RNA and mitochondrial (MT) reads of >15%, typically considered 'dead' cells, and these MT^{hi} cells were >75% PBs (Figures 3E and S9), something we had not seen in our previous studies on acute critical COVID-19 (11). Unsupervised clustering including these MThi cells identified five PB clusters ('0-5') all of which were CD19, CD20 (MS4A1), and IgD-negative (data not shown) but positive for other immunoglobulins and B-cell markers. Four PB clusters were exclusive to MIS-A and three represented MT^{hi} populations (Figures 3E, F and S9, 10). These MIS-A-specific Ig-expressing PB subpopulations could be differentially identified by MT RNA content, proliferation (MKI67), and chemokine receptor (CXCR4/CCR7/CCR10) expression (Figures 3E, H and S9, 10).

MIS-A is linked to autoreactive antibody production, microvascular damage, and coagulation

To determine potential pathogenic consequences of PB dysfunction, we investigated SARS-CoV2 and autoreactive antibody production. This indicated elevated total IgA, SARS-CoV2 antibody responses, and broad autoreactivity to multiple cytokines and human cardiac microvascular endothelial cells (HCMEC) in MIS-A (Figures 3I and 4A). We found that in addition to autoantibody binding specifically to cardiac but not lung endothelium (Supplementary Figure 12), MIS-A plasma also resulted in classical complement deposition and HCMEC disruption in vitro (Figures 4A–D). However, only inhibition of coagulation using hirudin, heparin, or activated protein C but not blockade of complement activity prevented endothelial disruption (Figures 4C–E). Using a more physiologic 3D microvascular assay (17, 18), we found acute MIS-A more so than severe COVID-19 plasma caused microvascular leak and coagulation that was also inhibited by hirudin, heparin, or activated protein C (Figures 4F–I, S13, 14, and Movie S1). Exploration of plasma markers of vascular dysfunction confirmed evidence of endothelial damage (Endoglin, PECAM-1, Ang-2, sEsel, sICAM1), neutrophil activation (MPO,

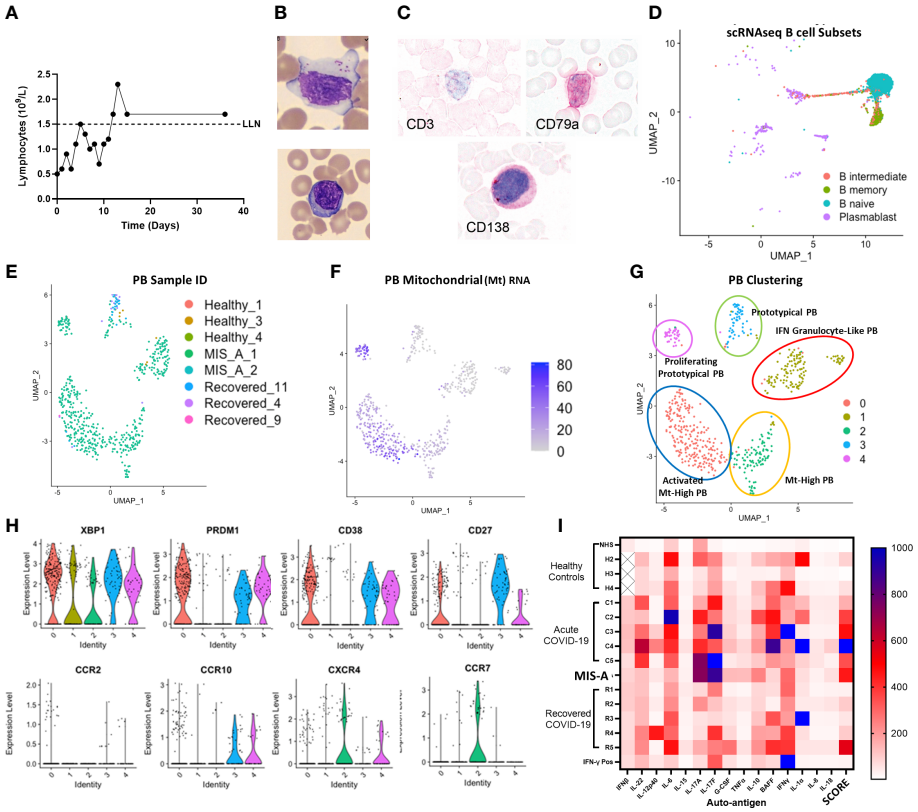

FIGURE 3
MIS-A is associated with lymphopenia but increased atypical lymphocytes, Plasmablast **(PB)** B cells and autoantibody production. **(A)** Lymphopenia in acute MIS-A on peripheral blood counts. **(B)** Emergence of atypical lymphocytes with increased cytoplasmic content **(i)** and less frequent observed but plasma cells (ii). **(C)** Staining of atypical lymphocytes demonstrate absence of T cell marker CD3 but presence of plasma/plasmablast markers CD79a and CD138 (red). **(D)** scRNAseq B-cell clustering using Azimuth reference database showing unknown but unique populations of plasmablasts (PB, purple). **(E)** Unsupervised clustering of scRNAseq plasmablasts shows increases in unique subpopulations with MIS-A. **(F)** Mitochrondrial (Mt) RNA content of PBs differentiates novel PB populations. **(G)** Proposed nomenclature for PB subsets based on top differentially expressed genes in PB subsets by scRNAseq. **(H)** Key PB genes (XBP1, PRDM1, CD38, CD27) and chemokine receptors (CCR2,7,10 and CXCR4) to differentiate PB subsets expressing Igs (see supplementary Supplementary Figure 9) and Mt RNA (panel F) in MIS-A and controls. **(I)** Serum auto-antibody reactivity to human cytokines from pooled normal healthy serum (NHS) and healthy (H2-4), acute severe COVID-19 (C1-5), MIS-A D1 and recovered COVID-19 (R1-6) patients versus known IFN-γ positive patient expressed as arbitrary units from assay. SCORE indicates an adjusted rank sum across each target to generate an autoimmunity 'score' for each patient. See methods for details.

GDF-15), and thrombosis (vWF, D-Dimer, sPsel) in MIS-A plasma but not healthy or convalescent controls (Figure 4J).

Discussion

Here we provide an in-depth immunologic analysis of an uncommon but severe late complication of COVID-19 predominantly in a young healthy male of non-Caucasian descent. Greater than 200 cases of MIS-A have now been reported with our patient being a prototypical severe case accompanied by elevated inflammatory markers (5). In contrast to MIS-C in children, MIS-A is often misdiagnosed or missed altogether in adults, which has led to difficulties in treating and examining the pathophysiology of the disease (19). Despite the syndromes striking clinical presentation, only a few case reports of MIS-A have investigated potential pathogenic features demonstrating evidence of cytokine dysregulation ('cytokine storm'), and vascular inflammation including microvascular neutrophil accumulation and complement deposition within the heart consistent with a vasculitis (1, 20, 21). In potentially related pediatric MIS-C, cytokine dysregulation, anti-endothelial autoantibody production (6, 10, 22), and inborn errors of OAS and RNAse- L antiviral signaling (10) are known to occur in a subset of patients but the interplay between these proposed pathways, terminal effectors, and relevance to MIS-A are unclear.

During our analysis, we found evidence of multiple striking immune cell alterations in neutrophil and B cell subpopulations. To our knowledge, no other scRNAseq analysis of MIS-A exists. Parallel studies in MIS-C exist and identify plasmablast and neutrophil dysfunction (6) with others showing acute NK and T cell alterations (22), or compare responses of convalescent samples stimulated with potentially unrelated agonists (10). Our results are difficult to compare to MIS-C data given other studies using

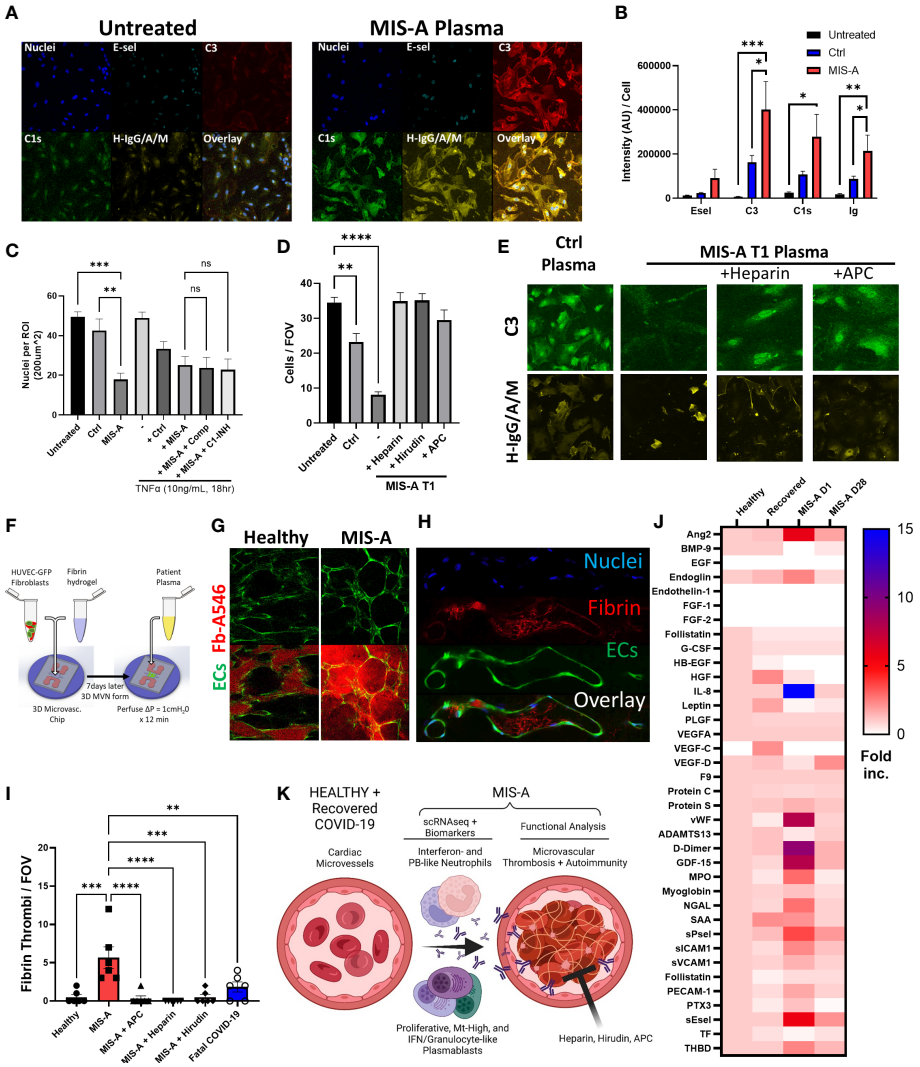

FIGURE 4
Microvascular dysfunction in MIS-A. **(A)** Primary human cardiac microvascular endothelial cells (HCMEC) untreated or treated for 30 minutes with MIS-A plasma and stained for nuclei, endothelial inflammatory markers (E-sel), complement (C3, C1s) and human IgG/A/M. **(B)** Quantitation of HCMEC staining from panel A including additional controls. **(C)** Quantitation of total endothelial cells (nuclei) as in panel A from control or MIS-A treated HCMEC pre-incubated with TNF-α (1ng/mL 18 hours) and or complement inhibitors, Compostatin (Comp) or C1 esterase inhibitor (C1-INH), as indicated. **(D)** Quantitation of total endothelial cells (nuclei) from control or MIS-A treated HCMEC pre-incubated with anti-coagulants heparin, hirudin, and activated protein C as indicated. **(E)** Representative images for C3 and H-IgG/A/M staining as in **(D–F)** 3D human microvascular model containing EGFP expressing human umbilical vein endothelial cells, normal human fibroblasts, and perfused with patient plasma containing Alexa 546-labeled fibrinogen. **(G)** Intra- and extra-vascular fibrin accumulation in healthy or MIS-A following 15-minute perfusion of patient plasma spiked with fibrinogen-Alexa546 (red) through microvascular networks (green). **(H)** Representative images of microvascular fibrinogen Alexa-546 accumulation in microvessels in response to MIS-A plasma for 15 minutes. **(I)** Quantitation fibrin accumulation as in B using patient plasma plus or minus addition of activated protein C (APC), heparin, or hirudin in comparison to healthy or fatal COVID-19 plasma. **(J)** Cytokine arrays from healthy controls (n=5) and acute *vs* convalescent MIS-A plasma (n=1 each) showing elevation in multiple vascular endothelial damage markers (Ang2, sEsel, THBD), neutrophil activation markers (MPO, NGAL) and pro-coagulants (D-Dimer, VWF, sPsel) as fold increase from healthy. **(K)** Summary of findings including emergence of plasmablast subsets, auto-antibody production, neutrophil activation, and thrombosis culminating in vascular damage in acute MIS-A. ns = nonsignificant, **p<0.01, ***p<0.001 by one-way ANOVA with *post-hoc* Tukey's test. *p < 0.05 and ****p < 0.0001.

scRNAseq have used PBMCs that underrepresent neutrophil responses (11) and are also confounded by potential differences between pediatric and adult immune systems (23).

In MIS-A, we specifically identified increased immature neutrophil populations that appear to overlap somewhat with those in other disease states (11, 14, 15, 24). However, none of the overlap with previously reported neutrophil subsets was strong suggesting that although loose connections between neutrophil populations are present in different diseases, there remains significant plasticity in human neutrophil phenotypes in different disease states that is not easily reconciled even by scRNAseq. The most unexpected neutrophil difference in our study was the emergence of B-cell gene expression in neutrophils which has been seen in severe COVID-19 (14, 15). In conjunction with known rapid induction of and clearance of PBs including unique populations identified here, it is tempting to speculate that neutrophil subsets may be activating or clearing PBs in MIS-A and possibly other conditions. Confirming the presence and

mechanisms of neutrophil-PB interactions in MIS-A may identify novel therapeutic targets for this and related conditions.

Conclusions

The pathological importance of potential neutrophil and B-cell dysregulation in MIS-A to date has remained unclear. The possibly overlapping syndrome of MIS-C suggests autoantibodies and neutrophil activation lead to damage of the vasculature (6). However, a terminal pathway downstream of neutrophil and B-cell activation driving vascular dysfunction in our hands appears to be microvascular coagulation (Figure 4K). This concept is supported by derangements in multiple coagulation markers from MIS-A plasma, most notably the common finding of elevated fibrin degradation products (D-dimer) (5). The process of coagulation in the context of inflammation and neutrophil activation is often referred to as immunothrombosis (25). It may be that MIS-A represents a complication from a delayed inflammatory phase of severe acute COVID-19 where IgA antibodies have been shown to cause neutrophil activation via release of neutrophil extracellular traps (NETs) (26). Our 2D and 3D in vitro assays suggest that anticoagulation using direct inhibitors of the coagulation cascade including heparin, hirudin, or activated protein C (APC) may be a way to prevent vascular dysfunction. APC is particularly intriguing because it also has potent vascular protective functions through the endothelial protein C receptor (EPCR), independent of anti-coagulant activity (27).

Limitations and future directions

Our study represents a single case of this rare condition and is therefore limited in its broad applicability but does provide a detailed roadmap for ongoing investigations of MIS-A and similar post-infectious conditions. These other conditions include MIS-C, Kawasaki disease, and even Long COVID-19, the latter of which our patient would have later fulfilled criteria for based on approximately six months of significant lingering fatigue, abdominal, and neurocognitive ('brain fog') symptoms. Our results demonstrate the presence of potentially novel human subpopulations of neutrophil and B cells that require further exploration in other cases of MIS-A and inflammatory conditions. Importantly, although we define differences in circulating numbers, morphologic features, and gene expression in these cells, all potential identifications by scRNAseq are proposed and do not imply functional properties. Utilization of cell surface markers are required to select and interrogate functional properties of these subpopulations. Important functional readouts to explore in subpopulations include PB cytokine and immunoglobulin production and neutrophil ROS, NET release, and degranulation. Ascertaining microvascular function in the heart and other organs of these patients would also be of benefit (28). Finally, clinical trials of proposed interventions, including anti-coagulation or APC, are desperately needed for this and other post-infectious syndromes.

Data availability statement

The datasets presented in this study can be found in online repositories. The names of the repository/repositories and accession number(s) can be found below: https://www.ncbi.nlm.nih.gov/geo/, GSE171052, https://www.ncbi.nlm.nih.gov/geo/, GSE157789.

Ethics statement

The studies involving human participants were reviewed and approved by Research Ethics Board, University of Calgary. The patients/participants provided their written informed consent to participate in this study. Written informed consent was obtained from the individual(s) for the publication of any potentially identifiable images or data included in this article.

Author contributions

MG, NR, MF, BY and JB designed the study. MG, NR, HK, RF, AN, KV, MF, and EM performed the experiments and analyzed data. NR and SS performed scRNAseq and bioinformatic analysis. MG, NR, MF, and BY wrote the manuscript. All authors contributed to the article and approved the submitted version.

Funding

MG received Canadian Institutes of Health Research, Canadian Foundation for Innovation, and Univ. of Calgary Clinical Research COVID-19 funding. FastGrant from the Thistledown Foundation (JB and BY) and the Calgary Firefighters Burn Treatment Society (JB) was also obtained for scRNASeq studies. SS received CIHR Vanier, Alberta Innovates and Killam doctoral scholarships. BY is a Tier II Canada Research Chair in Pulmonary Immunology, Inflammation and Host Defence.

Acknowledgments

Thank you to all the volunteers and patients, particularly our patient with MIS-A, for agreeing to be a part of this study and sharing their story. Also thank you to the clinical teams for supporting their care and this study. The graphical abstract was created using Biorender.

Conflict of interest

MF is the medical director of Mitogen Diagnostics Corporation MitogenDx and Eve Technologies, and has received honoraria from Inova Diagnostics Inc.

The remaining authors declare that the research was conducted in the absence of any commercial or financial relationships that could be construed as a potential conflict of interest.

Publisher's note

All claims expressed in this article are solely those of the authors and do not necessarily represent those of their affiliated organizations, or those of the publisher, the editors and the reviewers. Any product that may be evaluated in this article, or claim that may be made by its manufacturer, is not guaranteed or endorsed by the publisher.

Supplementary material

The Supplementary Material for this article can be found online at: https://www.frontiersin.org/articles/10.3389/fimmu.2023.1125960/full#supplementary-material

References

1. Jiang L, Tang K, Levin M, Irfan O, Morris SK, Wilson K, et al. Review COVID-19 and multisystem inflammatory syndrome in children and adolescents. *Lancet Infect Dis* (2020) 20(11):e276–88. doi: 10.1016/S1473-3099(20)30651-4

2. Feldstein LR, Tenforde MW, Friedman KG, Newhams M, Rose EB, Dapul H, et al. Characteristics and outcomes of US children and adolescents with multisystem inflammatory syndrome in children (MIS-c) compared with severe acute COVID-19. *JAMA* (2021) 325(11):1074–87. doi: 10.1001/jama.2021.2091

3. Morris SB, Schwartz NG, Patel P, Abbo L, Beauchamps L, Balan S. Case series of multisystem inflammatory syndrome in adults associated with SARS-CoV-2 infection — united kingdom and united states, march – august 2020. *MMWR* (2020) 69 (40):1450–6. doi: 10.15585/mmwr.mm6940e1

4. Centers for Disease Control and Prevention. *Multisystem inflammatory syndrome in adults (MIS-a)* (2021). Available at: https://www.cdc.gov/mis/mis-a.html.

5. Patel P, Decuir J, Abrams J, Campbell AP, Godfred-cato S, Belay ED. Clinical characteristics of multisystem inflammatory syndrome in adults a systematic review. *JAMA Netw Open* (2022) 4(9):e2126456. doi: 10.1001/jamanetworkopen.2021.26456

6. Ramaswamy A, Brodsky NN, Sumida TS, Pierce RW, Hafler DA, Lucas CL. Immune dysregulation and autoreactivity correlate with disease severity in SARS-CoV-2-associated multisystem inflammatory syndrome in children ll article immune dysregulation and autoreactivity correlate with disease severity in SARS-CoV-2-associated mult. *Immunity* (2021) 54(5):1083–1095.e7. doi: 10.1016/j.immuni.2021.04.003

7. Bartsch YC, Wang C, Zohar T, Fischinger S, Atyeo C, Burke JS, et al. Humoral signatures of protective and pathological SARS-CoV-2 infection in children. *Nat Med* (2021) 27:454–62. doi: 10.1038/s41591-021-01263-3

8. Bajaj R, Sinclair HC, Patel K, Low B, Pericao A, Manisty C, et al. Delayed-onset myocarditis following COVID-19. *Lancet Respir Med* (2021) 9(4):e32–4. doi: 10.1016/S2213-2600(21)00085-0

9. Chau VQ, Giustino G, Mahmood K, Oliveros E, Neibart E, Oloomi M, et al. Cardiogenic shock and hyperinflammatory syndrome in young males with COVID-19. *Circ Hear Fail* (2020) 13(e007485):556–9. doi: 10.1161/CIRCHEARTFAILURE.120.007485

10. Lee D, Lee D, Le Pen J, Yatim A, Dong B, Aquino Y, et al. Inborn errors of OAS – RNase l in SARS-CoV-2 – related multisystem inflammatory syndrome in children. *Science* (2022) 3627(December):1–35. doi: 10.1126/science.abo3627

11. Sinha S, Rosin NL, Arora R, Labit E, Jaffer A, Cao L, et al. Dexamethasone modulates immature neutrophils and interferon programming in severe COVID-19. *Nat Med* (2022) 28:201–11. doi: 10.1038/s41591-021-01576-3

12. Huang C, Wang Y, Li X, Ren L, Zhao J, Hu Y, et al. Articles clinical features of patients infected with 2019 novel coronavirus in wuhan , China. *Lancet* (2020) 395:497–506. doi: 10.1016/S0140-6736(20)30183-5

13. Mahler M, Meroni P-L, Infantino M, Buhler KA, Fritzler MJ. Circulating calprotectin as a biomarker of COVID-19 severity. *Expert Rev Clin Immunol* (2021) 17(5):431–43. doi: 10.1080/1744666X.2021.1905526

14. Bernardes JP, Mishra N, Tran F, Rosenstiel P. Longitudinal multi-omics analyses identify responses of megakaryocytes , erythroid cells , and plasmablasts as hallmarks of severe COVID-19. *Immunity* (2020) 53:1296–314. doi: 10.1016/j.immuni.2020.11.017

15. Wilk AJ, Rustagi A, Zhao NQ, Roque J, Martínez-colón GJ, Mckechnie JL, et al. A single-cell atlas of the peripheral immune response in patients with severe COVID-19. *Nat Med* (2020) 26(July):1070–6. doi: 10.1038/s41591-020-0944-y

16. Stephenson E, Reynolds G, Botting RA, Calero-nieto FJ, Morgan MD, Tuong ZK, et al. Response in COVID-19. *Nat Med* (2021) 27(May):904–16. doi: 10.1038/s41591-021-01329-2

17. Giovanni SO, Haase K, Gillrie MR, Li R, Morozova O, Hickman D, et al. An on-chip model of protein paracellular and transcellular permeability in the microcirculation. *Biomaterials* (2019) 212(January):115–25. doi: 10.1016/j.biomaterials.2019.05.022

18. Chen MB, Whisler JA, Fröse J, Yu C, Shin Y, Kamm RD. On-chip human microvasculature assay for visualization and quantification of tumor cell extravasation dynamics. *Nat Protoc* (2017) 12(5):865–80. doi: 10.1038/nprot.2017.018

19. Davogustto GE, Clark DE, Hardison E, Yanis AH, Lowery BD, Halasa NB, et al. Characteristics associated with multisystem inflammatory syndrome among adults with SARS-CoV-2 infection. *JAMA Netw Open* (2021) 4(5):e2110323. doi: 10.1001/jamanetworkopen.2021.10323

20. Fox SE, Lameira FS, Rinker EB, Vander Heide RS. Cardiac endotheliitis and multisystem inflammatory syndrome after COVID-19. *Ann Intern Med* (2020) 173 (12):1025–7. doi: 10.7326/L20-0882

21. Magro C, Mulvey JJ, Berlin D, Nuovo G, Salvatore S, Harp J, et al. Complement associated microvascular injury and thrombosis in the pathogenesis of severe COVID-19 infection : A report of five cases. *Transl Res* (2020) 220:1–13. doi: 10.1016/j.trsl.2020.04.007

22. Hoste L, Roels L, Naesens L, Bosteels V, Vanhee S, Dupont S, et al. TIM3 + TRBV11-2 T cells and IFN γ signature in patrolling monocytes and CD16 + NK cells delineate MIS-c. *J Exp Med* (2022) 219(2):e20211381. doi: 10.1084/jem.20211381

23. Mogilenko DA, Shchukina I, Artyomov MN. Immune ageing at single-cell resolution. *Nat Immunol* (2022) 22(August):486–98. doi: 10.1038/s41577-021-00646-4

24. Xie X, Shi Q, Wu P, Zhang X, Kambara H, Su J, et al. Single-cell transcriptome profiling reveals neutrophil heterogeneity in homeostasis and infection. *Nat Immunol* (2020) 21(September):1119–33. doi: 10.1038/s41590-020-0736-z

25. Bonaventura A, Vecchié A, Dagna L, Martinod K, Dixon DL, Van Tassell BW, et al. Endothelial dysfunction and immunothrombosis as key pathogenic mechanisms in COVID-19. *Nat Rev Immunol* (2021) 21(5):319–29. doi: 10.1038/s41577-021-00536-9

26. Stacey HD, Golubeva D, Posca A, Ang JC, Novakowski KE, Zahoor MA, et al. IgA potentiates NETosis in response to viral infection. *Proc Natl Acad Sci* (2021) 118 (27):e2101497118. doi: 10.1073/pnas.2101497118

27. Mohan Rao LV, Esmon CT, Pendurthi UR. Endothelial cell protein c receptor: a multiliganded and multifunctional receptor. *Blood* (2014) 124(10):1553–62. doi: 10.1182/blood-2014-05-578328

28. Masi S, Rizzoni D, Taddei S, Widmer RJ, Montezano AC, Lüscher TF, et al. Assessment and pathophysiology of microvascular disease: Recent progress and clinical implications. *Eur Heart J* (2021) 42(26):2590–604. doi: 10.1093/eurheartj/ehaa857

frontiers | Frontiers in Immunology

TYPE Original Research
PUBLISHED 28 February 2023
DOI 10.3389/fimmu.2023.1123497

OPEN ACCESS

EDITED BY
Pietro Ghezzi,
University of Urbino Carlo Bo, Italy

REVIEWED BY
Andreu Comas-Garcia,
Autonomous University of San Luis Potosí, Mexico
Andrew Weber,
Northwell Health, United States
Antonio Lalueza,
University Hospital October 12, Spain

*CORRESPONDENCE
Jaime Alfonso M. Aherrera
jimbz11@gmail.com

SPECIALTY SECTION
This article was submitted to Inflammation, a section of the journal Frontiers in Immunology

RECEIVED 14 December 2022
ACCEPTED 14 February 2023
PUBLISHED 28 February 2023

CITATION
Punzalan FER, Aherrera JAM, de Paz-Silava SLM, Mondragon AV, Malundo AFG, Tan JJE, Tantengco OAG, Quebral EPB, Uy MNAR, Lintao RCV, Dela Rosa JGL, Mercado MEP, Avenilla KC, Poblete JB, Albay AB Jr, David-Wang AS and Alejandria MM (2023) Utility of laboratory and immune biomarkers in predicting disease progression and mortality among patients with moderate to severe COVID-19 disease at a Philippine tertiary hospital.
Front. Immunol. 14:1123497.
doi: 10.3389/fimmu.2023.1123497

Utility of laboratory and immune biomarkers in predicting disease progression and mortality among patients with moderate to severe COVID-19 disease at a Philippine tertiary hospital

Felix Eduardo R. Punzalan[1,2], Jaime Alfonso M. Aherrera[1,2]*, Sheriah Laine M. de Paz-Silava[3], Alric V. Mondragon[1,2], Anna Flor G. Malundo[1,2], Joanne Jennifer E. Tan[1,2], Ourlad Alzeus G. Tantengco[4,5], Elgin Paul B. Quebral[2], Mary Nadine Alessandra R. Uy[1,2], Ryan C. V. Lintao[2], Jared Gabriel L. Dela Rosa[2], Maria Elizabeth P. Mercado[6], Krisha Camille Avenilla[2], Jonnel B. Poblete[1], Albert B. Albay Jr.[1,2], Aileen S. David-Wang[1,2] and Marissa M. Alejandria[1,2,7]

[1]Department of Medicine, Philippine General Hospital, University of the Philippines Manila, Manila, Philippines, [2]College of Medicine, University of the Philippines Manila, Manila, Philippines, [3]College of Public Health, University of the Philippines Manila, Manila, Philippines, [4]Department of Physiology, College of Medicine, University of the Philippines Manila, Manila, Philippines, [5]Department of Biology, College of Science, De La Salle University, Manila, Philippines, [6]Department of Clinical Epidemiology, Faculty of Medicine and Surgery, University of Santo Tomas, Manila, Philippines, [7]Institute of Clinical Epidemiology, National Institutes of Health, University of the Philippines Manila, Manila, Philippines

Purpose: This study was performed to determine the clinical biomarkers and cytokines that may be associated with disease progression and in-hospital mortality in a cohort of hospitalized patients with RT-PCR confirmed moderate to severe COVID-19 infection from October 2020 to September 2021, during the first wave of COVID-19 pandemic before the advent of vaccination.

Patients and methods: Clinical profile was obtained from the medical records. Laboratory parameters (complete blood count [CBC], albumin, LDH, CRP, ferritin, D-dimer, and procalcitonin) and serum concentrations of cytokines (IL-1β, IL-2, IL-4, IL-6, IL-8, IL-10, IL-18, IFN-γ, IP-10, TNF-α) were measured on Days 0-3, 4-10, 11-14 and beyond Day 14 from the onset of illness. Regression analysis was done to determine the association of the clinical laboratory biomarkers and cytokines with the primary outcomes of disease progression and mortality. ROC curves were generated to determine the predictive performance of the cytokines.

Results: We included 400 hospitalized patients with COVID-19 infection, 69% had severe to critical COVID-19 on admission. Disease progression occurred in

139 (35%) patients, while 18% of the total cohort died (73 out of 400). High D-dimer >1 μg/mL (RR 3.5 95%CI 1.83–6.69), elevated LDH >359.5 U/L (RR 1.85 95% CI 1.05–3.25), lymphopenia (RR 1.91 95%CI 1.14–3.19), and hypoalbuminemia (RR 2.67, 95%CI 1.05–6.78) were significantly associated with disease progression. High D-dimer (RR 3.95, 95%CI 1.62–9.61) and high LDH (RR 5.43, 95%CI 2.39–12.37) were also significantly associated with increased risk of in-hospital mortality. Nonsurvivors had significantly higher IP-10 levels at 0 to 3, 4 to 10, and 11 to 14 days from illness onset ($p<0.01$), IL-6 levels at 0 to 3 days of illness ($p=0.03$) and IL-18 levels at days 11-14 of illness ($p<0.001$) compared to survivors. IP-10 had the best predictive performance for disease progression at days 0-3 (AUC 0.81, 95%CI: 0.68–0.95), followed by IL-6 at 11-14 days of illness (AUC 0.67, 95%CI: 0.61–0.73). IP-10 predicted mortality at 11-14 days of illness (AUC 0.77, 95%CI: 0.70–0.84), and IL-6 beyond 14 days of illness (AUC 0.75, 95% CI: 0.68–0.82).

Conclusion: Elevated D-dimer, elevated LDH, lymphopenia and hypoalbuminemia are prognostic markers of disease progression. High IP-10 and IL-6 within the 14 days of illness herald disease progression. Additionally, elevated D-dimer and LDH, high IP-10, IL-6 and IL-18 were also associated with mortality. Timely utilization of these biomarkers can guide clinical monitoring and management decisions for COVID-19 patients in the Philippines.

KEYWORDS

biomarkers, cytokines, disease progression, mortality, COVID-19, Filipino

1 Introduction

Coronavirus disease 2019 (COVID-19) has taken the world by storm prompting the World Health Organization (WHO) to declare it a pandemic last March 11, 2020. COVID-19 primarily presents as fever, cough, fatigue, and dyspnea, but the clinical presentation can vary, from asymptomatic infection to severe, life-threatening symptoms. Most patients infected with the SARS-CoV-2 experience mild symptoms or remain asymptomatic, while 15% have severe, life-threatening diseases (1). Disease progression has often been linked to acute respiratory distress syndrome (ARDS) and cytokine storm. Furthermore, patients with COVID-19 with comorbidities, such as hypertension, cardiovascular disease, diabetes mellitus, chronic obstructive pulmonary disease (COPD), asthma, and immunocompromising conditions such as human immunodeficiency virus (HIV) infection, chronic steroid use, and active malignancy, are more likely to develop a more severe course and progression of the disease (2, 3). Current evidence points to a dysregulated immune response to the virus causing these known syndromes in COVID-19. Laboratory parameters in COVID-19 also differ with disease severity. Recent meta-analyses have described various biomarkers, such as lymphopenia, thrombocytopenia, elevated procalcitonin (PCT), C-reactive protein (CRP), lactate dehydrogenase (LDH), aspartate aminotransferase (AST), alanine aminotransferase (ALT), serum amyloid A (SSA), D-dimer, ferritin, troponin, B-type natriuretic peptides, creatinine and blood urea nitrogen (BUN), and elevated cytokines, including IL-6, TNF-α, IFN-γ, IL-8, and IL-10, to be associated with worse clinical outcomes and mortality in COVID-19 (4–10).

Most deaths from COVID-19 are from severe and critical diseases. Hence, studies have investigated biomarkers that may be predictive of progression to severe disease and adverse outcomes as shown in Supplementary Table 1. Data from a large cohort of patients admitted to a tertiary COVID-19 referral center in the Philippines reported the following factors to be predictive of severe disease: increasing age, diabetes mellitus (DM), chronic kidney disease (CKD), chronic obstructive pulmonary disease (COPD), hypertension, coronary artery disease, or metabolic syndrome. Likewise, patients with severe disease had significantly higher LDH, ferritin, D-dimer, and CRP (11). With the massive effect of cytokines in the development of cytokine storms and other complications in COVID-19, its utility as a predictive biomarker has been explored by several studies. If proven useful, these cytokines would be helpful in early recognition and intervention before disease progression becomes uncontrollable. IL-6 has already been predicted as a useful biomarker in managing COVID-19. Elevations in IL-6 have commonly been reported in several studies and are strongly associated in severe and critically ill patients with an increased risk for ICU admission, respiratory failure, and overall poor prognosis (12–19). Moreover, C-reactive protein (CRP) was also included among the strongest predictors for ICU admission or death at 30 days in COVID-19 (20, 21). Interferon-gamma (IFN-γ) has also been increased in severe cases compared to milder cases or

even with healthy controls (4, 15, 19). Early robust IFN-γ response is protective against COVID-19 infection. However, a delayed IFN-γ response did not limit viral load and led to increased inflammation and collateral damage (22). Other chemokines such as CCL2 and CXCL2 are likewise reported to be higher in infected cases (14, 22). Several chemokines, such as CXCL1 and CXCL5, have also been elevated in severe COVID-19 patients (23).

More studies are needed to better understand potential biomarkers that can predict cytokine storm-like syndrome associated with COVID-19 in Filipino population (24). Moreover, there is very limited data regarding genetic difference associated with different disease phenotypes among Filipino COVID-19 patients. Identifying biomarkers that are associated with clinical deterioration may help in treatment decisions. In this study, we studied different biomarkers (complete blood count [CBC], albumin, LDH, CRP, ferritin, D-dimer, and procalcitonin) and cytokines (IL-1β, IL-2, IL-4, IL-6, IL-8, IL-10, IL-18, IFN-γ, IP-10, TNF-α) associated with disease progression and mortality among patients with confirmed moderate to severe COVID-19 infection in the University of the Philippines - Philippine General Hospital (UP-PGH).

2 Patients and methods

2.1 Study design and setting

This was a prospective cohort study of adults with confirmed moderate to severe COVID-19 infection admitted in the University of the Philippines – Philippine General Hospital (UP-PGH) from October 2020 to September 2021. UP-PGH is a tertiary university hospital and a COVID-19 referral center in the National Capital Region (NCR) where cases of COVID-19 in the Philippines are the highest (25). The conduct of the study was approved by the University of the Philippines Manila Research Ethics Board (UPMREB 2020-251-01).

Potential participants were recruited upon admission through referral from attending physicians. Once consent is obtained, blood samples were collected on specific time points (i.e., days 0 – 3, 4 – 10, 11 – 14, and >14 from the onset of COVID-19 symptoms) to measure serum concentrations of selected pro-inflammatory and anti-inflammatory cytokines, namely IL-1β, IL-2, IL-4, IL-6, IL-8, IL-10, IL-18, IFN-γ, IP-10, TNF-α. The Milliplex Cytokine Storm Panel (Merck) that utilized the Luminex xMAP technology as per manufacturer's instructions was used for cytokine measurement. We also obtained the results of common laboratory tests requested by attending physicians specifically, CBC, albumin, LDH, CRP, ferritin, D-dimer, and procalcitonin. The primary outcomes of interest were: 1) disease progression and 2) in-hospital mortality. We monitored the occurrence of outcomes daily from enrolment until death or hospital discharge.

2.2 Participants

Eligible patients included hospitalized adults (18 years and above) with confirmed COVID-19 infection, classified as moderate or severe disease. We excluded pregnant patients, patients with known immunodeficiencies such as those with active malignancies and autoimmunity, and those receiving immunosuppressive medications. Quota sampling was employed.

2.3 Definitions

A *confirmed COVID-19 case* was defined as a patient with laboratory-confirmed positive RT-PCR test for SARS-CoV-2. We used the Philippine COVID-19 Living Recommendations for severity classification (26). *Moderate COVID-19* include those with clinical (cough, fever, and tachypnea) and/or radiographic evidence of pneumonia but without difficulty breathing or shortness of breath, respiratory rate <30 breaths/minute, or peripheral oxygen saturation (SpO2) ≥ 94% on room air. It also includes symptomatic patients without pneumonia but with risk factors for progression namely hypertension, cardiovascular disease, diabetes mellitus, chronic obstructive pulmonary disease (COPD), asthma, and immunocompromising conditions such as human immunodeficiency virus (HIV) infection, chronic steroid use, and active malignancy. *Severe COVID-19* includes those with pneumonia and any of the following: signs of respiratory distress, SpO2 <94% at room air, respiratory rate ≥30 breaths/minute, or requiring oxygen supplementation. Patients with impending respiratory failure requiring high flow oxygen or ventilatory support, ARDS, sepsis, or septic shock, deteriorating sensorium, multi-organ failure, and thrombosis already have *critical COVID-19*.

Disease progression is present if any of the following develop during the course of hospitalization: 1) ARDS or worsening of ARDS based on the Berlin Criteria (27), 2) need for mechanical ventilation, 3) acute kidney injury defined as an increase in serum creatinine by >0.3 mg/dL within 48 hours or 1.5 x from baseline occurring within the prior seven days or a decrease in urine output of less than 0.5 mL/kg/h for 24 hours, 4) need for acute renal replacement therapy, 5) symptomatic cerebro- or cardiovascular thrombotic events such as stroke documented by CT-scan, acute myocardial infarction with rise in troponin-I values by >20%, acute limb ischemia, or venous thromboembolism documented by imaging, 6) acute myocarditis with findings of new wall motion abnormalities or worsening ejection fraction to <45%, 7) ICU admission, and 8) in-hospital mortality. *In-hospital mortality* is death from any cause during admission.

2.4 Sample size

To detect the association of clinically relevant biomarkers with disease progression and mortality with an odds ratio of at least 2.00, the computed sample size was 400 at an alpha of 0.05 and a beta of 0.20. For the baseline estimate of the risk of death, the 16.7% case-fatality rate in UP PGH was used (28). Estimates for disease progression were based on the reported odds ratio from recent studies (5, 29, 30). The study was powered for most of the clinically usable biomarkers in resource-limited settings based on the

Philippine Society for Microbiology and Infectious Diseases (PSMID) Rapid Evidence Reviews on COVID-19 (31).

2.5 Data collection

Demographic and clinical data extracted from electronic medical records and the results of routine laboratory tests and cytokine analysis were encoded into a standard data collection form in the Research Electronic Data Capture (REDCap), a secure web-based application commonly used to capture data for clinical research and to create databases (32).

2.6 Statistical analysis

Shapiro-Wilk test and graphical representation were done using the data on patients' age. The data were normally distributed. Demographic and clinical characteristics were compared according to the main outcomes of mortality and disease progression using t-test for continuous variables and Fisher's exact test for dichotomous variables.

To determine the temporal changes in mean clinical laboratory biomarker levels between the outcome groups, the day of illness was grouped into four distinct time points: day 0-3, day 4-10, day 11-14, and day > 14 from the onset of illness. The mean biomarker levels and their confidence intervals were plotted against these four time points using R.

To determine the association between clinical laboratory biomarker levels and outcomes of interest, the following actions were made. First, for clinical applicability, biomarker levels were dichotomized using the following published cut-offs: NLR >3 (15), D-Dimer >1 μg/mL (33), Ferritin >300 μg/mL (33), hs-CRP >5 mg/dL (18), and LDH >359.50 U/L (34). Second, since patients usually get admitted on the 4^{th} to 10^{th} day of illness, we selected this period as reference for the analysis of prediction of disease progression and mortality. A generalized linear model for the binomial family was used to estimate the risk ratio for disease progression and in-hospital mortality using binary forms of the biomarker as the predictor variables. Separate models were created for each biomarker and each outcome of interest. Analysis was adjusted to age using a cutoff of 55 years, presence of CKD, presence of DM, treatment with tocilizumab, and treatment with dexamethasone during hospitalization. Association between laboratory results and outcomes of interest were reported as risk ratios with 95% confidence intervals.

We used a repeated measures mixed model regression analysis to determine the association between cytokine levels and outcomes over four time points. Main effects (time and outcome) with statistically significant results were subjected to *post-hoc* analysis to identify specific comparison pairs. Dot plots were used to graphically represent the trends in cytokine levels across time points and between groups. Statistical significance was set at a *p*-value of <0.05. The analysis was adjusted for age, comorbidities (CKD, DM), and treatment (tocilizumab, dexamethasone). Data were presented using linear prediction graphs. *Post-hoc* significance similarly used Šidák-Holm adjusted p-values. The prognostic utility of the cytokines in predicting disease progression and mortality was evaluated using ROC curves. Statistical analyses were performed in STATA/IC 15.1, GraphPad Prism version 8 for Windows, and R version 3.3.1.

3 Results

3.1 Patient demographics and profile

We analyzed 400 hospitalized adult patients with moderate to critical COVID 19. The demographic and clinical characteristics of the patients are summarized in Table 1. The mean age of the cohort was 56 years, and majority were males (61%). Hypertension (56%), diabetes mellitus (32%), and cardiac disease (12%) were the most common comorbid conditions. On admission, 123 (31%) had nonsevere disease (moderate COVID-19 infection), while 277 (69%) had severe to critical disease. Common presenting symptoms were cough (74%), shortness of breath (73%), fever (58%), generalized weakness (24%), and decreased appetite (23%). In the cohort, 139 (35%) exhibited disease progression. No comorbidities were associated with disease progression in this cohort. Patients with disease progression were generally older (p = 0.01) and presented with shortness of breath (p = 0.01) and sensorial changes (altered sensorium, delusions, hallucinations, and behavioral changes) (p < 0.001). On the other hand, the in-hospital mortality rate of the cohort was 18%. More patients who died were older (p = 0.01), had diabetes (p = 0.01), had chronic kidney disease (p = 0.03), presented with shortness of breath (p = 0.02), and sensorial changes (p < 0.001). Many also received therapeutic interventions, namely dexamethasone (78%), remdesivir (56%), tocilizumab (52%), anticoagulants, and antithrombotics (88%). The administration of remdesivir (p = 0.001), dexamethasone (p = 0.01), tocilizumab (p = 0.01), and anticoagulants/antithrombotics (p = 0.01) was higher among patients who progressed to the severe-critical stage. Meanwhile, more nonsurvivors received dexamethasone (p = 0.03) and tocilizumab (p = 0.04). Illness severity on admission was associated with both disease progression and in-hospital mortality (p < 0.001). More patients who progressed to more severe disease (82%) or died (86%) already had severe-critical COVID-19 on admission.

3.2 Trends in laboratory parameters

Serum ferritin, LDH, CRP, and NLR (i.e., inflammatory markers), were elevated throughout the course of illness among those who exhibited disease progression (Figures 1A–C, F). Moreover, their WBC counts were consistently above normal (WBC $>10^9$/L) compared to those who did not exhibit disease progression (Figure 1E). D-dimer, a marker of ongoing activation of the hemostatic system and overall inflammation, also showed a similar pattern as other inflammatory markers (Figure 1I). Albumin, a negative acute phase reactant, exhibited a marked decline to below normal levels among those with disease

10.3389/fimmu.2023.1123497

TABLE 1 Comparison of demographic and clinical characteristics of hospitalized adult patients with confirmed COVID-19 according to outcomes of disease progression and mortality.

Characteristics	Total (*N*=400)	Disease Progression			Mortality		
		Without disease progression (*n*=261)	With disease progression, (*n*=139)	*p*-value	Survivor (*n*=327)	Non-Survivor (*n*=73)	*p*-value
Age, years; mean (SD)	56 (15)	55 (15)	59 (14)	0.01	55 (15)	60 (13)	0.01
Male, n (%)	243 (61%)	157 (60%)	86 (62%)	0.75	201 (61%)	42 (58%)	0.60
Length of hospitalization; mean (SD)	15.65 (9.63)	15.60 (8.03)	15.75 (12.13)	0.89	16.43 (9.19)	12.18 (10.84)	<0.001
On Mechanical Ventilation at admission; n (%)	44 (11)	5 (2)	39 (28)	<0.001	18 (6)	26 (36)	< 0.001
COVID-19 Severity Classification on Admission							
Nonsevere	123 (31%)	98 (38%)	25 (18%)	<0.001	63 (35%)	10 (14%)	<0.001
Severe – Critical	277 (69%)	163 (62%)	114 (82%)		214 (65%)	63 (86%)	
Comorbidities							
Diabetes Mellitus	127 (32%)	75 (29%)	52 (37%)	0.09	94 (29%)	33 (45%)	0.01
Hypertension	224 (56%)	140 (54%)	84 (60%)	0.21	179 (55%)	45 (62%)	0.30
Cardiac disease	46 (12%)	31 (12%)	15 (11%)	0.87	38 (12%)	8 (11%)	1.00
Liver disease	3 (1%)	2 (1%)	1 (1%)	1.00	2 (1%)	1 (1%)	0.45
Chronic kidney disease	32 (8%)	16 (6%)	16 (11%)	0.08	21 (6%)	11 (15%)	0.03
COPD	4 (1%)	3 (1%)	1 (1%)	1.00	3 (1%)	1 (1%)	0.55
Asthma	26 (7%)	18 (7%)	8 (6%)	0.83	19 (6%)	7 (10%)	0.29
Active tuberculosis	6 (2%)	5 (2%)	1 (1%)	0.67	5 (2%)	1 (1%)	1.00
HIV/AIDS	0 (0%)	0 (0%)	0 (0%)	–	0 (0%)	0 (0%)	–
Malignancy	3 (1%)	2 (1%)	1 (1%)	1.00	3 (1%)	0 (0%)	1.00
Neurologic disease	14 (4%)	8 (3%)	6 (4%)	0.57	9 (3%)	5 (7%)	0.15
Smoking History							
Non-smoker	255 (64%)	167 (64%)	88 (63%)	0.37	208 (64%)	47 (64%)	0.36
Previous smoker	111 (28%)	68 (26%)	43 (31%)		88 (27%)	23 (32%)	
Current smoker	32 (8%)	24 (9%)	8 (6%)		29 (9%)	3 (4%)	
Treatments/Interventions							
Dexamethasone	311 (78%)	193 (74%)	118 (85%)	0.01	247 (76%)	64 (88%)	0.03
Remdesivir	224 (56%)	131 (50%)	93 (67%)	0.001	177 (54%)	47 (64%)	0.12
Tocilizumab	207 (52%)	122 (47%)	85 (61%)	0.01	161 (49%)	46 (63%)	0.04
Anticoagulation/antthrombotics	353 (88%)	223 (85%)	130 (94%)	0.02	285 (87%)	68 (93%)	0.23
Convalescent Plasma	14 (3%)	7 (3%)	7 (5%)	0.26	11 (3%)	3 (4%)	0.73

progression (Figure 1D). The differences between those who did and did not progress to a more severe disease were more obvious on days 4 to 14 of illness.

Throughout the course of illness, hemoglobin and platelet values were lower among those with disease progression compared to those without (Figures 1G, H). Nevertheless, hemoglobin and platelet values remained near normal for both groups (Normal values: Hemoglobin, Male 13.5 – 17.5 g/L, Female 12.0 – 16.0 g/L; Platelet 150 – 399 x 10^9/L).

A distinct peak in the procalcitonin level was observed on days 4-10 of illness, followed by a rapid decline towards the second week among those with disease progression (Figure 1J). The opposite was observed among nonprogressors, showing a steady increase in procalcitonin levels. Note that we only had at most 19 procalcitonin test results available for analysis in each observation period. Similarly for troponin, the tests were mostly done on days 4-10, with only 75 test results included in the analysis. Troponin was generally elevated, but the trends

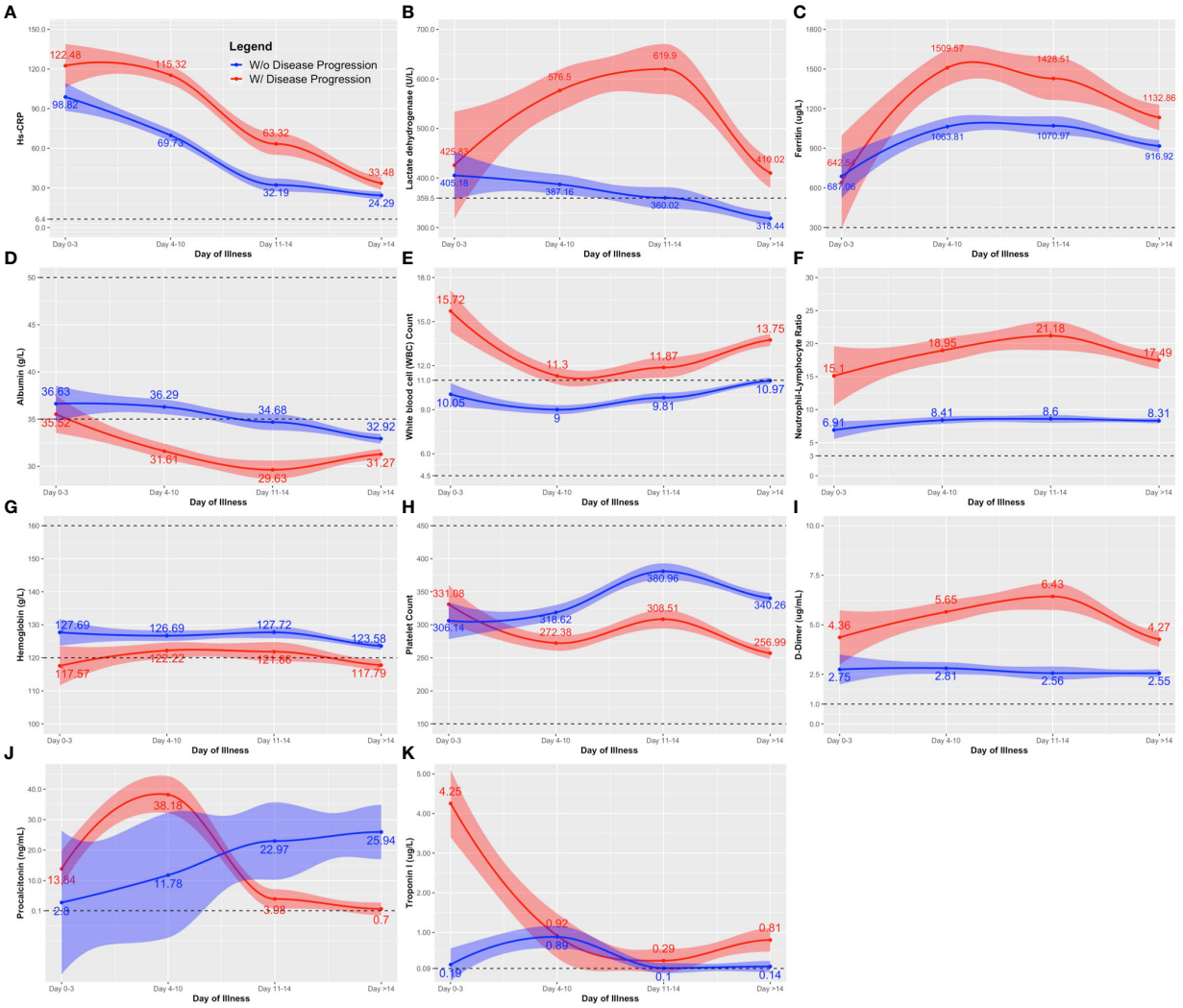

FIGURE 1
Comparison of the clinical laboratory biomarkers throughout the course of illness between COVID-19 patients with and without disease progression. The clinical biomarkers are: **(A)** hs-CRP; **(B)** lactose dehydrogenase (LDH); **(C)** Ferritin; **(D)** albumin; **(E)** white blood cell (WBC); **(F)** neutrophil-lymphocyte ratio; **(G)** hemoglobin; **(H)** platelet count; **(I)** D-dimer; **(J)** procalcitonin; and **(K)** Troponin. Line estimates were created using Locally Weighted Scatterplot Smoothing (LOWESS) showing 95% CI as shaded area around the line estimate. Points at each day interval represent mean estimate computed at that time point. Broken lines show the normal ranges of the tests.

did not reveal marked deviation between those who did and did not exhibit disease progression (Figure 1K).

For routine laboratory tests, nonsurvivors exhibited a similar pattern as patients with disease progression (Figures 1, 2), except that anemia was observed among nonsurvivors (Figure 2G), and the initial peak in procalcitonin levels was not observed among nonsurvivors (Figure 2J).

We also checked the general trend of the serum cytokine levels for all COVID-19 patients included in this study. The serum concentrations of IFN-γ, IL-1β, IL-2, IL-4, IL-6, IL-10, IL-18, and TNF-α did not change significantly throughout the course of illness (Supplementary Figure 1). The IP-10, considered to be an "early cytokine", peaked (1819.70 ng/mL; IQR: 549.54 – 8912.51) within ten days of illness onset and declined steadily thereafter (Figure 3A). On the other hand, IL-8, a "late" cytokine, increased after ten days and peaked 14 days after illness onset (446.68 ng/mL; IQR: 158.49 – 1071.52) (Figure 3B).

3.3 Association of biomarkers with disease progression and mortality

Among the routine laboratory tests taken on days 4 to 10, high NLR (RR 8.49), high D-dimer (RR 4.14), high LDH (RR 2.62), low ALC (RR 2.31), and low albumin levels (RR 3.22) were associated with disease progression ($p < 0.05$). Except for NLR ($p = 0.10$), the associations remained statistically significant after adjustment for age, comorbidities (DM, CKD), and interventions (tocilizumab, dexamethasone). On the other hand, elevated D-dimer, elevated LDH, low albumin, and low ALC were associated with increased risk of in-hospital mortality ($p < 0.05$). After adjustment, only high D-dimer and high LDH remained statistically significant. See Table 2.

Repeated measures mixed model regression analysis showed that IP-10 and IL-6 levels were associated with disease progression and mortality, while IL-18 levels were associated only with mortality (Supplementary Figures 2-5). Generally, the IP-10 levels of COVID-

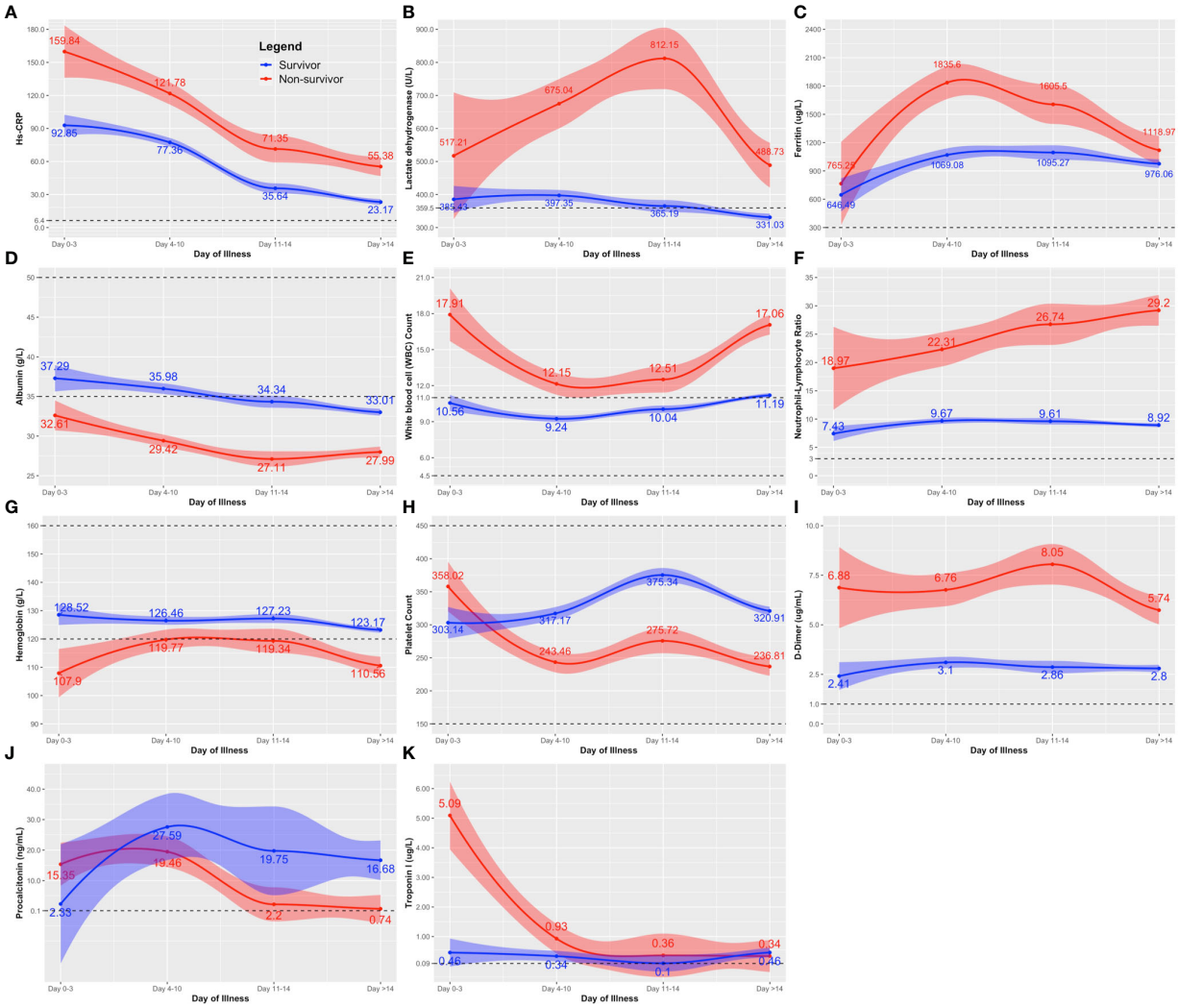

FIGURE 2
Comparison of the clinical laboratory biomarkers throughout the course of illness between COVID-19 survivors and nonsurvivors. The clinical biomarkers are: **(A)** hs-CRP; **(B)** lactose dehydrogenase (LDH); **(C)** Ferritin; **(D)** albumin; **(E)** white blood cell (WBC); **(F)** neutrophil-lymphocyte ratio; **(G)** hemoglobin; **(H)** platelet count; **(I)** D-dimer; **(J)** procalcitonin; and **(K)** Troponin. Line estimates were created using Locally Weighted Scatterplot Smoothing (LOWESS) showing 95% CI as shaded area around the line estimate. Points at each day interval represent mean estimate computed at that time point. Broken lines show the normal ranges of the tests.

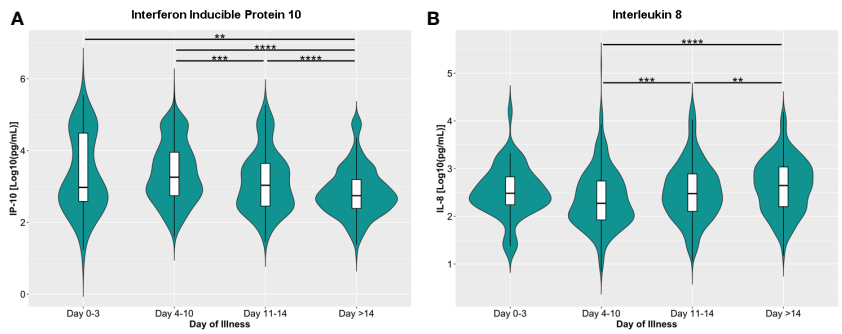

FIGURE 3
Dynamics of serum levels of **(A)** inducible protein 10 (IP-10) and **(B)** interleukin 8 (IL-8) during the disease course in the COVID-19 patient cohort. The cytokines were measured in terms of days from illness onset. All samples collected from 400 patients were stratified into four intervals starting from illness onset. The dots represent individual measurement, and the box plots represent medians with interquartile range. The different groups were compared using the Kruskal-Wallis test with Dunn's *post hoc* test. **p<0.01, ***p<0.001, ****p<0.0001.

19 patients were significantly higher during the early days of infection and then lowest levels were reached at >14 days from illness onset. IP-10 levels of patients with disease progression were higher at 0 to 3, 4 to 10, and 11 to 14 days from illness onset compared to patients without disease progression (Figure 4A). IL-6 levels were higher among those with disease progression (Figure 4B) compared to patients without disease progression beyond 14 days of illness onset.

IP-10 levels at 0 to 3, 4 to 10, and 11 to 14 days from illness onset were higher among nonsurvivors compared to survivors ($p < 0.01$) (Figure 4C). IL-6 levels of nonsurvivors (2454.46 ng/mL; IQR: 906.30 – 4002.63) were also elevated at 0 to 3 days of illness onset compared to survivors (523.47 ng/mL; IQR: -183.69 – 1230.63) ($p = 0.03$) (Figure 4D). For IL-18, levels were significantly higher among nonsurvivors (890.36 ng/mL; IQR: 668.33 – 1112.40) on days 11 to 14 compared to survivors (172.84 ng/mL; IQR: 81.39 – 264.30; $p < 0.001$) (Figure 4E). No significant differences were observed for the rest of the cytokines analyzed (Supplementary Figures 2, 3). For both outcomes, we did not observe a change in the statistical significance after adjusting the model for age, comorbidities, and interventions. Adjusted predictions of TNF-α for mortality outcomes could not be evaluated due to non-convergence of data using the adjusted model (Supplementary Tables 2, 3).

3.4 Temporal kinetics of biomarkers among COVID-19 patients

No statistical significance was observed when comparing the temporal differences in IL-6 levels among COVID-19 patients without disease progression. However, among COVID-19 patients with disease progression, a significant increase in IL-6 levels from days 4 – 10 (397.65 ng/mL; IQR: 5.55 – 800.86) to days >14 (1248.50 ng/mL; IQR: 798.47 – 1698.52) from illness onset was observed ($p < 0.05$). For both groups (i.e., with and without disease progression), higher IP-10 levels were observed during the earlier days of illness, days 0 – 3 and 4 – 10, compared to the latter days of illness (days 11 – 14 and days > 14) (Supplementary Table 2; Supplementary Figure 4).

Among nonsurvivors, significantly higher level of IL-6 was observed at >14 days (3037.35 ng/mL; IQR: 2320.95 – 3753.76) of illness compared to days 4 – 10 (421.17 ng/mL; IQR: -146.30 – 988.63; $p < 0.001$) and 11 – 14 (1014.34 ng/mL; IQR: 389.60 – 1639.08; $p < 0.001$). On the other hand, IL-18 significantly increased and peaked at days 11 – 14 (890.36 ng/mL; IQR: 668.33 – 1112.40) compared to days 4 – 10 (244.08 ng/mL; IQR: 46.92 – 441.25; $p < 0.001$). There was no significant difference in the levels of IL-6 and IL-18 among the survivors. For IP-10, the level peaked at days 0 – 3 (57367.50 ng/mL; IQR: 36903.53 – 77831.46) and was significantly higher compared to days 4 – 10 (24424.94 ng/mL; IQR: 16597.45 – 32252.43; $p < 0.05$) and >14 days of illness (36941.07 ng/mL; IQR: 28421.85 – 45460.29; $p < 0.001$) (Supplementary Table 3; Supplementary Figure 5).

3.5 Predictive performance of cytokines

The ROC curves for the individual cytokines as predictors for disease progression and mortality are shown in Figures 5A, B. IP-10 best predicted disease progression on days 0 to 3 of illness with an AUC of 0.81 (95% CI: 0.68 – 0.95), followed by IL-6 at 11 – 14 days of illness (AUC 0.67; 95% CI: 0.61 – 0.73) (Figure 5A; Supplementary Table 4). For predicting mortality, IP-10 had an AUC of 0.77 (95% CI: 0.70 – 0.84) at 11 to 14 days of illness. Beyond 14 days of illness, IL-6 predicted mortality with an AUC of 0.75 (95% CI: 0.68 – 0.82) while IL-18 had an AUC of 0.69 (95% CI: 0.60 – 0.77) at 11 to 14 days of illness (Figure 5B; Supplementary Table 5).

4 Discussion

The cohort in this study consists predominantly of patients with severe to critical COVID-19 disease (69%). This is higher compared

TABLE 2 Association of Selected Biomarkers (taken on Days 4-10) with Disease Progression and In-Hospital Mortality.

Biomarkers	Disease Progression					In-Hospital Mortality				
	N	Crude RR (95% CI)	*p*-value	Adjusted RR (95% CI)*	*p*-value	*N*	Crude RR (95% CI)	*p*-value	Adjusted RR (95% CI)*	*p*-value
Absolute Lymphocyte < 1.1×10^3 cells/μL	233	2.31 (1.39–3.81)	0.001	1.91 (1.14–3.19)	0.01	248	2.39 (1.25–4.56)	0.008	1.85 (0.95–3.59)	0.07
Neutrophil to lymphocyte ratio (NLR) > 3	234	8.49 (1.23–58.48)	0.03	5.21 (0.73–37.13)	0.10	249	5.55 (0.80–38.52)	0.08	3.19 (0.43–23.32)	0.25
D-dimer > 1 μg/mL	206	4.14 (2.16–7.96)	<0.0001	3.50 (1.83–6.69)	<0.0001	219	5.08 (2.07–12.44)	<0.0001	3.95 (1.62–9.61)	0.003
Albumin < 40 g/L	212	3.22 (1.25–8.33)	0.02	2.67 (1.05–6.78)	0.04	227	4.56 (1.15–18.04)	0.03	3.60 (0.91–14.24)	0.07
Lactate dehydrogenase (LDH) > 359.5 U/L	225	2.62 (1.57–4.38)	<0.0001	1.85 (1.05–3.25)	0.03	239	5.22 (2.30–11.85)	<0.0001	5.43 (2.39–12.37)	<0.0001
Serum Ferritin > 574.5 μg/mL	219	1.41 (0.86–2.30)	0.17	0.98 (0.60–1.60)	0.93	233	1.79 (0.91–3.54)	0.10	1.27 (0.63–2.56)	0.50
High-Sensitivity C-Reactive Protein (hsCRP) > 5 mg/dL	188	5.12 (0.76–34.56)	0.09	3.39 (0.47–24.67)	0.23	199	3.62 (0.53–24.75)	0.19	3.27 (0.44–24.55)	0.25

*Adjusted to age using a cutoff of 55 years, presence of CKD, presence of DM, treatment with tocilizumab, and treatment with dexamethasone during hospitalization.

10.3389/fimmu.2023.1123497

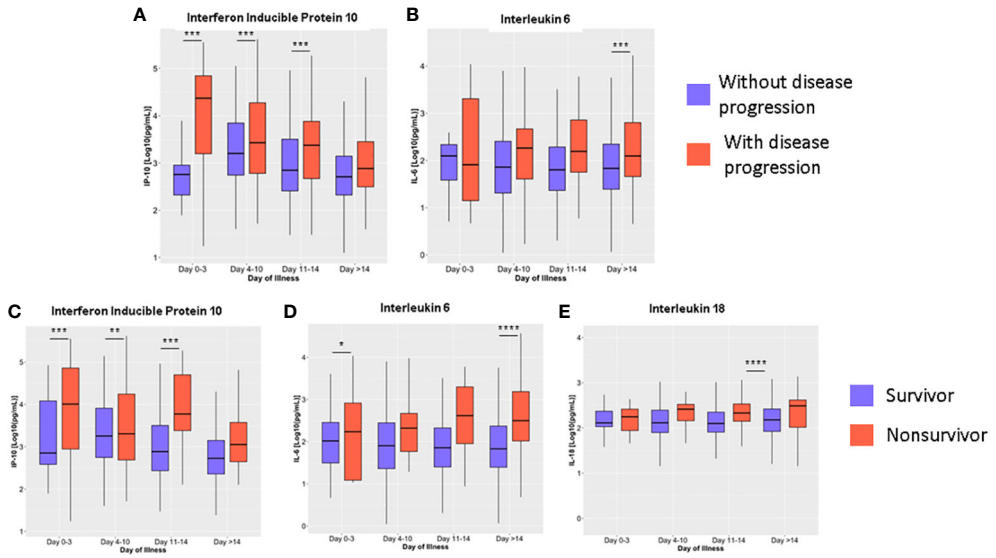

FIGURE 4
Dynamics of serum cytokine levels during the disease course in COVID-19 patients based on disease progression **(A, B)** and mortality **(C–E)**. The cytokines were measured in terms of days from illness onset. All samples collected from 400 patients were stratified into four intervals starting from illness onset. The dots represent individual measurements, and the box plots represent medians with interquartile range. The different groups were compared by repeated measures mixed model regression with *post hoc* test. *p<0.05, **p<0.01, ***p<0.001, ****p<0.0001.

to published data from the same institution (48.9%) and another tertiary referral center in Metro Manila (54.1%) even after excluding mild and asymptomatic patients (11, 35). The recorded mortality rate of 18% closely approximates the data from both reports, 15.1% in UP-PGH (11) and 20.8% in San Lazaro Hospital (35). The rate of disease progression was not reported in these local studies. But data from China show disease progression at 35.3% for patients with moderate and severe disease (36), similar to our study results at 35%. Given the high mortality and rates of progression, it is important to predict patients who will have poor outcomes to implement anticipatory care early in the course of the disease.

Older age, severe to critical illness on admission, existing comorbidities (DM, CKD), shortness of breath, and sensorial changes were associated with disease progression and mortality in this cohort. Age is an established risk factor for disease progression and mortality in multiple studies (10, 18, 33, 36, 37). Published data on comorbidities are variable but many studies reported DM and CKD to be associated with unfavorable outcomes among hospitalized patients with COVID-19 (1, 5, 18, 33, 36). Patients with severe disease were likely to die compared to their nonsevere counterparts. Expectedly, more nonsurvivors have received dexamethasone and tocilizumab. Local and international COVID-19 guidelines recommend the use of these agents to patients with severe disease (26, 38, 39). Corticosteroids have been shown to improve outcomes among patients with COVID-19 needing respiratory support (40), while tocilizumab on top of corticosteroids also improved outcomes also improved outcomes among patients with hypoxia and signs of systemic inflammation (41).

Our study showed that high D-dimer, high LDH, low ALC, and low albumin levels were associated with disease progression, while elevated D-dimer and LDH were associated with in-hospital mortality. These findings are consistent with other international and local reports on COVID-19 (11, 42–45). The finding of high D-dimer also provided evidence for SARS-CoV-2 infection as a hypercoagulable state (46), which further supports the use of prophylactic anticoagulation among patients with moderate to severe COVID-19. This hypercoagulable state can be attributed to neutrophil extracellular traps activation, which can trigger immunothrombosis in COVID-19 infection (47). In addition to what is already known, our study provided important insights about COVID-19: first, we provided the cut-off values and optimal time point for measurement of D-dimer (> 1 μg/mL), LDH, ALC (<1,100), and albumin (< 40 g/L); second, we reported cytokines that are significantly affected by COVID-19 and their use in predicting disease progression and mortality; third, we provided insights on the dynamics of IL-6 in the course of COVID-19 disease.

For routine laboratory tests, D-dimer >1 μg/mL and LDH >359.5 U/L obtained on the 4th to 10th day of illness may predict patients who are at high risk for disease progression and mortality, thus would warrant closer monitoring. Those who have ALC <1,100 and albumin <40 g/L should also be monitored due to high risk for mortality. Except for D-dimer, these are common tests available in most diagnostic facilities and hospitals. Incorporating them in clinical pathways for admitted patients with moderate to severe COVID-19 should not be a problem. As mentioned, high D-dimers are suggestive of a hypercoagulable state. It may be a marker of increased risk or even herald the presence of a thrombotic event. For D-dimer, our study does not only provide information on its predictive capacity, but also provides a research opportunity on the utility of D-dimer in guiding anticoagulant dosing among patients with COVID-19. A previous study showed that therapeutic-dose low molecular weight heparin decreased major thromboembolism and death compared with institutional standard heparin thromboprophylaxis among inpatients with COVID-19 with

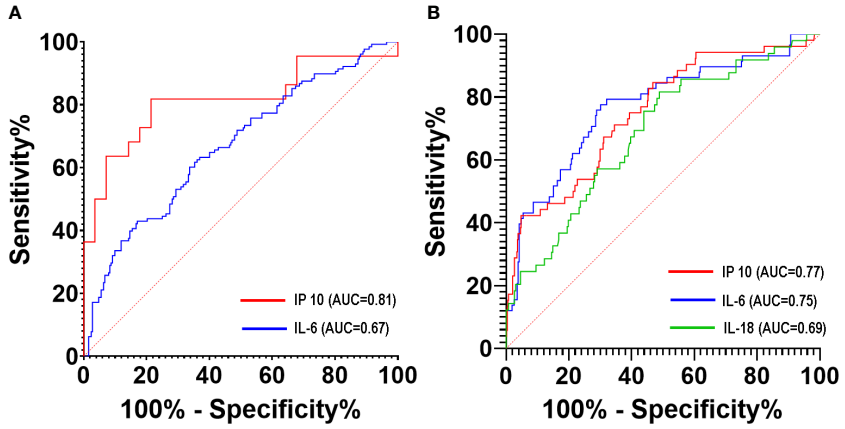

FIGURE 5
ROC curves of serum cytokine levels to predict disease progression **(A)** and mortality **(B)** of COVID-19 patients during hospitalization.

very elevated D-dimer levels (48). However, this benefit was only observed among noncritically ill patients with COVID-19 (48–50).

In addition to routine tests, our results agree with previous studies on the use of IP-10 as an early biomarker that distinguishes patients at risk for poor outcomes. Our results show clear divergence from day 0 to day 10 of illness – providing a wide window for clinicians as well as for researchers in terms of studying potential drug therapies. IP-10 is a protein secreted by various cell types such as monocytes, endothelial cells, and fibroblasts in response to IFNγ. IP-10 acts as a chemotactic factor for T cells, natural killer cells, monocytes, macrophages, and dendritic cells (51). IP-10 inhibits endothelial recovery independently of any other inflammatory factor, explaining the pervasive endothelialitis that is seen in severe and critical COVID-19 patients (52). Moreover, a critical factor for the exacerbation of the pathology of acute respiratory distress syndrome. It acts *via* autocrine signaling to promote oxidative burst and chemotaxis of inflamed neutrophils, leading to fulminant pulmonary inflammation (53). Neutrophilic infiltration has been observed post-mortem in pulmonary capillaries and alveolar space of patients who died from COVID-19 (54). Aside from the release of reactive oxygen species and cytokines to promote inflammation, neutrophils are known to produce neutrophil extracellular traps (NETs) composed of chromatin, anti-microbial proteins and oxidative enzymes meant to increase viscosity of respiratory tract mucus and eliminate pathogens (55). Although neutrophils act as first line of defense during infection of the lower respiratory tract, unregulated neutrophil activation can result to pneumonia and/or acute respiratory distress syndrome (56). Zuo et al. (57) has reported elevated NET markers such as myeloperoxidase-DNA complexes and citrullinated histone H3 (Cit-H3), the former of which was markedly elevated in hospitalized patients requiring mechanical ventilation (57).

A previous study also showed that IP-10 tends to elevate earlier in COVID-19 patients than other inflammatory cytokines (58). Several studies have shown that plasma levels of IP-10 are suitable biomarkers associated with the severity of COVID-19 diseases and may also be related to the risk of death in COVID-19 patients (59–62). Severe COVID-19 showed significantly higher levels of IP-10 than patients with mild COVID-19. Moreover, IP-10 levels were also positively correlated with SARS-CoV-2 titers in COVID-19 patients (63).

IL-6 is somewhat unique in that divergence was seen very early (0 – 3 days) and late (>14 days) in the course of the disease. This result highlights the usefulness of IL-6 as a prognostic biomarker for patients who presented to the hospital early or late in the course of the disease. This also shows that IL-6 can be used in monitoring patients with COVID-19 since IL-6 values can prognosticate disease progression and mortality even beyond 14 days after the onset of infection. However, IL-6 is only useful as a prognostic biomarker for patients not receiving tocilizumab. IL-6 is the main cytokine associated with several inflammatory diseases. Aside from being a pro-inflammatory cytokine, IL-6 promotes resistance to pathogens and tissue homeostasis (64). Previous studies showed that high serum levels of IL-6 are significantly related to adverse clinical outcomes such as admission to the intensive care unit, ARDS, and death (65, 66). Several studies recommended the early detection of serum IL-6 levels after admission to identify patients with the highest risk of disease progression and mortality (67–69).

IL-18, despite its "late" divergence, may still be useful especially for patients who present late in the course of their disease. IL-18 is a proinflammatory cytokine that facilitates IFN-γ production by Th1 cells. In the presence of IL-12, it also stimulates the production of IFN- by non-polarized T cells, NK cells, NKT cells, B cells, DC, and macrophages (70). A previous study in Brazil showed that fatal cases of COVID-19 had elevated levels of IL-18 (71). Multiple studies also showed that IL-18 is a marker of COVID-19 infection severity (71–73). Serum IL-18 levels in COVID-19 patients were noticeably higher compared to healthy controls, peaking in the group with severe pneumonia (74). IL-18 participates as an element of inflammasome activation among COVID-19 patients. Inflammasomes play a key role in the innate immune response to pathogen-associated molecular patterns. Inflammasomes release proinflammatory cytokines like IL-1 and IL-18 to the extracellular environment causing inflammation and cell death. Overactivation

of this process leads to exacerbation of COVID-19 infection (75, 76).

Our study has several limitations given its observational nature. First, the choice, the timing, and the frequency of routine laboratory tests were at the discretion of the attending physicians. Thus, it is likely that patients with more severe disease underwent extensive laboratory evaluation, earlier testing, and more frequent testing than patients with nonsevere disease. Second, the majority of the patients were admitted beyond four days of illness, hence fewer laboratory data were available for days 0 to 3. Although this could have missed significant deviation early in the course of the disease, our data reflected the most clinically relevant time point - *the time when most patients seek medical attention*. Third, we used cut-off values based on published studies for routine laboratory tests. Fourth, the COVID-19 pandemic is evolving along with the availability of vaccines and therapeutic agents. The vaccine roll-out began in March 2021. We were able to include therapeutic agents as shown in Table 1, but this is limited to those available and used in the hospital. Some patients may have tried "other agents" such as ivermectin, herbal supplements, and high dose vitamins – and the effect of such therapies cannot be controlled or considered in the analysis. Unfortunately, we were also unable to obtain the COVID-19 vaccination history of the patients. Cardiac magnetic resonance imaging was not done in any of the patients, which makes it very difficult to distinguish between acute myocardial infarction and myocarditis. Our study also had missing data. Some laboratory markers were not obtained from patients, or the values of the cytokines were beyond the range of detection. We did not run multiple imputations for these missing data. And finally, our study was conducted during the earlier waves of SARS-CoV-2, with the more virulent variants as opposed to the seemingly milder Omicron variant (77).

Future studies could explore the cost-effectiveness of these tests, especially since cytokine level determination is not widely available locally. For the biomarkers, monitoring trends before, during, and after treatment may be valuable in better understanding the immunopathologic mechanisms of COVID-19, as well as their association with clinical outcomes. These biomarkers may be studied as a predictor of the need for a higher FiO2 requirement. This can help clinicians better respond to acute complications, long-term sequelae, and possible future COVID-19 variants. This study emphasizes the need to develop research centers that can explore these critical immunologic mechanisms and be agile to respond to future pandemics and similar public health threats.

5 Conclusions

Among patients with moderate to severe COVID-19, elevated D-dimer (>1 μg/mL) or LDH (>359.5 U/L) obtained within ten days of illness onset were associated with disease progression and mortality. Additionally, lymphopenia and hypoalbuminemia were also associated with disease progression. For cytokines, elevated IP-10 within 14 days of illness, and elevated IL-6 beyond 14 days of illness were associated with disease progression and mortality. High levels of IL-18 on the 11th to 14th day of illness were also associated with mortality. Timely utilization of these biomarkers will better guide patient monitoring and management.

Data availability statement

The original contributions presented in the study are included in the article/Supplementary Material. Further inquiries can be directed to the corresponding author.

Ethics statement

This study was approved by the UP Manila Research Ethics Board (UPMREB 2020-251-01). The patients/participants provided their written informed consent to participate in this study.

Author contributions

Conceptualization: FP, JA, SP-S, AMo, AMa, JT, OT, EQ, MU, RL, JR, AD-W, and MA. Methodology: FP, JA, SP-S, AMo, AMa, JT, OT, EQ, MU, RL, JR, MM, KA, JP, AD-W, and MA. Formal analysis: FP, JA, SP-S, AMo, AMa, JT, OT, EQ, MU, RL, JR, MM, KA, AA, AD-W, and MA. Investigation: FP, JA, SP-S, AMo, AMa, JT, OT, EQ, MU, RL, JR, MM, KA, AD-W, and MA. Resources: FP, SP-S, and MA. Data curation: JA, SP-S, JT, OT, EQ, MU, RL, JR, MM, KA, and JP. Writing – original draft preparation: FP, JA, SP-S, AMo, AMa, JT, OT, EQ, MU, RL, JR, and MM. Writing – review & editing: FP, JA, SP-S, AMo, AMa, OT, MM, and MA. Supervision: FP, JA, SP-S, AMo, AMa, AD-W, and MA. Project administration: FP, JA, SP-S, AD-W, and MA. Funding acquisition: FP, JA, SP-S, AMo, AMa, JT, OT, EQ, MU, RL, JR, AD-W, and MA. All authors contributed to the article and approved the submitted version.

Funding

This study was funded by the Department of Science and Technology – Philippine Council for Health Research and Development.

Acknowledgments

The authors wish to acknowledge the University of the Philippines (UP) Manila COVID-19 Research Initiative whose collaboration with us made this study possible. We also thank the Philippine General Hospital Medical Research Laboratory and the UP National Institutes of Health for accommodating our experiments. We also thank Ms. Geraldine O. Soriano, Ms. Rhoda L. Montemayor, Ms. Angeline Macasinag, Ms. Maria Lourdes Hipolito, Dr. Clarissa Dayrit-Halum, Ms. Tine Dela Cruz, Mark Dale Imbag and Ms. Dana Santos for patiently assisting us in the implementation of the study.

Conflict of interest

The authors declare that the research was conducted in the absence of any commercial or financial relationships that could be construed as a potential conflict of interest.

Publisher's note

All claims expressed in this article are solely those of the authors and do not necessarily represent those of their affiliated organizations, or those of the publisher, the editors and the reviewers. Any product that may be evaluated in this article, or claim that may be made by its manufacturer, is not guaranteed or endorsed by the publisher.

Supplementary material

The Supplementary Material for this article can be found online at: https://www.frontiersin.org/articles/10.3389/fimmu.2023.1123497/full#supplementary-material

References

1. Huang C, Wang Y, Li X, Ren L, Zhao J, Hu Y, et al. Clinical features of patients infected with 2019 novel coronavirus in wuhan, China. *Lancet (London England)* (2020) 395:497–506. doi: 10.1016/S0140-6736(20)30183-5

2. Ejaz H, Alsrhani A, Zafar A, Javed H, Junaid K, Abdalla AE, et al. COVID-19 and comorbidities: Deleterious impact on infected patients. *J Infect Public Health* (2020) 13:1833–9. doi: 10.1016/j.jiph.2020.07.014

3. Sanyaolu A, Okorie C, Marinkovic A, Patidar R, Younis K, Desai P, et al. Comorbidity and its impact on patients with COVID-19. *SN Compr Clin Med* (2020) 2:1069–76. doi: 10.1007/s42399-020-00363-4

4. Han H, Ma Q, Li C, Liu R, Zhao L, Wang W, et al. Profiling serum cytokines in COVID-19 patients reveals IL-6 and IL-10 are disease severity predictors. *Emerg Microbes Infect* (2020) 9:1123–30. doi: 10.1080/22221751.2020.1770129

5. Li Lq, Huang T, Wang Yq, Wang Zp, Liang Y, Huang T, et al. COVID-19 patients' clinical characteristics, discharge rate, and fatality rate of meta-analysis. *J Med Virol* (2020) 92:577–83. doi: 10.1002/JMV.25757

6. Li X, To KKW. Biomarkers for severe COVID-19. *EBioMedicine* (2021) 68:103405. doi: 10.1016/j.ebiom.2021.103405

7. Malik P, Patel U, Mehta D, Patel N, Kelkar R, Akrmah M, et al. Biomarkers and outcomes of COVID-19 hospitalisations: Systematic review and meta-analysis. *BMJ Evidence-Based Med* (2021) 26:107–8. doi: 10.1136/BMJEBM-2020-111536

8. Omland T, Mills NL, Mueller C. Care the SG on b of the EA for AC. cardiovascular biomarkers in COVID-19. *Eur Hear J Acute Cardiovasc Care* (2021) 10:473–4. doi: 10.1093/EHJACC/ZUAB037

9. Segundo DS, de las Revillas FA, Lamadrid-Perojo P, Comins-Boo A, González-Rico C, Alonso-Peña M, et al. Innate and adaptive immune assessment at admission to predict clinical outcome in COVID-19 patients. *Biomedicines* (2021) 9(8):917. doi: 10.3390/BIOMEDICINES9080917

10. Shi C, Wang L, Ye J, Gu Z, Wang S, Xia J, et al. Predictors of mortality in patients with coronavirus disease 2019: A systematic review and meta-analysis. *BMC Infect Dis* (2021) 21(1):663. doi: 10.1186/S12879-021-06369-0

11. Malundo AFG, Abad CLR, Salamat MSS, Sandejas JCM, Planta JEG, Poblete JB, et al. Clinical characteristics of patients with asymptomatic and symptomatic COVID-19 admitted to a tertiary referral centre in the Philippines. *IJID Reg* (2022) 2:204–11. doi: 10.1016/j.ijregi.2022.02.002

12. Chen X, Zhao B, Qu Y, Chen Y, Xiong J, Feng Y, et al. Detectable serum severe acute respiratory syndrome coronavirus 2 viral load (RNAemia) is closely correlated with drastically elevated interleukin 6 level in critically ill patients with coronavirus disease 2019. *Clin Infect Dis* (2020) 71:1937–42. doi: 10.1093/CID/CIAA449

13. Gong J, Dong H, Xia QS, Huang Z, Wang Dk, Zhao Y, et al. Correlation analysis between disease severity and inflammation-related parameters in patients with COVID-19: A retrospective study. *BMC Infect Dis* (2020) 20(1):963. doi: 10.1186/S12879-020-05681-5

14. Hadjadj J, Yatim N, Barnabei L, Corneau A, Boussier J, Smith N, et al. Impaired type I interferon activity and inflammatory responses in severe COVID-19 patients. *Science* (2020) 369:718–24. doi: 10.1126/SCIENCE.ABC6027

15. Liu J, Li S, Liu J, Liang B, Wang X, Wang H, et al. Longitudinal characteristics of lymphocyte responses and cytokine profiles in the peripheral blood of SARS-CoV-2 infected patients. *EBioMedicine* (2020) 55:102763. doi: 10.1016/J.EBIOM.2020.102763

16. Liu T, Zhang J, Yang Y, Ma H, Li Z, Zhang J, et al. The role of interleukin-6 in monitoring severe case of coronavirus disease 2019. *EMBO Mol Med* (2020) 12(7): e12421. doi: 10.15252/EMMM.202012421

17. Pedersen SF, Ho YC. SARS-CoV-2: A storm is raging. *J Clin Invest* (2020) 130:2202–5. doi: 10.1172/JCI137647

18. Wu C, Chen X, Cai Y, Xia J, Zhou X, Xu S, et al. Risk factors associated with acute respiratory distress syndrome and death in patients with coronavirus disease 2019 pneumonia in wuhan, China. *JAMA Intern Med* (2020) 180:934–43. doi: 10.1001/JAMAINTERNMED.2020.0994

19. Zhou Y, Fu B, Zheng X, Wang D, Zhao C, Qi Y, et al. Pathogenic T-cells and inflammatory monocytes incite inflammatory storms in severe COVID-19 patients. *Natl Sci Rev* (2020) 7:998. doi: 10.1093/NSR/NWAA041

20. Lampart M, Zellweger N, Bassetti S, Tschudin-Sutter S, Rentsch KM, Siegemund M, et al. Clinical utility of inflammatory biomarkers in COVID-19 in direct comparison to other respiratory infections–a prospective cohort study. *PloS One* (2022) 17: e0269005. doi: 10.1371/journal.pone.0269005

21. Herold T, Jurinovic V, Arnreich C, Lipworth BJ, Hellmuth JC, von Bergwelt-Baildon M, et al. Elevated levels of IL-6 and CRP predict the need for mechanical ventilation in COVID-19. *J Allergy Clin Immunol* (2020) 146:128–136.e4. doi: 10.1016/j.jaci.2020.05.008

22. Blanco-Melo D, Nilsson-Payant BE, Liu WC, Uhl S, Hoagland D, Møller R, et al. Imbalanced host response to SARS-CoV-2 drives development of COVID-19. *Cell* (2020) 181:1036–1045.e9. doi: 10.1016/J.CELL.2020.04.026

23. Chu H, Chan JFW, Wang Y, Yuen TTT, Chai Y, Hou Y, et al. Comparative replication and immune activation profiles of SARS-CoV-2 and SARS-CoV in human lungs: An ex vivo study with implications for the pathogenesis of COVID-19. *Clin Infect Dis* (2020) 71:1400–9. doi: 10.1093/CID/CIAA410

24. Hu B, Huang S, Yin L. The cytokine storm and COVID-19. *J Med Virol* (2021) 93:250–6. doi: 10.1002/JMV.26232

25. Department of Health. *Philippines COVID-19 tracker* (2022). Available at: https://doh.gov.ph/covid19tracker.

26. Philippine COVID-19 Living Recommendations. (2022). Available at: https://www.psmid.org/philippine-covid-19-living-recommendations-3/.

27. Ranieri VM, Rubenfeld GD, Thompson BT, Ferguson ND, Caldwell E, Fan E, et al. Acute respiratory distress syndrome: The Berlin definition. *JAMA* (2012) 307:2526–33. doi: 10.1001/JAMA.2012.5669

28. Philippine General Hospital. *UP-PGH COVID-19 daily report*. (2020). [unpublished manuscript]

29. Chen N, Zhou M, Dong X, Qu J, Gong F, Han Y, et al. Epidemiological and clinical characteristics of 99 cases of 2019 novel coronavirus pneumonia in wuhan, China: a descriptive study. *Lancet* (2020) 395:507–13. doi: 10.1016/S0140-6736(20)30211-7

30. Zhang J, Wang X, Jia X, Li J, Hu K, Chen G, et al. Risk factors for disease severity, unimprovement, and mortality in COVID-19 patients in wuhan, China. *Clin Microbiol Infect* (2020) 26:767–72. doi: 10.1016/J.CMI.2020.04.012

31. Salido EO, Remalante PPM. Should laboratory markers be used for early prediction of severe and possibly fatal COVID-19? *Acta Med Philipp* (2020) 54. doi: 10.47895/amp.v54i0.1561

32. Patridge EF, Bardyn TP. Research electronic data capture (REDCap). *J Med Libr Assoc* (2018) 106:142–144–142–144. doi: 10.5195/JMLA.2018.319

33. Zhou F, Yu T, Du R, Fan G, Liu Y, Liu Z, et al. Clinical course and risk factors for mortality of adult inpatients with COVID-19 in wuhan, China: A retrospective cohort study. *Lancet (London England)* (2020) 395:1054–62. doi: 10.1016/S0140-6736(20)30566-3

34. Li C, Ye J, Chen Q, Hu W, Wang L, Fan Y, et al. Elevated lactate dehydrogenase (LDH) level as an independent risk factor for the severity and mortality of COVID-19. *Aging (Albany NY)* (2020) 12:15670–81. doi: 10.18632/AGING.103770

35. Agrupis KA, Smith C, Suzuki S, Villanueva AM, Ariyoshi K, Solante R, et al. Epidemiological and clinical characteristics of the first 500 confirmed COVID-19 inpatients in a tertiary infectious disease referral hospital in Manila, Philippines. *Trop Med Health* (2021) 49(1):48. doi: 10.1186/S41182-021-00340-0

36. Liu W, Tao ZW, Wang L, Yuan ML, Liu K, Zhou L, et al. Analysis of factors associated with disease outcomes in hospitalized patients with 2019 novel coronavirus disease. *Chin Med J (Engl)* (2020) 133:1032–8. doi: 10.1097/CM9.0000000000000775

37. Yanez ND, Weiss NS, Romand JA, Treggiari MM. COVID-19 mortality risk for older men and women. *BMC Public Health* (2020) 20(1):1742. doi: 10.1186/S12889-020-09826-8

38. *Interim guidance on the clinical management of adult patients with suspected or confirmed COVID-19 infection* (2020). Available at: https://www.psmid.org/interim-management-guidelines-for-covid-19-version-3-1/ (Accessed August 1, 2022).

39. World Health Organization. *Therapeutics and COVID-19: Living guideline* (2022). Available at: https://www.who.int/publications/i/item/WHO-2019-nCoV-therapeutics-2022.4 (Accessed August 1, 2022).

40. Horby P, Lim WS, Emberson JR, Mafham M, Bell JL, Linsell L, et al. Dexamethasone in hospitalized patients with covid-19. *N Engl J Med* (2021) 384:693–704. doi: 10.1056/NEJMoa2021436

41. Abani O, Abbas A, Abbas F, Abbas M, Abbasi S, Abbass H, et al. Tocilizumab in patients admitted to hospital with COVID-19 (RECOVERY): A randomised, controlled, open-label, platform trial. *Lancet (London England)* (2021) 397:1637–45. doi: 10.1016/S0140-6736(21)00676-0

42. Martha JW, Wibowo A, Pranata R. Prognostic value of elevated lactate dehydrogenase in patients with COVID-19: A systematic review and meta-analysis. *Postgrad Med J* (2022) 98(1160):422–7. doi: 10.1136/POSTGRADMEDJ-2020-139542

43. Xu Y, Yang H, Wang J, Li X, Xue C, Niu C, et al. Serum albumin levels are a predictor of COVID-19 patient prognosis: Evidence from a single cohort in chongqing, China. *Int J Gen Med* (2021) 14:2785–97. doi: 10.2147/IJGM.S312521

44. Zhan H, Chen H, Liu C, Cheng L, Yan S, Li H, et al. Diagnostic value of d-dimer in COVID-19: A meta-analysis and meta-regression. *Clin Appl Thromb Hemost* (2021) 27. doi: 10.1177/10760296211010976

45. Niu J, Sareli C, Mayer D, Visbal A, Sareli A. Lymphopenia as a predictor for adverse clinical outcomes in hospitalized patients with COVID-19: A single center retrospective study of 4485 cases. *J Clin Med* (2022) 11(3):700. doi: 10.3390/JCM11030700

46. Abou-Ismail MY, Diamond A, Kapoor S, Arafah Y, Nayak L. The hypercoagulable state in COVID-19: Incidence, pathophysiology, and management. *Thromb Res* (2020) 194:101. doi: 10.1016/J.THROMRES.2020.06.029

47. Middleton EA, He X-Y, Denorme F, Campbell RA, Ng D, Salvatore SP, et al. Neutrophil extracellular traps contribute to immunothrombosis in COVID-19 acute respiratory distress syndrome. *Blood* (2020) 136:1169–79. doi: 10.1182/blood.2020007008

48. Spyropoulos AC, Goldin M, Giannis D, Diab W, Wang J, Khanijo S, et al. Efficacy and safety of therapeutic-dose heparin vs standard prophylactic or intermediate-dose heparins for thromboprophylaxis in high-risk hospitalized patients with COVID-19: The HEP-COVID randomized clinical trial. *JAMA Intern Med* (2021) 181:1612–20. doi: 10.1001/jamainternmed.2021.6203

49. Lawler PR, Goligher EC, Berger JS, Neal MD, McVerry BJ, Nicolau JC, et al. Therapeutic anticoagulation with heparin in noncritically ill patients with covid-19. *N Engl J Med* (2021) 385:790–802. doi: 10.1056/NEJMoa2105911

50. Goligher EC, Bradbury CA, McVerry BJ, Lawler PR, Berger JS, Gong MN, et al. Therapeutic anticoagulation with heparin in critically ill patients with covid-19. *N Engl J Med* (2021) 385:777–89. doi: 10.1056/NEJMoa2103417

51. Van Den Borne P, Quax PHA, Hoefer IE, Pasterkamp G. The multifaceted functions of CXCL10 in cardiovascular disease. *BioMed Res Int* (2014) 2014:893106. doi: 10.1155/2014/893106

52. Lupieri A, Smirnova NF, Solinhac R, Malet N, Benamar M, Saoudi A, et al. Smooth muscle cells-derived CXCL10 prevents endothelial healing through PI3Kγ-dependent T cells response. *Cardiovasc Res* (2020) 116:438–49. doi: 10.1093/CVR/CVZ122

53. Ichikawa A, Kuba K, Morita M, Chida S, Tezuka H, Hara H, et al. CXCL10-CXCR3 enhances the development of neutrophil-mediated fulminant lung injury of viral and nonviral origin. *Am J Respir Crit Care Med* (2013) 187:65–77. doi: 10.1164/RCCM.201203-0508OC

54. Buja LM, Wolf DA, Zhao B, Akkanti B, McDonald M, Lelenwa L, et al. The emerging spectrum of cardiopulmonary pathology of the coronavirus disease 2019 (COVID-19): Report of 3 autopsies from Houston, Texas, and review of autopsy findings from other united states cities. *Cardiovasc Pathol Off J Soc Cardiovasc Pathol* (2020) 48:107233. doi: 10.1016/j.carpath.2020.107233

55. Vorobjeva NV, Chernyak BV. NETosis: Molecular mechanisms, role in physiology and pathology. *Biochem (Mosc)* (2020) 85:1178–90. doi: 10.1134/S0006297920100065

56. Wang J, Li Q, Yin Y, Zhang Y, Cao Y, Lin X, et al. Excessive neutrophils and neutrophil extracellular traps in COVID-19. *Front Immunol* (2020) 11:2063. doi: 10.3389/fimmu.2020.02063

57. Zuo Y, Yalavarthi S, Shi H, Gockman K, Zuo M, Madison JA, et al. Neutrophil extracellular traps in COVID-19. *JCI Insight* (2020) 5(11):e138999. doi: 10.1172/jci.insight.138999

58. Lu Q, Zhu Z, Tan C, Zhou H, Hu Y, Shen G, et al. Changes of serum IL-10, IL-1β, IL-6, MCP-1, TNF-α, IP-10 and IL-4 in COVID-19 patients. *Int J Clin Pract* (2021) 75(9):e14462. doi: 10.1111/IJCP.14462

59. Chen Y, Wang J, Liu C, Su L, Zhang D, Fan J, et al. IP-10 and MCP-1 as biomarkers associated with disease severity of COVID-19. *Mol Med* (2020) 26(1):97. doi: 10.1186/S10020-020-00230-X

60. Ozger HS, Karakus R, Kuscu EN, Bagriacik UE, Oruklu N, Yaman M, et al. Serial measurement of cytokines strongly predict COVID-19 outcome. *PloS One* (2021) 16 (12):e0260623. doi: 10.1371/journal.pone.0260623

61. Rizzi M, Costanzo M, Tonello S, Matino E, Casciaro FG, Croce A, et al. Prognostic markers in hospitalized COVID-19 patients: The role of IP-10 and c-reactive protein. *Dis Markers* (2022) 2022(1):119–127.e4. doi: 10.1155/2022/3528312

62. Yang Y, Shen C, Li J, Yuan J, Wei J, Huang F, et al. Plasma IP-10 and MCP-3 levels are highly associated with disease severity and predict the progression of COVID-19. *J Allergy Clin Immunol* (2020) 146(1):119–127.e4. doi: 10.1016/J.JACI.2020.04.027

63. Guo J, Wang S, Xia H, Shi D, Chen Y, Zheng S, et al. Cytokine signature associated with disease severity in COVID-19. *Front Immunol* (2021) 12:681516. doi: 10.3389/FIMMU.2021.681516

64. Jones SA, Hunter CA. Is IL-6 a key cytokine target for therapy in COVID-19? *Nat Rev Immunol* (2021) 21:337–9. doi: 10.1038/S41577-021-00553-8

65. Sabaka P, Koščálová A, Straka I, Hodosy J, Lipták R, Kmotorková B, et al. Role of interleukin 6 as a predictive factor for a severe course of covid-19: Retrospective data analysis of patients from a long-term care facility during covid-19 outbreak. *BMC Infect Dis* (2021) 21(1):308. doi: 10.1186/S12879-021-05945-8

66. Santa Cruz A, Mendes-Frias A, Oliveira AI, Dias L, Matos AR, Carvalho A, et al. Interleukin-6 is a biomarker for the development of fatal severe acute respiratory syndrome coronavirus 2 pneumonia. *Front Immunol* (2021) 12:613422. doi: 10.3389/FIMMU.2021.613422

67. Zhou J, He W, Liang J, Wang L, Yu X, Bao M, et al. Association of interleukin-6 levels with morbidity and mortality in patients with coronavirus disease 2019 (COVID-19). *Jpn J Infect Dis* (2021) 74:293–8. doi: 10.7883/YOKEN.JJID.2020.463

68. Gorham J, Moreau A, Corazza F, Peluso L, Ponthieux F, Talamonti M, et al. Interleukine-6 in critically ill COVID-19 patients: A retrospective analysis. *PloS One* (2020) 15(12):e0244628. doi: 10.1371/JOURNAL.PONE.0244628

69. Galván-Román JM, Rodríguez-García SC, Roy-Vallejo E, Marcos-Jiménez A, Sánchez-Alonso S, Fernández-Díaz C, et al. IL-6 serum levels predict severity and response to tocilizumab in COVID-19: An observational study. *J Allergy Clin Immunol* (2021) 147:72–80.e8. doi: 10.1016/J.JACI.2020.09.018

70. Yasuda K, Nakanishi K, Tsutsui H. Interleukin-18 in health and disease. *Int J Mol Sci* (2019) 20(3):649. doi: 10.3390/IJMS20030649

71. Coutinho LL, Oliveira CN, Albuquerque PL, Mota SM, Meneses GC, Martins AM, et al. Elevated IL-18 predicts poor prognosis in critically ill COVID-19 patients at a Brazilian hospital in 2020-21. *Future Microbiol* (2022) 17:1287–94. doi: 10.2217/FMB-2022-0057

72. Lucas C, Wong P, Klein J, Castro TBR, Silva J, Sundaram M, et al. Longitudinal analyses reveal immunological misfiring in severe COVID-19. *Nature* (2020) 584:463–9. doi: 10.1038/S41586-020-2588-Y

73. Tjan LH, Furukawa K, Nagano T, Kiriu T, Nishimura M, Arii J, et al. Early differences in cytokine production by severity of coronavirus disease 2019. *J Infect Dis* (2021) 223:1145–9. doi: 10.1093/INFDIS/JIAB005

74. Satış H, Özger HS, Aysert Yıldız P, Hızel K, Gulbahar Ö, Erbaş G, et al. Prognostic value of interleukin-18 and its association with other inflammatory markers and disease severity in COVID-19. *Cytokine* (2021) 137:155302. doi: 10.1016/J.CYTO.2020.155302

75. Rodrigues TS, de Sá KSG, Ishimoto AY, Becerra A, Oliveira S, Almeida L, et al. Inflammasomes are activated in response to SARS-CoV-2 infection and are associated with COVID-19 severity in patients. *J Exp Med* (2021) 218. doi: 10.1084/JEM.20201707

76. Cheon SY, Koo BN. Inflammatory response in COVID-19 patients resulting from the interaction of the inflammasome and SARS-CoV-2. *Int J Mol Sci* (2021) 22. doi: 10.3390/IJMS22157914

77. Xia B, Wang Y, Pan X, Cheng X, Ji H, Zuo X, et al. Why is the SARS-CoV-2 omicron variant milder? *Innov (Cambridge* (2022) 3. doi: 10.1016/J.XINN.2022.100251

frontiers | Frontiers in Immunology

TYPE Original Research
PUBLISHED 03 March 2023
DOI 10.3389/fimmu.2023.1098461

OPEN ACCESS

EDITED BY
Fabrice Cognasse,
INSERM U1059 SAnté INgéniérie BIOlogie, France

REVIEWED BY
Doreen Szollosi,
University of Saint Joseph, United States
Saidou Balam,
University Medical Center Regensburg, Germany
Philip Bufler,
Charité University Medicine Berlin, Germany

*CORRESPONDENCE
Yang-Kyu Choi
yangkyuc@konkuk.ac.kr
Soohyun Kim
soohyun@konkuk.ac.kr

†These authors have contributed equally to this work

SPECIALTY SECTION
This article was submitted to Inflammation, a section of the journal Frontiers in Immunology

RECEIVED 15 November 2022
ACCEPTED 25 January 2023
PUBLISHED 03 March 2023

CITATION
Hisham Y, Seo S-M, Kim S, Shim S, Hwang J, Yoo E-S, Kim N-W, Song C-S, Jhun H, Park H-Y, Lee Y, Shin K-C, Han S-Y, Seong JK, Choi Y-K and Kim S (2023) COVID-19 spike polypeptide vaccine reduces the pathogenesis and viral infection in a mouse model of SARS-CoV-2.
Front. Immunol. 14:1098461.
doi: 10.3389/fimmu.2023.1098461

COVID-19 spike polypeptide vaccine reduces the pathogenesis and viral infection in a mouse model of SARS-CoV-2

Yasmin Hisham[1†], Sun-Min Seo[2†], Sinae Kim[1,3†], Saerok Shim[1], Jihyeong Hwang[1], Eun-Seon Yoo[2], Na-Won Kim[2], Chang-Seon Song[3], Hyunjhung Jhun[4], Ho-Young Park[5], Youngmin Lee[6], Kyeong-Cheol Shin[7], Sun-Young Han[8], Je Kyung Seong[9,10], Yang-Kyu Choi[2*] and Soohyun Kim[1,3*]

[1]Laboratory of Cytokine Immunology, Department of Biomedical Science and Technology, Konkuk University, Seoul, Republic of Korea, [2]Department of Laboratory Animal Medicine, College of Veterinary Medicine, Konkuk University, Seoul, Republic of Korea, [3]College of Veterinary Medicine, Konkuk University, Seoul, Republic of Korea, [4]Food Industry Infrastructure Team, Korea Food Research Institute, Wanju, Republic of Korea, [5]Research Group of Functional Food Materials, Korea Food Research Institute, Wanju, Republic of Korea, [6]Department of Medicine, Pusan Paik Hospital, Inje University College of Medicine, Busan, Republic of Korea, [7]Center for Respiratory Disease, College of Medicine, Yeungnam University, Daegu, Republic of Korea, [8]College of Pharmacy and Research Institute of Pharmaceutical Sciences, Gyeongsang National University, Jinju, Gyeongsangnam, Republic of Korea, [9]Laboratory of Developmental Biology and Genomics, Research Institute for Veterinary Science, and BK21 PLUS Program for Creative Veterinary Science Research, College of Veterinary Medicine, Seoul National University, Seoul, Republic of Korea, [10]Korea Mouse Phenotyping Center, Interdisciplinary Program for Bioinformatics, and BioMAX Institute, Seoul National University, Seoul, Republic of Korea

The SARS-CoV-2 coronavirus, which causes a respiratory disease called COVID-19, has been declared a pandemic by the World Health Organization (WHO) and is still ongoing. Vaccination is the most important strategy to end the pandemic. Several vaccines have been approved, as evidenced by the ongoing global pandemic, but the pandemic is far from over and no fully effective vaccine is yet available. One of the most critical steps in vaccine development is the selection of appropriate antigens and their proper introduction into the immune system. Therefore, in this study, we developed and evaluated two proposed vaccines composed of single and multiple SARS-CoV-2 polypeptides derived from the spike protein, namely, vaccine A and vaccine B, respectively. The polypeptides were validated by the sera of COVID-19-vaccinated individuals and/or naturally infected COVID-19 patients to shortlist the starting pool of antigens followed by *in vivo* vaccination to hACE2 transgenic mice. The spike multiple polypeptide vaccine (vaccine B) was more potent to reduce the pathogenesis of organs, resulting in higher protection against the SARS-CoV-2 infection.

KEYWORDS

SARS-CoV-2, pathogenesis, COVID-19 vaccine, spike polypeptide, *in vivo* mouse model

Abbreviations: ACE2, angiotensin-converting enzyme 2; Ag, antigen; COVID-19, coronavirus disease 2019; ELISA, enzyme-linked immunosorbent assay; RBD, receptor-binding domain; PBS-T, phosphate-buffered saline, 0.1% Tween; SARS-CoV-2, severe acute respiratory syndrome coronavirus 2; S, spike; TG, transgenic mouse; WT, wild type.

1 Introduction

The recent and ongoing pandemic named COVID-19 caused by the coronavirus SARS-CoV-2 that first emerged in late 2019 continues to claim over 6 billion positive cases with higher than 6.5 million deaths (1). Symptoms are relatively similar to common cold symptoms and range from mild to severe conditions. These symptoms include coughing, shortness of breath, fatigue, and fever; the elderly especially those who have comorbidities such as hypertension, obesity, or diabetes are at higher risk for serious illness. In addition, another complication associated with SARS-CoV-2 is the development of a severe COVID-19-related "cytokine storm", possibly due to dysregulation of the IFN-I response that causes a serious condition known as acute respiratory distress syndrome (ARDS) (2–7). To note, among all shown SARS-CoV-2 variants, the Omicron variant outbreak was the highest wave worldwide (8–10).

Combining immunization with non-pharmaceutical interventions is the greatest approach to control a pandemic. Therefore, multiple vaccines against COVID-19 have been developed at an exceptional rate, delivering billions of doses worldwide and significantly reducing the number of deaths from the COVID-19 disease (11, 12). Although several vaccines have been approved, the pandemic is not over yet, as evidenced by the ongoing global pandemic since none of the commercially available vaccines is entirely effective to prevent COVID-19. Furthermore, a series of severe cases of COVID-19 among people who had already received two doses of the Pfizer vaccine were reported in Israel in late July and early August 2021, questioning the level of effectiveness of the vaccine (13). A recent analysis shows that the COVID-19 pandemic may end in 2022, but then again COVID-19 will be two times more lethal than seasonal flu by 2023 (14). Another analysis that was performed by the British government assumed that this pandemic could be over either by 2022/2023 or by 2023/2024, or may last till 2026 (15). Both assumptions signify the need for a proper effective vaccine against SARS-CoV-2.

The major transgene or its fragments thereof that are currently primarily focused on vaccine development for COVID-19 are the spike protein of SARS-CoV-2, especially the receptor-binding domain (RBD). Therefore, consideration of the variants and the mutational events of SARS-CoV-2 should not be neglected especially for the RBD region (16–20). Moreover, the spike protein facilitates viral entry into cells as it is located on the virion surface and is believed to bind to the human angiotensin-converting enzyme 2 (hACE2) receptor, making it susceptible to humoral antibody immune responses, thus considered a promising immunogen. Furthermore, data indicate that the spike protein is the primary target of neutralizing antibodies and some of identified neutralizing antibodies were applied as therapeutic neutralizing antibodies in different clinical trial phases such as Celltrion (NCT04602000) and Regeneron (NCT04425629, NCT04426695, and NCT04452318) (21, 22).

Among the vaccine types, subunit vaccines that are composed of viral proteins or protein fragments offer stably expressed, conformationally native antigenic peptides and high-throughput, scalable solutions. The most used platforms in designing the new vaccines for SARS-CoV-2 were mRNA vaccine-based and, to a lesser extent, DNA vaccine-based platforms (23). Still, although these vaccines restrict the severe cases of COVID-19 infections and relatively reduce the spreading, drawbacks including safety and immunogenicity, long-term efficacy, and stability especially for RNA, as it is highly susceptible to degradation, are among the challenges hindering vaccine development (24). Compared to these platforms, peptide-based vaccines exhibit superior properties and guarantee cytolytic T-cell induction and memory B-cell formation (25–27). Therefore, and in order not to depend on the transcriptional and/or translation machinery (peptide production) of the body and its variation among individuals, we chose to use the peptide-based vaccine platform.

Moreover, other than DNA and mRNA vaccines, subunit (peptide) vaccines guarantee to preserve the required conformation and its final concentration (28–31). Four used antigen polypeptides were selected by the structure and immunogenicity of spike protein (16, 32–34). In addition, polypeptide vaccines are easier and cheaper to manufacture on a large scale than mRNA vaccines and do not need ultra-cold storage. This may help get more vaccines to undeveloped parts of the world like Africa where vaccination rates are very low. Nevertheless, while vaccination remains the most important strategy to end the pandemic, achieving global vaccination coverage remains a major hurdle. In this context, we examined that the selected polypeptides of the COVID-19 spike were validated by sera of vaccinated individuals and infected patients following *in vivo* vaccination using the hACE2 transgenic mouse (TG) model of COVID-19 (35). Here, we report the result of two vaccines: vaccines A and B composed of single SARS-CoV-2 and multiple SARS-CoV-2 polypeptides, respectively, derived from the SARS-CoV-2 spike protein. Vaccine B sufficiently reduced the pathogenesis of different organs, resulting in protection of hACE2 TG mice from SARS-CoV-2 infection.

2 Materials and methods

2.1 Cloning, expression, and purification of polypeptides (antigens)

Polypeptide antigens of spike protein were cloned, expressed, and purified as described earlier (17, 36). Briefly, spike cDNA corresponding to polypeptide antigens were cloned into a pET21a vector (Takara, Shiga, Japan), followed by PCR, then PCR products were ligated into an expression vector using suitable restriction enzymes (Takara, Shiga, Japan). The positive clone containing the polypeptide cDNA insert was confirmed by analysis of their respective DNA sequencing (Cosmogen, Seoul, Korea). Next, expression vectors were transformed into BL21-CodonPlus (Stratagene, San Diego, CA, USA) through a heat-shock technique. After collecting the expressed polypeptides, they were purified using their 6 × his-tag at the C-terminus by TALON® Magnetic Beads (Takara) followed by HPLC purification. Their concentrations were verified *via* silver staining and Bradford assay.

2.2 Viral antibody testing and neutralization assay

Purified spike antigens were assessed for their neutralizing ability using serum samples from SARS-CoV-2-vaccinated and naturally infected people, which were approved by the Institutional Review Board of Yeungnam University Medical Center, Korea (approval no. 2020-07-063) (17). Homemade enzyme-linked immunosorbent assay (ELISA) was used to detect neutralizing antibodies (anti-SARS-CoV-2 antibodies) within human sera against a list of purified spike antigens, which was used to coat max-flat-bottom 96-well plates at a final concentration of 1 μg/ml and kept at 4°C 1 day before the assay. The next day (the day of the assay), the plates were washed three times with phosphate-buffered saline and 0.1% Tween (PBS-T) and blocked with 200 μl/well 2% BSA for 1 h at room temperature (RT), followed by washing with PBS-T three times, and then incubated with serially diluted serum samples for 2 h at RT. Next, the plates were washed three times with PBS-T, incubated on a rocker for 0.5 h at RT with antibody-HRP, washed three times with PBS-T, and incubated with TMP-substrate 100 μl/well for 20 min at RT followed by 100 μl/well of stop solution. The ELISA plate was read at 450 nm on a microplate reader. The same ELISA steps were used for the titration assay of mice serum.

2.3 Vaccine formulation, mice vaccinations, and infection

All the animal experiments were approved by the Institutional Animal Care and Use Committee (IACUC) at Konkuk University. Two vaccines, vaccine A and vaccine B, were designated among the purified spike antigens. Both were injected twice subcutaneously with 2-week intervals; the first injection (on day 21) was formulated with a complete adjuvant, and the second (on day 7) was formulated with an incomplete adjuvant. Antigens and adjuvants (Freund's adjuvant, a known solution of antigen emulsified in mineral oil used as an immunopotentiation; both complete and incomplete adjuvants were used: the complete adjuvant is made of inactivated and dried mycobacteria, and the incomplete adjuvant lacks the mycobacterial components) were mixed in a 1:1 ratio to the mentioned final concentration. Male mice of K18-hACE2 TG at 7 weeks of age were used; each group was injected with a dose of 2 μg per mouse, and all mice were preserved with food and water and weighted and monitored daily. The first group was vaccinated with vaccine A followed by those infected/challenged with SARS-CoV-2 virus (n = 5); the second group was vaccinated with vaccine B followed by those infected/challenged with SARS-CoV-2 (n = 5); and the control group was only infected/challenged with SARS-CoV-2 (n = 5), 1×10^5. The median tissue culture infectious dose ($TCID_{50}$) of SARS-CoV-2 virus (NCCP 43326) was given intranasally at day 0. The viral infection of SARS-CoV-2 by real-time RT-PCR was performed according to the guidelines of Korea Centers for Disease Control & Prevention (KCDC&P). Next, sera were collected on day 6 or 7, and all sera were kept at 4°C until use.

2.4 Mouse experiment for vaccine evaluation

The following elements were checked to evaluate changes and compare the three groups of mice: mouse weight, mouse activity, and survival rate until 7 dpi. Moreover, lung, spleen, and small intestine tissue excisions from sacrificed mice on day 7 were used for histopathological score measurements. Virus titer was measured for lung tissues, and tissue weight/body weight was measured for lung tissues.

2.5 Histopathological analysis of lung, spleen, and small intestine

Lung, spleen, and small intestine organs from sacrificed mice were collected on day 7 after infection. The collected tissues were fixed using 4% paraformaldehyde, paraffin-embedded, cut into sections equally, and stained with hematoxylin–eosin (H&E) staining for detection of histopathological changes. Inflammation, edema, and bronchiolitis lesions were measured for lung tissues. Spleen atrophy of the white pulp was measured in the spleen. The number of goblet cells was measured in the small intestine.

2.6 Statistical analysis

Statistical analysis was completed using Prism 8.0 (GraphPad Software). One-way ANOVA or two-way ANOVA, followed by Tukey's *post-hoc* correction, was used; P-value <0.05 was considered significant.

3 Results

3.1 Identifying potential protective antigens using serum samples from vaccinated and naturally infected patients

Various antigens/polypeptides of the spike protein were constructed and purified to be evaluated as a vaccine candidate. These antigens were checked for their ability to bind to neutralizing antibodies within the human sera of either vaccinated people or patients naturally infected with the SARS-CoV-2 virus. Among them, four antigens summarized in Table 1 were selected for further experiments. These antigens were used as a SARS-CoV-2 vaccine and to compare whether one antigen is sufficient to offer protection similar to multiple antigens. We used two vaccines as follows: vaccine A is composed of a single antigen-1 (Ag1), whereas vaccine B is a mixture of four antigens (Ag1, Ag2, Ag3, and Ag4). The scheme of the designed experiments is summarized in Figure 1. Briefly, mice were immunized with two different vaccines (two groups each with either vaccine A or vaccine B) subcutaneously in a final dose of 2 μg and scheduled within 3 weeks prior to infection as the first injection was at day 21 and the second injection was at day 7 (2-week interval), and then mice were infected with 10^5 PFU of SARS-CoV-2 virus at day 0, sera were collected, and mice were necropsied at day 7.

TABLE 1 Amino acid sequence of four spike antigens.

Antigen ID	Antigen Sequence (a a)	Length (aa)
Ag1 (14-134)	**M**QCVNLTTRTQLPPANNLDSKVGGNYNYLYRLFRKSNLKPFERDISTEIYQAGSTPCN GVEGFNCYFPLQSYGFQPTNGVGYQPYRVVVLSFELLHAPATVCGPKKSTNLVKNKC VNFNFNG**LE**HHHHHH*	**123aa**
Ag2 (358-683)	**M**ISNCVADYSVLYNSASFSTFKCYGVSPTKLNDLCFTNVYADSFVIRGDEVRQIAPGQT GKIADYNYKLPDDFTGCVIAWNSNNLDSKVGGNYNYLYRLFRKSNLKPFERDISTEIYQ AGSTPCNGVEGFNCYFPLQSYGFQPTNGVGYQPYRVVVLSFELLHAPATVCGPKKSTN LVKNKCVNFNFNGLTGTGVLTESNKKFLPFQQFGRDIADTTDAVRDPQTLEILDITPCS FGGVSVITPGTNTSNQVAVLYQDVNCTEVPVAIHADQLTPTWRVYSTGSNVFQTRAG CLIGAEHVNNSYECDIPIGAGICASYQTQTNSPRR**LE**HHHHHH*	**326aa**
Ag3 (507-683)	**M**PYRVVVLSFELLHAPATVCGPKKSTNLVKNKCVNFNFNGLTGTGVLTESNKKFLPFQ QFGRDIADTTDAVRDPQTLEILDITPCSFGGVSVITPGTNTSNQVAVLYQDVNCTEVPV AIHADQLTPTWRVYSTGSNVFQTRAGCLIGAEHVNNSYECDIPIGAGICASYQTQTNSP RR**LE**HHHHHH*	**179aa**
Ag4 (1040-1213)	**M**VDFCGKGYHLMSFPQSAPHGVVFLHVTYVPAQEKNFTTAPAICHDGKAHFPREGVF VSNGTHWFVTQRNFYEPQIITTDNTFVSGNCDVVIGIVNNTVYDPLQPELDSFKEELDK YFKNHTSPDVDLGDISGINASVVNIQKEIDRLNEVAKNLNESLIDLQELGKYEQYIKWP**LE** HHHHHH*	**176aa**

The list of potential vaccine candidates of spike protein and their IDs, amino acid sequence, and length. Amino acids in black bold emphasis represent the starting residue. M, methionine. Amino acids in red are the Histidine tags at the C-terminus; red asterisk symbol (*) represents the stop codon.
The underlined values showed the immunogenic part of the antigen (epitope/motif).

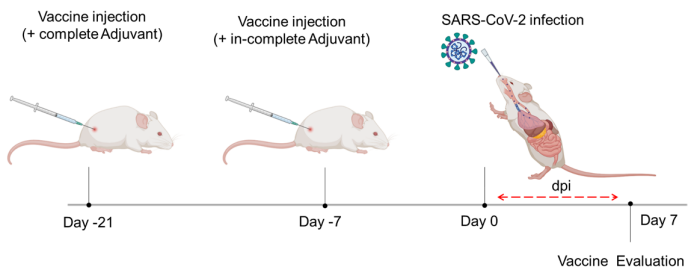

FIGURE 1
Schematic drawing showing the experimental design of the vaccination. K18-hACE2 TG mice were injected twice with 2 µg or either vaccine A or vaccine B subcutaneously at intervals of 2 weeks. After a week of a second injection, mice were infected with SARS-CoV-2 (10^5 PFU) through the intranasal route, and 7 days postinfection changes were assessed.

Two-step purified recombinant antigens were visualized by 10% SDS-PAGE and silver staining (Supplementary Figure 1). These four antigens were selected to be examined as vaccine candidates because of their highest binding ability (higher OD_{450}) with vaccinated or naturally infected human serum samples. COVID-19 patient 2's resulting titer against all four antigens was high and tightly associated with the COVID-19 neutralizing index 640 (Figure 2A). However, the vaccinated human sera exhibited very low titers compared to naturally infected patients' sera. In addition, the vaccinated mouse sera were examined for their titers using the four antigens (Figure 2B). In general, the multiple spike polypeptide (vaccine B)-immunized group exhibited higher titers compared with the single polypeptide (vaccine A)-immunized group.

3.2 Evaluation of survival, weight, and activity changes in mice after SARS-CoV-2 infection

After the vaccination schedule was performed as shown in Figure 1, the three groups of K18-hACE2 TG mice were intranasally infected and on day 7 sacrificed for collection of organ tissue and blood samples. Prior to and postinfection, the weight of mice was monitored for the two groups that have been vaccinated, that is, those vaccinated with vaccine A and those vaccinated with vaccine B, till the day of infection in which there was no difference in the body weight of these two groups. From day 0 up to day 7 postinfection, the three groups—the control group (infected only) was added—were compared for their body weight changes as percent change (Figure 3A, upper panel). At 6 dpi, both the SARS-CoV-2-infected group and the vaccine A-administrated group showed a body weight loss of nearly 15%, whereas the vaccine B-administrated group revealed an 11% loss of body weight. From 4 to 7 dpi, three mice of the vaccine-administered groups (one from the vaccine-A group and two from the vaccine-B group) recovered their weight after weight loss (Figure 3A, bottom panel). Although there was no statistical significance between the three groups in body weight changes, the vaccine B-administrated group demonstrated the lowest body weight loss and improved recovery (Supplementary Figure 2).

In addition, the activity of the three groups was observed and the changes were summarized as percentages (Figure 3B, upper panel). The activity in the SARS-CoV-2-infected group started to decrease at 5 dpi and continuously worsened leading to a moribund state at 7 dpi, whereas in the vaccine-administered group, the activity decreased

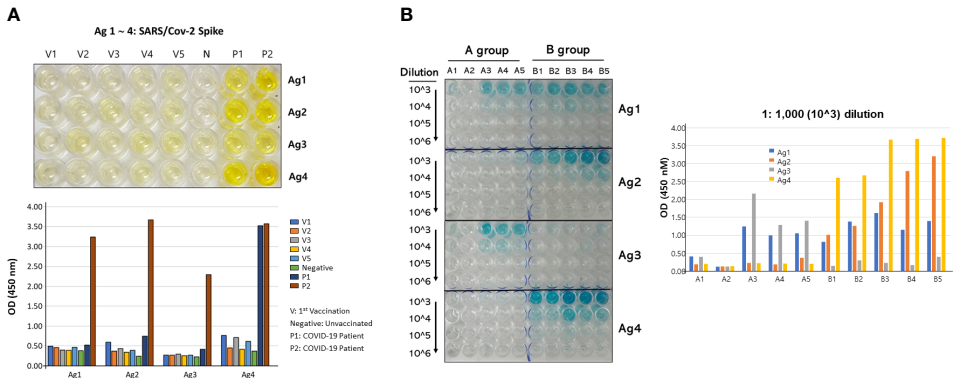

FIGURE 2
Antibody titers of serum against the four antigens. **(A)** ELISA plate showed the binding of the antigens with antibodies from sera of vaccinated (V1~V5), negative (N), and naturally infected patients (P1/2) (upper panel), and their numerical OD_{450} values (lower panel). The patient 1 and 2 COVID-19 neutralizing indexes were 20 and 640, respectively. **(B)** ELISA plate showed the titration results of the antigens with antibodies formed in the two vaccinated mice groups (left) and their numerical OD_{450} values (right). The antibody titration was performed by serial dilution from 1:1,000 (10^3) to 1:1,000,000 (10^6). All vaccinated people included in this study were vaccinated by Pfizer mRNA vaccine.

from 6 dpi and then continued to decrease leading to a moribund status in some mice at 7 dpi. Moreover, the activity of two mice in the vaccine-A group as well as two mice in the vaccine-B group remained 100% up to 7 dpi, and a moribund status was observed in two mice of the vaccine-A group but one mouse of the vaccine-B group (Figure 3B, bottom panel). As indicated also in the survival outcomes that were monitored up to 7 dpi, all mice were sacrificed on day 7 (Figure 3C). There was no significant difference between the three groups in the tested measurements; body weight changes, activity, and survival; however, the mice of group vaccine-B showed the most promising results.

3.3 SARS-CoV-2 titer in lung and histopathological changes in infected mice with and without vaccine

The three groups of mice were sacrificed at 7 dpi, and the viral titers and histopathologic changes were evaluated. In the lung, both viral titers and histopathologic changes are as shown in Figure 4. The vaccine-B group had a markedly lower viral titer (2.1×10^4) compared with those of SARS-CoV-2 infection only (3.7×10^7). Also, the virus titer of the vaccine-A group (9.2×10^5) showed a decrease compared with the SARS-CoV-2-infected group (Figure 4A), although there was no statistically significant difference. On the other hand, histopathological changes in the lungs of mice of the vaccine B-administered group were not greatly improved compared with the group of SARS-CoV-2-infected mice but was not worsened as in the vaccine A-administered group (Figures 4B–E). The total histopathological score showed a non-significant difference between the three groups (Figure 4D). However, for lung edema (Figure 4B), the vaccine A-administered mice showed higher edema compared with SARS-CoV-2-infected mice and vaccine B-administered mice (lowest edema score). In addition, out of five mice, two mice of the vaccine B-administered group revealed the lowest histopathological score when comparing all 15 mice of the three groups (Figure 4D, right panel). These quantitative histopathological scores were confirmed with the histopathological analysis of the mice's lungs (Figure 4E). Lung granulomas are highly formed in the mice of SARS-CoV-2 infection, followed by the vaccine A-administered group, and the least granuloma formation was in the vaccine B-administered group. Thus, taking all together, this suggests that vaccine B confers a promising vaccine nomination as it showed lower viral titers and histopathological scores.

3.4 Histopathological changes in vaccinated and non-vaccinated mice after SARS-CoV-2 infection

We investigated the histopathological changes in the spleen and small intestine, other than the lung, to evaluate the degree of spreading of the infection and how vaccines impact these organs (Figures 5, 6). The changes in spleen pathology of the three groups are shown in Figure 5, and the changes in other tissue weight over body weight (liver, spleen, right and left kidneys, and lung) are shown in Supplementary Figure 3. The spleen-to-body weight ratio showed significantly higher percentages in the vaccinated groups (vaccine A; *p = 0.025 and vaccine-B; *p = 0.042) compared with the SARS-CoV-2-infected group (Figure 5A). The spleen showed to be enlarged under infectious conditions due to the increased immune cell proliferation and differentiation against infected pathogens such as SARS-CoV-2. Thus far, the severity of the damage after infection or injury is mainly measured by the white pulp atrophy rather than spleen enlargement, whereas the atrophy lesion in the splenic white pulp was shown to be increased in the vaccine A-administered group with no significant difference in the vaccine B-and SARS-CoV-2-infected groups (Figures 5B, C). Furthermore, small intestine goblet cells are known for their participation in the immune response; however, increasing the number of these cells indicated worsening of the case and mucus hypersecretion will result in goblet cell hyperplasia (37). In Figure 6, the histopathological changes in terms of goblet cell number of the three mice were evaluated. As the results showed, the vaccine B-administered group represents a statistically significant low number of goblet cell in villi (*p = 0.027), representing a healthier intestine among the three groups.

10.3389/fimmu.2023.1098461

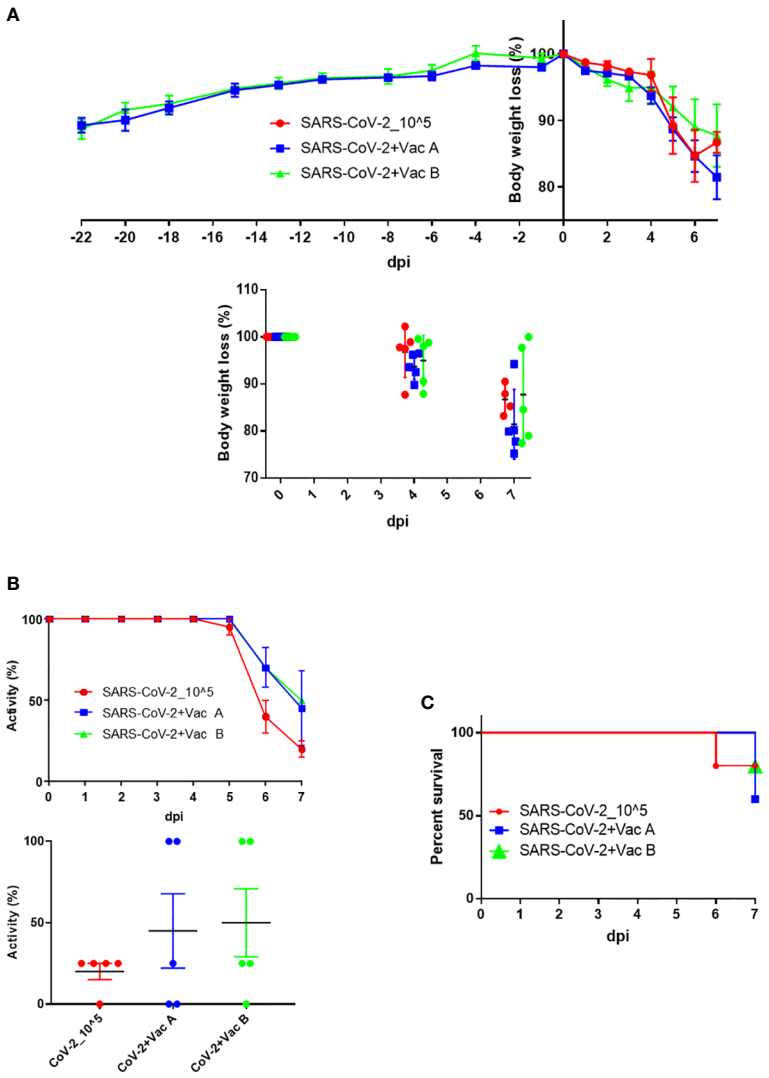

FIGURE 3
Body weight, activity, and survival changes in SARS-CoV-2-vaccinated and infected mice. **(A)** Weight changes starting from injection time (upper panel) and/or while infection (lower panel) plotted as percent change to compare the weight change of three groups (each group has n = 5); both the SARS-CoV-2-infected group (vaccine A, and vaccine B) and the vaccine-treated groups were autopsied; thus, mice's body weights were monitored until 7 days postinfection (dpi). **(B)** Activity changes from day 0 up to day 7 postinfection (upper panel), and the overall activity changes (lower panel) plotted as percent change to compare the activity change of three groups after infection (each group has n = 5); both the SARS-CoV-2-infected group and the vaccine-treated groups (vaccine A and vaccine B). **(C)** The survival of mice was monitored every day until mice of the three groups were autopsied on day 7 dpi. Means with SD are presented, and there was no significance among groups.

4 Discussion

Effective vaccine development has been a critical concern throughout the last pandemic caused by SARS-CoV-2. The need emerged from the start of this pandemic in late 2019, which encouraged many companies to work on a solution in a highly accelerated time frame (32, 38–42). Despite the several vaccines produced, there is still a need for more effective and safe vaccines against COVID-19 as the causing virus, SARS-CoV-2, continues to spread worldwide (33). It is true for a number of vaccines that it was successful in developing a vaccine in record time, yet many challenges remain to be solved to overcome the COVID-19 pandemic emergency (11, 34).

Here, in this study, we were able to select potential spike antigens after evaluation of a list of antigens using infected and vaccinated human sera. In addition, we compared a single antigen versus a mixture of antigens to assess, which could be the best vaccination strategy. Moreover, our results demonstrated the mixture of antigens; vaccine B has promising properties for the development of a vaccine against SARS-CoV-2. In developing peptide-based vaccines, choosing the appropriate epitopes/antigens is the most critical step. The spike (*S*) protein is a crucial protein on the SARS-CoV-2 viral surface as it binds to the host cell surface and mediates the invasion (43, 44). Thus, it is the foremost target of the majority of the anti-COVID-19 vaccines currently offered. Therefore, by narrowing a pool of spike antigens, we aimed to maximize the effectiveness of vaccine candidates. We started with various antigens/epitopes reaching four potential antigens by evaluating the binding of antigens with neutralizing antibodies in the sera of vaccinated and infected patients; these four selected antigens were subjected to further *in vivo* analysis.

10.3389/fimmu.2023.1098461

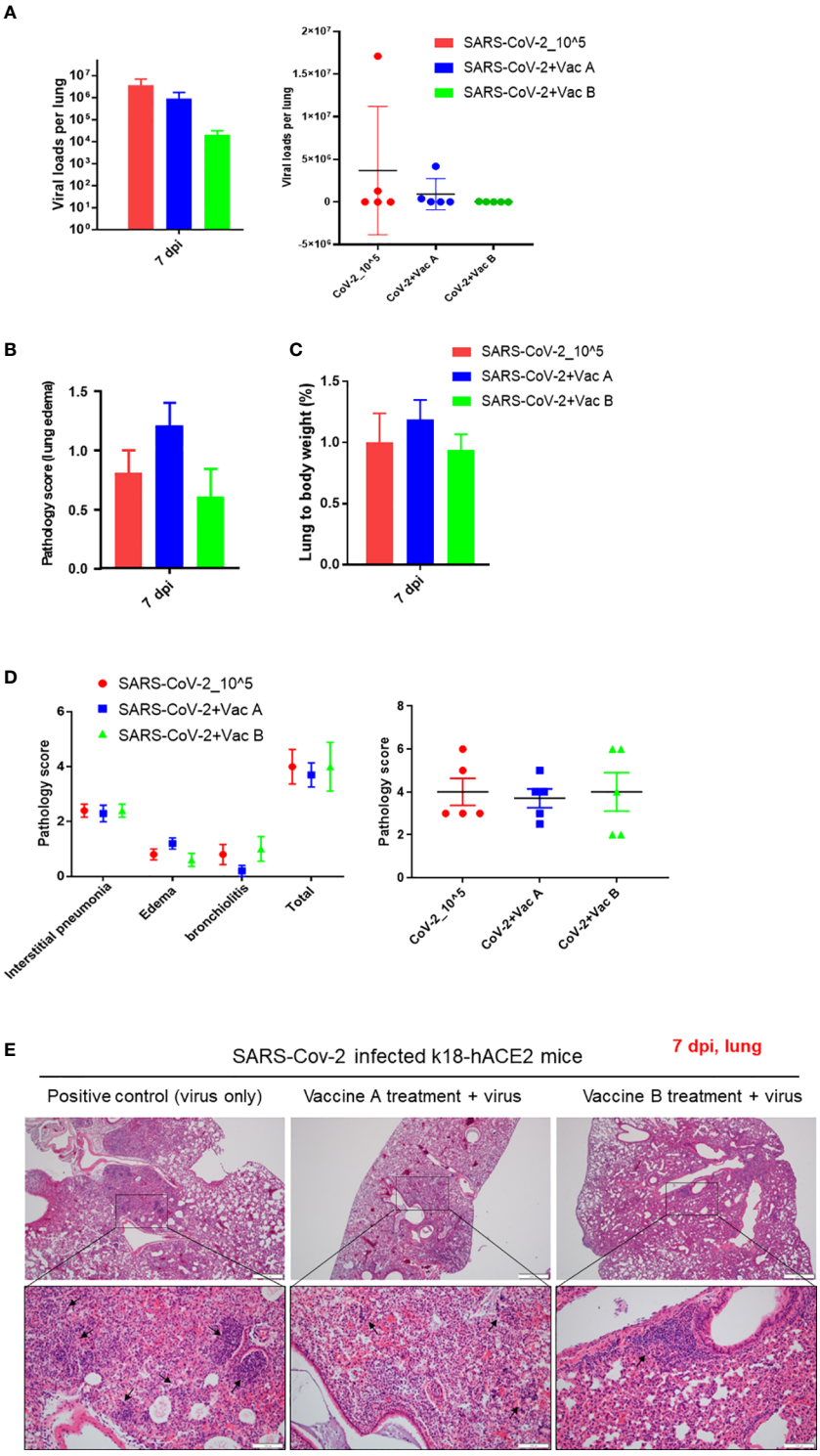

FIGURE 4
Pathological changes of K18-hACE2 TG mouse lungs after SARS-CoV-2 infection with and without vaccine. **(A)** The viral load measurements in the three groups of mice; vaccine A-administered group, vaccine B-administered group, and SARS-CoV-2-infected group (each n = 5) represented as cumulative viral load in each group in the *left* bar graph. The viral load measurements showed individual viral load in each mouse within the three groups of mice as represented in the *right* graph. Means with SD are presented, and there was no significance among groups. **(B)** Histopathological score of changes in lung edema. **(C)** Lung to body weight %. **(D)** Total pathology score. **(E)** Histopathology of mouse lungs after being paraffin-embedded, cut, and stained with hematoxylin–eosin (H&E). Lung granulomas are indicated in black arrows. Scale bars 50 μm (upper line) and100 μm (lower line).

Next, we want to evaluate the impact of the number of antigens per vaccine, so we designed two vaccines, which are vaccine A, which is composed of one antigen (Ag1), and vaccine B, which is composed of an equal mixture of the four selected antigens (Ag1–Ag4). Our results demonstrated that vaccine B with a mixture of antigens provides better outcomes in terms of viral load and histopathological changes than that of a single antigen, vaccine A. Moreover, when we validated the formation of antibodies by titration assay for both vaccinated groups

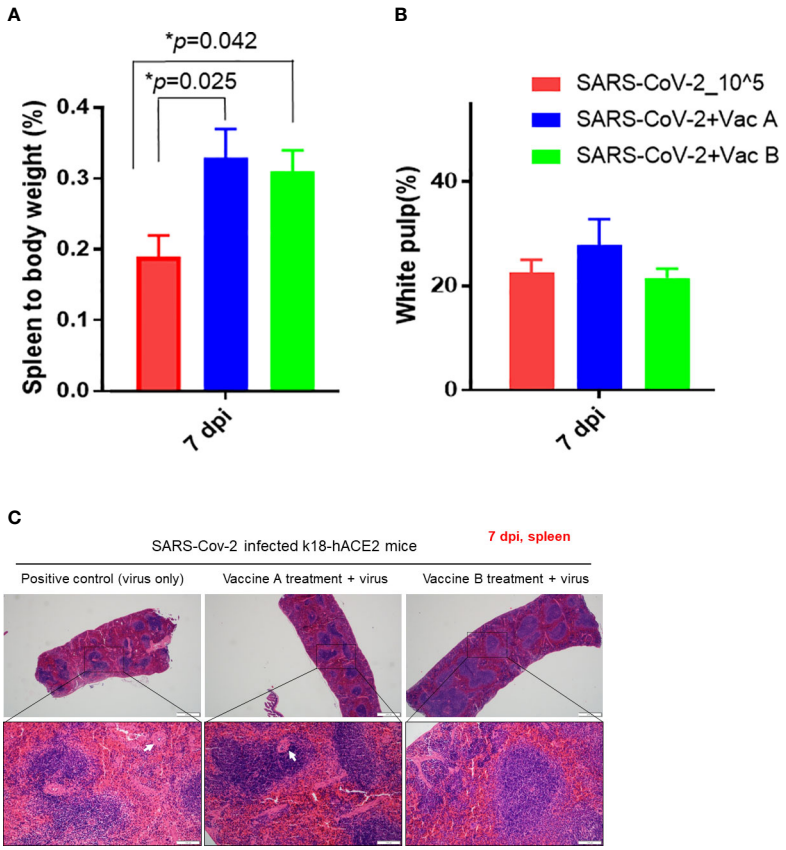

FIGURE 5
Pathological changes of K18-hACE2 TG mouse spleens after SARS-CoV-2 infection with and without vaccines. **(A)** Spleen to body weight %. **(B)** White pulp atrophy %. **(C)** Histopathology of mouse spleens after being paraffin-embedded and processed for hematoxylin–eosin (H&E) staining. Splenic white pulp atrophy is indicated in white arrows. Scale bars 50 μm (upper line) and100 μm (lower line). *p < 0.05.

(Figure 2B), as expected, the vaccine-B group showed binding with all four antigens, especially with Ag4. The vaccine-A group revealed binding with Ag1 as expected but also showed a cross-reactivity with Ag3. Interestingly, the vaccine-A group showed high affinity binding to Ag3, although vaccine A does not contain Ag3. Moreover, the OD_{450} of three mice (A3–A5) for Ag3 was slightly higher than Ag1 in this group, indicating a cross-reactivity occurrence that might be developed by a possible shared epitope structure resulting from a short stretch of amino acids. Furthermore, it is interesting that vaccine-B group mice did not develop an antibody against Ag3, although vaccine B contains Ag3. These data indicate that within a mixture of antigens, some antigens tend to be more visible to the immune system than others.

On the other hand, vaccine B owns four polypeptides of spike protein that interestingly have some amino acid stretches mentioned for their

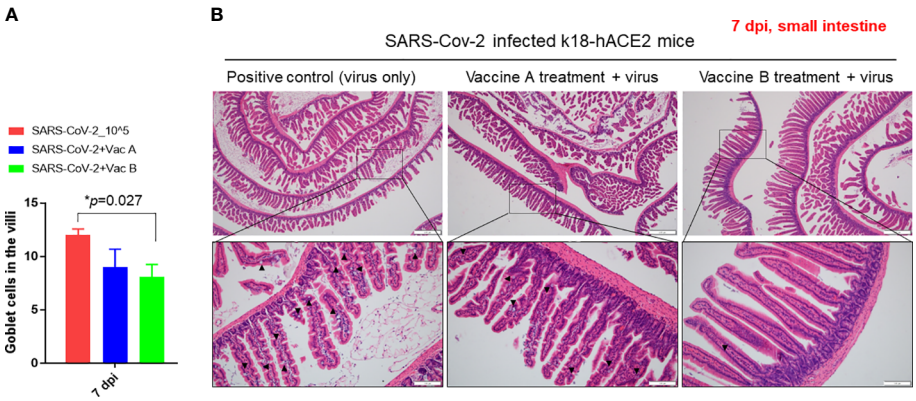

FIGURE 6
Pathological changes of K18-hACE2 TG mouse small intestines after SARS-CoV-2 infection, with and without vaccines. **(A)** Bar graph showing the number of goblet cells in villi in the three groups of mice. **(B)** Histopathology of mouse small intestine after being paraffin-embedded and stained with hematoxylin–eosin (H&E). Goblet cells are indicated in black arrows. Scale bars 50 μm (upper line) and 100 μm (lower line). *p < 0.05.

immunogenicity in previous studies (underlined in Table 1). The epitope/motif QCVNLTTRT in Ag1 was predicted for its antigenicity that was examined for the mutational events and thus, being a highly potential vaccine candidate, was already validated by our assessment (45). In addition, an epitope KPFERDISTEIYQAG STPCNGVEGFNCYFPLQS, found within Ag1 and Ag2, was recognized earlier among other epitopes that induce long-term immunity (46). However, Ag2 and Ag4 present higher titration results indicating higher binding with the formed antibodies (Figure 2B). Yet, all four antigens as one vaccine offer the overall outcome. More detailed investigations are needed to evaluate which antigens produce higher immunity.

In conclusion, it has been well established that vaccination is the most effective strategy for controlling and eradicating infectious diseases. In this study, we sought to evaluate the efficacy of two proposed SARS-CoV-2 vaccines, vaccine A and vaccine B, in providing protection against infection with the virus. Vaccine A was composed of a single SARS-CoV-2 polypeptide derived from the viral spike protein, whereas vaccine B consisted of multiple polypeptides also derived from the spike protein. Upon administering the vaccines to a group of study subjects, we observed that vaccine B was able to attenuate histopathological changes in organs and provided superior protection against SARS-CoV-2 infection compared with vaccine A, as shown in Figures 4–6. These findings suggest that multivalent spike protein-based vaccines may be more effective at inducing immunity against SARS-CoV-2. To the best of our knowledge, this is the first study to compare the efficacy of mono- and multi-peptide vaccine formulations against SARS-CoV-2. Based on the promising results of this study, further investigation into the use of multi-peptide-based vaccines such as vaccine B may hold promise as a potential candidate for the development of an effective COVID-19 vaccine.

Data availability statement

The original contributions presented in the study are included in the article/Supplementary Material. Further inquiries can be directed to the corresponding authors.

Ethics statement

All the animal experiments were approved by the Institutional Animal Care and Use Committee (IACUC) at Konkuk University. Written informed consent was obtained from the owners for the participation of their animals in this study.

Author contributions

YH, S-MS, and SK designed the study, analyzed the data, and performed the experiments. SS, JH, E-SY, and N-WK, performed the experiments. YH, C-SS, HJ, H-YP, YL, K-CS, and S-YH analyzed the data. Funding acquisition: H-YP, JS, Y-KC, and SHK. YH and S-MS examined the data. YH edited the manuscript. Y-KC and SHK designed the study, supervised the project, and wrote the manuscript.

Funding

This work was supported by the National Research Foundation of Korea (NRF-2021R1F1A1057397). This research was supported by the National research foundation of Korea (NRF) grant funded by the Korea government (MSIT) (2021M3H9A1030260). This research was supported by the Main Research Program (E0210602-02) of the Korea Food Research Institute (KFRI) funded by the Ministry of Science and ICT.

Conflict of interest

The authors declare that the research was conducted in the absence of any commercial or financial relationships that could be construed as a potential conflict of interest.

Publisher's note

All claims expressed in this article are solely those of the authors and do not necessarily represent those of their affiliated organizations, or those of the publisher, the editors and the reviewers. Any product that may be evaluated in this article, or claim that may be made by its manufacturer, is not guaranteed or endorsed by the publisher.

Supplementary material

The Supplementary Material for this article can be found online at: https://www.frontiersin.org/articles/10.3389/fimmu.2023.1098461/full#supplementary-material

References

1. Who covid-19 dashboard. *Geneva: World Health Organization 2020* (2022).

2. Hadjadj J, Yatim N, Barnabei L, Corneau A, Boussier J, Smith N, et al. Impaired type I interferon activity and inflammatory responses in severe covid-19 patients. *Science* (2020) 369(6504):718–24. doi: 10.1126/science.abc6027

3. Gong J, Dong H, Xia QS, Huang ZY, Wang DK, Zhao Y, et al. Correlation analysis between disease severity and inflammation-related parameters in patients with covid-19: A retrospective study. *BMC Infect Dis* (2020) 20(1):963. doi: 10.1186/s12879-020-05681-5

4. Richardson S, Hirsch JS, Narasimhan M, Crawford JM, McGinn T, Davidson KW, et al. Presenting characteristics, comorbidities, and outcomes among 5700 patients hospitalized with covid-19 in the new York city area. *JAMA* (2020) 323(20):2052–9. doi: 10.1001/jama.2020.6775

5. Long B, Carius BM, Chavez S, Liang SY, Brady WJ, Koyfman A, et al. Clinical update on covid-19 for the emergency clinician: Presentation and evaluation. *Am J Emerg Med* (2022) 54:46–57. doi: 10.1016/j.ajem.2022.01.028

6. Huang C, Wang Y, Li X, Ren L, Zhao J, Hu Y, et al. Clinical features of patients infected with 2019 novel coronavirus in wuhan, China. *Lancet* (2020) 395(10223):497–506. doi: 10.1016/S0140-6736(20)30183-5

7. Feldstein LR, Tenforde MW, Friedman KG, Newhams M, Rose EB, Dapul H, et al. Characteristics and outcomes of us children and adolescents with multisystem inflammatory syndrome in children (Mis-c) compared with severe acute covid-19. *JAMA* (2021) 325(11):1074–87. doi: 10.1001/jama.2021.2091

8. Kim S, Nguyen TT, Taitt AS, Jhun H, Park HY, Kim SH, et al. Sars-Cov-2 omicron mutation is faster than the chase: Multiple mutations on Spike/Ace2 interaction residues. *Immune Netw* (2021) 21(6):e38. doi: 10.4110/in.2021.21.e38

9. Ahmad A, Fawaz MAM, Aisha A. A comparative overview of sars-Cov-2 and its variants of concern. *Infez Med* (2022) 30(3):328–43. doi: 10.53854/liim-3003-2

10. Hoteit R, Yassine HM. Biological properties of sars-Cov-2 variants: Epidemiological impact and clinical consequences. *Vaccines (Basel)* (2022) 10(6):919. doi: 10.3390/vaccines10060919

11. Lipsitch M, Krammer F, Regev-Yochay G, Lustig Y, Balicer RD. Sars-Cov-2 breakthrough infections in vaccinated individuals: Measurement, causes and impact. *Nat Rev Immunol* (2022) 22(1):57–65. doi: 10.1038/s41577-021-00662-4

12. Tregoning JS, Flight KE, Higham SL, Wang Z, Pierce BF. Progress of the covid-19 vaccine effort: Viruses, vaccines and variants versus efficacy, effectiveness and escape. *Nat Rev Immunol* (2021) 21(10):626–36. doi: 10.1038/s41577-021-00592-1

13. Health IMo. Israel Ministry of health covid-19 dashboard. (2021).

14. Kidoguchi M, Morii W, Noguchi E, Yuta A, Ogawa Y, Nakamura T, et al. Hla-Dpb1*05:01 genotype is associated with poor response to sublingual immunotherapy for Japanese cedar pollinosis. *Allergy* (2022) 77(5):1633–5. doi: 10.1111/all.15254

15. Ghebreyesus TA, World Health Organization. WHO Director-General's opening remarks at the media briefing on COVID-19-25 May 2020.Ghebreyesus, T.A., World Health Organization. WHO Director-General's opening remarks at the media briefing on COVID-19-25 May 2020

16. Hong J, Jhun H, Choi YO, Taitt AS, Bae S, Lee Y, et al. Structure of sars-Cov-2 spike glycoprotein for therapeutic and preventive target. *Immune Netw* (2021) 21(1):e8. doi: 10.4110/in.2021.21.e8

17. Kim S, Lee JH, Lee S, Shim S, Nguyen TT, Hwang J, et al. The progression of sars coronavirus 2 (Sars-Cov2): Mutation in the receptor binding domain of spike gene. *Immune Netw* (2020) 20(5):e41. doi: 10.4110/in.2020.20.e41

18. He Y, Li J, Jiang S. A single amino acid substitution (R441a) in the receptor-binding domain of sars coronavirus spike protein disrupts the antigenic structure and binding activity. *Biochem Biophys Res Commun* (2006) 344(1):106–13. doi: 10.1016/j.bbrc.2006.03.139

19. Jhun H, Park HY, Hisham Y, Song CS, Kim S. Sars-Cov-2 delta (B.1.617.2) variant: A unique T478k mutation in receptor binding motif (Rbm) of spike gene. *Immune Netw* (2021) 21(5):e32. doi: 10.4110/in.2021.21.e32

20. Aleem A, Akbar Samad AB, Slenker AK. Emerging variants of sars-Cov-2 and novel therapeutics against coronavirus (Covid-19). In: *Statpearls*. FL: Treasure Island (2022).

21. Kim C, Ryu DK, Lee J, Kim YI, Seo JM, Kim YG, et al. A therapeutic neutralizing antibody targeting receptor binding domain of sars-Cov-2 spike protein. *Nat Commun* (2021) 12(1):288. doi: 10.1038/s41467-020-20602-5

22. Taylor PC, Adams AC, Hufford MM, de la Torre I, Winthrop K, Gottlieb RL. Neutralizing monoclonal antibodies for treatment of covid-19. *Nat Rev Immunol* (2021) 21(6):382–93. doi: 10.1038/s41577-021-00542-x

23. Doerfler W. Adenoviral vector DNA- and sars-Cov-2 mrna-based covid-19 vaccines: Possible integration into the human genome - are adenoviral genes expressed in vector-based vaccines? *Virus Res* (2021) 302:198466. doi: 10.1016/j.virusres.2021.198466

24. Ita K. Coronavirus disease (Covid-19): Current status and prospects for drug and vaccine development. *Arch Med Res* (2021) 52(1):15–24. doi: 10.1016/j.arcmed.2020.09.010

25. Pollet J, Chen WH, Strych U. Recombinant protein vaccines, a proven approach against coronavirus pandemics. *Adv Drug Delivery Rev* (2021) 170:71–82. doi: 10.1016/j.addr.2021.01.001

26. Francis MJ. Recent advances in vaccine technologies. *Vet Clin North Am Small Anim Pract* (2018) 48(2):231–41. doi: 10.1016/j.cvsm.2017.10.002

27. Sell S. How vaccines work: Immune effector mechanisms and designer vaccines. *Expert Rev Vaccines* (2019) 18(10):993–1015. doi: 10.1080/14760584.2019.1674144

28. Schiller JT, Lowy DR. Raising expectations for subunit vaccine. *J Infect Dis* (2015) 211(9):1373–5. doi: 10.1093/infdis/jiu648

29. Hansson M, Nygren PA, Stahl S. Design and production of recombinant subunit vaccines. *Biotechnol Appl Biochem* (2000) 32(2):95–107. doi: 10.1042/ba20000034

30. Mazur NI, Terstappen J, Baral R, Bardaji A, Beutels P, Buchholz UJ, et al. Respiratory syncytial virus prevention within reach: The vaccine and monoclonal antibody landscape. *Lancet Infect Dis* (2022) 23(1):e2–e21. doi: 10.1016/S1473-3099(22)00291-2

31. Cid R, Bolivar J. Platforms for production of protein-based vaccines: From classical to next-generation strategies. *Biomolecules* (2021) 11(8):1072. doi: 10.3390/biom11081072

32. Baden LR, El Sahly HM, Essink B, Kotloff K, Frey S, Novak R, et al. Efficacy and safety of the mrna-1273 sars-Cov-2 vaccine. *N Engl J Med* (2021) 384(5):403–16. doi: 10.1056/NEJMoa2035389

33. Vitiello A, Ferrara F, Troiano V, La Porta R. Covid-19 vaccines and decreased transmission of sars-Cov-2. *Inflammopharmacology* (2021) 29(5):1357–60. doi: 10.1007/s10787-021-00847-2

34. Cervantes-Torres J, Rosales-Mendoza S, Cabello C, Montero L, Hernandez-Aceves J, Granados G, et al. Towards the development of an epitope-focused vaccine for sars-Cov-2. *Vaccine* (2022) 40(45):6489–98. doi: 10.1016/j.vaccine.2022.09.059

35. Jiang RD, Liu MQ, Chen Y, Shan C, Zhou YW, Shen XR, et al. Pathogenesis of sars-Cov-2 in transgenic mice expressing human angiotensin-converting enzyme 2. *Cell* (2020) 182(1):50–8.e8. doi: 10.1016/j.cell.2020.05.027

36. Choi JD, Bae SY, Hong JW, Azam T, Dinarello CA, Her E, et al. Identification of the most active interleukin-32 isoform. *Immunology* (2009) 126(4):535–42. doi: 10.1111/j.1365-2567.2008.02917.x

37. Zhang M, Wu C. The relationship between intestinal goblet cells and the immune response. *Biosci Rep* (2020) 40(10). doi: 10.1042/BSR20201471

38. Knoll MD, Wonodi C. Oxford-Astrazeneca covid-19 vaccine efficacy. *Lancet* (2021) 397(10269):72–4. doi: 10.1016/S0140-6736(20)32623-4

39. Levine-Tiefenbrun M, Yelin I, Katz R, Herzel E, Golan Z, Schreiber L, et al. Initial report of decreased sars-Cov-2 viral load after inoculation with the Bnt162b2 vaccine. *Nat Med* (2021) 27(5):790–2. doi: 10.1038/s41591-021-01316-7

40. Sadoff J, Le Gars M, Shukarev G, Heerwegh D, Truyers C, de Groot AM, et al. Interim results of a phase 1-2a trial of Ad26.Cov2.S covid-19 vaccine. *N Engl J Med* (2021) 384(19):1824–35. doi: 10.1056/NEJMoa2034201

41. Voysey M, Clemens SAC, Madhi SA, Weckx LY, Folegatti PM, Aley PK, et al. Safety and efficacy of the Chadox1 ncov-19 vaccine (Azd1222) against sars-Cov-2: An interim analysis of four randomised controlled trials in Brazil, south Africa, and the uk. *Lancet* (2021) 397(10269):99–111. doi: 10.1016/S0140-6736(20)32661-1

42. Lurie N, Saville M, Hatchett R, Halton J. Developing covid-19 vaccines at pandemic speed. *N Engl J Med* (2020) 382(21):1969–73. doi: 10.1056/NEJMp2005630

43. Chen Y, Guo Y, Pan Y, Zhao ZJ. Structure analysis of the receptor binding of 2019-ncov. *Biochem Biophys Res Commun* (2020) 525(1):135–140. doi: 10.1016/j.bbrc.2020.02.071

44. Wrapp D, Wang N, Corbett KS, Goldsmith JA, Hsieh CL, Abiona O, et al. Cryo-em structure of the 2019-ncov spike in the prefusion conformation. *Science* (2020) 367 (6483):1260–3. doi: 10.1126/science.abb2507

45. Hisham Y, Ashhab Y, Hwang SH, Kim DE. Identification of highly conserved sars-Cov-2 antigenic epitopes with wide coverage using reverse vaccinology approach. *Viruses* (2021) 13(5):787. doi: 10.3390/v13050787

46. Yarmarkovich M, Warrington JM, Farrel A, Maris JM. Identification of sars-Cov-2 vaccine epitopes predicted to induce long-term population-scale immunity. *Cell Rep Med* (2020) 1(3):100036. doi: 10.1016/j.xcrm.2020.100036

frontiers | Frontiers in Immunology

TYPE Brief Research Report
PUBLISHED 04 April 2023
DOI 10.3389/fimmu.2023.1110874

OPEN ACCESS

EDITED BY
Fabrice Cognasse,
INSERM U1059 SAnté INgéniérie BIOlogie, France

REVIEWED BY
Parizad Torabi-Parizi,
NIH, United States
Insoo Kang,
Yale University, United States

*CORRESPONDENCE
Hyun Mu Shin
hyunmu.shin@snu.ac.kr
Hang-Rae Kim
hangrae2@snu.ac.kr
Wan Beom Park
wbpark1@snu.ac.kr

†These authors have contributed equally to this work and share first authorship

‡These authors have contributed equally to this work and share senior authorship

SPECIALTY SECTION
This article was submitted to Inflammation, a section of the journal Frontiers in Immunology

RECEIVED 29 November 2022
ACCEPTED 27 March 2023
PUBLISHED 04 April 2023

CITATION
Lee CM, Kim M, Kang CK, Choe PG, Kim NJ, Bang H, Cho T, Shin HM, Kim H-R, Park WB and Oh M-d (2023) Different degree of cytokinemia and T-cell activation according to serum IL-6 levels in critical COVID-19. *Front. Immunol.* 14:1110874. doi: 10.3389/fimmu.2023.1110874

Different degree of cytokinemia and T-cell activation according to serum IL-6 levels in critical COVID-19

Chan Mi Lee[1†], Minji Kim[2,3,4†], Chang Kyung Kang[1], Pyoeng Gyun Choe[1], Nam Joong Kim[1], Hyeeun Bang[5], Taeeun Cho[5], Hyun Mu Shin[2,4,6*‡], Hang-Rae Kim[2,3,4,6,7*‡], Wan Beom Park[1*‡] and Myoung-don Oh[1]

[1]Department of Internal Medicine, Seoul National University College of Medicine, Seoul, Republic of Korea, [2]Department of Biomedical Sciences, Seoul National University College of Medicine, Seoul, Republic of Korea, [3]Department of Anatomy & Cell Biology and Biomedical Sciences, Seoul National University College of Medicine, Seoul, Republic of Korea, [4]BK21 FOUR Biomedical Science Project, Seoul National University College of Medicine, Seoul, Republic of Korea, [5]Research and development team 2, Molecular Diagnostics Division, Quantamatrix Inc., Seoul, Republic of Korea, [6]Wide River Institute of Immunology, Seoul National University, Hongcheon, Republic of Korea, [7]Medical Research Institute, Seoul National University College of Medicine, Seoul, Republic of Korea

Introduction: Tocilizumab, a humanized anti-interleukin-6 receptor (IL-6R) antibody, is recommended for the treatment of severe to critical coronavirus diseases 2019 (COVID-19). However, there were conflicting results on the efficacy of tocilizumab. Therefore, we hypothesized that the differences in tocilizumab efficacy may stem from the different immune responses of critical COVID-19 patients. In this study, we described two groups of immunologically distinct COVID-19 patients, based on their IL-6 response.

Methods: We prospectively enrolled critical COVID-19 patients, requiring oxygen support with a high flow nasal cannula or a mechanical ventilator, and analyzed their serial samples. An enzyme-linked immunosorbent assay and flow cytometry were used to evaluate the cytokine kinetics and cellular immune responses, respectively.

Results: A total of nine patients with critical COVID-19 were included. The high (n = 5) and low IL-6 (n = 4) groups were distinguished by their peak serum IL-6 levels, using 400 pg/mL as the cut-off value. Although the difference of flow cytometric data did not reach the level of statistical significance, the levels of pro-inflammatory cytokines and the frequencies of intermediate monocytes ($CD14^+CD16^+$), IFN-γ^+ $CD4^+$ or $CD8^+$ T cells, and HLA-$DR^+PD\text{-}1^+$ $CD4^+$ T cells were higher in the high IL-6 group than in the low IL-6 group.

Conclusion: There were distinctive two groups of critical COVID-19 according to serum IL-6 levels having different degrees of cytokinemia and T-cell responses. Our results indicate that the use of immune modulators should be more tailored in patients with critical COVID-19.

KEYWORDS

immune response, cytokine, IL-6, T cell, critical COVID-19

Introduction

About 5% of patients with coronavirus disease 2019 (COVID-19) experience critical illness, characterized by respiratory failure, septic shock, and multiorgan failure (1, 2). T-cell hyperactivation (3), cytokine storm (4), and expansion of monocyte subpopulation (5) have been suggested as typical immunological features of severe COVID-19; thus immune modulators such as corticosteroid, baricitinib, or tocilizumab are used for the treatment of severe to critical COVID-19 (6).

Although the National Institutes of Health guidelines recommend the use of tocilizumab, a humanized monoclonal antibody against the interleukin-6 receptor (IL-6R), for the treatment of critical COVID-19 (7), there have been conflicting results relating to the efficacy of this drug (8–10). This raises the question of whether patients with critical COVID-19 differ in their immune responses. If different immunopathologies, rather than viral pathological mechanisms, contribute to disease severity in patients with critical COVID-19, more tailored anti-inflammatory strategies could be pursued. Therefore, we aimed to describe and classify immune responses especially according to IL-6 response, among patients with critical COVID-19.

Method

Study population and design

In this study, adult (≥ 18 years old) patients with critical acute respiratory syndrome coronavirus 2 (SARS-CoV-2) infection, hospitalized to the Seoul National University Hospital between August to December 2021, were prospectively enrolled. All SARS-CoV-2 infection was laboratory-confirmed by quantitative real-time reverse transcription polymerase chain reaction (qRT-PCR). Critical COVID-19 was defined as patients requiring respiratory support such as high flow nasal cannula (HFNC) oxygen therapy or mechanical ventilation.

Serial blood and nasopharyngeal swab samples were collected around the onset of critical illness. Clinical data, including demographics, underlying comorbidities, COVID-19 vaccination status, disease severity, COVID-19 specific treatment, duration of isolation, and clinical outcome were collected. The levels of C-reactive protein (CRP) were also retrospectively collected.

This study was approved by the Institutional Review Board (IRB) of Seoul National University Hospital (IRB no. 2104-181-1215). All participants provided written informed consent in accordance with the Declaration of Helsinki.

Measurement of anti-S1 immunoglobulin G

Serum anti-SARS-CoV-2 S1 domain (*i.e.*, S1) immunoglobulin (Ig) G titers were semi-quantitatively measured using the anti-SARS-CoV-2 enzyme-linked immunosorbent assay (ELISA) IgG kit (Euroimmun, Lübeck, Germany), according to the manufacturer's instructions. The optical density ($O.D._{450\ nm}$) ratios were interpreted as follows: ≥ 1.1, positive; ≥ 0.8 to < 1.1, borderline; < 0.8, negative.

Quantification of serum cytokines

The levels of IL-6, monocyte chemoattractant protein (MCP)-1, interferon-gamma (IFN-γ), and tumor necrosis factor-alpha (TNF-α) were measured in serum samples using the Human IL-6 ELISA Kit II (#550799, BD Biosciences, San Jose, CA, USA), Human MCP-1 ELISA Kit (#559017, BD Biosciences), Human IFN-γ Quantikine ELISA Kit (R&D Systems, Inc., Minneapolis, MN, USA), and Human TNF ELISA Kit (#550610, BD Biosciences) respectively, according to the manufacturer's instruction.

A previous study set the threshold of IL-6 > 406 pg/mL for predicting intensive care unit (ICU) mortality of COVID-19 patients (11). Therefore, in our study, patients were classified as the high IL-6 group if their peak IL-6 levels were over 400 pg/mL; otherwise, they were classified as the low IL-6 group.

Detection of SARS-CoV-2 RNA using qRT-PCR

Viral RNA was extracted from nasopharyngeal swab samples using the QIAamp Viral RNA Mini kit (Qiagen, Hilden, Germany), according to the manufacturer's instructions. Briefly, 140 μL of nasopharyngeal swabs was mixed with 560 μL of lysis buffer and incubated for 10 min at 37°C. The supernatant containing the viral RNA was purified, and the extracted RNA was eluted in 50 μL of

elution buffer and stored at –70°C until use. qRT-PCR for detection of SARS-CoV-2 was performed using the QPLEX™ COVID-19 Test (QMCOVID02, QuantaMatrix Inc., Seoul, Republic of Korea). A 20 µL of PCR mixture contained 10 µL of 2× One-step Premix, 5 µL of Oligo Mix, 5 µL of extracted RNA, and primer and probe sequences targeting the *RdRp* gene of SARS-CoV-2. Thermal cycling was performed at 25°C for 10 min for the uracil-DNA glycosylase incubation step, at 52°C for 5 min for the reverse transcription step, followed by 95°C for 10 sec, 5 cycles of pre-amplification (95°C for 10 sec and 55°C for 30 sec), and 35 cycles of the PCR reaction (95°C for 10 sec and 55°C for 30 sec) using the CFX-96 *In Vitro* Diagnostics Real-Time PCR System (Bio-Rad Laboratories, Inc., Hercules, CA, USA). A cycle threshold (Ct) value higher than 32 was defined as negative.

Peripheral blood mononuclear cells isolation

Human peripheral blood mononuclear cells (PBMCs) were isolated from heparinized blood by Ficoll–Plaque PLUS (1.077 g/mL; GE Healthcare Life Sciences, Piscataway, NJ, USA) density gradient centrifugation. Purified PBMCs were cryopreserved in 50% fetal bovine serum (FBS), 10% dimethyl sulfoxide, and 40% RPMI-1640 (all reagents from Thermo Fisher Scientific, Waltham, MA, USA) at 5×10^6 cells/mL and thawed prior to use (12).

Flow cytometric analysis

After thawing the PBMCs, cells were pelleted by centrifugation and resuspended in phosphate-buffered saline (pH 7.4) supplemented with 1% FBS at a final density of 1×10^7 cells/mL. Cells were stained using brilliant violet 711 (BV711)–anti-human CD3 (clone, UCHT1), brilliant ultra violet 805 (BUV805)–anti-human CD14 (clone, MØpq), and allophycocyanin-H7–anti-human CD16 (clone, 3G8) antibodies (Abs) (all from BD Biosciences). Brilliant Stain Buffer (BD Biosciences) was added to each sample.

For the staining of activation markers and cytokines, the PBMCs (at 1×10^7 cells/mL) were stimulated with 50 ng/mL of phorbol 12-myristate 13-acetate and 1 µg/mL of ionomycin (both reagents from Sigma-Aldrich, St. Louis, MO, USA) and then, 1 h later, treated with BD Golgistop™ (Monensin, BD Biosciences) for an additional 3 h. BV605–anti-human CD4 Ab (clone, OKT-4; Biolegend, San Diego, CA, USA) was applied concomitantly during stimulation. Stimulated cells were stained with BV711–anti-human CD3 (clone, UCHT1), BUV496–anti-human CD8 (clone, RPA-T8), BUV395–anti-human PD-1 (clone, MIH4), and phycoerythrin (PE)-cyanine-5–anti-human HLA-DR (clone, G46-6) Abs (all from BD Biosciences). After fixation and permeabilization with the Cytofix/Cytoperm kit (BD Biosciences), cells were incubated with the PE–anti-human IFN-γ Ab (clone, B27; BD Biosciences). Samples were acquired on a BD LSRII flow cytometer (BD Biosciences) and analyzed using FlowJo software version 10.7.1 (TreeStar, Ashland, OR, USA). The percentages of target cell populations in unstimulated specimens were subtracted from those in stimulated specimens (13).

Statistical analyses

The experimental data were presented as the median with interquartile range (IQR). The Mann–Whitney *U* test was used to compare continuous variables. Statistical analyses were conducted using SPSS Statistics, version 26.0 (IBM Corp., Armonk, NY, USA). *P*-values < 0.05 were considered as a measure of statistical significance. GraphPad Prism 9 (GraphPad Software, La Jolla, CA, USA) was used to generate graphs.

Results

Study participants and kinetics of serum SARS-CoV-2 antibody

A total of nine patients with critical COVID-19 were enrolled during the study period (Table 1). The high IL-6 group included five (55.6%) patients and the low IL-6 group included four (44.4%) patients (Table 1). Among the nine patients, seven patients (77.8%) were male and the median (range) age was 70 (58–84). All patients had multiple underlying comorbidities, such as hypertension (6/9, 66.7%) or diabetes mellitus (5/9, 55.6%) and were fully vaccinated with the AZD1222 (5/9, 55.6%) or BNT162b2 (4/9, 44.4%); the diagnosis of COVID-19 was made more than 14 days after their second vaccine dose (14). All patients were treated with remdesivir and steroids, and four (44.4%) patients were treated with tocilizumab. Two (2/5, 40%) patients from the high IL-6 group and one (1/4, 25%) patients from the low IL-6 group required mechanical ventilation, although all patients enrolled in this study made a full recovery.

The kinetics of viral load, the anti-S1 IgG and CRP levels, and the use of immune modulators in the high and low IL-6 groups are presented in Supplementary Figure S1A, B, respectively. The day of HFNC oxygen therapy initiation was designated as day 0. We found that the viral load decreased with time and all patients acquired anti-S1 IgG during their clinical course. In most patients, the level of CRP peaked near the onset of critical illness. Serial serum samples were used to evaluate cytokine levels and representative PBMC samples were used for the characterization of the cellular immune response.

Cytokine levels and kinetics vary according to IL-6 response

The levels of cytokines (IL-6, MCP-1, IFN-γ, and TNF-α) and CRP according to the groups are shown in Figures 1A, B, respectively. The cytokine levels measured within 0–5 days of initiating high flow nasal cannula oxygen therapy, at the closest point to the onset of critical illness, have been presented. The specific time point during the clinical course is indicated with pink arrows in Supplementary Figure S1A, B, allowing for a

TABLE 1 Clinical information of study participants.

IL-6 Group	Pt #	Age	Sex	Underlying disease	Vaccine status	Vaccine type	Severity of COVID-19	Treatment for COVID-19	Days of isolation	Outcome
High	1	76	Female	HTN, DM, DL	Fully vaccinated	BNT162b2	High flow	Remdesivir Steroid	17	Recovery
High	2	58	Male	LC, DM	Fully vaccinated	BNT162b2	Mechanical ventilator	Remdesivir Steroid Tocilizumab	18	Recovery
High	3	79	Female	Atrial fibrillation, aortic stenosis	Fully vaccinated	BNT162b2	Mechanical ventilator	Remdesivir Steroid Tocilizumab	30	Recovery
High	4	63	Male	HTN, DM	Fully vaccinated	AZD1222	High flow	Remdesivir Steroid Baricitinib	20	Recovery
High	5	68	Male	DM, HTN, DL	Fully vaccinated	AZD1222	High flow	Remdesivir Steroid Tocilizumab	21	Recovery
Low	6	60	Male	Angina, HTN, DL	Fully vaccinated	AZD1222	High flow	Remdesivir Steroid Baricitinib	10	Recovery
Low	7	84	Male	HTN, BPH	Fully vaccinated	BNT162b2	Mechanical ventilator	Remdesivir Steroid Tocilizumab	25	Recovery
Low	8	65	Male	HTN, DM, peripheral artery disease	Fully vaccinated	AZD1222	High flow	Remdesivir Steroid Baricitinib	7	Recovery
Low	9	70	Male	Chronic DVT	Fully vaccinated	AZD1222	High flow	Remdesivir Steroid Baricitinib	11	Recovery

IL-6, interleukin-6; HTN, hypertension; DM, diabetes mellitus; DL, dyslipidemia; LC, liver cirrhosis; BPH, benign prostate hyperplasia; DVT, deep vein thrombosis.
Fully vaccinated refers to individuals who were diagnosed with COVID-19 more than 14 days after their second COVID-19 vaccine dose.

simultaneous evaluation with the administration of immune modulators. The levels of IL-6 and IFN-γ were significantly higher in the high IL-6 group than in the low IL-6 group (median [IQR], 419 pg/mL [283–710] vs. 63 pg/mL [11–107], $P = 0.016$; 6.11 pg/mL [4.84–12.04] vs. 1.16 pg/mL [0.00–2.56], $P = 0.016$, respectively). While not statistically significant, the levels of MCP-1 and CRP were also higher in the high IL-6 group than in the low IL-6 group (median [IQR], 6,700 pg/mL [2,535–8,417] vs. 1,492 pg/mL [615–1,684], $P = 0.111$; 9.49 mg/dL [5.69–27.61] vs. 5.49 mg/dL [3.60–8.40], $P = 0.191$, respectively). The levels of TNF-α did not show significant difference between the high and low IL-6 groups (median [IQR], 0.08 pg/mL [0.00–27.53] vs. 1.36 pg/mL [0.32–41.89], $P = 0.714$).

The kinetics of cytokine levels in individual patients are presented in Supplementary Figure S1C, according to the days from critical illness. Overall, the low IL-6 group had lower levels of IL-6, MCP-1, and IFN-γ than the high IL-6 group.

Monocyte subpopulation and cellular immune response against SARS-CoV-2

To provide a temporal context for the flow cytometric analysis samples in relation to the clinical course and immune modulator treatment, we marked the respective time points with green arrows in Supplementary Figure S1A, B. The high IL-6 group showed a higher frequency of intermediate monocytes (CD14+CD16+) compared to the low IL-6 group, although the difference was not statistically significant (%, median [IQR], 1.51 [0.59–11.20] vs. 1.24 [0.82–1.88], $P = 0.730$; Figure 2A). On the other hand, the high IL-6 group had higher frequencies of IFN-γ+ in CD4+ and CD8+ T cells compared to the low IL-6 group (%, median [IQR], 7.07 [3.12–13.35] vs. 5.09 [2.24–10.73], $P = 0.730$; 23.6 [13.6–59.8] vs. 22.7 [9.7–30.5], $P = 0.730$; Figure 2B).

Regarding activated T cells based on the expression of HLA-DR and PD-1, the high IL-6 group had a slightly higher proportion of HLA-DR+PD-1+ CD4+ T cells compared to the low IL-6 group, although the difference was not statistically significant (%, median [IQR], 0.27 [0.08–0.49] vs. 0.25 [0.12–0.27], $P = 0.492$). In contrast, the high IL-6 group had a lower proportion of HLA-DR+PD-1+ CD8 + T cells compared to the low IL-6 group, but the difference was not statistically significant either (%, median [IQR], 0.18 [0.09–0.33] vs. 0.25 [0.08–0.43], $P = 0.730$; Figure 2C). The flow cytometric data from all samples are presented in Supplementary Figure S2.

Discussion

In this study, we found that patients with critical COVID-19 can be classified by two distinctive groups in terms of cytokinemia

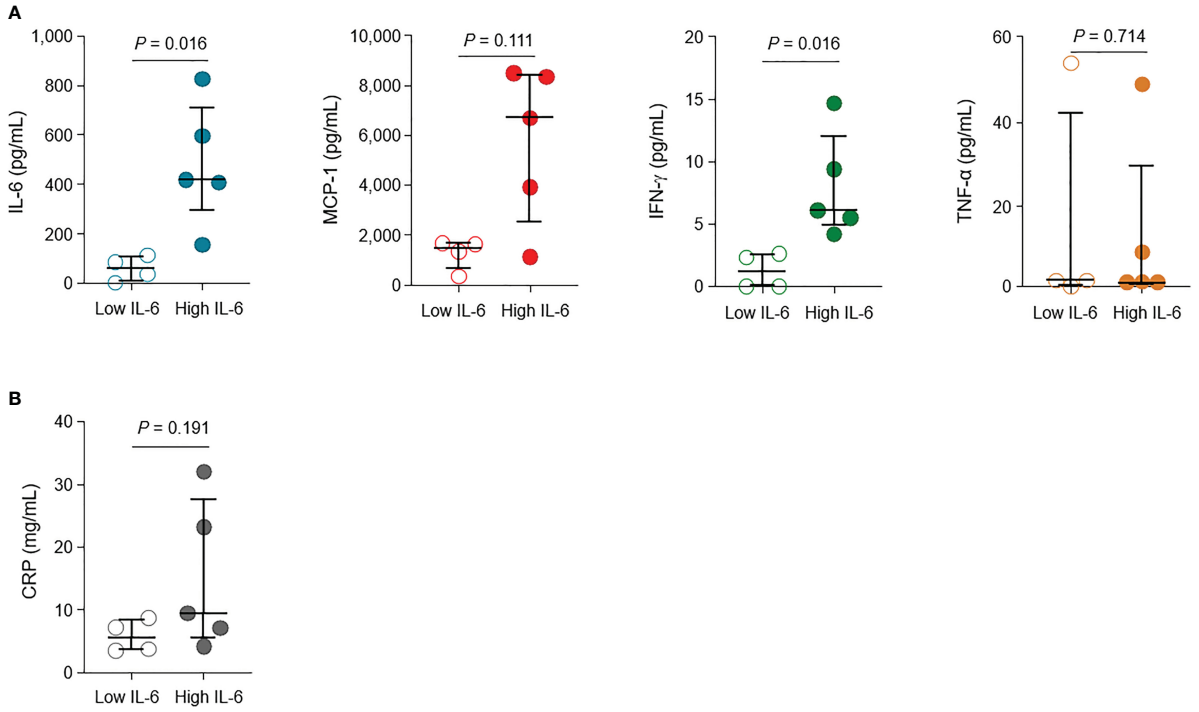

FIGURE 1
Levels of cytokines and inflammatory marker in patients with critical COVID-19. **(A)** The levels of interleukin (IL)-6, monocyte chemoattractant protein (MCP)-1, interferon (IFN)-γ, and tumor necrosis factor (TNF)-α in the high IL-6 (n = 5) and low IL-6 (n = 4) groups. **(B)** Levels of C-reactive protein (CRP) in the high IL-6 and low IL-6 groups. Vertical and horizontal lines indicate the median with the interquartile range. The cytokine and CRP levels at the closest point to the onset of critical illness (within 0–5 days of high flow nasal cannula oxygen therapy initiation) are shown.

and T-cell activation levels, according to their levels of serum IL-6. The high IL-6 group had higher levels of pro-inflammatory cytokines and cellular immune responses than the low IL-6 group. The hypercytokinemia and T-cell hyperactivation of the high IL-6 group suggest that immunological features could differ among patients with critical COVID-19, despite similar clinical characteristics.

Since IL-6 is considered as an important immunological factor in severe/critical COVID-19 (15, 16), clinical trials of tocilizumab for the treatment of severe COVID-19 have been conducted. For instance, the RECOVERY trial found that tocilizumab improved the clinical outcomes of COVID-19 patients with hypoxia (oxygen saturation < 92%) and CRP levels ≥ 7.5 mg/dL (17). However, other studies did not show the efficacy of tocilizumab in patients with severe COVID-19 (9, 10). One retrospective study also reported that the early use of tocilizumab was associated with improvement of oxygenation in patients with high IL-6 levels (18). These conflicting results led us to perform the present study, to elucidate whether certain immunological features, and especially the IL-6 response, differed among patients with critical COVID-19.

Results from the early phase of SARS-CoV-2 pandemic suggested that the host immune response, such as levels of cytokinemia, might play an important role in the pathogenesis of severe COVID-19 (19). For instance, the plasma levels of several cytokines, including MCP-1 and TNF-α, were shown to be higher in ICU than non-ICU COVID-19 patients (16). Another study demonstrated that the levels of several cytokines (e.g., IL-6, IL-10, and MCP-1) positively correlated with COVID-19 severity; moreover, MCP-1 was correlated with days on mechanical ventilation (20). A previous study has shown that increased levels of IL-6 are strongly associated with disease severity at admission and the need for ICU care in COVID-19 patients, regardless of age (21). In our present study, we aimed to demonstrate that cytokine levels could vary significantly among critically ill COVID-19 patients, using serum IL-6 levels as a surrogate marker. Our findings suggest that IL-6 could be an important marker for classifying COVID-19 patients, even after the general population has been vaccinated, as all patients in our study were vaccinated.

In addition, we detected higher frequencies of intermediate monocytes ($CD14^+CD16^+$) in the high IL-6 group than in the low IL-6 group. Intermediate monocytes expand in patients with systemic infection and secrete cytokines, such as TNF-α, IL-1β, and IL-6, implying their role in pathogen defense (22). A previous study suggested that $CD14^+CD16^+$ monocytes may exhibit dysregulated production of IL-6 (23). Another study also reported that monocyte-mediated hypercytokinemia is prominent in critical COVID-19 (24). Moreover, the frequencies of intermediate monocytes were higher in COVID-19 patients admitted to ICU (5). The higher levels of cytokines in the high IL-6 group might therefore correlate with the higher frequency of intermediate monocytes.

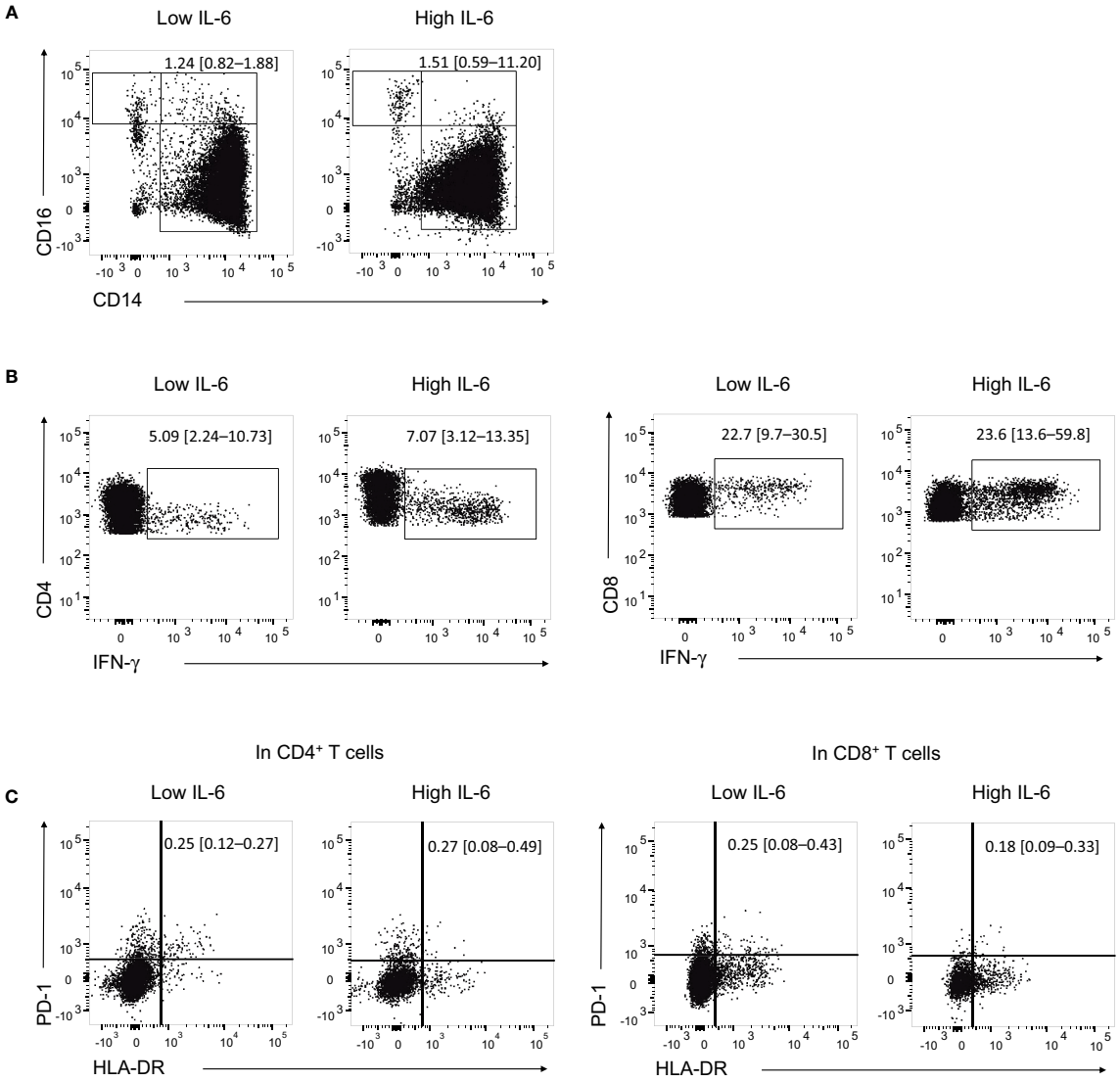

FIGURE 2
Proportion of monocyte subpopulation and expression levels of cytokine and activation markers in T cells. **(A)** Representative flow cytometry dot plots showing the identification of intermediate monocytes ($CD14^+CD16^+$) in the high IL-6 (n = 5) and low IL-6 (n = 4) groups. **(B)** Representative flow cytometry dot plots showing the identification of IFN-γ^+ $CD4^+$ T cells and $CD8^+$ T cells in the high IL-6 and low IL-6 groups. **(C)** Representative flow cytometry dot plots showing the identification of HLA-$DR^+PD\text{-}1^+$ $CD4^+$ T cells and $CD8^+$ T cells in the high IL-6 and low IL-6 groups. Numbers indicate population frequencies as the median with interquartile range.

We showed that the high IL-6 group exhibited stronger cellular immune responses than the low IL-6 group, based on the expression of cytokines and T-cell activation markers. Although T-cell hyperactivation is a key immunological feature of severe COVID-19 (3, 25), the results of the present study suggest that the magnitude of T-cell responses could vary even in clinically similar critical COVID-19. Corticosteroid might attenuate T-cell responses as well as cytokinemia in critical COVID-19, however, we could find distinctive two groups of critical COVID-19 in this study.

In conclusion, we identified that patients with critical COVID-19 could be divided into two groups with different degrees of cytokinemia and T-cell responses, according to their serum IL-6 levels. Our results suggest that a more tailored use of immune modulators should be sought in the treatment of critical COVID-19.

Data availability statement

The original contributions presented in the study are included in the article/Supplementary Material. Further inquiries can be directed to the corresponding authors.

Ethics statement

The studies involving human participants were reviewed and approved by the Institutional Review Board (IRB) of Seoul National University Hospital. The patients/participants provided their written informed consent to participate in this study.

Author contributions

CL, MK, CK, HS, H-RK, and WP conceived and designed the study. CL, CK, PC, NK, WP, and M-DO collected the samples. CL, MK, CK, HB, TC, HS, H-RK, and WP performed data analysis. NK, HS, H-RK, WP, and M-DO revised and edited the final manuscript. All authors contributed to the article and approved the submitted version.

Funding

This work was supported by the New Faculty Startup Fund from Seoul National University (to WP), the Bio and Medical Technology Development Program of the National Research Foundation (NF) and funded by the Korean government (MSIT) (2021M3A9I2080496 to H-RK and WP; 2018M3A9H4055197 to H-RK), and the Creative-Pioneering Researchers Program through Seoul National University (to H-RK).

Conflict of interest

Author HB and TC are employed by QuantaMatrix.

The remaining authors declare that the research was conducted in the absence of any commercial or financial relationships that could be construed as a potential conflict of interest.

Publisher's note

All claims expressed in this article are solely those of the authors and do not necessarily represent those of their affiliated organizations, or those of the publisher, the editors and the reviewers. Any product that may be evaluated in this article, or claim that may be made by its manufacturer, is not guaranteed or endorsed by the publisher.

Supplementary material

The Supplementary Material for this article can be found online at: https://www.frontiersin.org/articles/10.3389/fimmu.2023.1110874/full#supplementary-material

References

1. Wu Z, McGoogan JM. Characteristics of and important lessons from the coronavirus disease 2019 (COVID-19) outbreak in China: Summary of a report of 72314 cases from the Chinese center for disease control and prevention. *JAMA* (2020) 323(13):1239–42. doi: 10.1001/jama.2020.2648

2. Petrilli CM, Jones SA, Yang J, Rajagopalan H, O'Donnell L, Chernyak Y, et al. Factors associated with hospital admission and critical illness among 5279 people with coronavirus disease 2019 in new York city: prospective cohort study. *BMJ* (2020) 369: m1966. doi: 10.1136/bmj.m1966

3. Kang CK, Han GC, Kim M, Kim G, Shin HM, Song KH, et al. Aberrant hyperactivation of cytotoxic T-cell as a potential determinant of COVID-19 severity. *Int J Infect Dis* (2020) 97:313–21. doi: 10.1016/j.ijid.2020.05.106

4. Chen R, Lan Z, Ye J, Pang L, Liu Y, Wu W, et al. Cytokine storm: The primary determinant for the pathophysiological evolution of COVID-19 deterioration. *Front Immunol* (2021) 12:589095. doi: 10.3389/fimmu.2021.589095

5. Zhou Y, Fu B, Zheng X, Wang D, Zhao C, Qi Y, et al. Pathogenic T-cells and inflammatory monocytes incite inflammatory storms in severe COVID-19 patients. *Natl Sci Rev* (2020) 7(6):998–1002. doi: 10.1093/nsr/nwaa041

6. Bhimraj A, Morgan RL, Shumaker AH, Baden L, Cheng VCC, Edwards KM, et al. Infectious diseases society of America guidelines on the treatment and management of patients with COVID-19. *Clin Infect Dis* (2022), ciac724. doi: 10.1093/cid/ciac724

7. COVID-19 Treatment Guidelines Panel. *Coronavirus Disease 2019 (COVID-19) Treatment Guidelines*. Bethesda, MD: National Institutes of Health (2022). Available at: https://www.covid19treatmentguidelines.nih.gov/. Accessed 20 November 2022.

8. Investigators R-C, Gordon AC, Mouncey PR, Al-Beidh F, Rowan KM, Nichol AD, et al. Interleukin-6 receptor antagonists in critically ill patients with covid-19. *N Engl J Med* (2021) 384(16):1491–502. doi: 10.1056/NEJMoa2100433

9. Stone JH, Frigault MJ, Serling-Boyd NJ, Fernandes AD, Harvey L, Foulkes AS, et al. Efficacy of tocilizumab in patients hospitalized with covid-19. *N Engl J Med* (2020) 383(24):2333–44. doi: 10.1056/NEJMoa2028836

10. Rosas IO, Brau N, Waters M, Go RC, Hunter BD, Bhagani S, et al. Tocilizumab in hospitalized patients with severe covid-19 pneumonia. *N Engl J Med* (2021) 384 (16):1503–16. doi: 10.1056/NEJMoa2028700

11. Gorham J, Moreau A, Corazza F, Peluso L, Ponthieux F, Talamonti M, et al. Interleukine-6 in critically ill COVID-19 patients: A retrospective analysis. *PloS One* (2020) 15(12):e0244628. doi: 10.1371/journal.pone.0244628

12. Kim HR, Hong MS, Dan JM, Kang I. Altered IL-7Ralpha expression with aging and the potential implications of IL-7 therapy on CD8+ T-cell immune responses. *Blood* (2006) 107(7):2855–62. doi: 10.1182/blood-2005-09-3560

13. Kang CK, Kim HR, Song KH, Keam B, Choi SJ, Choe PG, et al. Cell-mediated immunogenicity of influenza vaccination in patients with cancer receiving immune checkpoint inhibitors. *J Infect Dis* (2020) 222(11):1902–9. doi: 10.1093/infdis/jiaa291

14. Abu-Raddad LJ, Chemaitelly H, Ayoub HH, Yassine HM, Benslimane FM, Al Khatib HA, et al. Association of prior SARS-CoV-2 infection with risk of breakthrough infection following mRNA vaccination in Qatar. *JAMA* (2021) 326(19):1930–9. doi: 10.1001/jama.2021.19623

15. Han H, Ma Q, Li C, Liu R, Zhao L, Wang W, et al. Profiling serum cytokines in COVID-19 patients reveals IL-6 and IL-10 are disease severity predictors. *Emerg Microbes Infect* (2020) 9(1):1123–30. doi: 10.1080/22221751.2020.1770129

16. Huang C, Wang Y, Li X, Ren L, Zhao J, Hu Y, et al. Clinical features of patients infected with 2019 novel coronavirus in wuhan, China. *Lancet* (2020) 395(10223):497–506. doi: 10.1016/S0140-6736(20)30183-5

17. Group RC. Tocilizumab in patients admitted to hospital with COVID-19 (RECOVERY): A randomised, controlled, open-label, platform trial. *Lancet* (2021) 397(10285):1637–45.

18. Galvan-Roman JM, Rodriguez-Garcia SC, Roy-Vallejo E, Marcos-Jimenez A, Sanchez-Alonso S, Fernandez-Diaz C, et al. IL-6 serum levels predict severity and response to tocilizumab in COVID-19: An observational study. *J Allergy Clin Immunol* (2021) 147(1):72–80 e8. doi: 10.1016/j.jaci.2020.09.018

19. Siddiqi HK, Mehra MR. COVID-19 illness in native and immunosuppressed states: A clinical-therapeutic staging proposal. *J Heart Lung Transplant.* (2020) 39 (5):405–7. doi: 10.1016/j.healun.2020.03.012

20. Ling L, Chen Z, Lui G, Wong CK, Wong WT, Ng RWY, et al. Longitudinal cytokine profile in patients with mild to critical COVID-19. *Front Immunol* (2021) 12:763292. doi: 10.3389/fimmu.2021.763292

21. Shin JJ, Jeon S, Unlu S, Par-Young J, Shin MS, Kuster JK, et al. A distinct association of inflammatory molecules with outcomes of COVID-19 in younger versus older adults. *Clin Immunol* (2021) 232:108857. doi: 10.1016/j.clim.2021.108857

22. Kapellos TS, Bonaguro L, Gemund I, Reusch N, Saglam A, Hinkley ER, et al. Human monocyte subsets and phenotypes in major chronic inflammatory diseases. *Front Immunol* (2019) 10:2035. doi: 10.3389/fimmu.2019.02035

23. Kong BS, Kim Y, Kim GY, Hyun JW, Kim SH, Jeong A, et al. Increased frequency of IL-6-producing non-classical monocytes in neuromyelitis optica spectrum disorder. *J Neuroinflammation.* (2017) 14(1):191. doi: 10.1186/s12974-017-0961-z

24. Vanderbeke L, Van Mol P, Van Herck Y, De Smet F, Humblet-Baron S, Martinod K, et al. Monocyte-driven atypical cytokine storm and aberrant neutrophil activation as key mediators of COVID-19 disease severity. *Nat Commun* (2021) 12 (1):4117. doi: 10.1038/s41467-021-24360-w

25. Kalfaoglu B, Almeida-Santos J, Tye CA, Satou Y, Ono M. T-Cell hyperactivation and paralysis in severe COVID-19 infection revealed by single-cell analysis. *Front Immunol* (2020) 11:589380. doi: 10.3389/fimmu.2020.589380

frontiers | Frontiers in Immunology

TYPE Original Research
PUBLISHED 03 May 2023
DOI 10.3389/fimmu.2023.1085610

OPEN ACCESS

EDITED BY
Gilles Kaplanski,
Assistance Publique Hôpitaux de Marseille, France

REVIEWED BY
Caroline Subra,
Henry M Jackson Foundation for the Advancement of Military Medicine (HJF), United States
Shie-Liang Hsieh,
Academia Sinica, Taiwan
Laura Mathae,
Karolinska Institutet (KI), Sweden

*CORRESPONDENCE
Lucia Catani
lucia.catani@unibo.it

†These authors have contributed equally to this work and share first authorship

‡These authors have contributed equally to this work and share last authorship

RECEIVED 31 October 2022
ACCEPTED 11 April 2023
PUBLISHED 03 May 2023

CITATION
Forte D, Pellegrino RM, Trabanelli S, Tonetti T, Ricci F, Cenerenti M, Comai G, Tazzari P, Lazzarotto T, Buratta S, Urbanelli L, Narimanfar G, Alabed HBR, Mecucci C, La Manna G, Emiliani C, Jandus C, Ranieri VM, Cavo M, Catani L and Palandri F (2023) Circulating extracellular particles from severe COVID-19 patients show altered profiling and innate lymphoid cell-modulating ability. *Front. Immunol.* 14:1085610. doi: 10.3389/fimmu.2023.1085610

Circulating extracellular particles from severe COVID-19 patients show altered profiling and innate lymphoid cell-modulating ability

Dorian Forte[1†], Roberto Maria Pellegrino[2†], Sara Trabanelli[3,4†], Tommaso Tonetti[5,6], Francesca Ricci[7], Mara Cenerenti[3,4], Giorgia Comai[8], Pierluigi Tazzari[7], Tiziana Lazzarotto[5,9], Sandra Buratta[2], Lorena Urbanelli[2], Ghazal Narimanfar[1], Husam B. R. Alabed[2], Cristina Mecucci[10], Gaetano La Manna[8], Carla Emiliani[2], Camilla Jandus[3,4], Vito Marco Ranieri[5,6], Michele Cavo[1,11‡], Lucia Catani[1,11*‡] and Francesca Palandri[11‡]

[1]Department of Medical and Surgical Sciences (DIMEC), Institute of Hematology 'Seràgnoli', University of Bologna, Bologna, Italy, [2]Department of Chemistry, Biology and Biotechnology, Biochemistry and Molecular Biology Section, University of Perugia, Perugia, Italy, [3]Department of Pathology and Immunology, Faculty of Medicine, University of Geneva, Geneva, Switzerland, [4]Ludwig Institute for Cancer Research, Lausanne Branch, Lausanne, Switzerland, [5]Department of Medical and Surgical Sciences (DIMEC), University of Bologna, Bologna, Italy, [6]Anesthesia and Intensive Care Medicine, IRCCS Azienda Ospealiero-Universitaria di Bologna, Bologna, Italy, [7]Immunohematology and blood bank, IRCCS Azienda Ospedaliero-Universitaria di Bologna, Bologna, Italy, [8]Nephrology, Dialysis and Renal Transplant Unit, IRCCS Azienda Ospedaliero-Universitaria di Bologna, Bologna, Italy, [9]Microbiology Unit, IRCCS Azienda Ospedaliero-Universitaria di Bologna, Bologna, Italy, [10]Department of Medicine and Surgery, Center for Hemato-Oncology Research (C.R.E.O.), University of Perugia, Perugia, Italy, [11]Istituto di Ematologia "Seràgnoli", IRCCS Azienda Ospedaliero-Universitaria di Bologna, Bologna, Italy

Introduction: Extracellular vesicles (EVs) and particles (EPs) represent reliable biomarkers for disease detection. Their role in the inflammatory microenvironment of severe COVID-19 patients is not well determined. Here, we characterized the immunophenotype, the lipidomic cargo and the functional activity of circulating EPs from severe COVID-19 patients (Co-19-EPs) and healthy controls (HC-EPs) correlating the data with the clinical parameters including the partial pressure of oxygen to fraction of inspired oxygen ratio (PaO2/FiO2) and the sequential organ failure assessment (SOFA) score.

Methods: Peripheral blood (PB) was collected from COVID-19 patients (n=10) and HC (n=10). EPs were purified from platelet-poor plasma by size exclusion chromatography (SEC) and ultrafiltration. Plasma cytokines and EPs were characterized by multiplex bead-based assay. Quantitative lipidomic profiling of EPs was performed by liquid chromatography/mass spectrometry combined with quadrupole time-of-flight (LC/MS Q-TOF). Innate lymphoid cells (ILC) were characterized by flow cytometry after co-cultures with HC-EPs or Co-19-EPs.

Results: We observed that EPs from severe COVID-19 patients: 1) display an altered surface signature as assessed by multiplex protein analysis; 2) are characterized by distinct lipidomic profiling; 3) show correlations between lipidomic profiling and disease aggressiveness scores; 4) fail to dampen type 2

10.3389/fimmu.2023.1085610

innate lymphoid cells (ILC2) cytokine secretion. As a consequence, ILC2 from severe COVID-19 patients show a more activated phenotype due to the presence of Co-19-EPs.

Discussion: In summary, these data highlight that abnormal circulating EPs promote ILC2-driven inflammatory signals in severe COVID-19 patients and support further exploration to unravel the role of EPs (and EVs) in COVID-19 pathogenesis.

KEYWORDS

COVID-19, SARS-CoV-2, extracellular vesicles and particles, innate lymphoid cells, type 2 innate lymphoid cell, lipidomic

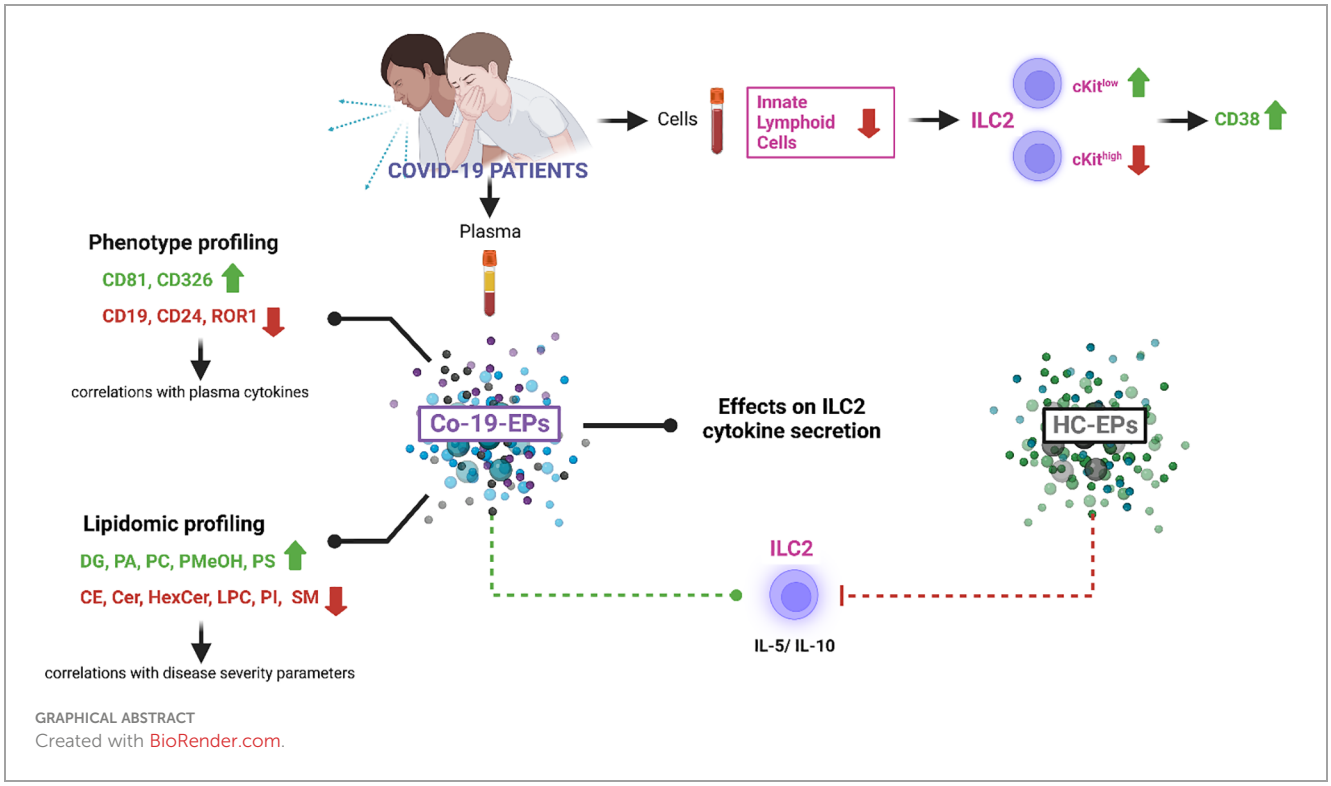

GRAPHICAL ABSTRACT
Created with BioRender.com.

Introduction

Coronavirus disease 2019 (COVID-19) is caused by Severe Acute Respiratory Syndrome Coronavirus 2 (SARS-CoV-2). Although most infected patients have mild to moderate symptoms or are even asymptomatic, older patients and those with pre-existing chronic diseases (e.g., hypertension, diabetes, obesity) are at greater risk of developing serious complications, such as pneumonia, cytokine storm and multiple organ failure (1, 2).

The critical production of (pro)inflammatory cytokines and chemokines detected during COVID-19 infection is mainly responsible for the broad and uncontrolled tissue damage observed in patients (3–11). Along with cytokine storm, immune dysregulation with quantitative abnormalities and impaired functional activity of innate and adaptive immune cells including innate lymphoid cells (ILC), monocytes/macrophages, dendritic cells, NK cells and T/B cells has been observed in COVID-19 patients (6, 12–14).

Specifically, ILC play a pivotal role in immune surveillance and form the front line of immune defense. Natural killer cells (NK), one of the ILC subsets belonging to the group 1 ILC (15), are known to perform lytic functions, instead ILC1, ILC2, and ILC3 subsets have mainly helper functions through secretion of Type 1, Type 2 and Type 17 cytokines, respectively (16, 17). In peripheral blood, an

additional subset of ILCs has been identified and named ILC precursor (ILCP) because of its ability to give rise, both *in vitro* and *in vivo*, to all ILC subsets (18). ILC are largely depleted from the circulation of COVID-19 patients (13, 19). The remaining circulating ILC reveal decreased frequencies of ILC2 in severe COVID-19, with a concomitant decrease of ILCP, as compared with HC. ILC2 and ILCP show an activated phenotype with increased CD69 expression which is positively correlated with the levels of IL-6 and IL-10, while frequencies of ILC subsets are correlated with clinical and biochemical laboratory parameters associated with disease severity (19, 20). However, the mechanism (s) leading to altered ILC activation and/or function in COVID-19 is yet to be determined.

Extracellular vesicles (EVs) are lipid bilayer structures with a key role within the inflammatory network. They are released from a broad variety of cells during homeostasis and cell activation with pleiotropic effects on cell-cell signaling, by transferring bioactive molecules into recipient cells or by regulating the downstream signal cascades of receptors on target cells. Based on size and biogenesis, small and large EVs can be identified. EVs contain functionally relevant biomolecules such as proteins, nucleic acids and lipids. They have been detected in various biological fluids including blood (21–23).

Recently, it has been described that EVs are involved in SARS-CoV-2 infection (24, 25). Circulating platelet-derived EVs have been described to be increased in COVID-19 patients (26–28). EVs may be also involved in 1) virus entry and spreading through the expression of the SARS-CoV-2 receptors angiotensin-converting enzyme (ACE)-2 (29) and CD9 (30, 31), 2) immune dysregulation, cytokine storm development and maintenance (30), 3) inflammation and thrombosis (32). In addition, a diagnostic (33) and prognostic (34, 35) role of EVs has been suggested.

In this work, considering the EV identity defined by MISEV 2018 (22) and their heterogeneity, we collectively referred to them as extracellular particles (EPs). To further understand the impact of EPs on COVID-19 infection, here we studied the lipid cargo/phenotype of EPs in COVID-19 patients and the functional activity of circulating EPs on ILC in severe COVID-19 patients as reported by the Graphical Abstract.

Materials and methods

Patients' characteristics

Ten COVID-19 patients, admitted to the Intensive Care Unit of the IRCCS Azienda Ospedaliero-Universitaria di Bologna, were enrolled in the study. Patients were diagnosed with COVID-19 using reverse-transcriptase polymerase chain reaction viral detection of oropharyngeal or nasopharyngeal swabs. We considered only critical patients for this study with respiratory failure and admitted to the intensive care unit with the need for mechanical ventilation.

Demographic and laboratory findings of all recruited COVID-19 patients are summarized in Table 1. In addition to age, sex, hospitalization duration, clinical outcome and date/timing of peripheral blood sample collection, patients were assessed for the presence or the absence of the following pre-existing medical condition: lung disease (asthma, chronic obstructive pulmonary disease (COPD)), heart disease (coronary artery disease, heart failure), peripheral vascular disease, hypertension, diabetes, obesity (BMI >30), kidney disease, autoimmune disorders, cancer, chemotherapy for cancer. Laboratory parameters at the time of sample collection were analyzed and the serum levels of ferritin, C-reactive protein, D-dimer, and lactate dehydrogenase were recorded for each patient as well as the number of white blood cells (WBC), platelets (PLT), hematocrit and hemoglobin.

Regarding COVID-19 disease severity parameters, the partial pressure of oxygen to fraction of inspired oxygen ratio (PaO_2/FiO_2) and the sequential organ failure assessment (SOFA) score were recorded. The use of specific COVID-19-targeted treatment has been also reported. Specimens from anonymous pre-screened healthy blood controls (HC; n=10), matched for sex and age, were collected from the blood donor center. This study was approved by the Ethics Committee of the IRCSS Azienda Ospedaliero-Universitaria di Bologna and written informed consent was obtained from all patients/controls enrolled in the study.

Blood sample collection and plasma preparation

Venous EDTA-blood was kept vertically at room temperature and processed within 1 hour. After the first centrifugation of 15 min 2,500 x g at room temperature, plasma was collected and subjected to second centrifugation of 15 min 2,500 x g at room temperature to obtain platelet-free plasma. Platelet-free plasma was then stored at -80°C until use.

EP isolation

Samples were defrosted at room temperature and EP isolation was achieved by size-exclusion chromatography (SEC; qEVoriginal/70 nm Gen 2 Column, Izon) following the manufacturer's instructions. In brief, the column was equilibrated with PBS before loading the sample (500 µl) on top of the column. Next, four fractions were collected after void volume. Then, where indicated, EP-enriched fractions were pooled for maximizing yield for downstream experiments using MWCO 30 kDa Amicon Ultra-2 Centrifugal Filters (Millipore, Merck, USA). Finally, all samples were used or stored at -80°C until use. The protein content of the EPs was determined using the Bradford assay according to the manufacturer's instructions.

10.3389/fimmu.2023.1085610

TABLE 1 Clinical and demographic characteristics of COVID-19 patients and HC.

		COVID-19 PATIENTS	HEALTHY CONTROLS
Number		10	10
Age	Years, median(range)	67 (56–76)	67.5 (43–72)
Female/Male	n°	2/8	3/7
Comorbidities	Arterial hypertension, n° (%)	5 (50%)	NA
	Peripheral artery disease, n° (%)	1 (10%)	NA
	COPD, n° (%)	2 (20%)	NA
	Diabetes, n° (%)	2 (20%)	NA
	Acute myocardial infarction, n° (%)	1 (10%)	NA
	Others, n° (%)	4 (40%)	NA
Treatment at time of sampling	Anticoagulant, n° (%)	10 (100%)	
	Antibiotics, n° (%)	9 (90%)	
	Glucocorticoids, n° (%)	5 (50%)	
At time of sampling	Platelets x 10^9/L, median(range)	239 (139–512)	200.5 (154–261)
	White Blood Cells x 10^9/L, median(range)	7.9 (3.8-15.6)	5,9 (4.0-9.0)
	c-Reactive Protein (CRP), median(range)	2.6 (0.33-13.9)	NA
	PaO_2, mm Hg median (range)	83 (57–132)	NA
	$PaCO_2$, mm Hg median (range)	49.5 (40-76)	NA
Ventilation mode at time of blood sampling	Pressure/volume control, n° (%)	3 (30%)	NA
	Pressure support, n° (%)	5 (50%)	NA
	Spontaneous, n° (%)	2 (20%)	NA
Intensive Care Unit stay	Days at time of sampling, median(range)	28.5 (8-43)	NA
PaO_2/FiO_2 score	median(range)	186 (113-330)	NA
SOFA score	median(range)	2.5 (1-8)	NA

EP lipid extraction and LC/MS Q-TOF analysis

The EP lipidome was quantified using an untargeted lipidomic approach. Specifically, lipids were extracted from EP samples according to the one-phase extraction method described by (36) with minor modifications. In brief, 18mL of MMC extraction solvent was prepared by adding 5mL of methanol (MeOH), 6mL of chloroform ($CHCl_3$), 6mL of metil-t-butil etere (MTBE) and 1mL of Internal Standard mixture Splash I Lipidomix (Avanti Polar Lipids, USA) diluted 1:10 in MeOH. Each sample was added with 600 µl of MMC, vortexed for 10 seconds and shaken at 1600 rpm at 20°C in a T-Shaker (Euroclone). At the end, the tubes were centrifuged for 20 min at 16,000 x g at 4°C. The supernatant was transferred to a 1.5mL glass vial and flushed to dryness with a gentle stream of nitrogen. The residue was resuspended with 200 µl of a 9:1 mixture (MeOH/Toluene) and subjected to LC/MS Q-TOF analysis.

LC/MS Q-TOF analysis was carried out according to (37), after adaptation to the different instrumental configurations and using a 1260 Infinity II LC System coupled with an Agilent 6530 Q-TOF spectrometer (Agilent Technologies, Santa Clara, CA USA). Separation was carried out on a reverse phase C18 column (Agilent InfinityLab Poroshell 120 EC-C18, 3.0 × 100 mm, 2.7 µm) at 50°C and 0.6 mL/min flow. Mobile phase consisted of a mixture of water (A), Acetonitrile (can) (B), MeOH (C) and Isopropanol (IPA) (D) all containing a concentration of 10 mM ammonium acetate and 0.2 mM of ammonium fluoride except for ACN. Gradient was time 0-1 min isocratic at A 27%, B 14%, C 24%, D 35%; time from 1 to 3.5min: linear gradient to A 12.6%, B 17.2%, C 27.2%, D 43%; time 3.5-10 min isocratic; time from 10 to 11 min: linear gradient to A 0%, B 20%, C 30%, D 50%; time 11-17 min isocratic; time 17-17.1 min: linear gradient to A 27%, B 14%, C 24%, D 35%; time 20 min: stop run. Spectrometric data were acquired in the 40-1700 m/z range both in negative and positive polarity. An iterative MS/MS acquisition mode on three technical

replicates for each sample was used. The Agilent JetStream source operated as follows: Gas Temp (N2) 200°C, Drying Gas 10 L/min, Nebulizer 50 psi, Sheath Gas temp: 300°C at 12 L/min. MS/MS spectra were obtained using N2 at 30V CE.

Acquired raw data were processed using the MS-DIAL software (4.48) (38) to perform peak-picking, alignment, annotation and quantification. Lipid annotation and quantification were carried out according to the recommendations of Lipid Standard Initiative (39).

At the end of the workflow, a data matrix containing the concentration in nmol/mL of the annotated lipids distributed over various lipid classes was obtained. The tool LipidOne was used to perform an in-depth analysis in lipid compositions, called lipid building blocks (40). The volcano plot and network graphs were created with Excel (Microsoft) and Graph Editor (https://csacademy.com/app/graph_editor/) by processing the data obtained with LipidOne. MetaboAnalist 5.0 web platform was used to perform multivariate statistical and chemoinformatic analysis (41).

MACSPlex

MACSPlex analysis was performed using the MACSPlex Exosome Kit, human (Miltenyi Biotec, Bergisch-Gladbach, Germany) according to the manufacturer's instructions. Briefly, EP-enriched pool were diluted with MACSPlex buffer and MACSPlex Exosome Capture Beads were added. After overnight incubation at room temperature in agitation, MACSPlex Exosome Detection Reagent for CD9, CD63, and CD81 were added to each sample followed by incubation for 1 hour at room temperature. Flow cytometric analysis was carried out on a CytoFLEX flow cytometer followed by Kaluza Analysis 2.1 (Beckman and Coulter Life Sciences, CA, USA). Exosomal surface epitope expression (median APC fluorescence intensity) was then recorded. Median fluorescence intensity (MFI) was evaluated for each capture bead subsets and corrected by subtracting the respective MFI of blank control (PBS, vehicle) and normalized by the mean MFI of CD9, CD63, and CD81.

Plasma cytokine concentration

Plasma from HC and COVID-19 patients were analyzed using BioLegend's LEGENDplex™ bead-based immunoassays to quantify IL-2, IL-4, IL-5, IL-6, IL-9, IL-10, IL-13, IL-17A, IL-17F, IL-22, IFN-γ and TNF-α (Human Th Cytokine Panel (12-plex)) and to quantify IL-1β, IL-6, TNF-α, IP-10, IFN-λ1, IL-8, IL-12p70, IFN-α2, IFN-λ2/3, GM-CSF, IFN-β, IL-10 and IFN-γ (Human Anti-Virus Response Panel (13-plex)). A customized Human Th Cytokine Panel, including only IL-4, IL-5, IL-9, IL-10 and IL-13, was also used to quantify these cytokines in the supernatants of *in vitro* stimulated ILC2. The analyses were performed according to the manufacturer's instructions.

ILC phenotype, isolation and expansion

ILC were identified by flow cytometry using the following antibodies:

FITC-conjugated anti-CD3 (clone: UCHT1), anti-CD4 (clone: RPA-T4), anti-CD8 (lot: 276276, Immunotools), anti-CD14 (clone: HCD14), anti-CD15 (clone: HI98), anti-CD16 (lot: 7464017, Beckman Coulter), anti-CD19 (clone: HIB19), anti-CD20 (clone: 2H7), anti-CD33 (clone: HIM3-4), anti-CD34 (clone: 561), anti-CD203c (clone: NP4D6), anti-FcεRI (clone: AER-37) all from Biolegend); BUV737-conjugated anti-CD56 (clone: NTAM16.2, BD); BV421-conjugated anti-CD127 (clone: A019D5, Biolegend); BV605-conjugated anti-CD117 (cKit, clone: 104D2, Biolegend); BUV395-conjugated anti-CRTH2 (clone: BM16, BD Biosciences). Total ILC were identified as Lineage$^-$ (CD3$^-$, CD4$^-$, CD8$^-$, CD14$^-$, CD15$^-$, CD16$^-$, CD19$^-$, CD20$^-$, CD33$^-$, CD34$^-$, CD203c$^-$, FcεRI$^-$), CD56$^-$, CD127$^+$ lymphocytes. From total ILC, ILC1 were identified as CRTH2$^-$cKit$^-$, ILC2s as CRTH2$^+$cKit$^{+/-}$ and ILCP as CRTH2$^-$cKit$^+$. The gating strategy is shown in Supplementary Figure S1.

ILC2 phenotype was analysed by using: APC-conjugated anti-CD69 (clone: FN50, BD Biosciences); BV650-conjugated anti-CD38 (clone: HB7, Biolegend); BV785-conjugated NKG2D (clone: 1D11, Biolegend). Dead cells were always excluded using a viability dye. Samples were acquired on a LSRFortessa flow cytometer (BD Biosciences) and data were analysed using FlowJo software V10.8.1 (TreeStar). For immunophenotyping, each marker was analysed on the PBMCs of at least 4 different donors.

ILC2 were isolated by Fluorescence Activated Cell Sorting (FACS) on a FACS Aria III (BD) from HC and expanded in StemSpanTM Serum-Free Expansion Medium II (SFEMII, from STEMCELL Technologies) in the presence of IL-2 (100U/ml) and IL-7 (10ng/ml, both from PeproTech).

EP/ILC2 co-culture assay

ILC2 were stimulated with a cytokine cocktail (IL-2, IP-10, IL-8, IL-6 at 20U/ml, 100ng/ml, 100ng/ml, 20ng/ml, respectively, PeproTech) alone or in combination with EPs isolated from either HC or COVID-19 patients. We set up co-cultures using a concentration of EPs ranging from 2 to 10 µg, that we tested not to kill the cells (data not shown). Supernatants were collected after 48 hours and cytokines were measured using a bead-based immunoassay flow assay, as stated above.

Statistics

All data are composed of at least three independent experiments. Data were analyzed with Graphpad Prism 9.4.1 for Windows (GraphPad Software, Inc., La Jolla, CA, USA). Due to the small sample size, the data were analyzed using the non-parametric Mann-Whitney test where two groups were compared and the non-parametric Kruskal-Wallis test followed by Dunn's posthoc test

10.3389/fimmu.2023.1085610

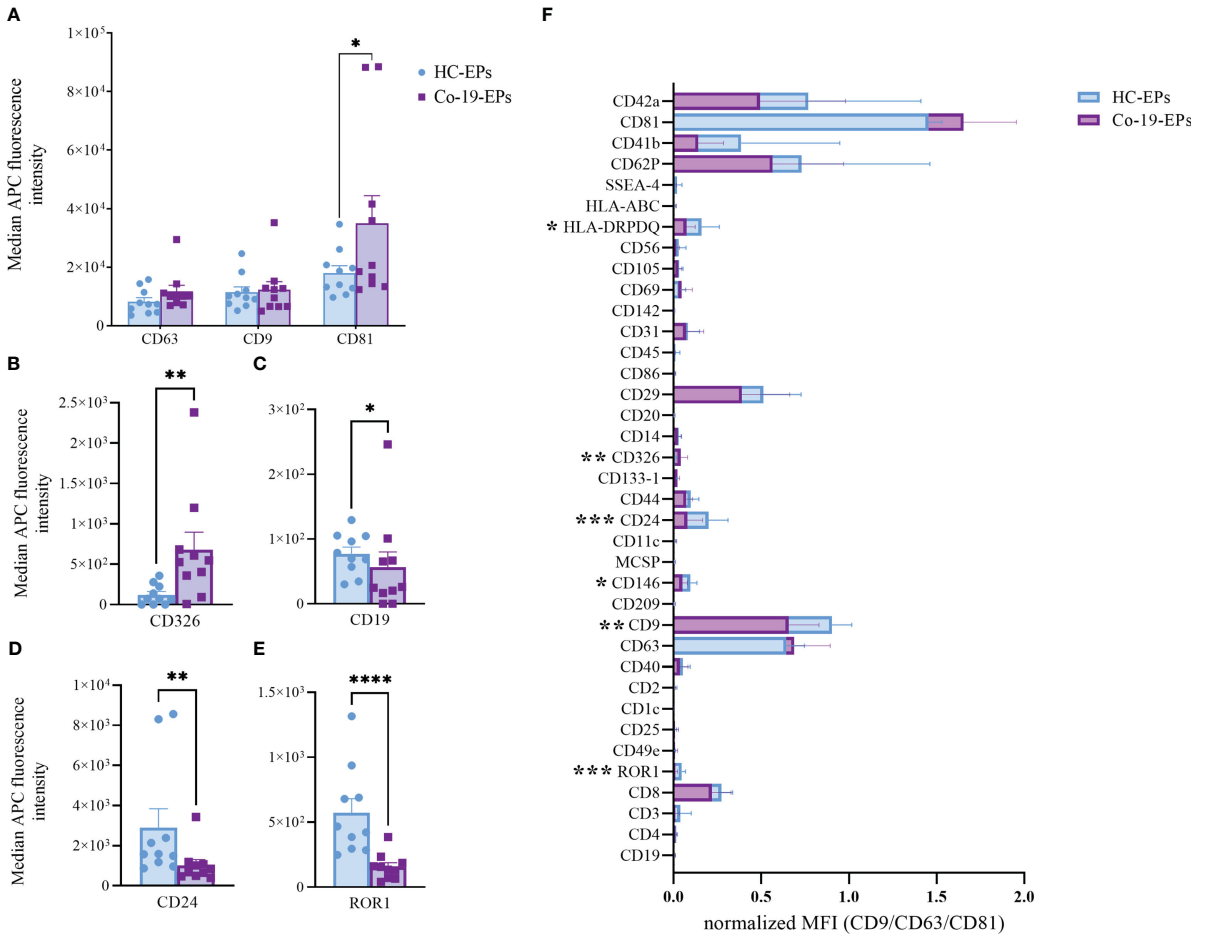

FIGURE 1
Comparison between EPs from COVID-19 patients (n=10) and HC (n=10) using MACSPlex exosome kit. Background-corrected median APC fluorescence intensity (MFI) for selected markers: **(A)** tetraspanins (CD9, CD63, CD81), **(B–E)** the only significantly different markers between COVID-19 patients and controls (CD326, CD19, CD24, ROR1). **(F)** Superimposed graph with background-corrected median APC fluorescence intensity normalized to exosome marker mean (CD9, CD63, CD81) for all 37 surface epitopes on the different purified EP preparations comparing patients and controls. *p<0.05, **p<0.01, ***p<0.001, ****p<0.001.

where more than two groups were compared. P-values ≤ 0.05 were considered statistically significant and are indicated in the graphs as reported by the analysis software: *$p<0.05$, **$p<0.01$, ***$p<0.001$, ****$p<0.0001$.

Results

Multiplex protein analysis shows altered EP surface signatures in severe COVID-19 patients and reveals a Co-19-EP identikit

To detect any signal produced by cells in the circulation after COVID-19 infection, we firstly evaluated the proteins expressed on the surface of the plasma-derived EPs isolated from COVID-19 patients (Co-19-EPs) and HC (HC-EPs) using bead-based multiplex EV analysis. Considering the overall median fluorescence intensity (MFI) for specific EV markers (i.e., tetraspanins CD63, CD9 and CD81; Figure 1A) we observed that only EV-specific tetraspanin CD81 was significantly higher in COVID-19 patients than controls ($P<0.05$). Similarly, the epithelial cell adhesion molecule CD326 (EpCAM) was significantly higher ($P<0.01$) in EPs derived from COVID-19 patients than in controls (Figure 1B). Conversely, among differentially expressed epitopes we also found lower expression for CD19, CD24 (B-cell related markers) and ROR1 (stemness marker) in EPs from patients than in controls (Figures 1C–E). In particular, most of the immunological-related proteins (CD1c, CD2, CD4, CD11c, CD20, CD25, CD69, CD86, CD209) as well as the hemopoietic marker (CD45) showed either very low expression or were not detected in both groups. Overall, the graph reported in Supplementary Figure S2 shows the MFI for each marker detected.

Then, we tested the MFI of individual markers after normalization to the mean MFI of the specific EV markers (namely CD9, CD63, and CD81) (nMFI; Figure 1F). In addition to the above-described markers (ROR1 and CD24, respectively), we observed that Co-19-EPs differed from controls for the other three markers including CD9 (tetraspanin, $P<0.01$), HLA-DR/DP/DQ (MHC-II, leukocyte, $P<0.05$), and CD146 (endothelial, $P<0.05$). All of them were relatively lower in Co-19-EPs compared to HC-

10.3389/fimmu.2023.1085610

derived EPs. CD326 (EpCAM) expression was detected only on Co-19-EPs ($P<0.01$).

Therefore, these data indicate that a phenotype-based signature on EPs may distinguish severe COVID-19 patients from HC suggesting further investigations on circulating EPs.

Circulating EPs from severe COVID-19 patients reveal abnormal lipidomic profiling

Within EV cargos, lipids are suggested to be involved in EV formation and biological functions (42). To investigate the cargo of circulating Co-19-EPs and eventually how SARS-CoV-2 might influence their cargo, untargeted lipidomic analyses were performed on EPs isolated from the plasma of COVID-19 patients and HC. Lipidomic analysis revealed 1112 lipid species annotated at the molecular species level, grouped into 26 lipid classes. As reported in Table 2, we found that almost 70% of the EP-associated lipids are free fatty acids (FA) (28%), cholesteryl ester (CE) (16%), triacylglycerol (TG) (13%) and phosphatidylcholine (PC) (12%). The most significantly different lipid classes between patients and HC were FA, CE, TG, PC, ceramide (Cer), diacylglycerol (DG), lysophophatidylcholine (LPC) and sphingomyelin (SM). Indeed, the volcano plot showed that the amount of SM, HexCer, LPC and Cer is

TABLE 2 Summary of lipidomic data.

Class abbreviation	Explained class name	N molecular species	CV19 (nMol/mL)	CV19 SEM (n=10)	HC (nMol/mL)	HC SEM (n=10)	P-value	average Amount (%)
BMP	Bismonoacyl glycerophosphate	3	19.5	2.4	15.9	1.8	0.12	0.18
CAR	AcylCarnitine	16	11.9	0.7	12.4	2.3	0.41	0.12
CE	Cholesteryl ester	9	1246.8	236.9	2012.0	261.1	0.02	16.16
Cer	Ceramide	85	576.5	53.6	852.5	50.6	0.0007	7.08
CL	Cardiolipin	14	172.8	9.6	150.0	12.3	0.08	1.60
DG	Diacylglycerol	74	807.1	113.4	541.3	59.4	0.02	6.68
DMPE	Dimethyl-Phosphatidyl ethanolamine	18	9.9	1.9	12.6	4.0	0.27	0.11
FA	Free fatty acid	59	2989.9	94.3	2675.6	50.5	0.004	28.09
FAHFA	Fatty acid ester of hydroxyl fatty acid	31	67.3	6.4	53.8	2.8	0.03	0.60
HexCer	Hexosylceramide	11	14.3	1.5	31.2	3.8	0.0002	0.23
LPC	Lysophophatidylcholine	54	223.5	7.3	312.0	19.5	0.0002	2.65
LPE	Lysophosphatidyl ethanolamine	5	3.5	0.2	3.1	0.3	0.11	0.03
MG	Monoacylglycerol	3	3.8	0.2	3.4	0.5	0.21	0.04
MMPE	monomethyl-phosphatidyl ethanolamine	9	7.6	0.6	10.4	2.2	0.12	0.09
NAE	N-acyl ethanolamines	41	111.5	4.1	137.5	24.0	0.15	1.23
NAOrn	N-acyl ornitines	20	14.1	0.9	12.2	1.2	0.11	0.13
PA	Glycerophosphate	4	119.2	17.1	43.5	8.0	0.0004	0.81
PC	Phosphatidylcholine	114	1126.7	61.2	1324	77.7	0.03	12.15
PE	Phosphatidyl Ethanolamine	75	120.9	9.1	122.5	18.5	0.46	1.21
PEtOH	Phosphatidyl ethanol	29	36	4.9	25.5	3.3	0.04	0.30
PG	Phosphatidyl glycerol	16	411.6	20.7	354.5	28.7	0.06	3.80
PI	Phosphatidylinositol	20	20.0	1.4	26.1	1.4	0.002	0.23
PMeOH	Phosphatidyl Methanol	14	16.9	1.4	11.7	0.4	0.0008	0.14
PS	Phosphatidylserine	5	4.5	0.5	3.2	0.3	0.01	0.04
SM	Sphingomyelin	26	226.9	12.1	385.7	25.0	1.03E-05	3.04
TG	Triacylglycerol	357	1335	186.5	1341.8	209.1	0.49	13.27

The synthetic class name, extended name, number of molecular species annotated, concentration and standard error of the mean (SEM) for both the COVID-19 (CV19, n=10) and HC groups (n=10) of EP samples and p-value of difference are reported for each lipid class. The last column shows the percentage of the mean amount for both groups.

lower (P<0.001, respectively) while that of phosphatidylmethanol (PMeHO; P = 0.0008) and phosphatidic acid (PA; P = 0.0004) is higher in Co-19-EPs compared to HC-EPs (Figure 2A). Using known biosynthetic pathways as a reference in Figure 2B we show some metabolic pathways activated in COVID-19 patients. Interestingly, we found an inverse correlation between O-acyl-R-carnitine (CAR) and EP markers expressed on Co-19-EPs such as CD3, CD56, and HLA-ABC. Also, lysophosphatidylethanolamine (LPE) reported a negative correlation with the expression of CD4 on Co-19-EPs. By contrast, CE positively correlated with CD86 expression on Co-19-EPs whereas PG lipid class correlated with the exosomal expression of CD81 (Figure 2C).

In addition, we identified the presence of oxidized molecular species using the LipidOne analyses. We reported the oxidized/unoxidized species ratio or the Ether/Esters linked ratio within each lipid class. The results are represented with the volcano plot showing that EPs from COVID-19 patients are enriched in selected lipid classes that contain oxidized lipid chains including phosphatidylethanolamine (PE; P<0.001), PC and phosphatidylglycerol (PG) (P<0.01) (Figure 2D). Conversely, considering the Ether/Ester ratio within the 27 lipid classes, only the phospholipids were found to contain ether bonds with enrichment on the PE class in HC (P<0.001; Figure 2E).

The entire lipidomic dataset was then processed using the MetaboAnalyst platform to perform univariate and multivariate analyses on lipid species. The most prominent observation reported from both the Volcano Plot and the Heat Map (Figures 3A, B) was a significant depletion of specific molecular species belonging to the following classes: SM, Cer and some Ether-phospholipids (PE-O) in COVID-19 patients. Indeed, as depicted by the heat map, several sphingolipids (e.g., SM 16:1:20_15:0; SM 22:1:20_8:0, SM 17:1:20_22:0; SM 18:1:20_14:0) were deeply underexpressed in Co-19-EPs. By contrast, several species of diacylglycerols (DG: DG 18:1_24:6/DG 18:1_20:4) and triacylglycerols (TG: TG 18:1_18:2_18:3/TG 20:0_18:1_18:2) were more abundant in Co-19-EPs. Overall data confirmed a pattern that determined the formation of the two clusters as shown in PCA (Figure 3C) and PLS-DA (Figure 3D) analyses. In both, the first component explains about 21% of the variance in the data. Next, despite the low number of patients, we explored any difference in specific lipids between survivors and non-survivors COVID-19 patients. Of note, we observed specific lipid enrichments discriminating survivors and non-survivors including bis(monoacylglycero)phosphate (BMP) 33:0; O-acyl-R-carnitine (CAR) 17:2; CE 17:4; DG 48:2; N-acylethanolamine (NAE) 20:2 (P<0.05, respectively). Also, within TG species, two TGs were significantly up-regulated in non-survivor COVID-19 patients (TG 40:1; TG 40:2, P<0.05) (Figure 3E).

Overall, we demonstrated that lipidome from EPs distinguishes severe COVID-19 patients from HC.

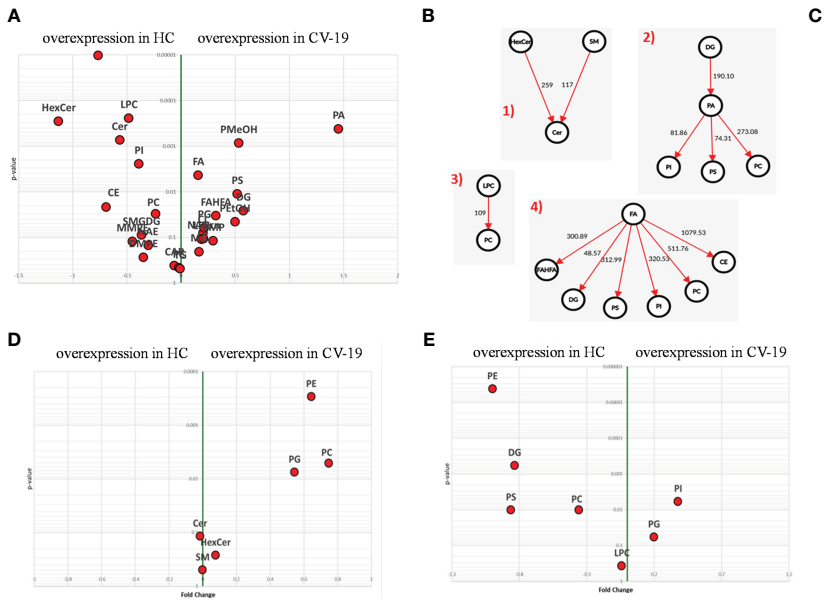

Lipid class	Co-19-EP markers	Spearman
CAR	CD3	r = -0,79 P = 0,008
CAR	CD56	r = -0,74 P = 0,01
CAR	HLA-ABC	r = -0,78 P = 0,01
LPE	CD4	r = -0,74 P = 0,01
CE	CD86	r = 0,77 P = 0,01
PG	CD81	r = 0,72 P = 0,02

FIGURE 2
(A) Volcano plot of lipid classes. Top left and top right show the lipid classes overexpressed in Co-19-EPs and HC-EPs, respectively. **(B)** Network of transformations between lipid classes: significant changes (P<0.05) between lipid classes can be interpreted using known biochemical pathways as reference. Both graphs were made with Excel and Graph Editor from data produced with the lipid class overview fiction of LipidOne. The numbers in the diagram indicate the intensity of the reaction on an arbitrary scale. **(C)** Table reporting the association between lipid classes and MFI of markers on Co-19-EPs using Spearman's correlation analysis and presented as rank coefficient (r) and P value. Volcano plot of the ratio of oxidized/reduced species **(D)** and the ether/ester-linked ratio **(E)**. The figure shows that the phosphatidylethanolamine (PE), phosphatidylcholine (PC) and Phosphatidylglycerol (PG) classes contain oxidized species and that EPs from COVID-19 patients are enriched in these oxidized species (P<0.01). In contrast, EPs from HC are enriched in lipid classes containing ether linkages (PE, diacylglycerol (DG), phosphatidylserine (PS) and PC) (P<0.01).

10.3389/fimmu.2023.1085610

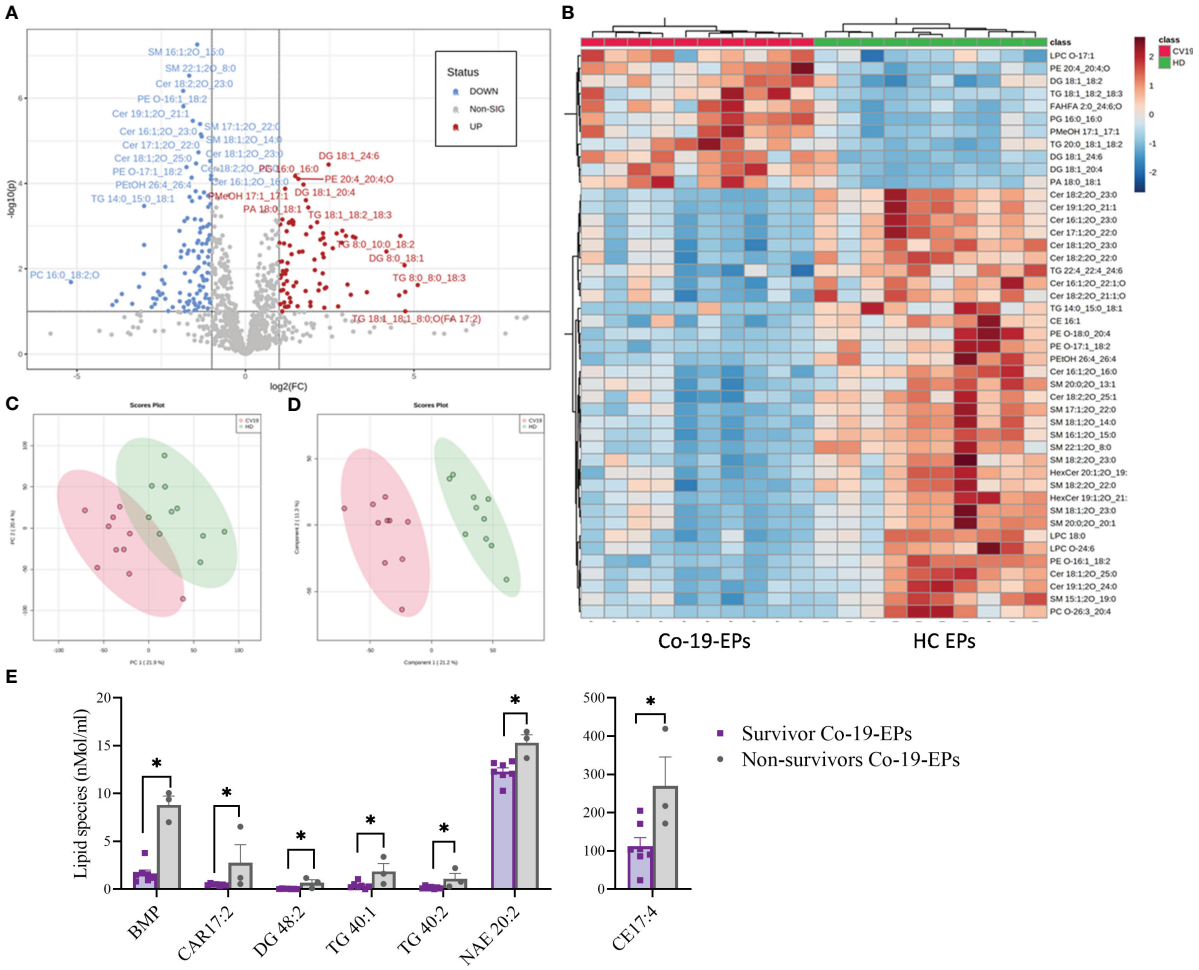

FIGURE 3
Volcano Plot **(A)**, Heat Map **(B)**, Principal Component Analysis (PCA) **(C)** and Partial least squares-discriminant analysis (PLS-DA) **(D)** of Lipidomic dataset for EPs from COVID-19 patients and HC (n=10, respectively). **(E)** Significant difference ins specific lipid species (namely Bis(monoacylglycero) phosphate (BMP), O-acyl-R-carnitine (CAR)17:2, diacylglycerol (DG) 48:2, triacylglycerol (TG) 40:1, TG 40:2, N-acylethanolamine (NAE) 20:2) between survivors and non-survivors COVID-19 patients (n=7 vs n=3). *P<0.05.

Specific lipid species detected in circulating Co-19-EPs correlate with disease aggressiveness scores

To explore the clinical impact of EP lipidome in COVID-19 patients, we investigated whether the lipidome profile of EPs was associated with disease severity parameters including SOFA and PaO_2/FiO_2 scores.

As stated above, we observed a strong depletion of SM lipid class in Co-19-EPs (Figure 3). Interestingly, we found a negative correlation between SM class and SOFA score (r= -0.82, P = 0.009) (data not shown). Taking into account the individual lipid species, Spearman's correlation analysis revealed that patients with higher SOFA scores had low levels of several lipids' species including SM 41:1;2O; SM 40:2;3O; SM 42:1;2O; SM 43:1;2O; SM 43:2;2O, monosialodihexosylganglioside (GM3) 38:1;2O and HexCer 42:2;3O. Notably, CL 86:0 reported the strongest negative association with SOFA score (r=-0.93, P = 0.0008). By contrast, specific DG and FA were positively correlated with SOFA scores (fatty acid esters of hydroxy fatty acids (FAHFA) 28:4;O/FA 34:0/DG 33:7 DG 36:6) (Supplementary Table S1).

Correlation analysis was also performed to detect any association with PaO_2/FiO_2 values. Regarding individual lipid species, we observed that FAHFA 22:0;O and two LPCs (LPC O-16:1, LPC O-18:1) were positively associated with PaO_2/FiO_2 score. Also, lipid species (SM 41:1;2O; SM 40:2;3O) were both positively correlated to PaO_2/FiO_2 score. Of interest, PE 40:3;O and phosphoinositides (PI) O-39:5 levels reported an inverse correlation with PaO_2/FiO_2 values (Supplementary Table S2).

Next, we investigated any relation between the expression of markers on Co-19-EPs and lipid cargo and clinical features. Both LPC O-16:1 and LPC O-18:1 lipid species, detected in Co-19-EPs, showed a positive association with MFI of CD8 in Co-19-EPs (r = 0.75, P = 0.01 and r = 0.90, P= 0.0008, respectively). Accordingly, a similar trend was found between CD8 MFI in Co-19-EPs and PaO_2/FiO_2 failure score (r = 0.87, P= 0.002) (Figures 4A, B).

Taken together these data indicate that lipidomic profiling refines the accuracy of disease aggressiveness assessment among

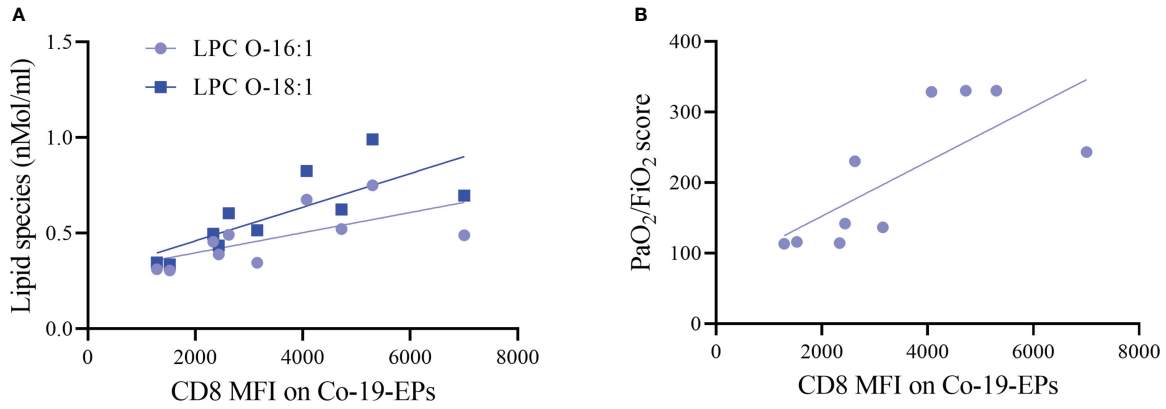

FIGURE 4
Association between lipid species or clinical score with MFI of markers on Co-19-EPs using Spearman's correlation analysis. **(A)** Correlations between lipid specie lysophosphatidylcholine (LPC) O-16:1 with CD8 MFI on Co-19-EPs (P = 0.01, r = 0.75). A similar association was reported for LPC O-18:1 found in Co-19-EPs and CD8 MFI on Co-19-EPs (P=0.0008, r=0.90). **(B)** Correlation between PaO_2/FiO_2 score and CD8 MFI on Co-19-EPs (P=0.0017, r=0.87).

severe COVID-19 patients and supports the hypothesis that selective lipid species might act as a prognostic tool for (severe) COVID-19 patients.

Co-19-EPs reduce the cytokine production ability of ILC2

ILC are lymphocytes known to respond to a large variety of stimuli, including cytokines, nutrients, neuropeptides and tumor-derived factors (43, 44). In particular, ILC2 were shown to be sensitive also to lipid mediators and EV stimulation (13, 19). To understand whether ILC2 could respond differently to EPs from COVID-19 patients, we firstly analyzed the profile of circulating ILC of COVID-19 patients and HC. Specifically, as already shown by others, total ILC were decreased in COVID-19 patients in comparison to HC (Figure 5A). Although we did not see any significant differences in the ILC subset distribution between COVID-19 patients and HC within the ILC2 subset, we found a significant decrease in the $cKit^{high}$ subpopulation, paralleled with a significant increase in the $cKit^{low}$ population, in COVID-19 patients (Figures 5B, C). Because the $cKit^{low}$ population has been proposed to be the ILC2 subpopulation more mature and fully committed (45, 46), our findings suggest that in COVID-19 patients only the ILC2 subset specifically secreting type 2 cytokines is enriched.

Next, we evaluated a total of 21 cytokines in plasma samples from patients with severe COVID-19 and HC (Figure 5D and Supplementary Figure S3). The plasma levels of IL-6 and IL-10 (P<0.0001, respectively) were significantly increased in patients with COVID-19 as compared to the HC (Figure 5D). Similarly, the levels of IL-8 (P=0.005), IP-10 (P=0.035) and IL-5 (P=0.01; Figure 5E) were higher in COVID-19 patients compared to HC. Comparing survivors and non-survivors, only IL-5 plasma levels were significantly increased in non-survivor COVID-19 patients (P=0.045) (Figure 5E). Furthermore, several Co-19-EP protein markers reported in Figure 1 were associated with plasma cytokine levels as reported in Figure 6. Most of the correlations reported were positive except for those between MFI CD3 with IL-2 and MFI SSEA-4 with IL-6. Of interest, among the significant plasma cytokines detected in COVID-19 patients, IL-8 showed a positive correlation with CD19, CD69 and ROR1 whereas IL-6 positively correlates with MFI CD24. Importantly, MFI CD63 expression on Co-19-EPs is linked to IL-5 plasma levels, the only cytokine different between survivor and non-survivor patients Figures 5E, 6.

To understand whether the combination of the pro-inflammatory cytokines IL-6, IL-8 and IP-10 together with the EPs isolated from HC and COVID-19 patients could impact the cytokine secretion ability of ILC2, we isolated and expanded human ILC2 from HC *in vitro* and stimulated them with IL-6, IL-8, IP-10 alone or in the presence of either HC-EPs or Co-19-EPs. We found that, while the EPs from HC inhibit IL-5 and IL-10 production, the EPs from COVID-19 patients failed in downregulating these two cytokines, suggesting that the composition of the EPs isolated from COVID-19 patients was supporting the ILC2 activation status (Figures 7A, B). Indeed, when we compared the phenotype of ILC2 present in the PBMC of HC and COVID-19 patients, we found that COVID-19 patients' ILC2 showed a more activated phenotype characterized by an increase in CD38 and CD69 expression and a trend for increased NKG2D (Figure 7C). CD38 upregulation was present both in the ILC2 $cKit^{low}$ and $cKit^{high}$ (Figure 7D–E).

Altogether these data highlight that the presence of a well-known inflammatory microenvironment in severe COVID-19 patients might be reflected in more activated ILC2 producing high concentrations of both IL-5 and IL-10. Interestingly, at variance with HC-EPs, Co-19-EPs are unable to dampen the activation status of ILC2 in severe COVID-19 patients.

10.3389/fimmu.2023.1085610

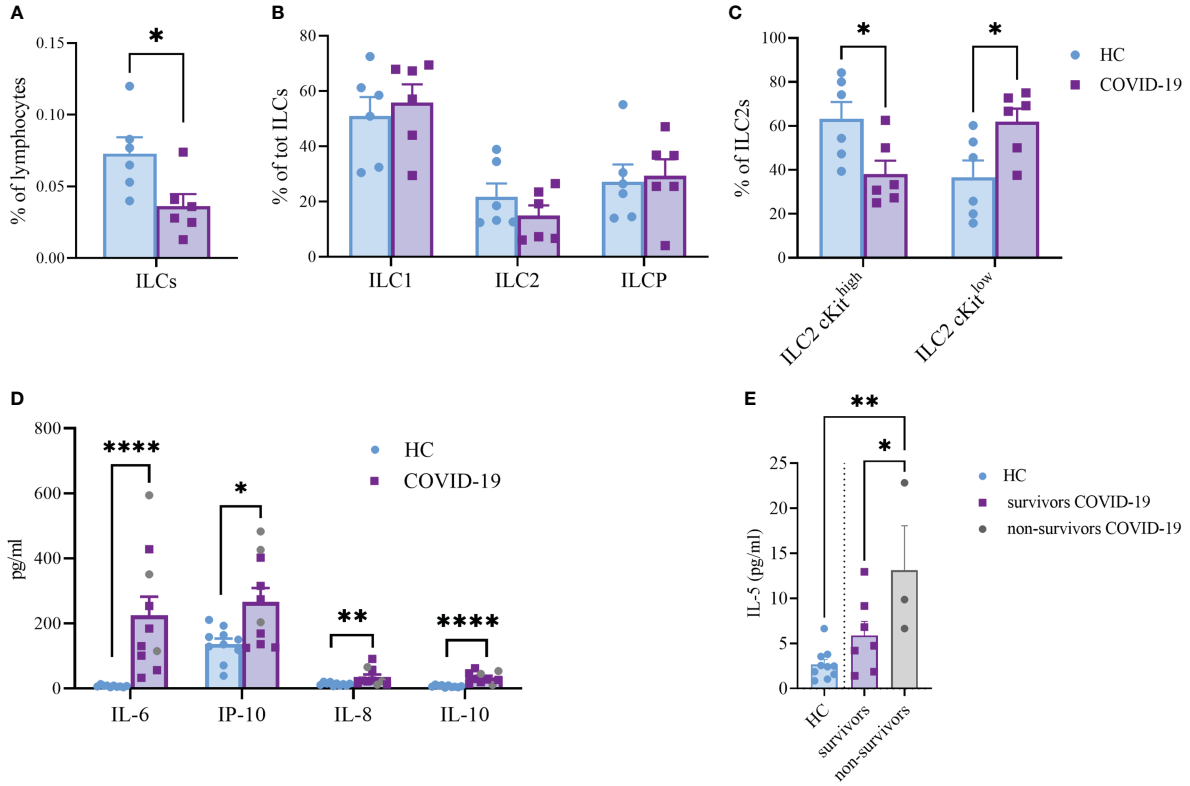

FIGURE 5
Frequency of total ILC **(A)**, (*P*<0.05), ILC subsets **(B)** and cKit^{high} vs cKit^{low} ILC2 **(C)**, (*P*<0.05) in the circulation of HC and COVID-19 patients (n=6, respectively). Plasma cytokines levels of COVID-19 patients (n=10) and HC (n=10) **(D)**. The plasma levels of IL-6 (*P*<0.0001); IL-10 (*P*<0.0001); IL-8 (*P*<0.01) and IP-10 (*P*<0.05) were significantly increased in COVID-19 patients. Significant difference reported for IL-5 plasma levels between non-survivors (n=3, grey dots) and survivor COVID-19 patients (n=7, *P*<0.05; purple squares) or HC (n=10, *P*<0.01; light blue dots) **(E)**. **p*<0.05, ***p*<0.01, *****p*<0.0001

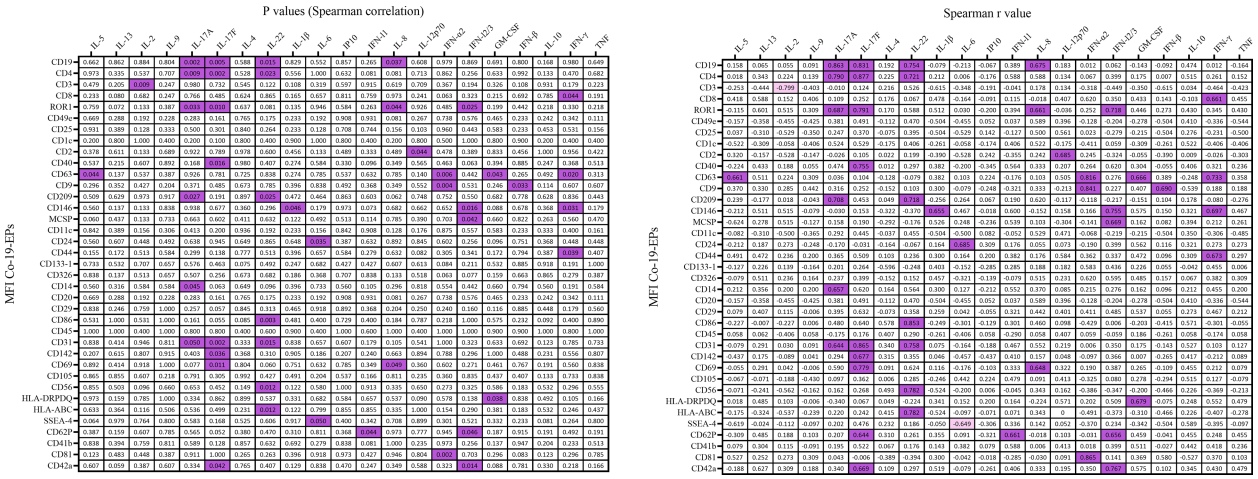

FIGURE 6
Correlation coefficient matrix heat map reporting any associations of plasma cytokines from COVID-19 patients (n=10). In figure, the color map with double gradient for Spearman correlation coefficient (significant values represented in purple for positive correlations and in light violet for negative correlations).

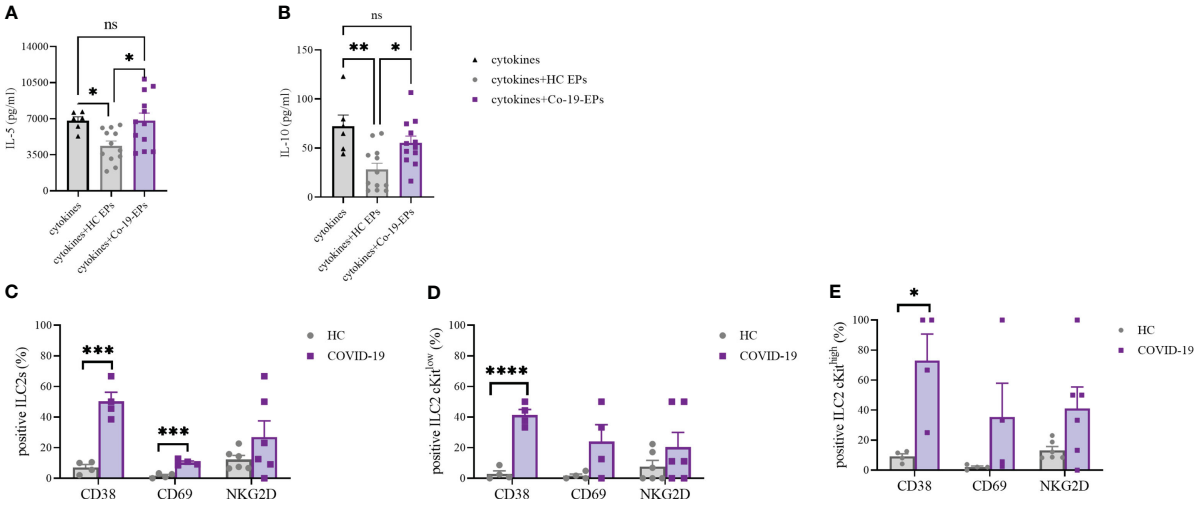

FIGURE 7
IL-5 **(A)** and IL-10 **(B)** secretion by short-term expanded ILC2 isolated from HC stimulated with cytokines (IL-6, IL-8 and IP-10) alone or in the presence of either HC-EPs or Co-19-EPs. HC-EPs inhibited IL-5 ($P<0.05$) and IL-10 ($P<0.01$) production. **(C–E)** Expression of the activation markers CD38, CD69 and NKG2D in total ILC2 **(C)** and in cKit^{low} **(D)** and cKit^{high} **(E)** ILC2 (4-6 different donors were analyzed for each marker). *p<0.05, **p<0.01, ***p<0.001, ****p<0.0001.

Discussion

In this study, we identify an EP-associated lipidomic and phenotypic signature of SARS-CoV-2 infected patients with severe disease. Most important, the EP lipid and their protein patterns are associated with the disease aggressiveness scores, highlighting the putative role of Co-19-EPs as a prognostic biomarker cargo in severe COVID-19 patients. Interestingly, critical correlations between EP profile, lipidomic cargo and the immune-inflammatory microenvironment have been found. In addition, these circulating Co-19-EPs are unable to dampen the activated phenotype (as assessed by the ability to produce IL-5 and IL-10) of ILC2 isolated from HC. Despite the limitations of the small number of patients, we developed a valuable method for detecting the effects of SARS-CoV-2 infection and novel insight for studying EPs in infectious diseases.

It has recently been described that EVs might play a role in the host response to SARS-CoV2 infection (47, 48). In the present study, the lipidomic analysis of the EPs from COVID-19 patients enrolled demonstrates the reduced expression of sphingomyelins. Together with glycerophospholipids, sphingolipids are important components of the cell membrane and regulate several processes, such as proliferation and inflammatory responses (49, 50). Moreover, sphingolipid metabolism is involved in exosome secretion (51). Inhibition of SM synthesis has been reported to slow Golgi-to-plasma membrane trafficking of vesicular stomatitis virus G protein, influenza hemagglutinin, and pancreatic adenocarcinoma up-regulated factor suggesting that the SM biosynthetic pathway is broadly required for secretory competence (52). Therefore, SM metabolism can be a potential biomarker for identifying crucial vulnerabilities in COVID-19 patients and a potential target for therapeutic intervention against COVID-19 virus infection. In addition, in this study, Hex Cer and several SM reveal an opposite association with SOFA score which demonstrated that the depletion of sphingolipid species may be closely related to the severity of the disease. We also observe the relative abundance of lipids involved in energy storage, such as triacyl- and diacylglycerols (TG and DG) in EPs from COVID-19 patients. TGs are the most abundant lipids in the human body and are the major source of energy that constitutes a critical component of the lipoproteins (50, 53). Of note, specific TGs (including TG 40:1 and TG 40:2) are selectively increased in non-survivor subjects. In line with this, a myriad of cardiovascular manifestations are observed in COVID-19 patients (54) and, based on the role of lipoproteins in thrombosis, our data may suggest an association between increased TG levels in EPs and cardiovascular events in COVID-19 patients.

The EP surface proteins were also investigated. We found that the exosome markers CD9, CD63 and CD81 are present in EPs isolated from all groups. Among differentially expressed proteins, CD24, CD146 and CD326 show remarkably higher expressions in EPs from COVID-19 patients.

CD24 is highly expressed by immune cells and cancer cells and it is known to play an inhibitory role in B-cell activation responses and the control of autoimmunity (55). It has recently been described that CD24 stimulation of B cells may trigger a transfer of receptors functional in recipient cells *via* EVs (56).

CD146, a membrane and immunoglobulin superfamily protein that is normally expressed by endothelial cells and Th17 cells, promotes the adhesion, rolling and extravasation of lymphocytes and monocytes across the endothelium. Indeed, functionally, CD146 is involved in angiogenesis and inflammation (57, 58).

Finally, CD326 is an adhesion molecule that is characteristic of some epithelia and many carcinomas and has been implicated in intercellular adhesion and metastasis (59). It has recently been described to play a role in coagulopathy (60, 61). Overall, the

phenotype of circulating EPs from severe COVID-19 patients suggests that the hyperexpression of these EV biomarkers might contribute to affecting the immune response and the inflammatory microenvironment. For instance, it is worth noticing that it has been previously reported a link between the LPC and T cell homeostatic turnover (62). Herein, we find a direct association between Co-19-EPs expressing CD8 and two specific lipid species (LPC O-16:1 and LPC O-18:1), suggesting a defective role in the release of EV by $CD8^+$ memory T cells in COVID-19 patients (62). This hypothesis is also confirmed by a corresponding association with the PaO_2/FiO_2 failure score that show a more aggressive disease in the patients with lower MFI for CD8 in Co-19-EPs.

The challenge of the COVID-19 pandemic is to predict intensive care admission or death of COVID-19 patients. Based on the explorative data of this study, in-depth phenotype and lipidome profiling of EP could be considered novel tools for better stratification of the patients, helping selection and decision for clinical studies, or avoiding the risk of therapy-related complications. Since few data concerning the role of EPs and their lipid-associated cargo in COVID-19 are available, further studies, combining lipidomic data with biological and immunological characterization, may help to elucidate specific (immuno) pathogenetic mechanisms and identify novel treatment strategies for virus infections. Importantly, considering EV trafficking, the lipid composition of EV membranes may play a role in the stability of these vesicles as well as facilitating binding to and uptake into recipient cells such as immune cells.

Along with lipidomic and surface protein expression, we also performed co-culture experiments with circulating EPs from HC or COVID-19 patients using ILC2 as a target. In line with others, we find that the ILC2 from severe COVID-19 patients show a more activated phenotype in terms of CD38, CD69 and a trend for NKG2D expression; the latter marker was already shown to be upregulated in patients showing no need for mechanical ventilation and a shorter hospitalization (63). Our data suggest that the activated phenotype of ILC2 as well as the higher capacity of producing IL-5 and IL-10 might be linked with the different cargo of the circulating EPs. Indeed, only HC-EPs are efficient in suppressing the ILC2 cytokine secretion capacity, while Co-19-EPs lose this property. Whether this inhibitory capacity is due to the different lipidic or protein composition of the EPs is yet to be investigated. Overall, although EVs may represent a mechanism by which the SARS-CoV-2 escapes the immune system, our data indicate that circulating EPs may alarm the innate immune system by modifying the production of inflammatory cytokines. These findings shed light on the diverse effects of circulating EPs on the inflammatory/immune response of COVID-19. Consistently, we found the plasma levels of IL-5, IL-6, IL-8, IL-10 and IP-10 to be significantly higher in severe COVID-19 patients compared with control plasma. Previous data identified IL-10 and IP-10 as putative biomarkers associated with poor outcomes. In this regard, IL-10 has been shown as a putative regulator of COVID-19 pathogenesis in association with IL-6 (64), whereas IP-10 has been investigated for its role in thrombosis in COVID-19 patients (65). For instance, IP-10 is secreted by many cell types in response to interferon-gamma IFN-including monocytes, endothelial cells and fibroblasts (66) and acts as a chemotactic agent for immune cells such as T cells, NK cells, monocytes/macrophages and dendritic cells (65). In addition, IL-6, TNF-α and IL-8 were considered strong and independent markers for patient survival (67–69). Notably, Li L et al. showed both IL-8 and IL-6 as biomarkers of disease prognosis for COVID-19 patients suggesting them as putative therapeutic targets (69). Of interest, IL-5 plays a crucial role in our cohort being significantly different not only between HC and COVID-19 patients but also between non-survivor and survivor patients. It is already known the role of IL-5 in the growth, survival, and activation of eosinophils (70). Despite we do not find any association between IL-5 and the absolute eosinophil count of our patients (data not shown), our results suggest that the Type 2 immune response is involved and may be aggravated by SARS-CoV-2-induced pneumonia (70). Following previous work (71), EVs from subcutaneous immunotherapy-treated mice exert effects on IL-5 production from ILC2 suggesting novel therapeutic options using EVs. Indeed, it has been also demonstrated the potential for using EVs as powerful and feasible cargo for drug delivery (72). The natural origin of EVs enables them to reduce immunogenicity compared with existing delivery systems. Thus, an EV-based drug delivery system may be an attractive candidate to manipulate also the cytokines secretion by specific cell subsets for a novel effective treatment for COVID-19. Overall, our data on circulating cytokines confirm and highlight the complex immune/inflammatory network of COVID-19 pathogenesis and suggest that blocking one cytokine alone could be an ineffective strategy (64, 67, 73).

At last, even though these findings depict an "EP signature" of severe COVID-19 patients, it should be highlighted that at the time of sample collection severe COVID-19 patients were under treatment; therefore, we can not rule out the possibility that treatment might have influenced the EP pattern.

In summary, this study demonstrates that a distinct lipidomic and phenotypic signature characterizes EPs in severe COVID-19 patients. In addition, this study shed light on the mechanisms by which circulating EPs modulate the innate immune response. With the limitations related to the small cohort of COVID-19 patients included, these findings might have the potential for prognostic implications of EPs in severe COVID-19 patients. Since future and innovative therapeutic approaches in the COVID-19 current scenario may rely on signals carried by Co-19-EPs, our data represent a step toward the identification of a Co-19-EP-specific pattern of secret signals released in circulation in COVID-19 patients.

Data availability statement

The raw data supporting the conclusions of this article will be made available by the authors, without undue reservation.

Ethics statement

The studies involving human participants were reviewed and approved by Comitato Etico di Area Vasta Emilia Centro della

Regione Emilia-Romagna (CE-AVEC) (377/2020/Oss/AOUBo). The patients/participants provided their written informed consent to participate in this study.

Author contributions

DF, ST and LC contributed to the conception, research design and drafting of the paper and conceptualization methodology. TT and GC collected human samples. RP, HA, SB and LU performed the LC-MS/MS measurements and analysis. DF, RP, ST, MCe, GN and HA performed data curation. TT, GC, GM and VR provided clinical data and enrolled patients for the study. DF, FR PT performed the flow-cytometry analysis. DF, ST, MCe, CM, CE, CJ, MC, LC and FP reviewed and edited the manuscript. DF, MCa, LC, and FP provided supervision of the study. All authors contributed to the article and approved the submitted version.

Funding

DF was supported by Fondazione Umberto Veronesi. This research was funded by Olga Mayenfish Foundation. This work was also supported by Fondazione Cassa di Risparmio di Bologna (CARISBO).

Acknowledgments

The authors acknowledge the support from AIL Bologna ODV.

Conflict of interest

The authors declare that the research was conducted in the absence of any commercial or financial relationships that could be construed as a potential conflict of interest.

Publisher's note

All claims expressed in this article are solely those of the authors and do not necessarily represent those of their affiliated organizations, or those of the publisher, the editors and the reviewers. Any product that may be evaluated in this article, or claim that may be made by its manufacturer, is not guaranteed or endorsed by the publisher.

Supplementary material

The Supplementary Material for this article can be found online at: https://www.frontiersin.org/articles/10.3389/fimmu.2023.1085610/full#supplementary-material

References

1. Fajgenbaum DC, June CH. Cytokine storm. *N Engl J Med* (2020) 383(23):2255–73. doi: 10.1056/NEJMra2026131

2. Wanhella KJ, Fernandez-Patron C. Biomarkers of ageing and frailty may predict COVID-19 severity. *Ageing Res Rev* (2022) 73:101513. doi: 10.1016/j.arr.2021.101513

3. Blanco-Melo D, Nilsson-Payant BE, Liu WC, Uhl S, Hoagland D, Moller R, et al. Imbalanced host response to SARS-CoV-2 drives development of COVID-19. *Cell* (2020) 181(5):1036–45.e9. doi: 10.1016/j.cell.2020.04.026

4. Hadjadj J, Yatim N, Barnabei L, Corneau A, Boussier J, Smith N, et al. Impaired type I interferon activity and inflammatory responses in severe COVID-19 patients. *Science* (2020) 369(6504):718–24. doi: 10.1126/science.abc6027

5. Song JW, Lam SM, Fan X, Cao WJ, Wang SY, Tian H, et al. Omics-driven systems interrogation of metabolic dysregulation in COVID-19 pathogenesis. *Cell Metab* (2020) 32(2):188–202.e5. doi: 10.1016/j.cmet.2020.06.016

6. Guan J, Wei X, Qin S, Liu X, Jiang Y, Chen Y, et al. Continuous tracking of COVID-19 patients' immune status. *Int Immunopharmacol* (2020) 89(Pt A):107034. doi: 10.1016/j.intimp.2020.107034

7. Wu D, Yang XO. TH17 responses in cytokine storm of COVID-19: an emerging target of JAK2 inhibitor fedratinib. *J Microbiol Immunol Infect* (2020) 53(3):368–70. doi: 10.1016/j.jmii.2020.03.005

8. Cao X. COVID-19: immunopathology and its implications for therapy. *Nat Rev Immunol* (2020) 20(5):269–70. doi: 10.1038/s41577-020-0308-3

9. Lucas C, Wong P, Klein J, Castro TBR, Silva J, Sundaram M, et al. Longitudinal analyses reveal immunological misfiring in severe COVID-19. *Nature* (2020) 584 (7821):463–9. doi: 10.1038/s41586-020-2588-y

10. Merad M, Martin JC. Pathological inflammation in patients with COVID-19: a key role for monocytes and macrophages. *Nat Rev Immunol* (2020) 20(6):355–62. doi: 10.1038/s41577-020-0331-4

11. Hu B, Huang S, Yin L. The cytokine storm and COVID-19. *J Med Virol* (2021) 93(1):250–6. doi: 10.1002/jmv.26232

12. Wan S, Yi Q, Fan S, Lv J, Zhang X, Guo L, et al. Relationships among lymphocyte subsets, cytokines, and the pulmonary inflammation index in coronavirus (COVID-19) infected patients. *Br J Haematol* (2020) 189(3):428–37. doi: 10.1111/bjh.16659

13. Kuri-Cervantes L, Pampena MB, Meng W, Rosenfeld AM, Ittner CAG, Weisman AR, et al. Comprehensive mapping of immune perturbations associated with severe COVID-19. *Sci Immunol* (2020) 5(49):eabd7114. doi: 10.1126/sciimmunol.abd7114

14. Lagunas-Rangel FA, Chavez-Valencia V. What do we know about the antibody responses to SARS-CoV-2? *Immunobiology* (2021) 226(2):152054. doi: 10.1016/j.imbio.2021.152054

15. Vivier E, Artis D, Colonna M, Diefenbach A, Di Santo JP, Eberl G, et al. Innate lymphoid cells: 10 years on. *Cell* (2018) 174(5):1054–66. doi: 10.1016/j.cell.2018.07.017

16. Mortha A, Burrows K. Cytokine networks between innate lymphoid cells and myeloid cells. *Front Immunol* (2018) 9:191. doi: 10.3389/fimmu.2018.00191

17. Klose CS, Artis D. Innate lymphoid cells as regulators of immunity, inflammation and tissue homeostasis. *Nat Immunol* (2016) 17(7):765–74. doi: 10.1038/ni.3489

18. Lim AI, Li Y, Lopez-Lastra S, Stadhouders R, Paul F, Casrouge A, et al. Systemic human ILC precursors provide a substrate for tissue ILC differentiation. *Cell* (2017) 168 (6):1086–100.e10. doi: 10.1016/j.cell.2017.02.021

19. Garcia M, Kokkinou E, Carrasco Garcia A, Parrot T, Palma Medina LM, Maleki KT, et al. Innate lymphoid cell composition associates with COVID-19 disease severity. *Clin Transl Immunol* (2020) 9(12):e1224. doi: 10.1002/cti2.1224

20. Kumar A, Cao W, Endrias K, Kuchipudi SV, Mittal SK, Sambhara S. Innate lymphoid cells (ILC) in SARS-CoV-2 infection. *Mol Aspects Med* (2021) 80:101008. doi: 10.1016/j.mam.2021.101008

21. Tkach M, Kowal J, Théry C. Why the need and how to approach the functional diversity of extracellular vesicles. *Philos Trans R Soc Lond B Biol Sci* (2018) 373 (1737):20160479. doi: 10.1098/rstb.2016.0479

22. Théry C, Witwer K, Aikawa E, Alcaraz MJ, Anderson JD, Andriantsitohaina R, et al. Minimal information for studies of extracellular vesicles 2018 (MISEV2018): a

position statement of the international society for extracellular vesicles and update of the MISEV2014 guidelines. *J Extracell Vesicles* (2018) 7(1):1535750. doi: 10.1080/20013078.2018.1535750

23. Forte D, Barone M, Palandri F, Catani L. The "Vesicular intelligence" strategy of blood cancers. *Genes (Basel)* (2021) 12(3):416. doi: 10.3390/genes12030416

24. Hassanpour M, Rezaie J, Nouri M, Panahi Y. The role of extracellular vesicles in COVID-19 virus infection. *Infect Genet Evol* (2020) 85:104422. doi: 10.1016/j.meegid.2020.104422

25. Gurunathan S, Kang MH, Kim JH. Diverse effects of exosomes on COVID-19: a perspective of progress from transmission to therapeutic developments. *Front Immunol* (2021) 12:716407. doi: 10.3389/fimmu.2021.716407

26. Cappellano G, Raineri D, Rolla R, Giordano M, Puricelli C, Vilardo B, et al. Circulating platelet-derived extracellular vesicles are a hallmark of sars-Cov-2 infection. *Cells* (2021) 10(1):85. doi: 10.3390/cells10010085

27. Zaid Y, Puhm F, Allaeys I, Naya A, Oudghiri M, Khalki L, et al. Platelets can associate with SARS-Cov-2 RNA and are hyperactivated in COVID-19. *Circ Res* (2020) 127(11):1404–18. doi: 10.1161/CIRCRESAHA.120.317703

28. Puhm F, Flamand L, Boilard E. Platelet extracellular vesicles in COVID-19: potential markers and makers. *J Leukoc Biol* (2022) 111(1):63–74. doi: 10.1002/JLB.3MIR0221-100R

29. Wang J, Chen S, Bihl J. Exosome-mediated transfer of ACE2 (Angiotensin-converting enzyme 2) from endothelial progenitor cells promotes survival and function of endothelial cell. *Oxid Med Cell Longev* (2020) 2020:4213541. doi: 10.1155/2020/4213541

30. Xia X, Yuan P, Liu Y, Wang Y, Cao W, Zheng JC. Emerging roles of extracellular vesicles in COVID-19, a double-edged sword? *Immunology* (2021) 163(4):416–30. doi: 10.1111/imm.13329

31. Inal JM. Decoy ACE2-expressing extracellular vesicles that competitively bind SARS-CoV-2 as a possible COVID-19 therapy. *Clin Sci (Lond)* (2020) 134(12):1301–4. doi: 10.1042/CS20200623

32. Rosell A, Havervall S, von Meijenfeldt F, Hisada Y, Aguilera K, Grover SP, et al. Patients with COVID-19 have elevated levels of circulating extracellular vesicle tissue factor activity that is associated with severity and mortality-brief report. *Arterioscler Thromb Vasc Biol* (2021) 41(2):878–82. doi: 10.1161/ATVBAHA.120.315547

33. Goodlet KJ, Bansal S, Arjuna A, Nailor MD, Buddhdev B, Abdelrazek H, et al. COVID-19 in a lung transplant recipient: exploring the diagnostic role of circulating exosomes and the clinical impact of advanced immunosuppression. *Transpl Infect Dis* (2021) 23(2):e13480. doi: 10.1111/tid.13480

34. Inal J. Complement-mediated extracellular vesicle release as a measure of endothelial dysfunction and prognostic marker for COVID-19 in peripheral blood - letter to the Editor. *Clin Hemorheol Microcirc* (2020) 75(4):383–6. doi: 10.3233/CH-200958

35. Barberis E, Vanella VV, Falasca M, Caneapero V, Cappellano G, Raineri D, et al. Circulating exosomes are strongly involved in SARS-CoV-2 infection. *Front Mol Biosci* (2021) 8:632290. doi: 10.3389/fmolb.2021.632290

36. Pellegrino RM, Di Veroli A, Valeri A, Goracci L, Goracci L, Cruciani G, et al. LC/MS lipid profiling from human serum: a new method for global lipid extraction. *Anal Bioanal Chem* (2014) 406(30):7937–48. doi: 10.1007/s00216-014-8255-0

37. Koelmel J, Li X, Stow S, Sartain MJ, Murali A, Kemperman R, et al. Lipid annotator: towards accurate annotation in non-targeted liquid chromatography high-resolution tandem mass spectrometry (LC-HRMS/MS) lipidomics using a rapid and user-friendly software. *Metabolites* (2020) 10(3):101. doi: 10.3390/metabo10030101

38. Tsugawa H, Ikeda K, Takahashi M, Satoh A, Mori Y, Uchino H, et al. A lipidome atlas in MS-DIAL 4. *Nat Biotechnol* (2020) 38(10):1159–1163. doi: 10.1038/s41587-020-0531-2

39. Liebisch G, Fahy E, Aoki J, Dennis EA, Durand T, Ejsing CS, et al. Update on LIPID MAPS classification, nomenclature, and shorthand notation for MS-derived lipid structures. *J Lipid Res* (2020) 61(12):1539–1555. doi: 10.1194/jlr.S120001025

40. Pellegrino RM, Giulietti M, Alabed HBR, Buratta S, Urbanelli L, Piva F, et al. LipidOne: user-friendly lipidomic data analysis tool for a deeper interpretation in a systems biology scenario. *Bioinformatics* (2022) 38(6):1767–9. doi: 10.1093/bioinformatics/btab867

41. Pang Z, Zhou G, Ewald J, Chang L, Hacariz O, Basu N, et al. Using MetaboAnalyst 5.0 for LC-HRMS spectra processing, multi-omics integration and covariate adjustment of global metabolomics data. *Nat Protoc* (2022) 17(8):1750–2799. doi: 10.1038/s41596-022-00710-w

42. Record M, Silvente-Poirot S, Poirot M, Wakelam MJO. Extracellular vesicles: lipids as key components of their biogenesis and functions. *J Lipid Res* (2018) 59(8):1316–24. doi: 10.1194/jlr.E086173

43. Sahiner UM, Layhadi JA, Golebski K, Istvan Komlosi Z, Peng Y, Sekerel B, et al. Innate lymphoid cells: the missing part of a puzzle in food allergy. *Allergy* (2021) 76(7):2002–16. doi: 10.1111/all.14776

44. Trabanelli S, Chevalier MF, Martinez-Usatorre A, Gomez-Cadena A, Salome B, Lecciso M, et al. Tumour-derived PGD2 and NKp30-B7H6 engagement drives an immunosuppressive ILC2-MDSC axis. *Nat Commun* (2017) 8(1):593. doi: 10.1038/s41467-017-00678-2

45. Bernink JH, Ohne Y, Teunissen MBM, Wang J, Wu J, Krabbendam L, et al. C-kit-positive ILC2s exhibit an ILC3-like signature that may contribute to IL-17-mediated pathologies. *Nat Immunol* (2019) 20(8):992–1003. doi: 10.1038/s41590-019-0423-0

46. Hochdörfer T, Winkler C, Pardali K, Mjösberg J. Expression of c-kit discriminates between two functionally distinct subsets of human type 2 innate lymphoid cells. *Eur J Immunol* (2019) 49(6):884–93. doi: 10.1002/eji.201848006

47. Yan YY, Zhou WM, Wang YQ, Guo QR, Zhao FX, Zhu ZY, et al. The potential role of extracellular vesicles in COVID-19 treatment: opportunity and challenge. *Front Mol Biosci* (2021) 8:699929. doi: 10.3389/fmolb.2021.699929

48. Zani-Ruttenstock E, Antounians L, Khalaj K, Figueira RL, Zani A. The role of exosomes in the treatment, prevention, diagnosis, and pathogenesis of COVID-19. *Eur J Pediatr Surg* (2021) 31(4):326–34. doi: 10.1055/s-0041-1731294

49. Wu Q, Zhou L, Sun X, Yan Z, Hu C, Wu J, et al. Altered lipid metabolism in recovered SARS patients twelve years after infection. *Sci Rep* (2017) 7(1):9110. doi: 10.1038/s41598-017-09536-z

50. Skotland T, Sagini K, Sandvig K, Llorente A. An emerging focus on lipids in extracellular vesicles. *Adv Drug Deliv Rev* (2020) 159:308–21. doi: 10.1016/j.addr.2020.03.002

51. Yuyama K, Sun H, Mikami D, Mioka T, Mukai K, Igarashi Y. Lysosomal-associated transmembrane protein 4B regulates ceramide-induced exosome release. *FASEB J* (2020) 34(12):16022–33. doi: 10.1096/fj.202001599R

52. Deng Y, Rivera-Molina FE, Toomre DK, Burd CG. Sphingomyelin is sorted at the trans golgi network into a distinct class of secretory vesicle. *Proc Natl Acad Sci U S A* (2016) 113(24):6677–82. doi: 10.1073/pnas.1602875113

53. Sun Y, Saito K, Saito Y. Lipid profile characterization and lipoprotein comparison of extracellular vesicles from human plasma and serum. *Metabolites* (2019) 9(11):259. doi: 10.3390/metabo9110259

54. Thakkar S, Arora S, Kumar A, Jaswaney R, Faisaluddin M, Ammad Ud Din M, et al. A systematic review of the cardiovascular manifestations and outcomes in the setting of coronavirus-19 disease. *Clin Med Insights Cardiol* (2020) 14:1179546820977196. doi: 10.1177/1179546820977196

55. Altevogt P, Sammar M, Hüser L, Kristiansen G. Novel insights into the function of CD24: a driving force in cancer. *Int J Cancer* (2021) 148(3):546–59. doi: 10.1002/ijc.33249

56. Phan H, Longjohn M, Gormley D, Smith R, Dang-Lawson M, Matsuuchi L, et al. CD24 and IgM stimulation of b cells triggers transfer of functional b cell receptor to b cell recipients *Via* extracellular vesicles. *J Immunol* (2021) 207(12):3004–15. doi: 10.4049/jimmunol.2100025

57. Heim X, Joshkon A, Bermudez J, Bachelier R, Dubrou C, Boucraut J, et al. CD146/sCD146 in the pathogenesis and monitoring of angiogenic and inflammatory diseases. *Biomedicines* (2020) 8(12):592. doi: 10.3390/biomedicines8120592

58. Wu Z, Liu J, Chen G, Du J, Cai H, Chen X, et al. CD146 is a novel ANGPTL2 receptor that promotes obesity by manipulating lipid metabolism and energy expenditure. *Adv Sci (Weinh)* (2021) 8(6):2004032. doi: 10.1002/advs.202004032

59. Patriarca C, Macchi RM, Marschner AK, Marschner AK, Mellstedt H. Epithelial cell adhesion molecule expression (CD326) in cancer: a short review. *Cancer Treat Rev* (2012) 38(1):68–75. doi: 10.1016/j.ctrv.2011.04.002

60. Burrello J, Bianco G, Burrello A, Manno C, Maulucci F, Pileggi M, et al. Extracellular vesicle surface markers as a diagnostic tool in transient ischemic attacks. *Stroke* (2021) 52(10):3335–47. doi: 10.1161/STROKEAHA.120.033170

61. Bang OY, Chung JW, Lee MJ, Kim SJ, Cho YH, Kim GM, et al. Cancer cell-derived extracellular vesicles are associated with coagulopathy causing ischemic stroke *via* tissue factor-independent way: the OASIS-CANCER study. *PLoS One* (2016) 11(7):e0159170. doi: 10.1371/journal.pone.0159170

62. Piccirillo AR, Hyzny EJ, Beppu LY, Menk AV, Wallace CT, Hawse WF, et al. The lysophosphatidylcholine transporter MFSD2A is essential for CD8(+) memory T cell maintenance and secondary response to infection. *J Immunol* (2019) 203(1):117–26. doi: 10.4049/jimmunol.1801585

63. Gomez-Cadena A, Spehner L, Kroemer M, Khelil MB, Bouiller K, Verdeil G, et al. Severe COVID-19 patients exhibit an ILC2 NKG2D(+) population in their impaired ILC compartment. *Cell Mol Immunol* (2021) 18:484–6. doi: 10.1038/s41423-020-00596-2

64. Tang Y, Sun J, Pan H, Yao F, Yuan Y, Zeng M, et al. Aberrant cytokine expression in COVID-19 patients: associations between cytokines and disease severity. *Cytokine* (2021) 143:155523. doi: 10.1016/j.cyto.2021.155523

65. Chen Y, Wang J, Liu C, Su L, Zhang D, Fan J, et al. IP-10 and MCP-1 as biomarkers associated with disease severity of COVID-19. *Mol Med* (2020) 26(1):97. doi: 10.1186/s10020-020-00230-x

66. van den Borne P, Quax PH, Hoefer IE, Pasterkamp G. The multifaceted functions of CXCL10 in cardiovascular disease. *Biomed Res Int* (2014) 2014:893106. doi: 10.1155/2014/893106

67. Del Valle DM, Kim-Schulze S, Huang HH, Beckmann ND, Nirenberg S, Wang B, et al. An inflammatory cytokine signature predicts COVID-19 severity and survival. *Nat Med* (2020) 26(10):1636–43. doi: 10.1038/s41591-020-1051-9

68. Zhou F, Yu T, Du R, Fan G, Liu Y, Liu Z, et al. Clinical course and risk factors for mortality of adult inpatients with COVID-19 in wuhan, China: a retrospective cohort study. *Lancet* (2020) 395(10229):1054–62. doi: 10.1016/S0140-6736(20)30566-3

69. Li L, Li J, Gao M, Fan H, Wang Y, Xu X, et al. Interleukin-8 as a biomarker for disease prognosis of coronavirus disease-2019 patients. *Front Immunol* (2021) 11:602395. doi: 10.3389/fimmu.2020.602395

70. Pala D, Pistis M. Anti-IL5 drugs in COVID-19 patients: role of eosinophils in SARS-CoV-2-Induced immunopathology. *Front Pharmacol* (2021) 12:622554. doi: 10.3389/fphar.2021.622554

71. Matsuda M, Shimizu S, Kitatani K, Nabe T. Extracellular vesicles derived from allergen immunotherapy-treated mice suppressed IL-5 production from group 2 innate lymphoid cells. *Pathogens* (2022) 11(11):1373. doi: 10.3390/pathogens11111373

72. Wang Z, Mo H, He Z, Chen A, Cheng P. Extracellular vesicles as an emerging drug delivery system for cancer treatment: current strategies and recent advances. *BioMed Pharmacother* (2022) 153:113480. doi: 10.1016/j.biopha.2022.113480

73. Rowaiye A, Okpalefe O, Onuh Adejoke O, Ogidigo J, Hannah Oladipo O, Ogu A, et al. Attenuating the effects of novel COVID-19 (SARS-CoV-2) infection-induced cytokine storm and the implications. *J Inflamm Res* (2021) 14:1487–510. doi: 10.2147/JIR.S301784

frontiers | Frontiers in Immunology

TYPE Original Research
PUBLISHED 26 May 2023
DOI 10.3389/fimmu.2023.1185716

OPEN ACCESS

EDITED BY
Antonio Lalueza,
University Hospital October 12, Spain

REVIEWED BY
Andrew Weber,
Northwell Health, United States
Doreen E Szollosi,
University of Saint Joseph, United States

*CORRESPONDENCE
Robin Arcani
robin.arcani@ap-hm.fr

†These authors have contributed equally to this work and share first authorship

‡These authors have contributed equally to this work and share last authorship

RECEIVED 13 March 2023
ACCEPTED 15 May 2023
PUBLISHED 26 May 2023

CITATION
Arcani R, Correard F, Suchon P, Kaplanski G, Jean R, Cauchois R, Leprince M, Arcani V, Seguier J, De Sainte Marie B, Andre B, Koubi M, Rossi P, Gayet S, Gobin N, Garrido V, Weiland J, Jouve E, Couderc A-L, Villani P and Daumas A (2023) Tocilizumab versus anakinra in COVID-19: results from propensity score matching. *Front. Immunol.* 14:1185716. doi: 10.3389/fimmu.2023.1185716

Tocilizumab versus anakinra in COVID-19: results from propensity score matching

Robin Arcani[1,2*†], Florian Correard[3†], Pierre Suchon[4], Gilles Kaplanski[2,5], Rodolphe Jean[5], Raphael Cauchois[2,5], Marine Leprince[5], Vincent Arcani[3], Julie Seguier[6], Benjamin De Sainte Marie[6], Baptiste Andre[6], Marie Koubi[7], Pascal Rossi[7], Stéphane Gayet[1], Nirvina Gobin[1], Victoria Garrido[1], Joris Weiland[1], Elisabeth Jouve[8], Anne-Laure Couderc[9,10], Patrick Villani[1,10‡] and Aurélie Daumas[1,2‡]

[1]Internal Medicine and Therapeutics Department, CHU La Timone, Assistance Publique-Hôpitaux de Marseille (AP-HM), Marseille, France, [2]Center for Cardiovascular and Nutrition Research (C2VN), INRA 1260, INSERM UMR_S 1263, Aix-Marseille University, Marseille, France, [3]Pharmacy Department, CHU La Timone, AP-HM, Marseille, France, [4]Hematology Laboratory, CHU La Timone, Assistance Publique-Hôpitaux de Marseille (AP-HM), Marseille, France, [5]Internal Medicine and Clinical Immunology Department, CHU La Conception, Assistance Publique-Hôpitaux de Marseille (AP-HM), Marseille, France, [6]Internal Medicine Department, CHU La Timone, Assistance Publique-Hôpitaux de Marseille (AP-HM), Marseille, France, [7]Department of Internal Medicine, CHU Nord, Assistance Publique-Hôpitaux de Marseille (AP-HM), Marseille, France, [8]Service Evaluation Médicale, CHU la Conception, Assistance Publique-Hôpitaux de Marseille (AP-HM), Marseille, France, [9]Internal Medicine, Geriatrics and Therapeutic Department, CHU Sainte-Marguerite, Assistance Publique-Hôpitaux de Marseille (AP-HM), Marseille, France, [10]Aix-Marseille University, CNRS, EFS, ADES, Marseille, France

Background: Tocilizumab and anakinra are anti-interleukin drugs to treat severe coronavirus disease 2019 (COVID-19) refractory to corticosteroids. However, no studies compared the efficacy of tocilizumab versus anakinra to guide the choice of the therapy in clinical practice. We aimed to compare the outcomes of COVID-19 patients treated with tocilizumab or anakinra.

Methods: Our retrospective study was conducted in three French university hospitals between February 2021 and February 2022 and included all the consecutive hospitalized patients with a laboratory-confirmed severe acute respiratory syndrome coronavirus 2 (SARS-CoV-2) infection assessed by RT-PCR who were treated with tocilizumab or anakinra. A propensity score matching was performed to minimize confounding effects due to the non-random allocation.

Results: Among 235 patients (mean age, 72 years; 60.9% of male patients), the 28-day mortality (29.4% *vs.* 31.2%, p = 0.76), the in-hospital mortality (31.7% *vs.* 33.0%, p = 0.83), the high-flow oxygen requirement (17.5% *vs.* 18.3%, p = 0.86), the intensive care unit admission rate (30.8% *vs.* 22.2%, p = 0.30), and the mechanical ventilation rate (15.4% *vs.* 11.1%, p = 0.50) were similar in patients receiving tocilizumab and those receiving anakinra. After propensity score

10.3389/fimmu.2023.1185716

matching, the 28-day mortality (29.1% *vs.* 30.4%, p = 1) and the rate of high-flow oxygen requirement (10.1% *vs.* 21.5%, p = 0.081) did not differ between patients receiving tocilizumab or anakinra. Secondary infection rates were similar between the tocilizumab and anakinra groups (6.3% *vs.* 9.2%, p = 0.44).

Conclusion: Our study showed comparable efficacy and safety profiles of tocilizumab and anakinra to treat severe COVID-19.

KEYWORDS

anakinra, tocilizumab, anti-interleukin drugs, COVID-19, mortality, SARS-CoV-2, anti-interleukin 6, interleukin 1 receptor antagonist

1 Introduction

Coronavirus disease 2019 (COVID-19) is caused by severe acute respiratory syndrome coronavirus 2 (SARS-CoV-2) (1) and has led to more than 6 million deaths around the world (2). COVID-19 can range from a simple asymptomatic viral infection to acute respiratory distress syndrome (ARDS) requiring intensive care; 15%–20% of hospitalized patients develop severe pneumonia (3, 4). Currently, the standard of care for in-hospitalized patients requiring oxygen is based on corticosteroids (5, 6), which have broad-spectrum anti-inflammatory actions. Despite the extensive use of dexamethasone, 15%–30% of patients remain refractory to corticosteroids and require intubation or progress to death (5–7).

Tocilizumab (an interleukin (IL)-6 receptor antagonist) and anakinra (an IL-1 receptor antagonist) have been proven effective in reducing mortality in patients with severe inflammatory COVID-19 (8–12). In France, since 2021, the French High Council for Public Health (HCSP) recommends adding anti-IL-6 or anti-IL-1 drugs in patients requiring high-flow oxygen therapy and having a marked inflammatory state in the absence of improvement (C-reactive protein (CRP) >75 mg/L) after 48 h of the standard of care, including dexamethasone (13). However, to date, there is no evidence showing which anti-IL drug is the most effective. Scarce data have compared the efficacy of tocilizumab versus anakinra in dexamethasone-refractory COVID-19 patients (14, 15). We aimed to retrospectively compare the outcomes of dexamethasone-refractory COVID-19 patients treated with tocilizumab or anakinra using propensity score matching.

2 Materials and methods

2.1 Patients

We retrospectively included all consecutive adult patients (aged ≥18 years) admitted with a laboratory-confirmed SARS-CoV-2 infection assessed by RT-PCR on nasopharyngeal swabs requiring oxygen, who were dexamethasone-refractory (defined by an absence of clinical improvement and/or an absence of a decrease in CRP after 72 h of dexamethasone) and treated with tocilizumab or anakinra between February 2021 and February 2022 in six internal medicine departments in three hospitals (La Timone, La Conception and Hôpital Nord, and University Hospitals of Marseille, France). Patients were not included if they had received both anti-IL drugs or one anti-IL and one JAK inhibitor to treat COVID-19 or if there were insufficient patient follow-up data to perform analysis (e.g., patient transferred to another hospital).

Clinical, biological, radiological, and follow-up data were collected from electronic medical records. Patients were divided into three groups based on low-dose chest computed tomography (CT) extent of lung parenchymal lesions (minimal, <10%; moderate, 10%–25%; and severe, >25%). The vaccine status of the patients was unvaccinated, partially vaccinated, or fully vaccinated (0, 1, or 2 doses received, respectively).

Patients received tocilizumab (8 mg/kg, 800 mg maximum) intravenously over a 1-h infusion once or repeated after 24 h, according to the opinion of the attending clinician. Patients were treated with subcutaneous anakinra 100 mg/day until clinical improvement (maximum 10 days) or with 300 mg/day for 5 days and then tapering 200 mg/day for 2 days and 100 mg/day for 1 day. All patients were treated with dexamethasone (6 mg/day, administered intravenously, until oxygen discontinuation). Patients could also have received anti-spike monoclonal antibodies [casirivimab/imdevimab (Ronapreve®), or sotrovimab (Xevudy®) according to the SARS-CoV-2 variants], antibiotics, and prophylactic (enoxaparin 40 mg/day), intermediate (enoxaparin 40 mg twice a day), or therapeutic (tinzaparin 175 anti-Xa IU/kg/day) thromboprophylaxis according to the current recommendations from the French Society of Critical Care (16) until discharge.

Patients were considered under immunosuppressive therapy when they took anti-rejection therapy, immunosuppressive therapy, corticosteroids > 10 mg/day, biotherapy, or chemotherapy before COVID-19. Patients were considered with a secondary infection when they needed a new antibiotic 48 h after the introduction of the anti-IL drug or when a new bacterial infection was identified (by culture or molecular testing).

Abbreviations: COVID-19, coronavirus disease 2019; SARS-CoV-2, severe acute respiratory syndrome coronavirus; ARDS, acute respiratory distress syndrome; IL, interleukin; HCSP, High Council for Public Health; CT, computed tomography; SD, standard deviations; ICU, intensive care unit.

2.2 Ethics

This study was approved by the Institutional Review Board of Assistance Publique - Hôpitaux de Marseille (GDPR number PADS22-339). The study was conducted in compliance with good clinical practices and the Declaration of Helsinki principles. Formal approval from an ethics committee was not required for this observational study.

2.3 Statistical analysis

Quantitative variables were described using means and standard deviations (SD); categorical variables were described using numbers and percentages. Quantitative data were compared using Student's t-test or the Mann–Whitney U test, while qualitative data were compared with the chi-square or Fisher's exact test when appropriate. A propensity score matching was performed to minimize confounding effects due to the non-random allocation. The propensity score matching function matched the two groups of patients with an anti-IL drug (tocilizumab or anakinra) as the dependent variable. Based on risk factors described in the literature (17–21), propensity score matching of 1:1 was performed with age, sex, vaccine status (partial/full versus none), the extent of lung involvement, comorbidities (hypertension, cancer, chronic kidney disease, diabetes, and obesity), a high-flow requirement before anti-IL introduction, CRP level at the anti-IL drug introduction, use of anti-spike monoclonal antibodies, and thromboprophylaxis as covariates using the optimal method. To confirm the results found with the optimal method, we performed the nearest neighbor propensity score matching method (caliper = 0.25). After matching, McNemar's test was used to test the association of the mortality rate/rate of high-flow oxygen requirement with the anti-IL drug between matched pairs. The tests were two-sided. p-Values <0.05 were considered significant. All analyses were performed with R software (R Foundation for Statistical Computing, Vienna, Austria), and the propensity score was performed with the MatchIt package.

3 Results

3.1 Characteristics of the population

During the study period, 259 patients were treated with anti-IL drugs; 19 patients were excluded because they received tocilizumab and anakinra (n = 16) or JAK inhibitor and anakinra (n = 3), and five patients were excluded because of a lack of follow-up data. A total of 235 patients were included in the analysis. The main characteristics of the population are presented in Table 1. The mean age was 72 ± 15 years (range, 28–99), with 143 male patients (60.9%). The main comorbidities were hypertension (51.5%), type 2 diabetes (34.0%), obesity (23.4%), overweight (19.4%), chronic kidney disease (18.7%), coronary artery disease (14.0%), pulmonary diseases (chronic obstructive pulmonary disease, asthma, or obstructive sleep apnea, 13.6%), and active cancer (13.2%). Of the total patients, 21 (8.9%) received previous immunosuppressive therapy, and 116 (49.4%) had a "not to be resuscitated" status.

Vaccine status was available for 229 patients: 61 patients (26.6%) received at least one dose of vaccine, 12 patients (5.2%) were partially vaccinated (only one dose of vaccine), and 49 (21.4%) were fully vaccinated (two doses of vaccine). Assessment of SARS-CoV-2 variants was available in 111 patients: 25 (22.5%) carried the alpha variant, 5 (4.5%) carried the beta variant, 51 (45.9%) carried the delta variant, and 30 (27.0%) carried the omicron variant. Lung CT showed typical lesions of COVID-19 in 212 out of 220 patients (96.4%), consisting of minimal, moderate, and severe lesions in 11.8%, 34.5%, and 50.0%, respectively. Of 152 patients (64.7%) who received antibiotics, 117 of them (49.8%) received third-generation cephalosporin, 83 patients (35.3%) received azithromycin, 56 patients (23.8%) received piperacillin–tazobactam, and 11 patients (4.7%) received carbapenem. Sixty-six patients (28.1%) received only one antibiotic, 61 patients (26.0%) received two antibiotics, 21 patients (8.9%) received three antibiotics, and four patients (1.7%) received four antibiotics. Of 235 patients, 231 (98.3%) were treated with low-molecular-weight heparin at prophylactic, intermediate, or therapeutic doses of 36.2%, 27.7%, and 34.5%, respectively; 22 patients (9.4%) were treated with monoclonal anti-spike antibodies; 150 patients (63.8%) were treated with an anti-IL drug once under high-flow oxygen. At the time of anti-IL introduction, ferritin was 1,496 ± 1,442 µg/L (range, 96–10,555), and C-reactive protein was 123 ± 77 mg/L (range, 8–351).

3.2 Comparisons of the baseline characteristics between patients receiving tocilizumab and anakinra

A total of 126 (53.6%) patients received tocilizumab, and 109 (46.4%) patients received anakinra (Table 1). The two cohorts were similar in age, gender, and main comorbidities (hypertension, coronaropathy disease, obesity, overweight, and cancer). There were some differences between the two cohorts in terms of vaccine status (fully vaccinated patients: 15.1% of the tocilizumab group *vs.* 29.1% of the anakinra group, p = 0.01), extent of lung involvement (42.0% of intermediate lesions in the tocilizumab group *vs.* 25.7% in the anakinra group, p = 0.011; 41.2% of severe lesions in the tocilizumab group *vs.* 60.4% in the anakinra group, p = 0.0045), SARS-CoV-2 variants (47.8% of alpha variant in the tocilizumab group *vs.* 4.6% in the anakinra group, p < 0.001; 2.2% of omicron variant in the tocilizumab group *vs.* 44.6% in the anakinra group, p < 0.001), comorbidities (9.5% of the tocilizumab group had pulmonary diseases *vs.* 18.3% of the anakinra group, p = 0.049; 11.9% of the tocilizumab group had chronic kidney disease *vs.* 24.4% of the anakinra group, p = 0.0040; 4.0% of the tocilizumab group were under immunosuppressive therapy *vs.* 14.7% of the anakinra group, p = 0.0041), severity of clinical state (82.5% of the tocilizumab group were under high-flow oxygen before anti-IL introduction *vs.* 42.2% of the anakinra group, p < 0.001), thromboprophylaxis management (45.2% of the tocilizumab group received prophylactic dose of low-molecular-weight

10.3389/fimmu.2023.1185716

TABLE 1 Description of the cohort.

Characteristics	Tocilizumab group (n = 126)	Anakinra group (n = 109)	Overall population (n = 235)	p-Value[a]
Age[b]	73 ± 15 (32–98)	72 ± 16 (28–99)	72 ± 15 (28–99)	0.71
Male gender	76 (60.3)	67 (61.5)	143 (60.9)	0.86
Length of hospitalization[b]	13 ± 10 (1–89)	13 ± 8 (4–44)	13 ± 9 (1–89)	0.95
Vaccinated - Partially - Fully	28 (22.2) 9 (7.1) 19 (15.1)	33/103 (32.0) 3/103 (2.9) 30/103 (29.1)	61/229 (26.6) 12/229 (5.2) 49/229 (21.4)	0.095 0.15 **0.0099**
Body mass index (kg/m^2) [b]	28 ± 7 (16–57)	26 ± 6 (16–43)	27 ± 6 (16–57)	0.20
Extent of lung involvement - No COVID-19 lesion - <10% - 10%–25% - >25%	 4/119 (3.4) 16/119 (13.4) 50/119 (42.0) 49/119 (41.2)	 4/101 (4.0) 10/101 (9.9) 26/101 (25.7) 61/101 (60.4)	 8/220 (3.6) 26/220 (11.8) 76/220 (34.5) 110/220 (50)	 0.81 0.42 **0.011** **0.0045**
SARS-CoV-2 variant - Alpha variant - Beta variant - Delta variant - Omicron variant	 22/46 (47.8) 2/46 (4.3) 21/46 (45.7) 1/46 (2.2)	 3/65 (4.6) 3/65 (4.6) 30/65 (46.2) 29/65 (44.6)	 25/111 (22.5) 5/111 (4.5) 51/111 (45.9) 30/111 (27.0)	 **<0.001** 0.95 0.96 **<0.001**
Comorbidities - Hypertension - Coronaropathy disease - Stroke - Venous thromboembolism - Pulmonary diseases - Cancer - Chronic kidney disease - Diabetes - Obesity - Overweight - Immunosuppressive therapy	 62 (49.2) 13 (10.3) 2 (1.6) 2 (1.6) 12 (9.5) 18 (14.3) 15 (11.9) 36 (28.6) 26/116 (22.4) 23/116 (19.8) 5 (4.0)	 59 (49.6) 20 (18.3) 7 (6.4) 2 (1.8) 20 (18.3) 13 (11.9) 29 (24.4) 44 (40.4) 21/85 (24.7) 16/85 (18.8) 16 (14.7)	 121 (51.5) 33 (14.0) 9 (3.8) 4 (1.7) 32 (13.6) 31 (13.2) 44 (18.7) 80 (34.0) 47/201 (23.4) 39/201 (19.4) 21 (8.9)	 0.45 0.077 0.054 0.88 **0.049** 0.59 **0.0040** 0.057 0.70 0.86 **0.0041**
High-flow oxygen introduction before anti-interleukin introduction	104 (82.5)	46 (42.2)	150 (63.8)	**<0.001**
Ferritin (µg/L) at anti-interleukin introduction[b]	1,393 ± 1,225 (118–6,607)	1,571 ± 1,584 (96–10,555)	1,496 ± 1,442 (96–10,555)	0.42
CRP (mg/L) at anti-interleukin introduction[b]	119 ± 76 (8–349)	129 ± 79 (17–351)	123 ± 77 (8–351)	0.30
Associated therapies - Anti-spike monoclonal antibody - Any antibiotics - Third-generation cephalosporin - Azithromycin - Piperacillin–tazobactam - Carbapenem - Prophylactic thromboprophylaxis - Intermediate thromboprophylaxis - Therapeutic thromboprophylaxis	 0 (0) 56 (44.4) 41 (32.5) 15 (11.9) 17 (13.5) 0 (0) 57 (45.2) 30 (23.8) 37 (29.4)	 22 (20.2) 96 (88.1) 76 (69.7) 68 (62.4) 39 (35.8) 11 (10.1) 28 (25.7) 35 (32.1) 44 (40.4)	 22 (9.4) 152 (64.7) 117 (49.8) 83 (35.3) 56 (23.8) 11 (4.7) 85 (36.2) 65 (27.7) 81 (34.5)	 **<0.001** **<0.001** **<0.001** **<0.001** **<0.001** **<0.001** **0.0019** 0.16 0.077

Note. p-Value <0.05 in bold.
CRP, C-reactive protein.
[a]Comparison between tocilizumab and anakinra groups.
[b]Mean ± standard deviation (range).

heparin *vs.* 25.7% of the anakinra group, p = 0.0019), or associated therapies (0% of the tocilizumab group received anti-spike monoclonal antibody *vs.* 20.2% of the anakinra group, p < 0.001; 44.4% of the tocilizumab group received antibiotics *vs.* 88.1% of the anakinra group, p < 0.001).

After propensity score matching using the optimal method (Table 2), 79 patients treated with tocilizumab and 79 patients treated with anakinra had similar characteristics (except for anti-spike monoclonal antibodies; no patients in the tocilizumab group received anti-spike monoclonal antibodies *vs.* 26.6% of the anakinra

10.3389/fimmu.2023.1185716

TABLE 2 Patient characteristics after matching (optimal method).

Characteristics	Tocilizumab group (n = 79)	Anakinra group (n = 79)	p-Value[a]
Age[b]	74 (15)	70 (16)	0.11
Male gender	44 (55.7)	51 (64.6)	0.33
Vaccinated (partially or fully)	22 (27.8)	23 (29.1)	1
Extent of lung involvement - No COVID-19 lesion - <10% - 10%–25% - >25%	 5 (6.3) 10 (12.7) 25 (31.6) 35 (44.3)	 5 (6.3) 8 (10.1) 19 (24.1) 44 (55.7)	0.70
Hypertension	42 (53.2)	39 (49.4)	0.7
Cancer	10 (12.7)	8 (10.1)	0.80
Chronic kidney disease	11 (13.9)	18 (22.8)	0.22
Diabetes	23 (29.1)	29 (36.7)	0.40
Obesity	14 (17.7)	21 (26.6)	0.25
CRP (mg/L) at anti-interleukin introduction[b]	125 (82)	130 (80)	0.70
Anti-spike monoclonal antibody	0 (0)	21 (26.6)	**<0.001**
Associated anticoagulant: - No anticoagulant - Prophylactic thromboprophylaxis - Intermediate thromboprophylaxis - Therapeutic thromboprophylaxis	 2 (2.5) 24 (30.4) 26 (32.9) 27 (34.2)	 1 (1.3) 21 (26.6) 29 (36.7) 28 (35.4)	0.87
High-flow oxygen introduction before anti-interleukin introduction	58 (73.4)	34 (43.0)	**<0.001**

Note. p-Value <0.05 in bold.
CRP, C-reactive protein.
[a]Comparison between tocilizumab and anakinra groups.
[b]Mean ± standard deviation (range).

group, p < 0.001; for high-flow oxygen introduction before anti-IL introduction, 73.4% were under high-flow oxygen at tocilizumab introduction *vs.* 43.0% at anakinra introduction). Because of the imbalance of covariates between the two groups, we performed a propensity score matching using the nearest neighbor method (Table 3). Similar characteristics were found in 36 patients treated with tocilizumab and 36 patients treated with anakinra.

3.3 Outcomes of patients under anti-IL drugs

The 28-day mortality was similar between the two groups (29.4% in the tocilizumab group *vs.* 31.2% in the anakinra group, p = 0.76), as was in-hospital mortality (31.7% in the tocilizumab group *vs.* 33.0% in the anakinra group, p = 0.83). High-flow oxygen was required in similar proportions (17.5% in the tocilizumab group *vs.* 18.3% in the anakinra group, p = 0.86). Among patients without a "not to be resuscitated" status (n = 119), the transfer rate into intensive care units (ICUs) was similar between the two groups (30.8% in the tocilizumab group *vs.* 22.2% in the anakinra group, p = 0.30). The secondary infections following anti-IL drugs were quite scarce (6.3% in the tocilizumab group *vs.* 9.2% in the anakinra group, p = 0.44) (Table 4).

After propensity score matching using the optimal method, the 28-day mortality (29.1% in the tocilizumab group *vs.* 30.4% in the anakinra group, p = 1) and the rate of high-flow oxygen requirement (10.1% in the tocilizumab group *vs.* 21.5% in the anakinra group, p = 0.081) did not differ between the two groups. Using the nearest neighbor method, we found a similar 28-day mortality (33.3% in the tocilizumab group *vs.* 30.6% in the anakinra group, p = 1) and a similar rate of high-flow oxygen requirement (5.6% in the tocilizumab group *vs.* 13.9% in the anakinra group, p = 0.43) between the pseudo-populations.

4 Discussion

We reported a cohort of hospitalized COVID-19 before ICU admission and intubation who were treated with an anti-IL drug. We showed that the 28-day mortality and the high-flow oxygen requirement did not differ according to the treatment received, tocilizumab or anakinra. The two treatments had the same risk of infections.

These results follow the few data available about this subject. IL-1 and IL-6 are two cytokines mainly involved in cytokine storm initiation and amplification, particularly in COVID-19 ARDS (22). Anakinra is an IL-1-receptor antagonist blocking the effect of both

10.3389/fimmu.2023.1185716

TABLE 3 Patient characteristics after matching (nearest neighbor method).

Characteristics	Tocilizumab group (n = 36)	Anakinra group (n = 36)	p-Value[a]
Age[b]	74 (16)	69 (17)	0.25
Male gender	19 (52.8)	20 (55.6)	1
Vaccinated (partially or fully)	14 (38.9)	10 (27.8)	0.45
Extent of lung involvement - No COVID-19 lesion - <10% - 10%–25% - >25%	 2 (5.6) 5 (13.9) 8 (22.2) 18 (50)	 1 (2.8) 4 (11.1) 13 (36.1) 16 (44.4)	0.74
Hypertension	21 (58.3)	16 (44.4)	0.35
Cancer	4 (11.1)	3 (8.3)	1
Chronic kidney disease	7 (19.4)	5 (13.9)	0.75
Diabetes	9 (25)	9 (25)	1
Obesity	8 (22.2)	9 (25)	1
CRP (mg/L) at anti-interleukin introduction[b]	136 (79)	119 (75)	0.41
Monoclonal anti-spike antibody	0 (0)	0 (0)	
Associated anticoagulant: - No anticoagulant - Prophylactic thromboprophylaxis - Intermediate thromboprophylaxis - Therapeutic thromboprophylaxis	 1 (2.8) 14 (38.9) 11 (30.6) 10 (27.8)	 1 (2.8) 12 (33.3) 14 (38.9) 9 (25)	0.90
High-flow oxygen introduction before anti-interleukin introduction	12 (33.3)	14 (38.9)	0.81

Note. CRP, C-reactive protein.
[a]Comparison between tocilizumab and anakinra groups.
[b]Mean ± standard deviation (range).

IL-1α and IL-1β. IL-1β leads to the production of IL-6 (23). However, tocilizumab blocks IL-6-mediated signal transduction by targeting both the membrane and soluble forms of the IL-6 receptor (24). Thus, it seems logical that the use of tocilizumab or anakinra could be effective in COVID-19. A large amount of data in the literature confirm the efficacy of the two anti-IL drugs (10, 25–27).

However, to date, randomized trials comparing the efficacy of different agents are lacking. The effect of tocilizumab and anakinra seems similar among all the meta-analyses (28–31). One Turkish study compared many patients receiving tocilizumab or anakinra using propensity score matching (15). The authors concluded a lower mortality and ICU transfer rate in the anakinra group. However, in this cohort, patients received very high doses of anakinra (600 mg daily mean versus 100 mg daily in most studies) and were also treated with hydroxychloroquine and favipiravir. Finally, the patients in the tocilizumab group received less corticosteroid than in the anakinra group, which is a major bias. Langer-Gould et al. (32) compared 52 patients treated with tocilizumab to 41 patients treated with anakinra using a propensity score matching and found no statistical difference in mortality. Some other studies, with a few participants, have directly compared tocilizumab to anakinra. Iglesias-Julian et al. (33) showed the same mortality under tocilizumab or anakinra. Patoulias et al.

TABLE 4 Outcomes of the cohort.

Outcome	Tocilizumab group (n = 126)	Anakinra group (n = 109)	Overall population (n = 235)	p-Value[a]
Secondary infection	8 (6.3)	10 (9.2)	16 (6.8)	0.44
High-flow oxygen	22 (17.5)	20 (18.3)	42 (17.9)	0.86
Intensive care unit transfer	20/65 (30.8)	12/54 (22.2)	32/119 (26.9)	0.30
Mechanical ventilation	10/65 (15.4)	6/54 (11.1)	16/119 (13.4)	0.50
28-day mortality	37 (29.4)	34 (31.2)	71 (30.2)	0.76
In-hospital mortality	40 (31.7)	36 (33.0)	76 (32.2)	0.83

[a]Comparison between tocilizumab and anakinra groups.

(14) performed a meta-analysis on three non-randomized studies comparing 125 patients under tocilizumab to 112 patients under anakinra and found lower mortality in the anakinra group. Unfortunately, they did not adjust their results with confounding factors. To the best of our knowledge, here, we report one of the largest cohorts of patients treated with tocilizumab compared to anakinra using an adjustment on confounding factors.

We acknowledge some limitations of this study. First, it was retrospective, but we could compare the patients using propensity score matching despite the absence of randomization. We used a combination of clinical, biological, and radiological prognosis factors to build our propensity score matching. Second, the patients were recruited over a large period, including patients infected by different variants of SARS-CoV-2. We could not add variants in the propensity score matching because there were too much missing data, which would have led to the inability to build the propensity score matching. Furthermore, we included a few patients with the omicron variant, which is now dominating. However, there is no evidence that the SARS-CoV-2 omicron variant changes the response to the anti-inflammatory therapy (34, 35). In effect, even if the omicron variant is less severe than the others, thanks to the propensity score matching, we could compare patients with COVID-19 with the same severity (according to the extent of lung involvement, the CRP level, or the rate of high-flow requirement before anti-IL introduction, which are well-known factors of severity). We also acknowledge the lack of assessment of inflammatory biomarkers such as interleukin-6 and soluble urokinase plasminogen activator receptor (suPAR) at baseline. Nevertheless, their utility was not clear, hyperinflammation was defined by CRP and ferritin levels, and IL-6 and suPAR are not routinely available biomarkers in all the centers. Furthermore, the two groups could not be matched on anti-spike monoclonal antibodies (using the optimal method) because no patients in the tocilizumab group have received these treatments (they were not available during the second and third waves when most patients receiving tocilizumab were included). Therefore, we performed a second propensity score matching, in which the use of anti-spike monoclonal antibodies was balanced between the two groups. Despite the small sample size, similar results were found with this method. Moreover, the rate of antibiotic prescriptions was different between the two groups. However, there is no evidence in the literature showing that antibiotics influence the response to anti-IL drugs or the evolution of COVID-19 (36–38).

Since the efficacy of tocilizumab seems to be similar to the efficacy of anakinra, clinicians should consider the cost of the treatment to choose it. In France, the cost of a 10-day anakinra course is lower than that of an 8 mg/kg dose of tocilizumab. In our study, the average cost of tocilizumab per patient was 1,052€/1,124 USD compared to 189€/202 USD per patient treated with anakinra. Moreover, the half-life of anakinra [a few hours (39)] is lower than that of tocilizumab [14–21 days (40)]. In patients with secondary infection due to the anti-IL drug, the infection would be easier to manage with a short half-life therapy such as anakinra than with tocilizumab.

Despite the small sample sizes of groups after propensity score matching, our study showed the same efficacy and secondary infection risk of tocilizumab and anakinra to treat severe COVID-19. Thus, anakinra and tocilizumab represented equivalent therapies in conjunction with corticosteroids. Our results need to be confirmed in larger randomized studies in order to choose the most effective and personalized treatment plans for each patient.

Data availability statement

The raw data supporting the conclusions of this article will be made available by the corresponding authors, upon reasonable request.

Ethics statement

The studies involving human participants were reviewed and approved by Portail d'Accès aux Données de Santé - Assistance Publique Hôpitaux de Marseille. Written informed consent for participation was not required for this study in accordance with the national legislation and the institutional requirements.

Author contributions

RA, FC, PS, PV and AD contributed to the design of the study. All the authors participated in the enrolment of study participants and data collection. RA and PS analyzed the data. RA, FC, PV and AD drafted the manuscript. All authors contributed to the data interpretation and in revising the final manuscript. All authors contributed to the article and approved the submitted version.

Conflict of interest

GK has received from ROCHE-CHUGAI Research Grants < €20,000 and fees from Sobi France for scientific presentations < €4,000 and participated in a SOBI Advisory Board on COVID unpaid and an OLATEC Monitoring Board unpaid.

The remaining authors declare that the research was conducted in the absence of any commercial or financial relationships that could be construed as a potential conflict of interest.

Publisher's note

References

1. *WHO director-general's remarks at the media briefing on 2019-nCoV on 11 February 2020*. Available at: https://www.who.int/director-general/speeches/detail/who-director-general-s-remarks-at-the-media-briefing-on-2019-ncov-on-11-february-2020 (Accessed February 3, 2021).

2. *WHO coronavirus (COVID-19) dashboard*. Available at: https://covid19.who.int (Accessed April 25, 2021).

3. Chen G, Wu D, Guo W, Cao Y, Huang D, Wang H, et al. Clinical and immunological features of severe and moderate coronavirus disease 2019. *J Clin Invest* (2022) 130:2620–9. doi: 10.1172/JCI137244

4. Ramasamy S, Subbian S. Critical determinants of cytokine storm and type I interferon response in COVID-19 pathogenesis. *Clin Microbiol Rev* (2021) 34:e00299-20. doi: 10.1128/CMR.00299-20

5. RECOVERY Collaborative Group, Horby P, Lim WS, Emberson JR, Mafham M, Bell JL, et al. Dexamethasone in hospitalized patients with covid-19. *N Engl J Med* (2021) 384:693–704. doi: 10.1056/NEJMoa2021436

6. Arcani R, Cauchois R, Suchon P, Jean R, Jarrot P-A, Gomes De Pinho Q, et al. Factors associated with dexamethasone efficacy in COVID-19. a retrospective investigative cohort study. *J Med Virol* (2022) 94:3169–75. doi: 10.1002/jmv.27712

7. Munch MW, Myatra SN, Vijayaraghavan BKT, Saseedharan S, Benfield T, Wahlin RR, et al. Effect of 12 mg vs 6 mg of dexamethasone on the number of days alive without life support in adults with COVID-19 and severe hypoxemia. *JAMA* (2021) 326:1–11. doi: 10.1001/jama.2021.18295

8. Salama C, Han J, Yau L, Reiss WG, Kramer B, Neidhart JD, et al. Tocilizumab in patients hospitalized with covid-19 pneumonia. *N Engl J Med* (2021) 384:20–30. doi: 10.1056/NEJMoa2030340

9. RECOVERY Collaborative Group. Tocilizumab in patients admitted to hospital with COVID-19 (RECOVERY): a randomised, controlled, open-label, platform trial. *Lancet* (2021) 397:1637–45. doi: 10.1016/S0140-6736(21)00676-0

10. Kyriazopoulou E, Huet T, Cavalli G, Gori A, Kyprianou M, Pickkers P, et al. Effect of anakinra on mortality in patients with COVID-19: a systematic review and patient-level meta-analysis. *Lancet Rheumatol* (2021) 3:e690–7. doi: 10.1016/S2665-9913(21)00216-2

11. Kyriazopoulou E, Poulakou G, Milionis H, Metallidis S, Adamis G, Tsiakos K, et al. Early treatment of COVID-19 with anakinra guided by soluble urokinase plasminogen receptor plasma levels: a double-blind, randomized controlled phase 3 trial. *Nat Med* (2021) 27:1752–60. doi: 10.1038/s41591-021-01499-z

12. Cavalli G, De Luca G, Campochiaro C, Della-Torre E, Ripa M, Canetti D, et al. Interleukin-1 blockade with high-dose anakinra in patients with COVID-19, acute respiratory distress syndrome, and hyperinflammation: a retrospective cohort study. *Lancet Rheumatol* (2020) 2:e325–31. doi: 10.1016/S2665-9913(20)30127-2

13. *Covid-19: IL1 and IL6 antagonist treatment recommendations*. Available at: https://www.hcsp.fr/Explore.cgi/AvisRapportsDomaine?clefr=1110 (Accessed August 26, 2022).

14. Patoulias D, Dimosiari A, Michailidis T. Anakinra or tocilizumab for prevention of COVID-19 death? a big dilemma. *Eur J Intern Med* (2021) 90:107–8. doi: 10.1016/j.ejim.2021.05.039

15. Küçükşahin O, Erden A, Karakaş Ö, Güven SC, Armağan B, Şahiner EŞ, et al. Comparison of anakinra and tocilizumab in management of severe COVID-19: a retrospective cohort study. *Turk J Med Sci* (2022) 52:1486–94. doi: 10.55730/1300-0144.5487

16. *Propositions du GFHT/GIHP pour le traitement anticoagulant pour la prévention du risque thrombotique chez un patient hospitalisé avec COVID-19. groupe d'etude sur l'hemostase et la thrombose*. Available at: https://site.geht.org/actu/propositions-du-gfht-gihp-pour-le-traitement-anticoagulant-pour-la-prevention-du-risque-thrombotique-chez-un-patient-hospitalise-avec-covid-19/ (Accessed December 19, 2022).

17. Gupta A, Gonzalez-Rojas Y, Juarez E, Crespo Casal M, Moya J, Falci DR, et al. Early treatment for covid-19 with SARS-CoV-2 neutralizing antibody sotrovimab. *N Engl J Med* (2021) 385:1941–50. doi: 10.1056/NEJMoa2107934

18. RECOVERY Collaborative Group. Casirivimab and imdevimab in patients admitted to hospital with COVID-19 (RECOVERY): a randomised, controlled, open-label, platform trial. *Lancet* (2022) 399:665–76. doi: 10.1016/S0140-6736(22)00163-5

19. Gao Y-D, Ding M, Dong X, Zhang J-J, Kursat Azkur A, Azkur D, et al. Risk factors for severe and critically ill COVID-19 patients: a review. *Allergy* (2021) 76:428–55. doi: 10.1111/all.14657

20. Dessie ZG, Zewotir T. Mortality-related risk factors of COVID-19: a systematic review and meta-analysis of 42 studies and 423,117 patients. *BMC Infect Dis* (2021) 21:855. doi: 10.1186/s12879-021-06536-3

21. Zhang J-J, Dong X, Liu G-H, Gao Y-D. Risk and protective factors for COVID-19 morbidity, severity, and mortality. *Clin Rev Allergy Immunol* (2023) 64:90–107. doi: 10.1007/s12016-022-08921-5

22. Fajgenbaum DC, June CH. Cytokine storm. *N Engl J Med* (2020) 383:2255–73. doi: 10.1056/NEJMra2026131

23. Kozak W, Kluger MJ, Soszynski D, Conn CA, Rudolph K, Leon LR, et al. IL-6 and IL-1β in fever: studies using cytokine-deficient (Knockout) micea. *Ann New York Acad Sci* (1998) 856:33–47. doi: 10.1111/j.1749-6632.1998.tb08310.x

24. Aliyu M, Zohora FT, Anka AU, Ali K, Maleknia S, Saffarioun M, et al. Interleukin-6 cytokine: an overview of the immune regulation, immune dysregulation, and therapeutic approach. *Int Immunopharmacol* (2022) 111:109130. doi: 10.1016/j.intimp.2022.109130

25. Hermine O, Mariette X, Tharaux P-L, Resche-Rigon M, Porcher R, Ravaud P, et al. Effect of tocilizumab vs usual care in adults hospitalized with COVID-19 and moderate or severe pneumonia: a randomized clinical trial. *JAMA Intern Med* (2021) 181:32–40. doi: 10.1001/jamainternmed.2020.6820

26. Tleyjeh IM, Kashour Z, Damlaj M, Riaz M, Tlayjeh H, Altannir M, et al. Efficacy and safety of tocilizumab in COVID-19 patients: a living systematic review and meta-analysis. *Clin Microbiol Infect* (2021) 27:215–27. doi: 10.1016/j.cmi.2020.10.036

27. Pasin L, Cavalli G, Navalesi P, Sella N, Landoni G, Yavorovskiy AG, et al. Anakinra for patients with COVID-19: a meta-analysis of non-randomized cohort studies. *Eur J Intern Med* (2021) 86:34–40. doi: 10.1016/j.ejim.2021.01.016

28. Khan FA, Stewart I, Fabbri L, Moss S, Robinson K, Smyth AR, et al. Systematic review and meta-analysis of anakinra, sarilumab, siltuximab and tocilizumab for COVID-19. *Thorax* (2021) 76:907–19. doi: 10.1136/thoraxjnl-2020-215266

29. Peng J, Fu M, Mei H, Zheng H, Liang G, She X, et al. Efficacy and secondary infection risk of tocilizumab, sarilumab and anakinra in COVID-19 patients: a systematic review and meta-analysis. *Rev Med Virol* (2022) 32:e2295. doi: 10.1002/rmv.2295

30. Davidson M, Menon S, Chaimani A, Evrenoglou T, Ghosn L, Graña C, et al. Interleukin-1 blocking agents for treating COVID-19. *Cochrane Database Systematic Rev* (2022). doi: 10.1002/14651858.CD015308

31. Albuquerque AM, Eckert I, Tramujas L, Butler-Laporte G, McDonald EG, Brophy JM, et al. Effect of tocilizumab, sarilumab, and baricitinib on mortality among patients hospitalized for COVID-19 treated with corticosteroids: a systematic review and meta-analysis. *Clin Microbiol Infect* (2022) 29(1):13–21. doi: 10.1016/j.cmi.2022.07.008

32. Langer-Gould A, Smith JB, Gonzales EG, Castillo RD, Figueroa JG, Ramanathan A, et al. Early identification of COVID-19 cytokine storm and treatment with anakinra or tocilizumab. *Int J Infect Dis* (2020) 99:291–7. doi: 10.1016/j.ijid.2020.07.081

33. Iglesias-Julián E, López-Veloso M, de-la-Torre-Ferrera N, Barraza-Vengoechea JC, Delgado-López PD, Colazo-Burlato M, et al. High dose subcutaneous anakinra to treat acute respiratory distress syndrome secondary to cytokine storm syndrome among severely ill COVID-19 patients. *J Autoimmun* (2020) 115:102537. doi: 10.1016/j.jaut.2020.102537

34. Atluri K, Aimlin I, Arora S. Current effective therapeutics in management of COVID-19. *J Clin Med* (2022) 11:3838. doi: 10.3390/jcm11133838

35. Oliynyk O, Barg W, Oliynyk Y, Dubrov S, Gurianov V, Rorat M. Lack of difference in tocilizumab efficacy in the treatment of severe COVID-19 caused by different SARS-CoV-2 variants. *J Pers Med* (2022) 12:1103. doi: 10.3390/jpm12071103

36. Chedid M, Waked R, Haddad E, Chetata N, Saliba G, Choucair J. Antibiotics in treatment of COVID-19 complications: a review of frequency, indications, and efficacy. *J Infect Public Health* (2021) 14:570–6. doi: 10.1016/j.jiph.2021.02.001

37. Popp M, Stegemann M, Riemer M, Metzendorf M-I, Romero CS, Mikolajewska A, et al. Antibiotics for the treatment of COVID-19. *Cochrane Database Syst Rev* (2021) 10:CD015025. doi: 10.1002/14651858.CD015025

38. Akbari A, Razmi M, Sedaghat A, Alavi Dana SMM, Amiri M, Halvani AM, et al. Comparative effectiveness of pharmacological interventions on mortality and the average length of hospital stay of patients with COVID-19: a systematic review and meta-analysis of randomized controlled trials. *Expert Rev Anti Infect Ther* (2022) 20:585–609. doi: 10.1080/14787210.2022.1997587

39. Yang B-B, Gozzi P, Sullivan JT. Pharmacokinetics of anakinra in subjects of heavier vs. lighter body weights. *Clin Transl Sci* (2019) 12:371–8. doi: 10.1111/cts.12622

40. EMA. *RoActemra* (2018). European Medicines Agency. Available at: https://www.ema.europa.eu/en/medicines/human/EPAR/roactemra (Accessed December 19, 2022).

Frontiers in Immunology

Explores novel approaches and diagnoses to treat immune disorders.

The official journal of the International Union of Immunological Societies (IUIS) and the most cited in its field, leading the way for research across basic, translational and clinical immunology.

Discover the latest Research Topics

See more →

Frontiers

Avenue du Tribunal-Fédéral 34
1005 Lausanne, Switzerland
frontiersin.org

Contact us

+41 (0)21 510 17 00
frontiersin.org/about/contact